Lewis Acid Mediated Approaches for the Generation of 4- and 5-Membered Ring Systems

by

Shorena Gelozia

A thesis submitted in partial fulfillment of the requirements for the degree of

Doctor of Philosophy

Department of Chemistry
University of Alberta

Abstract

The presence of complex polycyclic skeletons is a commonly encountered phenomenon in natural products and biologically active compounds. Having diverse synthetic approaches for accessing them is vital for the effective development of the pharmaceutical industry. Among other strategies, pericyclic reactions, such as electrocyclizations and cycloadditions, are very powerful tools to generate cyclic templates. While Nazarov electrocyclization is a well-known method for synthesizing cyclopentanones, intercepting the reaction intermediates opens the door for their further functionalization. The [2+2] cycloaddition is a step-economical procedure to obtain strained cyclobutane structures. This thesis will discuss some recent advances in a relatively new concept of double interrupted Nazarov cyclization mediated by organoaluminum reagent, as well as a less commonly used thermal approach for the synthesis of cyclobutane derivatives.

Chapter 1 describes fundamentals of 4π and 6π electrocyclization reactions, along with some recent advances in this field. Conceptual differences in their photochemical and thermal variants will be showcased in a multitude of examples. Their practical usefulness will be demonstrated by their use in the total synthesis of natural products and bioactive substrates.

Chapter 2 tells the detailed story about organoaluminum mediated double interrupted Nazarov cyclization, in which the sequence of electrocyclization is productively combined with the subsequent nucleophilic trapping via methyl migration, followed by electrophilic capture through Simmons-Smith cyclopropanation. This new

approach allows the access to bicyclic alcohols, further derivatization of which could convert them into their 6-membered equivalents via various ring expansion strategies.

Conversion of the Nazarov substrates into their 6π analogues by adding extra conjugation and their treatment with Lewis acids instead of 6π electrocyclization underwent some unexpected formal [2+2] cycloadditions, the details of which will be disclosed in Chapter 3. Use of structurally similar but qualitatively different haloboranes resulted in dissimilar results, which along with product diversification emphasizes the versatility of the method.

To circumvent the problem of insufficient heart contraction, various calcium signaling pathways are attempted to be affected. Increasing myofilament sensitivity towards calcium without increasing intracellular ion concentration is one of the strategies which could be achieved via tight binding of small molecules to the target protein Troponin C. In Chapter 4, our attempts to synthesize a library of those small molecules with better calcium sensitizing effect will be described.

Preface

Part of Chapter 2 of this thesis has been published as S. Gelozia, Y. Kwon, R. McDonald, F. G. West, "One-Pot Generation of Bicyclo[3.1.0]hexanols and Cyclohexanones via Double Interrupted Nazarov Reaction," *Chem. Eur. J.* **2018**, *24*, 6052–6056. I was responsible for the experimental work, the data collection, and characterization of compounds as well as the manuscript composition. Y. Kwon was responsible for the concept formation, some preliminary optimization work, data collection and characterization of compounds **40a, 43a, 43a′, 44a, 44a′**(numbering from Chapter 2). R. MacDonald provided X-ray data for compounds **42a** and **43a**. F. G. West was the supervisory author and was involved with concept formation and manuscript composition.

Part of Chapter 3 of this thesis will be published as S. Gelozia, R. McDonald, M. J. Ferguson, F. G. West, "Lewis Acid Mediated Formal Crossed [2+2] Cycloaddition of *o*-Styrenyl Chalcones," *manuscript in preparation*. I was responsible for the experimental work, the data collection, and characterization of compounds as well as the manuscript composition. R. McDonald provided X-ray data for compounds **52a**, **52f′, 54a;** F. J. Ferguson provided X-ray data for compound **52l** (numbering from Chapter 3). F. G. West was the supervisory author and wasinvolved with concept formation and manuscript composition.

Part of Chapter 4 of this thesis has been published as F. Cai, M. X. Li, S. E. Pineda-Sanabria, S. Gelozia, S. Lindert, F. G. West, B. D. Sykes, P. M. Hwang, "Structures Reveal Details of Small Molecule Binding to Cardiac Troponin" *J. Mol.*

Cell. Cardiol. **2016**, *101*, 134–144. I was responsible for the experimental work, the data collection and characterization of compounds **10, 11, 12, 13, 18, 19, 30, 33, 34, 35, 36, 37, 38, 39**, **51** (numbering from Chapter 4) as well as composition of supporting information of the manuscript. F. Cai, and M. X. Li were responsible for protein preparation and obtaining NMR titration data (biology data) as well as manuscript composition. P. M. Hwang F. G. West and B. D. Sykes were the supervisory authors and were involved with concept formation and manuscript composition.

Acknowledgements

In the first place, I would like to express my sincere gratitude to my supervisor Prof. Dr. West for accommodating me in his lab and allowing do the high level research, for his continuous support and guidance. In retrospect to who I was when I joined the group and now I can feel the dramatic difference. The merit for growing as a chemist and improving my theoretical knowledge and practical skills can be in most part attributed to him. The freedom he provides in his group forged the feeling of independence and self-confidence which in turn encouraged me to delve into new adventures of chemistry world and challenge myself.

I would like to thank Prof. Dr. Robert Campbell, Prof. Dr. Derrick Clive and Dr. John Vederas for being my supervisory committee members and expressing their willingness to support me in my academic life.

Next, I would like to thank those of my group members who could be seen as an example of collegiality, friendliness and generosity and giving me moral support at certain stages of my graduate studies (Tianmin, Yaseen, Ahmed Elmenoufy and Ahmed Oraby, Yury, Olivier, Natasha, Luna, Kyle, Peter). My special thanks need to go to Marius Constantin who constantly provided positive atmosphere in the lab and made arduous lab work more fun. His perpetual readiness to help makes him a special person. I feel lucky that his work space (in both lab and office) was assigned next to mine and I acquired such a colleague. Baolei Wang was another remarkable person who I was fortunate to meet. His fairness and all-forgiving attitude were features which allowed me to create the bonds of friendship. I would like to thank my mentee Dana Boe for accepting my mentorship and guidance and making me feel useful. Fortunately, some

people from other research groups were kind enough to grant their warmth and gentleness which I am infinitely grateful to them for (Eva Rodriguez-Lopez, Pariza Rezghi, Mohammad Khadem).

Mark Miskolzie from NMR facility lab, Jing Zheng and Angie Morales from MS lab, Jason Dibbs from glass shop, staff from IR and X-Ray service labs are people who deserve my special appreciation for their readiness to help and invaluable support. Thank you so much for being so approachable and treating me as equal.

Table of Contents

List of Tables

List of Figures

List of Schemes

List of Symbols and Abbreviations

^{1}H	proton
^{13}C	carbon-13
^{19}F	fluorine-19
A	acid
Å	Angstrom
Ac	acetyl
Ac_2O	acetic anhydride
acac	acetylacetonate
app.	apparent (spectral)
APPI	atmospheric pressure photoionization (mass spectrometry)
aq	aqueous solution
Ar	aryl
ATP	adenosine triphosphate
BA	Brønsted acid
BINOL	1,1′-binaphthalene-2,2′-diol
BINAP	2,2′-bis(diphenylphosphino)-1,1′-binaphthalene
Bn	benzyl
Boc	*tert*-butyloxycarbonyl
Bpin	bis(pinacolato)boron
Br	broad (spectral)
Bu	butyl
ºC	degrees Celsius
Calcd	calculated
cat.	indicates that the reagent was used in a catalytic amount
CFL	compact fluorescent lamp
cm^{-1}	wave numbers
COSY	H-H correlation spectroscopy
conc.	concentrated
CVD	cardiovascular disease

d	day(s); doublet (spectral)
dba	tris(dibenzylideneacetone
DBU	1,8-diazabicyclo[5.4.0]undec-7-ene
DCE	1,2-dichloroethane
DCM	dichloromethane
dd	doublet of doublets (spectral)
ddd	doublet of doublets of doublets (spectral)
dddd	doublet of doublets of doublets of doublets (spectral)
DHF	diastolic heart failure
DIBAL-H	diisobutylaluminum hydride
DIPEA	*N,N*-diisopropylethylamine
DMAP	4-diemthylamino pyridine
DMF	dimethylformamide
DMSO	dimethyl sulfoxide
de	diastereomeric excess
dig	digonal
DPA	diphenylamine
dq	doublet of quartets (spectral)
dr	diastereomeric ratio
dt	doublet of triplets (spectral)
e^-	electron
E^+	an unspecified electrophile
EDG	electron-donating group
ee	enantiomeric excess
EI	electron impact (mass spectrometry)
endo	endocyclic
equiv	equivalent(s)
er	enantiomeric ratio
ESI	electrospray inonization (mass spectrometry)
Et	ethyl
EtOAc	ethyl acetate

EWG	electron-withdrawing group
exo	exocyclic
FLP	frustrated Lewis pair
FMO	frontier molecular orbitals
FT-IR	Fourier-transform infrared spectroscopy
g	gram(s)
h	hour(s)
HF	heart failure
HMBC	heteronuclear multiple bond coherence (spectral)
HOMO	highest occupied molecular orbital
HSQC	heteronuclear single quantum coherence (spectral)
HRMS	high resolution mass spectrometry
hν	light
Hz	hertz
i-Bu	isobutyl
i-Pr	isopropyl
ISC	intersystem crossing
J	coupling constant
kcal	kilocalorie
K_D	dissociation constant
kJ	kilojoules
L	liter(s); unspecified ligand
LA	Lewis acid
LAH	lithium aluminum hydride
LDA	lithium diisopropylamide
LED	light-emitting diode
LiHMDS	lithium hexamethyldisilazane
LUMO	lowest unoccupied molecular orbital
M	molar
m	multiplet (spectral)
M^+	generalized Lewis acid or protic acid; molecular ion

Me	methyl
mg	milligram(s)
MHz	megahertz
min	minute(s)
mL	milliliter(s)
mmol	millimole(s)
mol	mole(s)
mp	melting point
MS	molecular sieves
Ms	methanesulfonyl
m/z	mass to charge ratio
NFSI	fluoro-*o*-benzenedisulfonimide
nm	nanometer(s)
NMR	nuclear magnetic resonance
NOE	nuclear Overhauser enhancement
n-Pr	normal propyl
Nu	an unspecified nucleophile
o/n	overnight
ORTEP	Oak Ridge thermal-ellipsoid plot
Ph	phenyl
PMP	*p*-methoxyphenyl
pp	pages
ppm	parts per million
Pr	propyl
Py	pyridine
q	quartet (spectral)
qt	quartet of triplet
quint	quintet
R	generalized alkyl group of substituent
rac	racemate
R_f	retention factor (in chromatography)

rt	room temperature
rxn	reaction
s	singlet (spectral)
SAR	structure activity relationship
SDNC	silicon directed Nazarov cyclization
sept	septet (spectral)
SET	single electron transfer
SHF	systolic heart failure
SHOMO	second highest occupied molecular orbital
SM	starting material
S_N	nucleophilic substitution
SOMO	singly occupied molecular orbital
t	triplet (spectral)
T	temperature
TBDMS	tert-Butyldimethylsilyl
t-Bu	*tert*-butyl
TEA	triethylamine
TEMPO	(2,2,6,6-Tetramethylpiperidin-1-yl)oxyl
tet	tetrahedral
Tf	trifluoromethanesulfonyl
TFA	trifluoroacetic acid
THF	tetrahydrofuran
TLC	thin layer chromatography
Tm	tropomyosin
TMS	trimethylsilyl
Tn	Troponin
TOCSY	total correlation spectroscopy
Tq	triplet of quartet
Trig	trigonal
TROESY	transverse rotating-frame overhauser enhancement spectroscopy
Ts	*p*-toluenesulfonyl

tt	triplet of triplet
p-TsOH(pTSA)	*p*-toluenesulfonic acid
UV	ultra violet light
W	watt
wt.	weight
Δ	applied heat
δ	chemical shift
λ	wavelength
μ	micro

Chapter 1

4π and 6π Electrocyclic Reactions

1.1 Fundamentals of Electrocyclization

Among diverse synthetic strategies en route to structurally complex cyclic scaffolds which are present in many biologically active natural compounds and drugs, electrocyclic reactions constitute a powerful class of reactions for the stereoselective construction of new rings.[1] In contrast to cycloaddition reactions in which two new σ-bonds form at the expense of two π-bonds, in electrocyclization only one σ-bond forming event takes place (Figure 1.1).[2] Due to the highly ordered cyclic transition state and necessity of conservation of orbital symmetry, electrocyclic reactions are characterized by high degree of stereospecificity as demonstrated by Woodward-Hoffmann rules.[3] Like all pericyclic reactions, electrocyclization is a concerted process which means that bond-breaking and bond formation happens simultaneously.

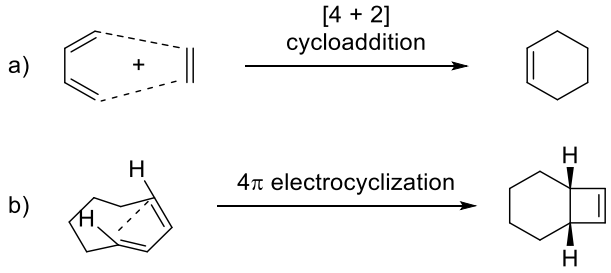

Figure 1.1 Pericyclic reactions.

According to the *Frontier Molecular Orbital Theory* (FMO), conrotatory ring-closure (two terminal substituents rotate in the same direction) of highest occupied molecular orbitals (HOMO) is general for 4π electron conjugated systems under thermal conditions while only disrotatory motion (two terminal substituents rotate in opposite direction) can provide positive overlap of orbitals for 6π electron systems. The opposite scenario can explain bond formation in photochemically induced species when highest *singly occupied molecular orbitals* (SOMO) are involved in ring closure (Figure 1.2).

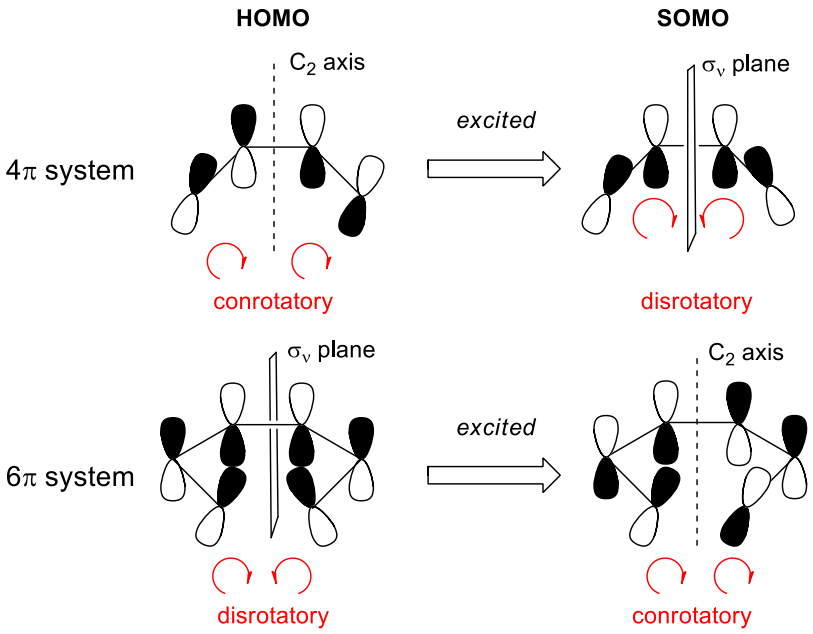

Figure 1.2 Woodward-Hoffmann rules for electrtocyclization.

The driving force for electrocyclization reactions lies in the inherent structural features of reactants and the products which means the process is controlled by their relative stabilities. The reason why electrocyclization reactions are less explored compared to other pericyclic reactions is the need for high temperatures - the factor very disadvantageous for highly functionalized substrates. This fact provides a good incentive for the development of kinetically controlled variants with the use of catalytic and stoichiometric initiators.[4]

1.2. 4π Electrocyclization

Among other electrocyclic reactions, 4π electrocyclizations is obviously a very important strategy towards construction of various complex polycyclic skeletons including cyclopentanes, lactones and cyclohexanones. Natural products depicted in figure 1.3 demonstrate practical utility and usefulness of 4π electrocyclization, as the

later one was used as one of the key steps towards preparation of these complex structures.[5,6,7]

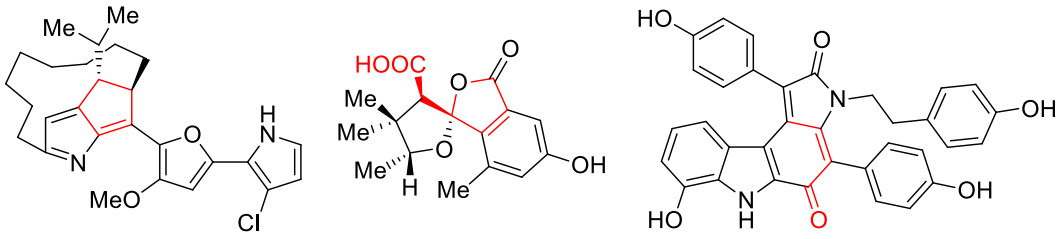

Figure 1.3 Natural products synthesized via 4π electrocyclization.

Depending on the number of atoms over which 4π electrons are delocalized, 4π electrocyclization can be split in to two subcategories: one involving 4-electron/4-atom neutral species and another proceeding through 4-electron/5-atom cationic species.

1.2.1 Photochemical Neutral 4π Electrocyclization

Cyclobutene was first prepared in 1905 by Willstätter[8,9] however, mechanistic studies on the formation and reactivity of cyclobutenes were not carried out until the 1950s.[10] Walter's report from 1958 states that cyclobutene, possessing ring strain of 32.5 kcal/mol, is prone to ring opening to form 1,3-butadiene at 150 °C in an unimolecular process.[11] Due to this strain, 4π electrocyclizations of 1,3-butadiene precursors **5** and **5′** are highly endothermic, therefore pushing equilibrium towards ring opening products under thermal conditions (Scheme 1.1).[12] However, photochemical irradiation of *E/E*-butadienes **4** with carefully selected wavelength at low temperature allows synthesis of *cis*-disubstituted cyclobutenes **5** as stable products via disrotatory ring closure. Competitive *E/Z*-isomerization of the diene precursor **4** can lead to the erosion of stereospecificity and formation of mixture of *cis* and *trans* cyclobutenes though.

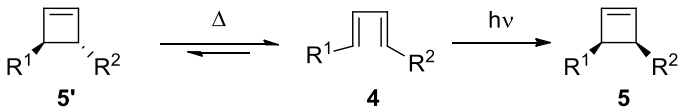

Scheme 1.1 Cyclobutene formation via 4π electrocyclization.

According to Corey's 1964 report, an ethereal solution of 2-pyrone **6** under ultraviolet irradiation affords in almost quantitative yield strained lactone **7** via disrotatory 4π electrocyclization (Scheme 1.2a).[13] Under the same reaction conditions, N-methyl-2-pyridone **8** yields lactam **9** although at slower rate (Scheme 1.2b). Structure assignments of products **7** and **9** were performed based on chemical and physical characteristics. Despite their air sensitivity, instability and explosive nature, these types of compounds reveal none of the above mentioned undesired features when handled in cold ethereal solutions.

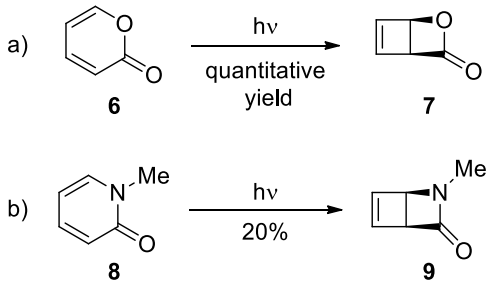

Scheme 1.2 Photochemical 4π electrocyclization of 2-pyrone and 2-pyridone.

In 2010, Maulide's group took advantage of instability of 2-pyrone **7** to use it as a synthetic handle in catalytic stereoselective transformation towards functionalized cyclobutenes.[14] In the presence of Pd(0), strained lactone **7** underwent ionization to afford the palladium-π-allyl complex, which was subsequently trappedin situ by malonates to produce 1,2 *cis*-substituted carboxylic acids which upon esterification afforded corresponding esters **10** (Scheme 1.3).

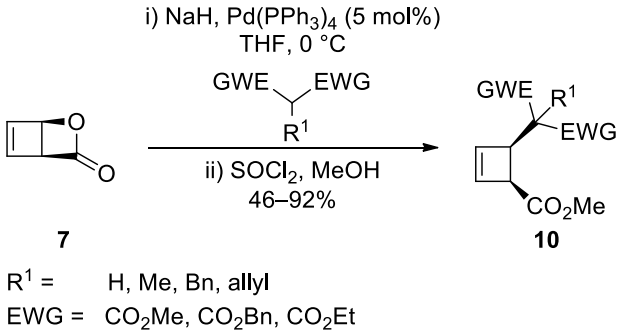

Scheme 1.3 Catalytic stereoselective functionalization of 2-pyrones.

As a prominent example of photochemical 4π electrocyclization can serve the light-induced electrocyclic ring closure of colchicine. There are several reports about colchicine and its solution to undergo some changes when exposed to sunlight.[15] However, as shown by Macht, only the shorter wavelength (blue) portion of the visible spectrum effects the photochemical rearrangement.[16]

Forbes in 1955 showcased that direct prolonged irradiation of colchicine **11** with summer sunlight initiates photochemical 4π disrotatory electrocyclization of involving tropolone moiety to give diastereomeric mixture of cyclobutenes **12** and **13** which were named as β – (**12)** and γ–lumicolchicines (**13)** respectively (Scheme 1.4).[17]

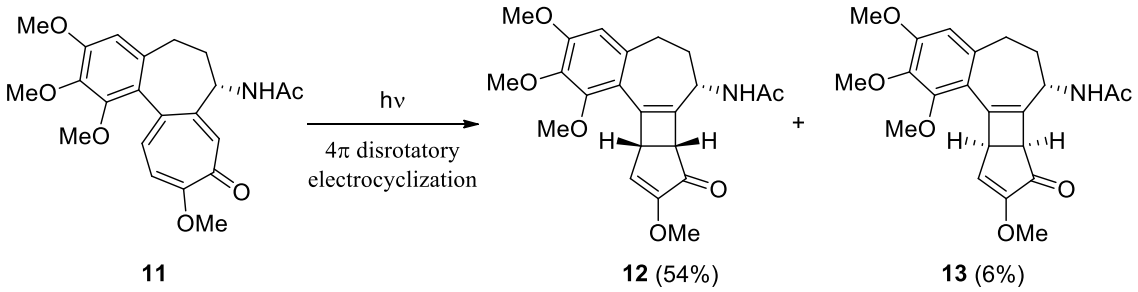

Scheme 1.4 Light induced 4π electrocyclization of colchicines.

1.2.2 Thermal Neutral 4π Electrocyclization

In 2004, Murakami's group published a work about dramatic effects of boryl substituents on thermal ring-closure of vinylallenes.[18] In contrast to the electrocyclization of 1,3-butadiene, instability of vinylallenes bearing boron substituents on the terminus of the alkene moiety made thermal 4π conrotatory ring closure a favorable process allowing the formation of thermodynamically more stable methylene cyclobutenes. Heating of *Z*-vinylallene **14** in xylene at 140 °C provided ring-closed product **15** in 96% yield (Scheme 1.5). The precursor with *trans* boron substituent also underwent cyclization to afford product **15**, however, at much lower rate. For comparison, vinylallene **16** lacking a boron group underwent only self-dimerization via [4+2] cycloaddition even at -30 °C; only heating at 140 °C for 8 h could produce 4π electrocyclization product **17**, although in 20% yield along with [4+2] cycloaddition product **18** and polymerization products (Scheme 1.6). This dramatic effect was attributed to the interaction of vacant *p*-orbitals of boryl substituents as electron acceptors with the frontier orbitals (second highest occupied molecular orbital - SHOMO) of the transition states.

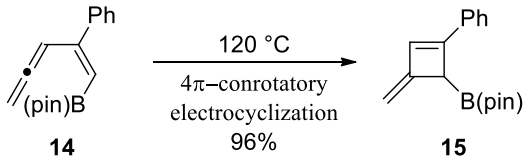

14 **15**

Scheme 1.5 4π Conrotatory ring closure of vinylallenes.

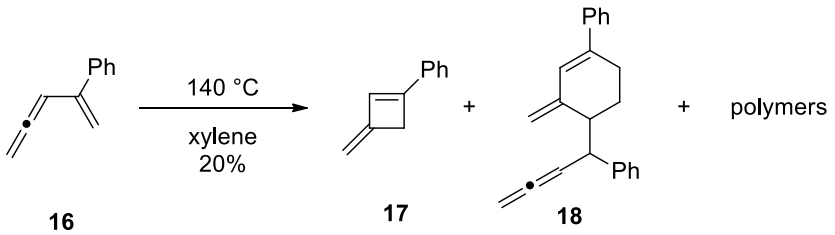

16 **17** **18**

Scheme 1.6 Effect of boron substituent on 4π electrocyclization.

In contrast to the thermodynamically unfavorable thermal 4π electrocyclizations of all carbon systems, introduction of heteroatom into dienes makes the ring-closing process exothermic, thus allowing the isolation of cyclic products. As an example, Pansuryia et al. in 2010 demonstrated synthesis of 1,2-diazetines via hetero 4π electrocyclization of corresponding coumarin azines.[19] Treatment of hydrazone **19** with aldehydes in DMSO containing HCl as a catalyst at 100 °C afforded 1,2-diazete products **21** via 4π conrotatory electrocyclization of coumarin azine intermediates **20** (Scheme 1.7). The stereochemical outcome of the reaction is consistent with the involvement of 4π conrotatory ring-closing process explaining formation of *trans*-1,2-diazetes as major products (Scheme 1.8).

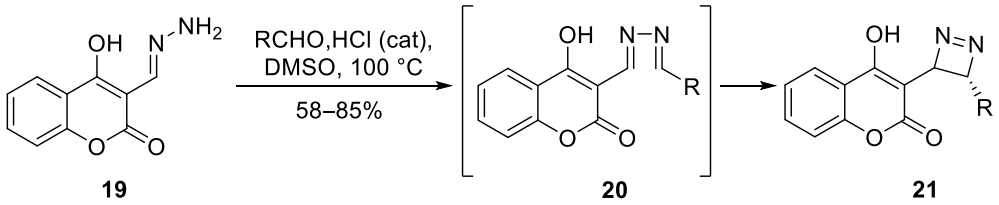

Scheme 1.7 Hetero 4π electrocyclic ring closure.

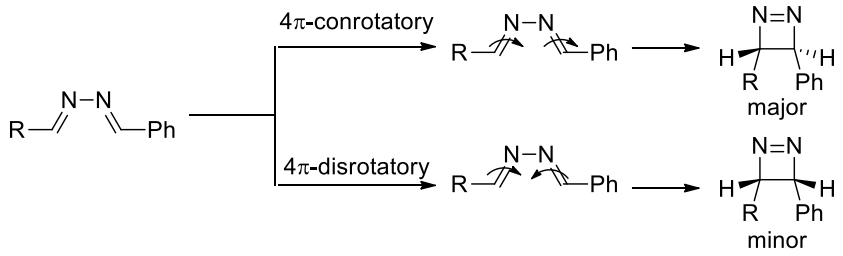

Scheme 1.8 Mechanistic insight into the analysis of reaction stereocontrol.

Recently, Liu group in collaboration with Houk and Merlic groups reported synthesis of strained cyclic dienes via Pd(II)-catalyzed oxidative cyclization of terminal bis(vinylboronate) ester **22**.[20] The reaction generated strained intermediate (*E,E*)-1,3-diene **23** which at room temperature spontaneously underwent 4π conrotatory cyclization to afford *trans*-cyclobutene **24** (Scheme 1.9). The authors postulated that

cyclobutene ring formation is driven by strain presented in medium-sized cyclic diene intermediates with strain energies predicted to lie between 15–46 kcal/mol.

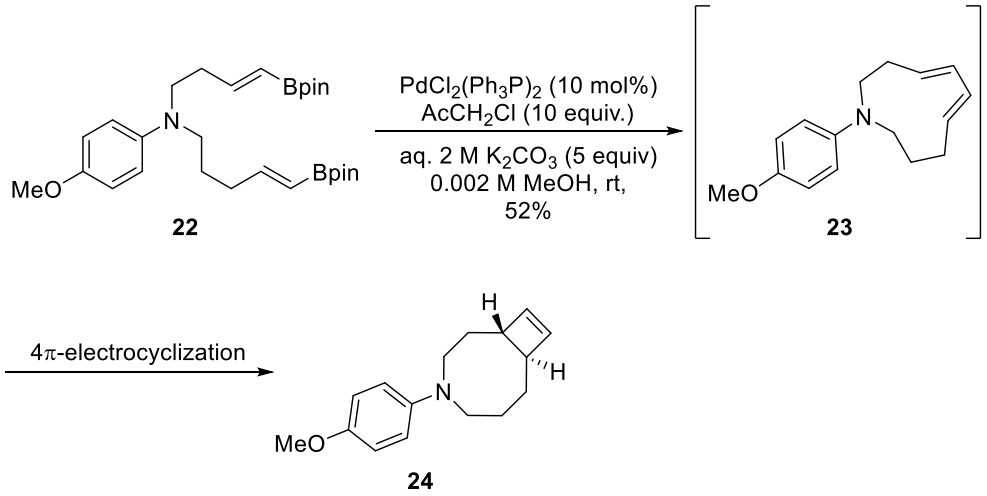

Scheme 1.9 Medium-sized strained ring 4π electrocyclization.

1.2.3 Cationic Thermal 4π Electrocyclization

1.2.3.1 Pentadienyl to Cyclopentenyl – Electrocyclization of Trienes

The simplest illustrative example of cationic thermal 4π electrocyclization is conversion of pentadienyl cations into cyclopentenyl cations. In 1964, Deno and co-worker reported that in strongly acidic medium aliphatic triene **25** can exist in equilibrium with its stable cationic counterpart **26** (Scheme 1.10a). In contrast, the pentadienyl cation **28** generated upon protonation of dienylic alcohol **27** in concentrated sulfuric acid, immediately converts into cyclopentenyl cation **30** via cyclization/rearrangement in quantitative yield (Scheme 1.10b).[21] The process is electrocyclic reaction and proceeds in conrotatory fashion in accordance with Woodward-Hoffmann rules.[22]

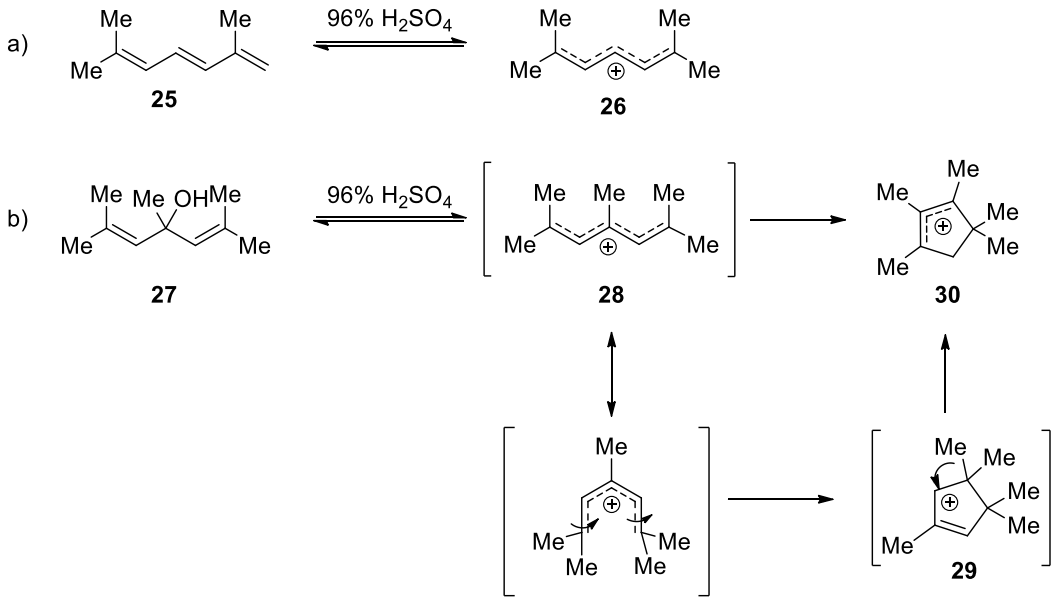

Scheme 1.10 Acid promoted generation of pentadienyl cations.

Later, Sorensen confirmed both reactions and further showed that **26** can in fact cyclize into its corresponding cyclopentenyl cation.[23] He further examined other less methylated homologues of **25** and **27**, and they all could successively be converted to their cyclic analogues. In 1965, Deno and co-workers further extended the scope of dienylic alcohols. The dienes generated from cyclopentenyl cations were reacted with maleic anhydride in Diels-Alder reaction to deliver diacid derivatives **33** (Scheme 1.11).

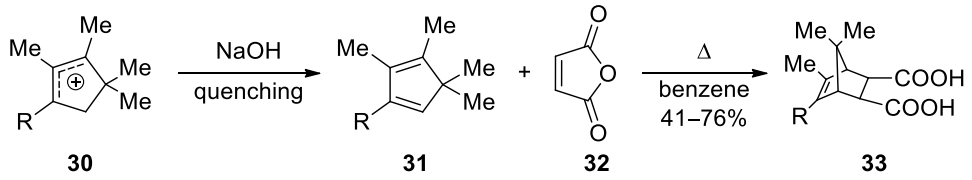

Scheme 1.11 Practical utility of cyclopentenyl cation.

1.2.3.2 The Nazarov Electrocyclization

The Nazarov reaction is the most prominent example of 4-electron/5-atom cationic electrocyclizations mediated by coordination of a Lewis or Brønsted acid

promoter to the divinyl ketone. Since its discovery in 1941, there has been an extensive research performed in this area and utilized in the synthesis of highly functionalized 5-membered carbocycles - frequently encountered structural motifs in various natural products and pharmaceuticals - from divinyl ketone precursors.[24]

The Nazarov cyclization was first documented in 1903 by Vorländer and Schroedter, who isolated an unknown ketol **35** while treating dibenzylideneacetone **34** with concentrated sulfuric acid in the presence of acetic anhydride followed by mild alkaline hydrolysis (Scheme 1.12).[25] Corrections were made by Allen and co-workers in 1955[26] for the originally misassigned structure of Vorländer's ketol **35**.

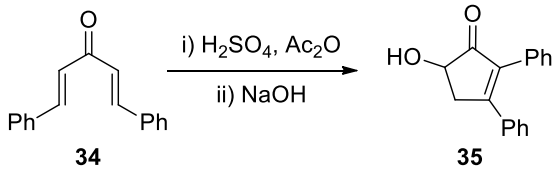

Scheme 1.12 First report of Nazarov cyclizaiton.

The reaction was rediscovered by Nazarov in 1940s during his extensive study of formation of allyl vinyl ketone **37** by hydration of dienyne **36** followed by acid catalyzed ring closure to 2-cyclopentenone **38** (Scheme 1.13).[27] However, the mechanism proposed by Nazarov for this transformation was incorrect and it was not until 1952 that the involvement of a pentadienyl cation derived from a rearranged α,α′-divinylketone was proposed by Braude and Coles.[28]

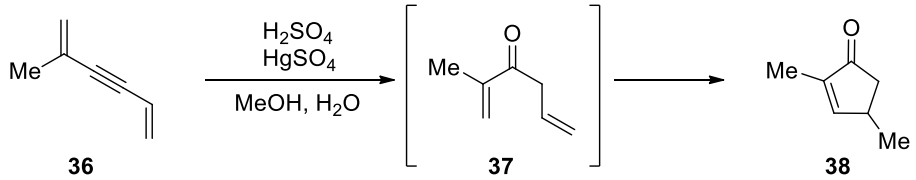

Scheme 1.13 Rediscovery of Nazarov reaction.

Subsequent work has confirmed the mechanistic proposal of Braude and Coles, and the generally accepted mechanism of the Nazarov reaction involves the sequential steps outlined below: (1) Neutral divinyl ketone **39** is activated by complexation with

strong Brønsted or Lewis acid (A). (2) The resulting pentadienyl cation **40** undergoes 4π conrotatory electrocyclization in a stereospecific manner as dictated by Woodward-Hoffmann rules to furnish more reactive oxyallyl cation **41** which upon proton elimination terminates with the formation of cyclopentenone **43** (Scheme 1.14).[29]

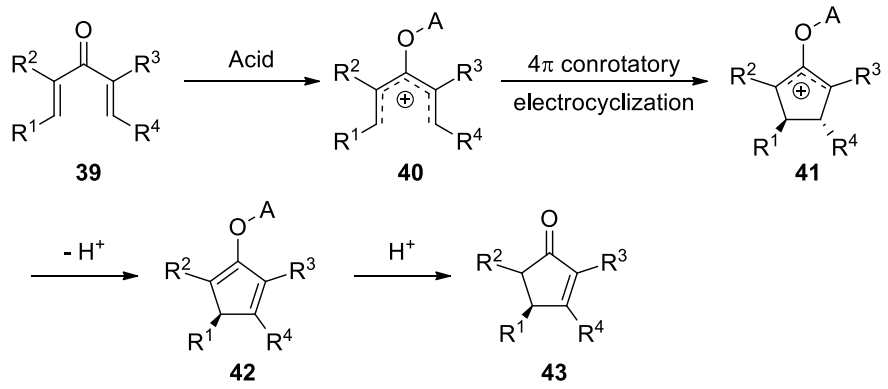

Scheme 1.14 Accepted mechanism for Nazarov electrocyclization.

1.2.3.2.1 Interrupted Nazarov Cyclization

1.2.3.2.1.1 Trapping with Nucleophiles

There is no doubt about the importance of straightforward Nazarov cyclization as a synthetic handle in the synthesis of more elaborate structures. Serious advances have been made in this area in terms of development of substrate variety and utilization of the methodology in natural product synthesis. However, termination of Nazarov cyclization with proton elimination is only one possible mode of exploiting reactive oxyallyl cation **41** which has a potential for further functionalization. Rather than simple deprotonation, this electrophilic intermediate can be intercepted with carbon- or heteroatom-based nucleophiles. Likewise, the enol or enolate resulting from either nucleophilic capture or elimination is subject to trapping with electrophilic reagents. Taken as a whole, these additional bond-forming processes are referred to as *"interrupted Nazarov reactions."*[24] The obvious advantages of the interruption process could be the introduction of an extra

carbon-carbon or carbon-heteroatom bonds to afford more functionalized cyclopentanoid scaffolds **44** and **46** (Scheme 1.15).

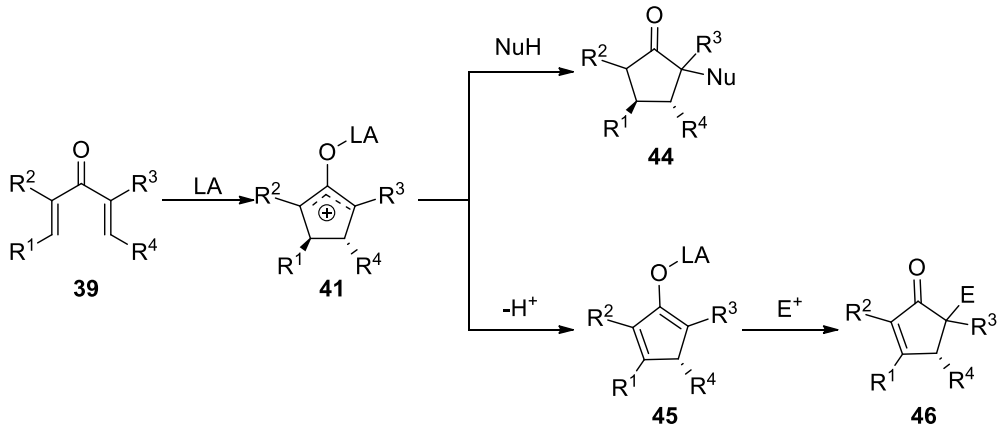

Scheme 1.15 Modes of interruption of Nazarov reaction.

The first example of intentional thermal interrupted Nazarov reaction was published by the West group in 1998.[30] Lewis acid activation of trienone **47** upon 4π conrotatory electrocyclization produced oxyallyl intermediate **48** which got trapped by pendant olefin in 5-exo-trig fashion. The tertiary carbocation present in the intermediate **49** underwent subsequent capture by enolate oxygen. Protonation of **50** in aqueous work-up delivered hemiketal **51** as a single product (Scheme 1.16).

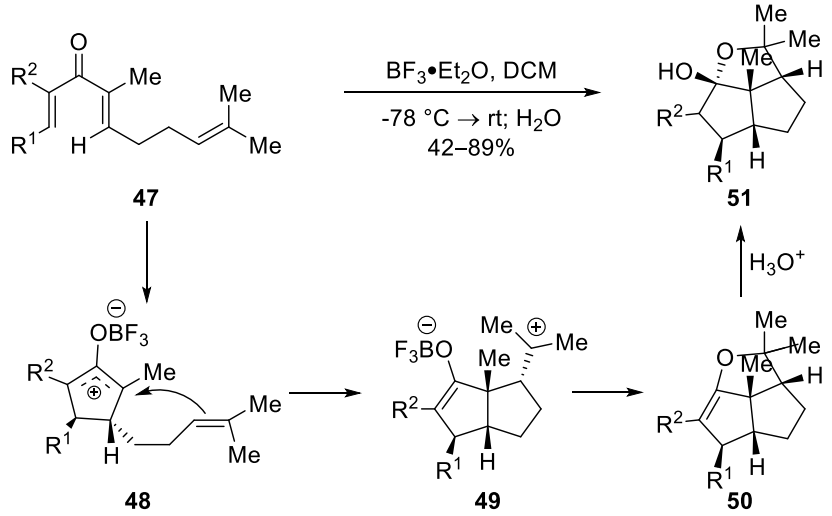

Scheme 1.16 First deliberate example of interrupted Nazarov cyclization.

In 2013, the West group first demonstrated the use of triorganoaluminum reagents in interrupted Nazarov processes. In this case, the organoaluminum species serves two essential functions. First, Lewis acid-base complexation to dienone **39** affords the necessary pentadienyl system to permit electrocyclization to oxyallyl intermediate **52** (Scheme 1.17). At this point, the now tetravalent aluminate can function as an internal nucleophile, transferring one of its ligands to the nearby terminus of the allyl cation (**53**). Importantly, this allows for interrupted Nazarov reaction with simple alkyl nucleophiles such as R = methyl. This methodology allows incorporation of alkyl group with good diastereselectivity to form densely substituted cyclopentanoid scaffolds.

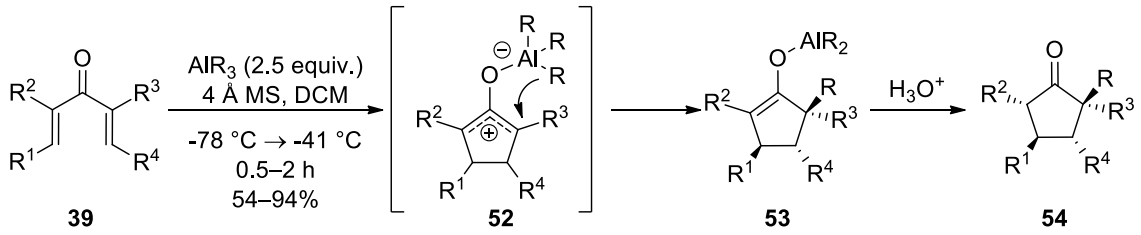

Scheme 1.17 Organoaluminum mediated interrupted Nazarov reaction.

Another recent example of interrupting oxyallyl cation with σ-nucleophile in a new modality has been reported by the Liu group in 2016.[31] Upon mixing potassium alkynyltrifluoroborate with $BF_3{\cdot}Et_2O$, Lewis acidic organodifluoroborane **55** was generated which effectively activated dienones **30** and formed zwitterionic pentadienyl cation intermediates **56**; 4π conrotatory ring closure followed by migration of the alkynyl group from the boron center to the oxyallyl cation formed enolates **57** which after protonation turned into α-alkynyl cyclopentanones **58** with high diastereoselectivity (Scheme 1.18). This was a first example of successful incorporation of sp-hybridized alkyne groups into cyclopentanone scaffolds using interrupted Nazarov reaction.

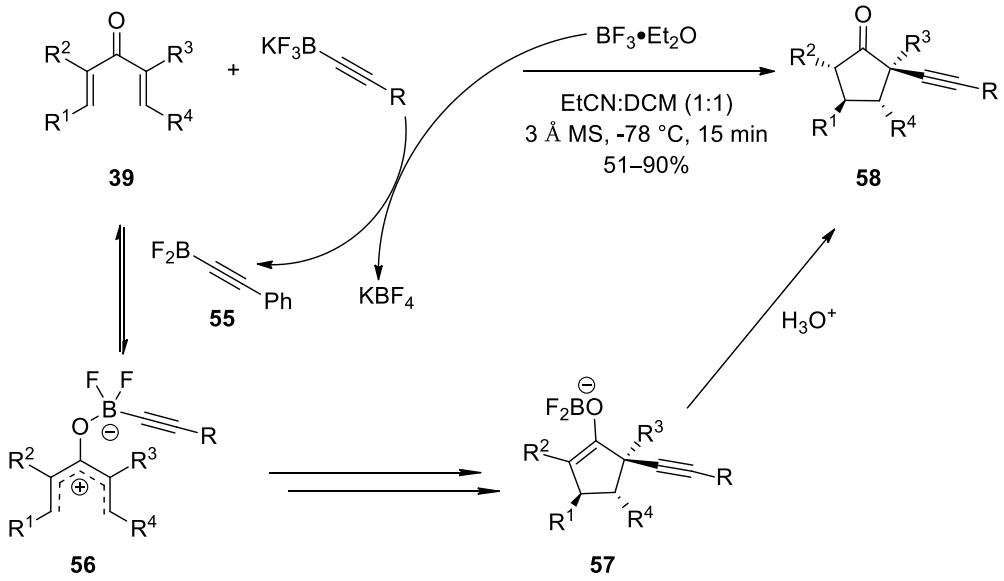

Scheme 1.18 Trapping of divinyl ketone with organotrifluoroborate.

1.2.3.2.1.2 Trapping with Electrophiles

Interrupted Nazarov cyclization with electrophilic trapping agents has also been investigated by various research groups. As noted above, in the absence of nucleophilic trapping agents, elimination is the predominant fate of the oxyallyl intermediate. This furnishes a nucleophilic dienolate that can participate in further bond-formation through reaction with a suitable electrophilic partner.

In 2007, Ma and co-workers took advantage of an already well established procedure of Knoevenagel condensation/Nazarov cyclization mediated by Lewis acid catalyst starting with β-ketoesters to afford 1-indanone derivatives. They developed one pot procedure in which the known cascade was extended to the subsequent electrophilic fluorination resulting in fluorinated 1-indanones.[32] In this three component triple cascade transformation consisting of β-ketoesters **59**, aldehydes and the fluorinating agent NFSI, a single Lewis acid ($AlCl_3$) was capable of catalyzingeach step of the sequence to provide fluorinated 1-indanones **60** (Scheme 1.19).

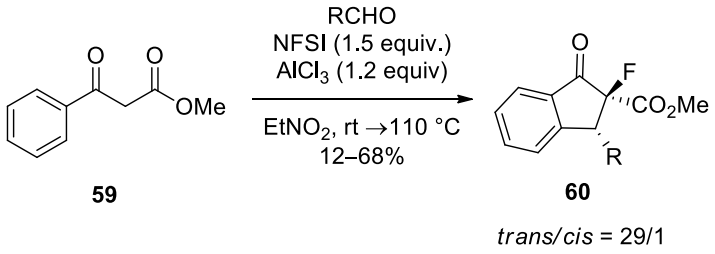

Scheme 1.19 Triple cascade transformation.

In 2018 an enantioselective variant of electrophilic fluorination was developed by Lu and co-workers. The authors reported a newly designed thiazoline iminopyridine ligand for the enantioselective interception of enolate with electrophilic fluorine source to prepare chiral α-fluoro cyclopentanone derivatives.[33] Activated by chiral cobalt catalyst, the precursor α-carboxymethyl divinyl ketones **61** underwent sequential Nazarov cyclization/electrophilic trapping in the presence of NFSI fluorinating agent affording fluorinated β-ketoesters **62** in good yields with good enantioselectivity. Decarboxylation in strongly acidic medium during reflux gave access to the diastereomeric mixture of α-fluoro cyclopentenones **63** and **63′** (Scheme 1.20).

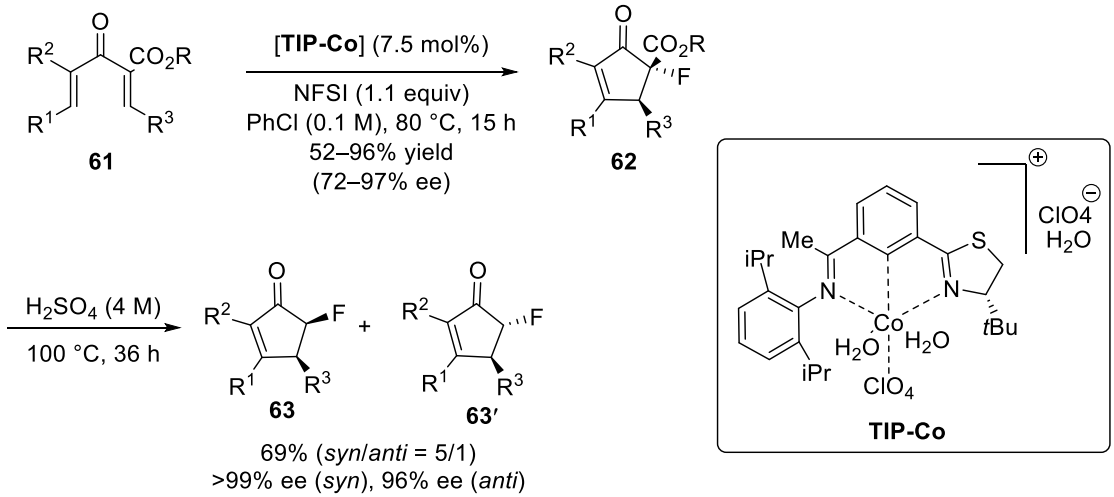

Scheme 1.20 Catalytic electrophilic fluorination of dienones.

1.2.3.2.1.3 Double Interrupted Nazarov Cyclization

The previous section discussed single interruption of the Nazarov reaction through either nucleophilic trapping of the oxyallyl cation or electrophilic trapping of the enolate formed after elimination. The concept of double interruption via sequential trapping has now begun to be explored. The enolate that results from nucleophilic trapping is also potentially capable of reaction with added electrophiles in a second bond-forming step to afford cyclopentanones with new functionality introduced on both sides of the carbonyl carbon. In order to accomplish this dual functionalization, the trapping nucleophile and electrophile must be mutually compatible, or else they must be introduced sequentially to avoid reaction with each other. Some advances have been made in this direction by the West group.

Synthesis of α-hydroxycyclopentanones could be accomplished in one pot via sequential nucleophilic/electrophilic trapping of the oxyallyl cation and its resulting enolate.[34] As already discussed above, during organoaluminum activation of dienones **39,** trapping of oxyallyl cations by methyl migration took place producing methylated aluminum enolates **53**. Passage of oxygen gas through the reaction vessel after complete consumption of starting material furnished epimeric mixture of α-hydroxycyclopentanones **64** and **64′** in moderate to good yields (Scheme 1.21). Although the exact mechanism of the oxidation process is not completely clear, intermediacy of alkylperoxyaluminum intermediates have been postulated, which upon aqueous work-up transforms into alcohols.

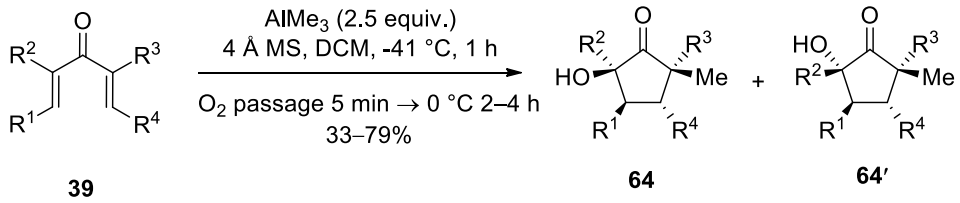

Scheme 1.21 $AlMe_3$ mediated Nazarov cyclization followed by oxidation.

Soon afterwards, unprecedented diatomic halogenation of the Nazarov intermediate was reported by the same group to prepare α,α′-dibrominated

cyclopentanones.[35] Treatment of dienones **39** with $BF_3{\cdot}Et_2O$ in the presence of pyridinium tribromide ($pyHBr_3$) as the bromine source delivered dibrominated symmetrical cyclopentanones **67** and **67′** with high diastereoselectivity (Scheme 1.22).

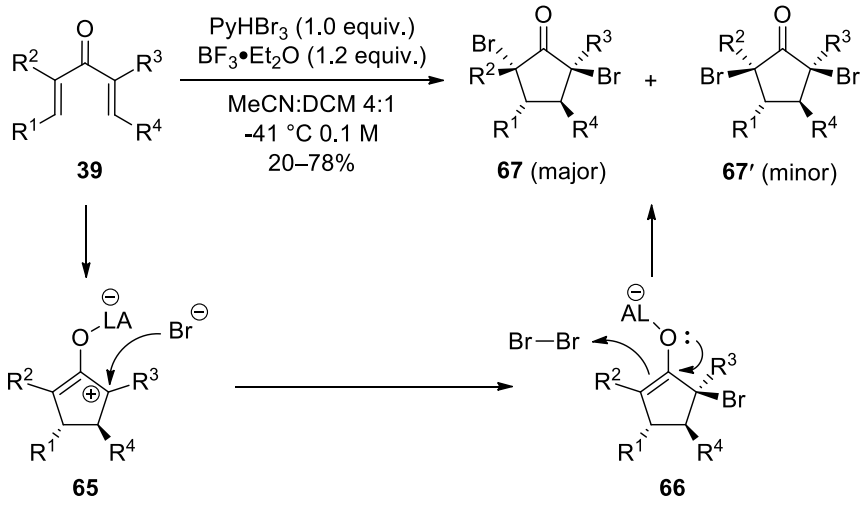

Scheme 1.22 Double bromination via Nazarov cyclization.

1.2.3.2.2 Photochemical Nazarov Cyclization

Nazarov cyclization can also be initiated by photochemical irradiation with photon source as an alternative to the thermal variant whose synthetic utility can be compromised by the use of strong Brønsted or Lewis acid. However, disrotatory ring closure in the former one sets substitutents in β-position in opposite *syn/anti* relationship tothatofthe thermal conditions (Figure 1.2).

The first example of intercepting oxyallyl cation took place during photo-induced Nazarov cyclization. The oxyallyl cation **69** formed from photochemical induction of 4-pyranone **68** can undergo bimolecular trapping with hydroxylic solvent such as MeOH to form **71** or [4+3] cycloaddition with furan to afford **72** (Scheme 1.23).[36] However, photochemical Nazarov methodology suffers from limited scope and necessity for the use of polar nonnucleophilic solvents such as trifluoroethanol.

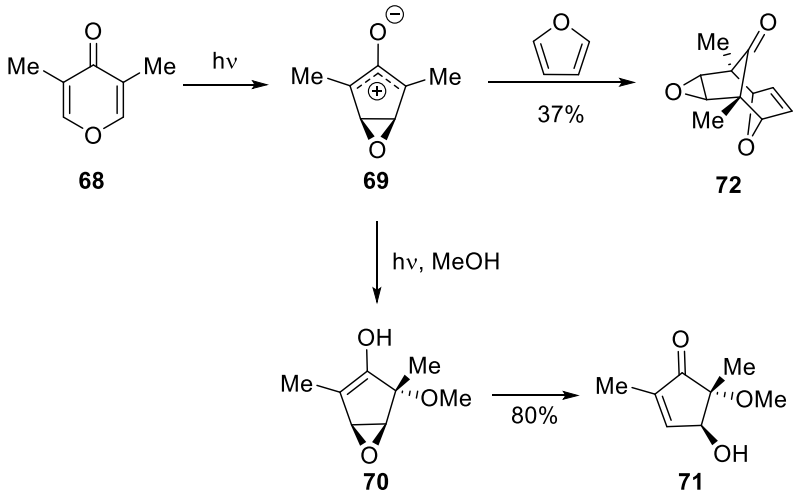

Scheme 1.23 Photochemical Nazarov cyclization of 4-pyranone.

Photochemical Nazarov cyclization was used by Gianni's group as one of the steps in their sequence towards the synthesis of 16-*epi*-terpendole**75**.[37] Intermediate **73** with prerequisite dienone subunit was irradiated at 350 nm to furnish cyclization product **74** in 80%. In four more steps **74** was successfully converted into target molecule 16-*epi*-terpendole **75** (Scheme 1.24).

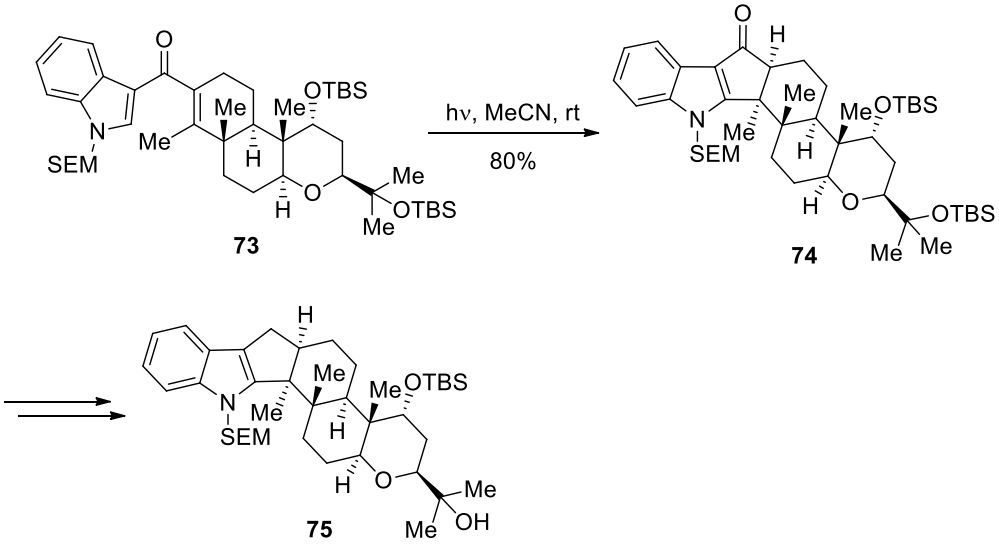

Scheme 1.24 Synthesis of 16-*epi*-terpendole.

UV-light induced Nazarov cyclization of aryl vinyl ketones bearing acid sensitive groups as well as cycloalkyl and unsaturated pyran moieties under neutral or basic conditions was reported by Gao group in 2014 (Scheme 1.25).[38] The authors applied this methodology to the formal synthesis of taiwaniaquinol B **80**. Starting with **78**, they produced advanced intermediate **79**, which has previously been converted to **80** in two steps (Scheme 1.26).[39]

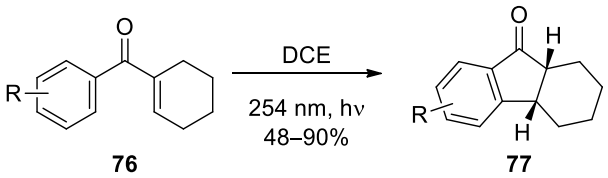

Scheme 1.25 Photochemical Nazarov cyclization of aryl vinyl ketones.

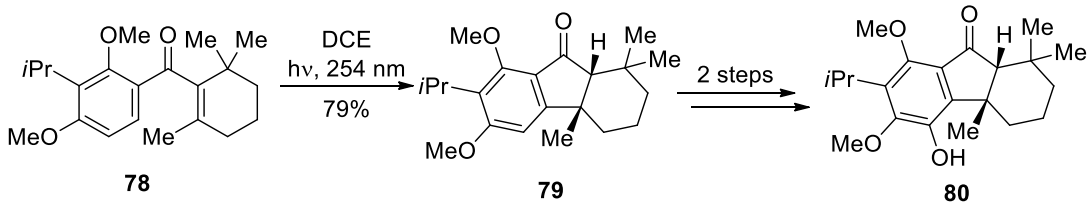

Scheme 1.26 Formal synthesis of taiwaniaquinol B.

1.3. 6π Electrocyclization

In its simplest manifestation, 6π electrocyclization can be viewed as the isomerization of (*E,E*)-1,3,5-hexatrienes **81** undergo thermal disrotatory or photochemical conrotatory ring closure to afford *cis*- **82** or *trans*-1,3-cyclohexadienes **82′** respectively (Scheme 1.27).[40]

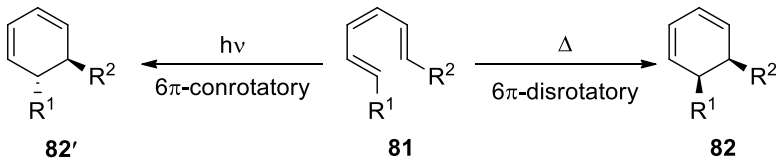

Scheme 1.27 Thermal and photochemical 6π electrocyclization.

Compared to other pericyclic reactions, 6π electrocyclizations find less utility in the synthesis of target molecules. Since its discovery in early 1960s,[41] the volume of scientific literature pertaining to 6π electrocyclizations did not expand significantly. This scarcity was attributed to the difficulty of preparing 1,3,5-hexatrienes with required alkene geometry. Another limiting factor is the high activation barrier of ring-closing process which necessitates use of higher temperatures for cyclization to happen at reasonable rates which in turn, undermines yields in poor functional group tolerance as well as higher number of possible side reactions.[42] However, introduction of substituents with different electronic nature around the conjugated 6π system or replacement of one of the carbon atoms with a more electronegative heteroatom can significantly lower the activation barrier and allow cyclization to proceed near or below room temperatures.[43] Relative stereochemistry of stereocenters generated upon cyclization of terminally substituted trienes can be predicted by Woodward-Hofmann rules.3[a]

Heptatrienyl cations **83** possessing the same number of π electrons can also cyclize either via 6π disrotatory ring closure to form cycloheptadienyl cations **84** or afford cyclopentenyl cations **85** through 4π conrotatory electrocyclization. However, according to the theoretical studies, for 6π-electron/7-atom systems ring closure towards cyclopentenyls is a favorable bond-forming event (Scheme 1.28).[12,44]

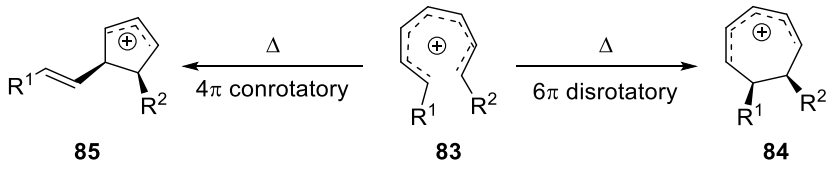

Scheme 1.28 Cyclization modes of heptatrienyl cation.

Examples of frequent occurrence of 6π electrocyclizations in nature are the biosynthesis of vitamin D and polyketides.[45] In the last decade, the volume of scientific literature pertaining use of 6π electrocyclization strategy for the construction of biologically active complex skeletons has increased significantly. Some representative

examples prepared via 6π electrocyclic ring closure (moieties highlighted in red) are illustrated in Figure 1.4.[46,47,48]

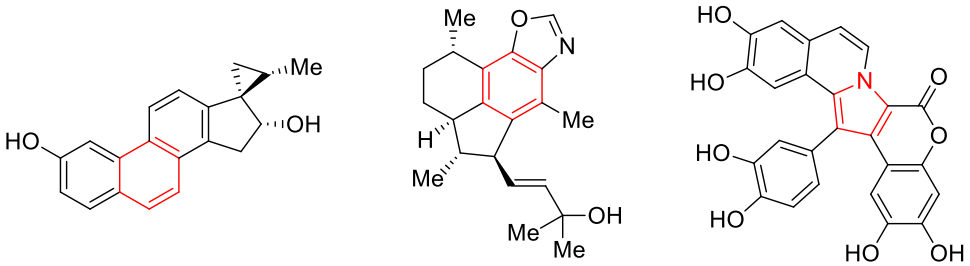

86
Ent(+)-cinanthrenol A

87
Ileabethoxazole

88
Lamellarin

Figure 1.4 Natural products made via 6π electrocyclization.

1.3.1. 6π Electrocyclizaton of 1,3,5-hexatrienes

Extensive experimental and computational studies of 1,3,5-hexatrienes have shown substituent effects on cyclization rates;[49] in particular, putting electron withdrawing or donating groups at C-2 position of the 1,3,5-hexatriene considerably lowers the activation barrier for the cyclization, sometimes even by 10 kcal/mol.[50]

In 2008, Trauner and co-workers reported 6π electrocyclization of hexatriene **89** and **91** bearing carbonyl substituents in the second position in the presence of stoichiometric amount of Me_2AlCl (Scheme 1.29a,b).[51] The experiments revealed reaction rate enhancement by 13 or 55 times compared to their thermal uncatalyzed variants. The reaction outcome was indicative of synergism of catalyst and the substituent effects as well as carbonyl groups being suitable functionalities in Lewis acid catalyzed 6π electrocyclization for broader spectrum of substrates.

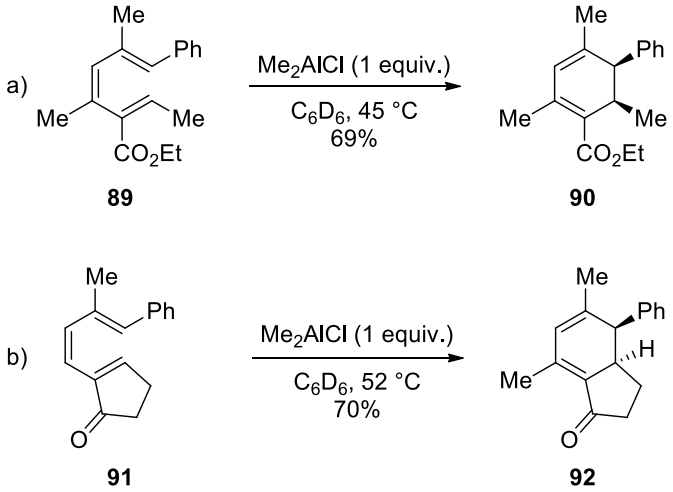

Scheme 1.29 Me_2AlCl catalized 6π electrocyclization of 2-substituted hexatriens.

Since setting the central double bond of 1,3,5-hexatriene in *cis*-configuration can be troublesome, incorporation of an auxiliary phenylsulfonyl group in the appropriate position of 6π-system can eliminate this stereochemical obstacle.[52] Heating 3-sulfonylated hexatrienes **93** at reflux in toluenecan afford *cis*-1,3-cyclohexadienes **94** in moderate yield. Inefficient mass recovery in some cases was attributed to decomposition pathways of both starting triene and cyclized product (Scheme 1.30).

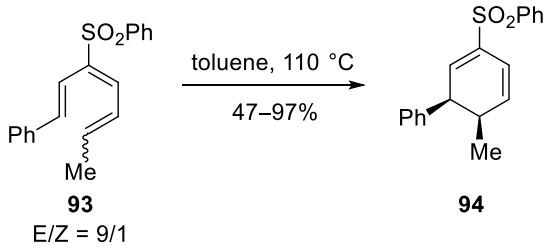

Scheme 1.30 Auxiliary mediated 6π electrocyclization.

Metal-stabilized conjugated enolates generated *in situ* by γ-deprotonation of the corresponding divinyl ketones belong to the family of 3-oxido-substituted 1,3,5-hexatrienes. Use of sterically demanding oxophilic organoaluminum Lewis acid **96** in the presence of Et_3N as a base can productively generate metal-stabilized dienolate **97** from the corresponding dienone **95** with the (*E*)-geometry at the middle C=C bond

required for 6π electrocyclization to happen successfully (Scheme 1.31).[53] The presence of electron withdrawing sulfone in the C-2 and electron donating enolate in the C-3 positions in hexatriene **97** is contributing to the lower activation barrier for the facile 6π electrocyclization to form cyclohexenone **98**.

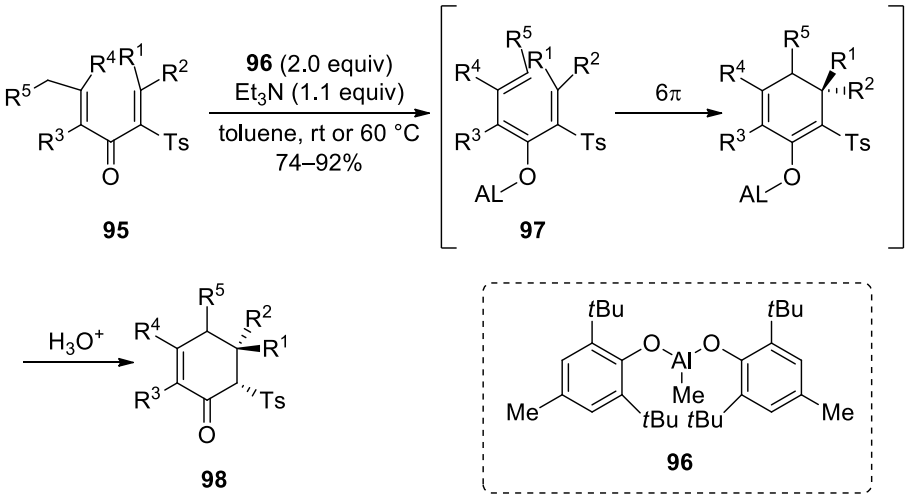

Scheme 1.31 Electrocyclization of in situ generated metal-stabilized enolates.

Torquoselective 6π electrocyclization can be achieved by installation of a remote stereocenter on the hexatriene. In 2010, the Hsung group reported the enantioselective synthesis of cyclohexadienes using 1,3,5-hexatrienes bearing remote chiral auxiliary.[54] Chiral 3-amido hexatriene **100,** generated via either thermal 1,3-hydrogen shift or protonation/deprotonation of the corresponding allenamide **99** was prone to 6π electrocyclic ring closure. However, instead of isolating amido-cyclohexadiene **101** as a direct product of cyclization, it isomerized into **102** via 1,5-hydrogen shift (Scheme 1.32).

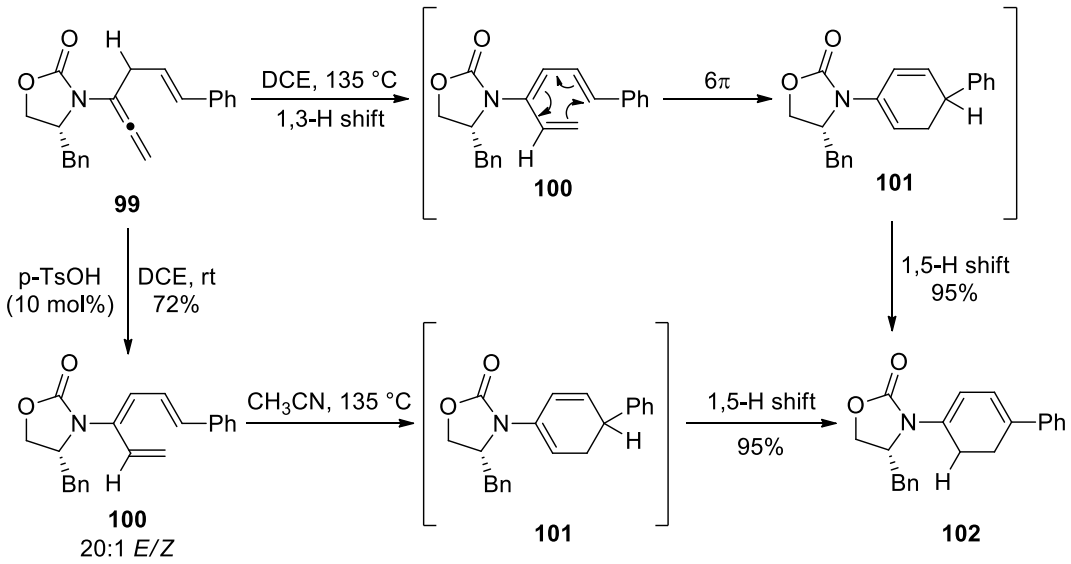

Scheme 1.32 Enantioselective 6π electrocyclization.

Involvement of photochemical 6π electrocyclization in the cascade reaction for the construction of fused polycyclic skeletons has been reported by Zhang and co-workers.[55] Precursor triene intermediates **105** formed upon UV light irradiation of 3-chloroisoquinolones **104** underwent 6π electrocyclization resulting in amides **106** which after subsequent autooxidation afforded the number of benzo[a]phenanthridein-5-one derivatives **107** (Scheme 1.33). Triene **105** itself ensued from the series of bond-cleavage/bond-forming events: C-Cl bond cleavage upon irradiation of **103** with UV light was followed by 5-exo-dig cyclization and subsequent chlorine trapping. Intermediate **104** was unstable under photolytic conditions and favored isomerization into triene **105**.

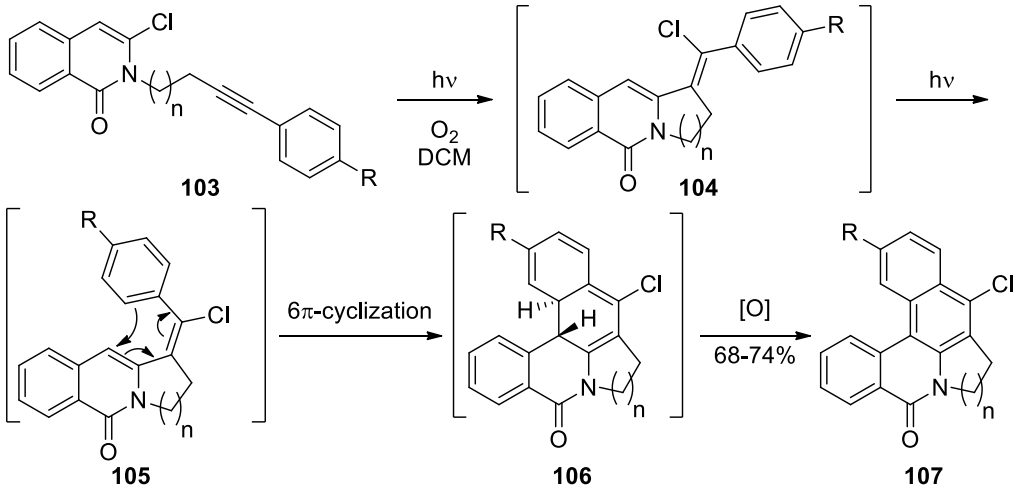

Scheme 1.33 Photo 6π electrocyclization in the cascade sequence.

As important building blocks in the synthesis of biologically active compounds, polycyclic aromatic hydrocarbons and the strategies for their preparation deserve much attention.[56] Catalytic method for the preparation of naphthalene derivatives from phenylene-bridged carbonyl compounds employing $Cu(OTf)_2$ as a catalyst was developed by the Narasaka group in 2012.[57] Experimental evidence revealed involvement of 6π electrocyclization of an intermediate hexatriene as a mechanistic step in this transformation. The tertiary carbocation **109** formed upon protonation of ketone **108** underwent deprotonation to give rise to hexatriene **110.** After 6π electrocyclization of **110,** dihydronaphthalene **111** rearomatized into naphthalene **112** via subsequent dehydration (Scheme 1.34). The authors postulated that $Cu(OTf)_2$ acted as a source of TfOH which is believed to be responsible for substrate activation.

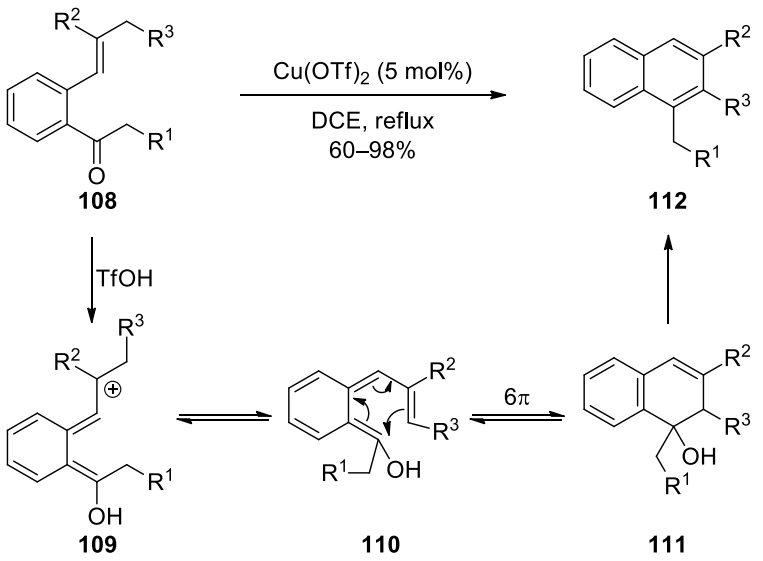

Scheme 1.34 Synthesis of polycylic aromatic hydrocarbons via 6π electrocyclization.

Recently, the Erker group developed the route towards preparation of phenylene-bridged phosphane/borane frustrated Lewis pairs (FLP).[58] Thermal 6π electrocyclizaiton of phosphorus/boron-substituted hexatrienes **113** upon heating at 80 °C neatly converted them into P/B-substituted cyclohexadiene derivatives **114** in very good yields (Scheme 1.35). Rearomatization of **114** by TEMPO oxidation afforded aromatic phenylene-bridged FLPs **115**. Thermal stability of **114** and **115** makes them desirable substrates for the development of new FLP methodologies.

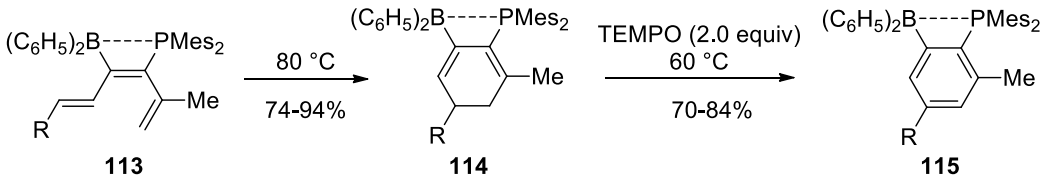

Scheme 1.35 6π Electrocyclization of frustrated Lewis pairs.

1.3.2 6π Electrocyclization of 6-Electron/7-Atom Systems

As already mentioned earlier, heptatrienyl cation **116** with 6π electrons delocalized over seven carbon atoms would preferentially cyclize via 4π conrotatory

electrocyclization. This is due to the higher energy state of the intermediate **116b** compared to its 5-atom counterpart **116a** which is associated with the difficulty of putting all the bonds in s-*cis*-configuration (Figure 1.5).[59,44] Therefore, the realization of a cationic 6π electrocyclization of conjugated systems with 6π electrons delocalized over 7 atoms is challenging.

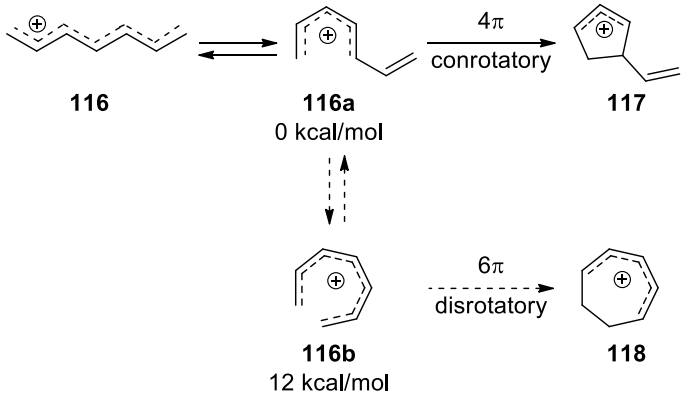

Figure 1.5 4π vs 6π electrocyclizaiton.

Based on the previously mentioned statement, the Nazarov cyclization is a well studied 4π conrotatory electrocyclziation to build 5-membered carbocycles. Except for traditional acid activated divinyl ketone variants, there are some advances in the area of "*vinylogous*"[60] and homo-Nazarov[61] cyclizations with modified substrates, however, they all deliver either 5- or 6-membered rings.

In 2016, Opatz and co-workers isolated unexpected 7-membered carbocycle in the photo-induced cascade process involving photoisomerization/condensation/cyclization sequence.[62] Azirine **120** was formed from isoxazole **119** by light-induced rearrangement, and this intermediate underwent cobalt-catalyzed condensation with acetylacetone to form 2,4-diacylpyrrole **121**. The unexpected 7-membered product **123** was formed via photochemical conrotatory 6π electrocyclizaiton of **121** followed by hydrogen shift (Scheme 1.36). Since no cyclization was observed with Lewis acid, the 6π electrocyclization step was strongly believed to require photochemical excitation to proceed. The authors believed that the thermal disrotatory electrocyclization would involve higher energy transition state due to unfavorably shaped π-system with a low

degree of conjugation. Additionally, in silico studies indeed indicated higher activation barrier for thermal conrotatory electrocyclization.

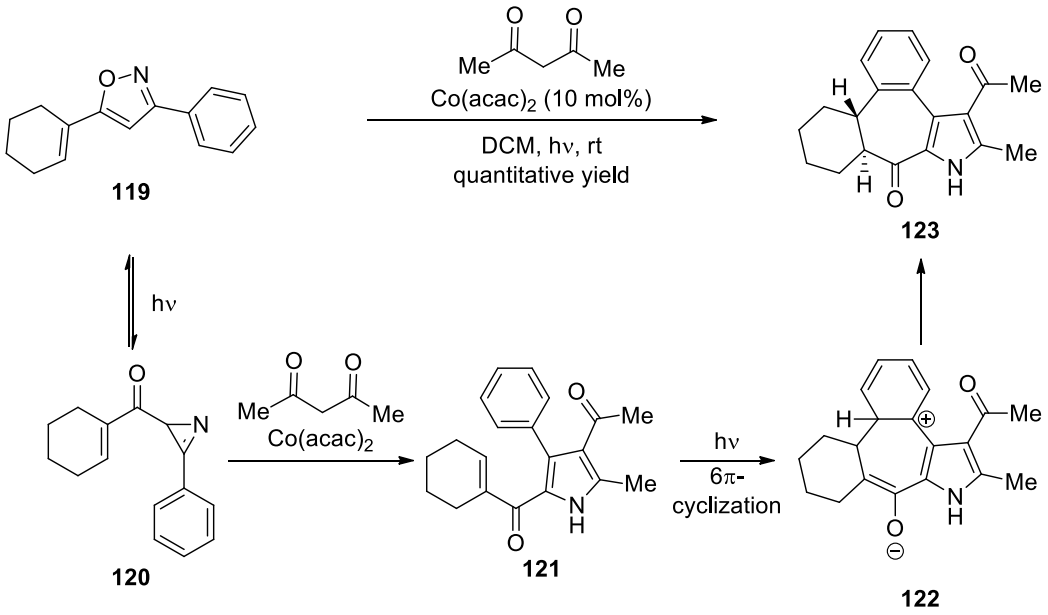

Scheme 1.36 Photoisomerization/condensation/cyclization cascade.

Recently, gold-catalyzed [4+3] annulation of 3-substituted 3-en-1-ynamides with isoxazolesto form 4*H*-azepines has been reported.[59] The annulation mechanism was postulated to involve unprecedented 6π electrocyclizaiton of 3-azaheptatrienyl system **128**. Attack of isoxazole **125** on gold-ynamide complex **124** after several bond rearrangements gave gold-stabilized intermediate **128**. Presence of substituents on **124** was crucial to achieve the required geometry in **128** for 6π electrocyclization to take place. Substituent R^1 being H favored conformation **128'** which underwent a 4π aza-Nazarov-type cyclizationwhile **128** was a predominant conformation when R^1 was a bulkier group, thus facilitating 6π electrocyclization. Loss of an acidic proton from 7-membered cation **130** afforded azepine **131** (Scheme 1.37).

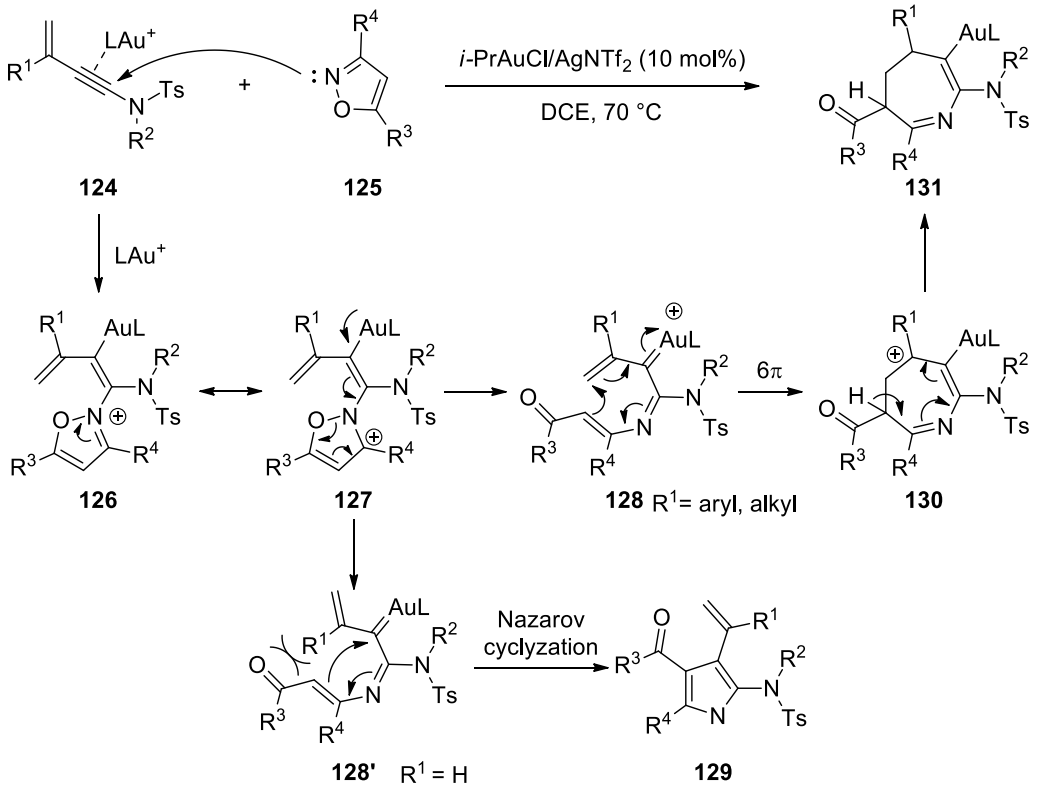

Scheme 1.37 6π Electrocyclization of 3-azaheptatrienyls.

1.4 Electrocyclizations in Natural Product Syntheses

Cyclobutanes found in nature are less probable to be formed via electrocyclization process because of their unfavorable thermodynamics caused by high torsionaland angle strain.1 However, the neoclerodane diterpene salvileucalin C is believed to be formed biosynthetically from its precursor salvileucalin D viaphotochemical 4π electrocyclization. The Ding group in 2014 employed this strategy in a biomimetic diastereoselective total synthesis of salvileucalin C to test the hypothesis.[63] Salvileucalin D **132** was prepared from commercially available starting materials in 11 steps involving Beckwith-Dowd ring expansion, a tandem diastereoselective Stille coupling/debromination/desilylation/lactonization reaction as a key transformation. UV induced 4π electrocyclization of **132** afforded salvileucalin C **133** in 84% yield (Scheme 1.38).

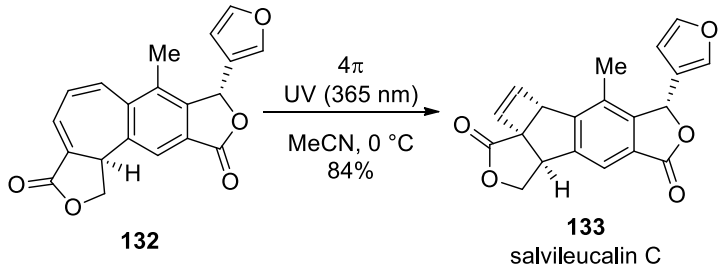

Scheme 1.38 4π Electrocyclization in the total synthesis of salvileucalin C.

In 2015, Smith's group showcased successful implementation of cationic 4π Nazarov electrocyclization reaction at the late stage of long 37-step sequence for the construction of congested polycyclic skeleton of (−)-calyciphylline N alkaloid **136**.[64] Nazarov precursor **134**, prepared via a multistep sequence, underwent one-pot Nazarov cyclization/proto-desilylation by treatment with HBF_4 Et_2O as an acid promoter for both steps to produce intermediate **135**. Formation of final product (−)-calyciphylline N **136** was achieved in extra ten steps (Scheme 1.39).

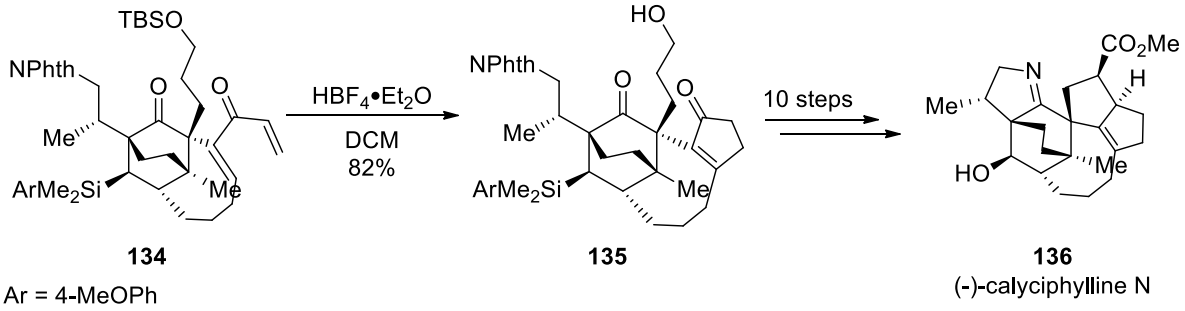

Scheme 1.39 Total synthesis of (−)-calyciphylline N.

A vivid example of the usefulness of 6π electrocyclization reactions in natural product synthesis can be seen in the total synthesis of the complex alkaloid daphenylline reports by the Li group in 2015.[65] The biggest synthetic challenge in this work was construction of the sterically congested tetrasubstituted arene ring, which could be overcome by 6π electrocyclization/aromatization sequence. Upon irradiation with a Hg-vapor lamp, trans-triene **137** underwent photoisomerization to afford desired *cis*-triene

isomer **138.** While the *cis*-triene **138** proved to be stubborn towards thermal electrocyclization using various Lewis acid promoters, it cleanly underwent conrotatory photochemical electrocyclization to form pentacyclic intermediate **139**. The authors suggested that disrotatory ring-closure was sterically more demanding than the conrotatory alternative. With **139** in hand, the target daphenylline **140** could be accessed via an additional 10-step sequence (Scheme 1.40).

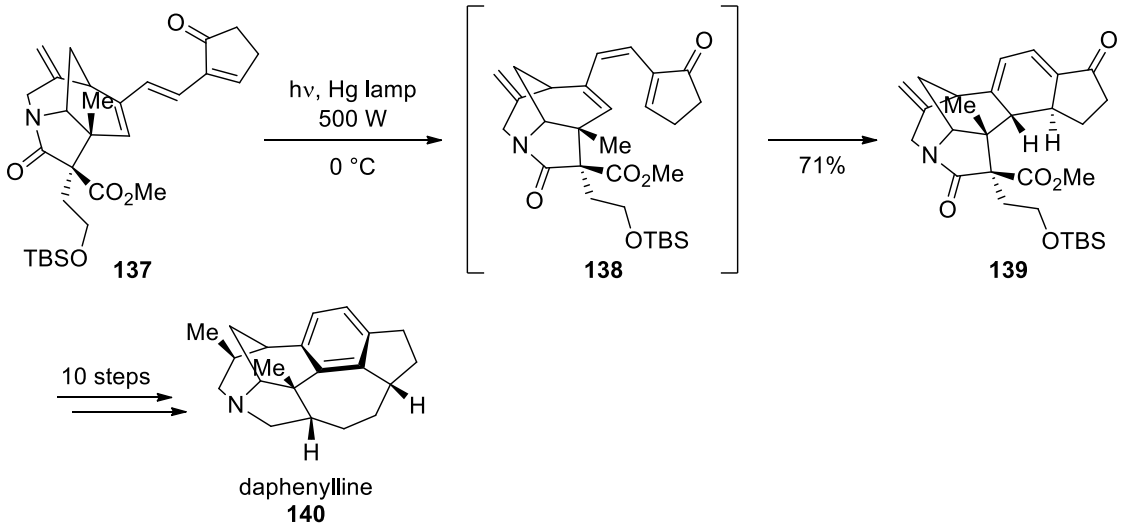

Scheme 1.40 Total synthesis of daphenylline.

1.5 Conclusion

Electrocyclizations belong to the important subclass of pericyclic reactions which have been widely used as a tool in the natural product synthesis for the construction of complex polycyclic scaffolds. Woodward-Hoffmann rules for the conservation of orbital symmetry makes realization of this strategy affordable in a stereocontrolled fashion.

Substrates with 4π electrons distributed over either four or five atoms, are used for the stereoselective synthesis of 4- and 5-membered ring systems. Depending on the mode of activation, the ring-closure can proceed in conrotatory (thermal) or disrotatory (photochemical) fashion. The conrotatory ring-closure of cross-conjugated dienones

well known as the Nazarov cyclization is a powerful method for the construction of cyclopentanoid scaffolds. There have been significant advances in this field in terms of developing substrate variety and the modes of interception of Nazarov intermediates. A concept of double interruption starts to emerge as a new tool for one-pot multifunctionalization of 5-membered carbocycles.

Synthesis of functionalized 6-membered cyclic fragments via 6π electrocyclization has garnered much attention in the last decades and new methodologies have been evolving to enrich this strategy. The ring closing process is characterized with the stereochemical outcome opposite to its 4π electron analogues. The vast majority of the literature pertaining 6π electrocyclizations deals with 6π-electron/6-atom systems, while only few occurrences have been reported about 6π-electron/7-atom ring closing occasions.

In chapter 2, a novel approach of double interruption of the Nazarov reaction will be described. Organoaluminum activation of divinyl ketones with subsequent trapping of the oxyallyl cation via methyl migration from tetracoordinate aluminum generated the aluminum enolate susceptible for the second trapping event in the process of Simmons-Smith cyclopropanation. The bicyclic alcohol generated via the cascade of process could further be rearranged into its 5- or 6-membered equivalents.

In Chapter 3, our attempts to generate 7-membered carbocycles via Lewis acid activation of modified-Nazarov substrates will be disclosed. The modification involved extension of conjugation of divinyl ketones and conversion into *o*-styrenyl chalcones. However, instead of intended 7-membered rings some unexpected course of reaction delivered formal [2+2] cycloadducts the details of which will be covered in Chapter 3.

Chapter 4 describes a medicinal chemistry project carried out earlier that is unrelated to the work detailed in Chapters 2 and 3. In it, I will discuss efforts to develop new calcium sensitizing agents for potential use in the treatment of heart failure.

Chapter 2

Organoaluminum-Mediated Double Interrupted Nazarov Cyclization: Nucleophilic Alkylation Followed by Simmons-Smith Type Cyclopropanation[66]

2.1 Introduction

Attention towards Nazarov cyclization as a convenient and easy method for accessing cyclopentanoid scaffolds from readily available 1,4-dien-3-ones has revived in recent years.[25,67,68] Particularly interesting areas of research in this field involve catalytic asymmetric versions of theNazarov reaction[69,70] along with development of alternativeprecursors,[71] and domino/cascade transformations.[72]

The new concept of "double interception" of reactive oxyallyl cations successively withnucleophiles and then with electrophiles in one pot is emerging as apowerful tool for double functionalization of cyclopentane frameworks at both α positions of the cyclopentanone carbonyl group. The electrophilic oxyallyl cation **2** formed upon acid activation of divinyl ketone **1** can be trapped in synthetically useful transformations by a variety of nucleophiles; the product arising from this trapping is enolate **3** which could be incorporated in additional bond-forming reactions to afford densely substituted complex cyclopentanoid scaffolds **4** with the potential for further functional manipulations (see Chapter 1 for Double Interrupted Nazarov Cyclization).

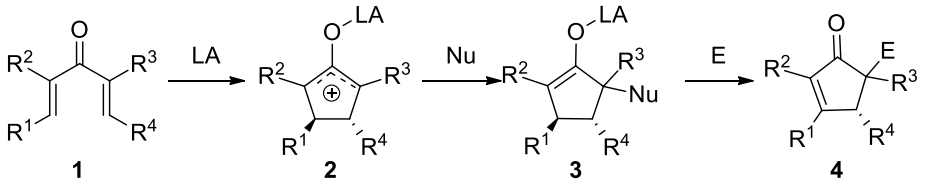

Scheme 2.1 Double interrupted Nazarov reaction.

2.2 Organoaluminum Reagents as Both Lewis Acids and Nucleophiles

The strong Lewis acidic nature of organoaluminum reagents results from the absence of a full electronic octet on trivalent aluminum, and is mediated through the vacant p orbital on the sp^2-hybridized aluminum center. Coordination of the aluminum atom to Lewis basic moieties such as carbonyls, imines, epoxides, etc., satisfies the electronic deficiency at that center, while simultaneously activating these functional groups as strong electrophiles. However, Lewis acidity is not their only feature. Upon complexation with Lewis basic heteroatoms, aliphatic or aromatic substituents on tetracoordinate aluminum can migrate to the activated substrate via 1,2- or 1,4-nucleophilic addition.[73]

The high dissociation energy of Al–O bonds (ca. 580 kJ/mol) explains the high oxophilicity of organoaluminum reagents which can productively be used in the activation of oxygen containing substrates. The first use of trialkylaluminum reagent for the activation and subsequent alkylation of epoxides was reported in 1970 by Lundeen et al. The reaction of excess triethylaluminum with *cis*-2,3-epoxybutane **5** at 80 °C productively formed *cis*-3-methyl-2-pentanol **6** (Scheme 2.2a). In case of nonsymmetrical substrates such as propylene oxide **7**, ring opening proceeded with predominant alkylation on the more substituted carbon center (Scheme 2.2b).[74] Since then, the use of organoaluminum in epoxide ring opening has been studied extensively.

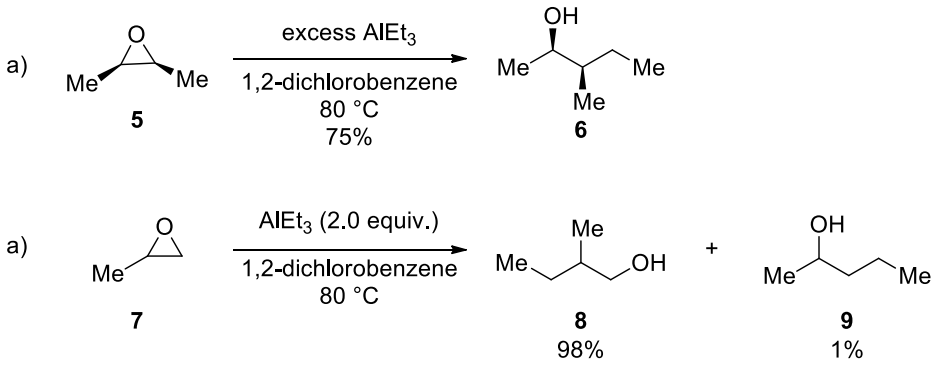

Scheme 2.2 Organoaluminum in epoxide ring opening.

With the same success, organoaluminum reagents can activate carbonyl groups. It has been known that migration of substituents on the aluminum center can proceed either via 1,2-or 1,4-addition. As described in an early report by Yu (1971), 4-*t*-butyl-cyclohexanone **10** activated by $AlMe_3$ in benzene underwent intramolecular methylation by methyl migration from the aluminum center to afford alcohol **12** (Scheme 2.3).[75] The use of 2 equivalents or higher excess of $AlMe_3$ favored formation of *trans* isomer **12**, which the authors, based on previous kinetic studies, attributed to 6-center transition state **11** involving two atoms of $AlMe_3$ and one molecule of ketone.[76]

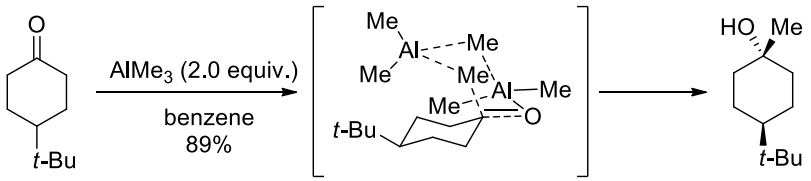

10 **11** **12**

Scheme 2.3 Activation of carbonyl group with $AlMe_3$.

In the recent years, there has been a substantial amount of work devoted to the development of new methodologies for the conjugate addition through the medium of organoaluminum as an alternative to organozinc and Grignard reagents. Due to their stronger Lewis acidity, challenging 1,4-conjugate additions to sterically hindered enones, which are inert to organozinc- or Grignard-based protocols, could be achieved via a Cu-catalyzed organoaluminum process.

The most successful trend of using trialkylaluminum reagents in asymmetric 1,4-additions started with the work of Iwata and Woodward. In 1996, Iwata's group reported the first Cu-catalyzed asymmetric 1,4-addition of a trialkyluminum reagent to enone **13** in the presence of 2-aryloxazoline **14** as a catalytic chiral ligand and *tert*-butyldimethylsilyl triflate as an additive (Scheme 2.4).[77] The role of oxazoline was described as crucial since it was able to coordinate to copper. The chiral induction of the conjugate addition was attributed to the chirality of C4-alkyl substituent in oxazoline ring. Use of additive was important in achieving high ee values.

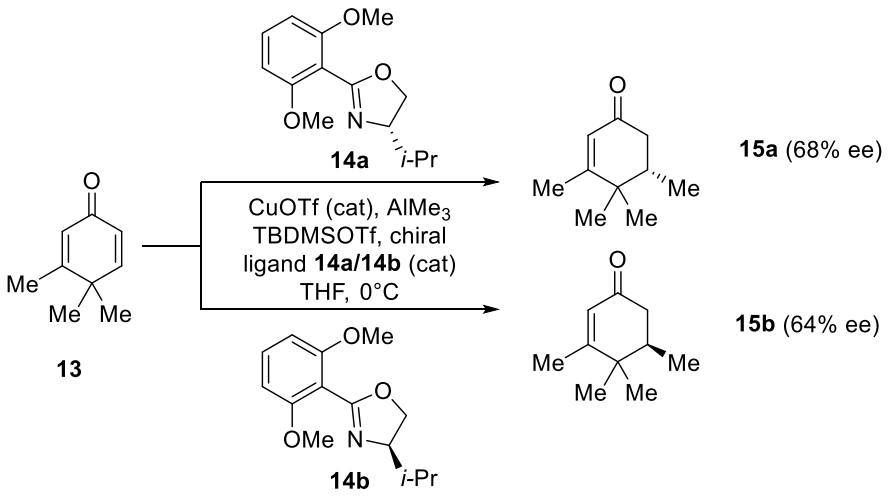

Scheme 2.4 Asymmetric Cu-catalyzed conjugate addition.

In the last decade, an immense number of chiral ligands have been applied to this process and phosphoroamidites **16**, diaryl N-phosphines **17**, and chiral N-heterocyclic carbenes **18** have been shown be the best in achieving highest enantioselectivities (Figure 2.1).[73]

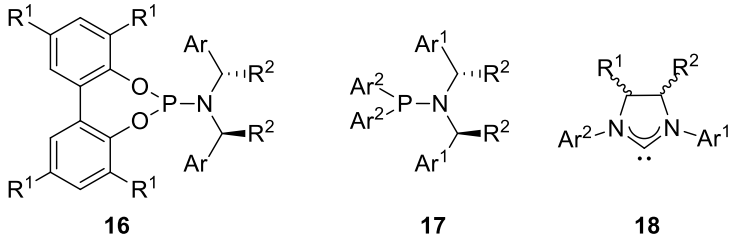

Figure 2.1 Ligands for achieving best enantioselectivity.

Trialkylaluminum reagents are competent Lewis acids for the activation of divinyl ketones in Nazarov cyclizations. Chapter 1 provides a detailed discussion of their application in this direction.

Trialkyl- or halodialkylaluminum reagents can also be employed as one of the ingredients for the formation of aluminum-based carbenoids in Simmons-Smith cyclopropanation. The upcoming subchapter 2.3 will disclose developments in this field in more details.[73]

2.3 Simmons-Smith Cyclopropanation

In late 1950s, almost 30 years after Emschwiller prepared $IZnCH_2I$,[78] Simmons and Smith discovered that the reagent formed upon mixing diiodomethane with zinc/copper couple could affect the cyclopropanation of olefins.[79] Treatment of cyclohexene **19** with CH_2I_2 and activated zinc afforded pure bicyclo[4.1.0]heptane (norcarane) **20** in 48% yield. The carbene source iodomethylzinc iodide $IZnCH_2I$ was generated via insertion of zinc into CH_2I_2 (Scheme 2.5).

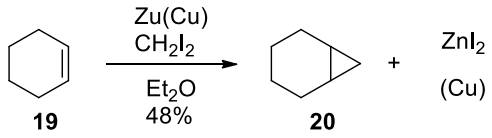

Scheme 2.5 Simmons-Smith cyclopropanation of cyclohexene.

Based on experimental evidence, it has been postulated that cyclopropanation proceeds via "butterfly type" transition state (Figure 2.2).[79b] The postulate is in agreement with theoretical studies that determined the butterfly transition state to be the energy minimum.[80]

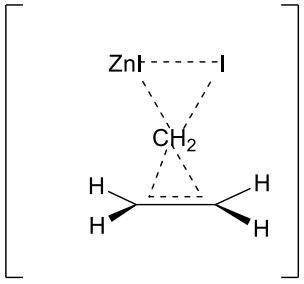

Figure 2.2 Butterfly type transition state.

Generation of zinc carbenoids using zinc-copper couple is a tedious process. Furthermore, variations in surface features on the heterogeneous alloy can affect the reproducibility of the reaction. For these reasons, newer protocols were developed for the Simmons-Smith cyclopropanation. In 1959, Wittig and Schwarzbach reported a new method of preparing zinc carbenoids **A** via exposure of diazomethane to zinc iodide to

form $IZnCH_2I$ (Figure 2.3).[81] Later, Furukawa developed new type of zinc carbenoids by treating CH_2I_2 with Et_2Zn to generate $EtZnCH_2I$ **B** (Figure 2.3).[82] Furukawa's carbenoids show high degree of reactivity with electron rich alkenes, while being less effective with unfunctionalized ones. Superior cyclopropanation can be achieved by carbenoids **C** (Figure 2.3) generated from Et_2Zn and $ClCH_2I$ as reported by Denmark in 1991.[83]

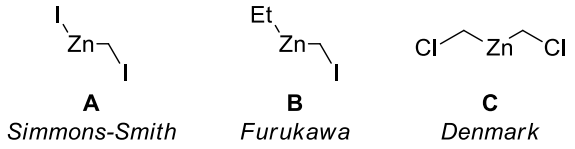

Figure 2.3 Modifications of zinc carbenoids.

Nowadays, the Simmons-Smith reaction is the most widely used approach to introduce a cyclopropane unit into complex molecular frameworks, mainly owing to its stereospecificity with respect to double bond geometry and tolerance of wide range of functional groups.[84] Electron rich alkenes undergo more facile cyclopropanation than their electron poor counterparts due to the electrophilicity of metal carbenoid species. Usually, the reaction is governed by steric effects and takes place on the less hindered face. However, use of allylic alcohols is more advantageous in terms of reaction rates and stereocontrol. Presence of proximal hydroxyl group can direct cyclopropanation so that the directing group and cyclopropane unit would end up on the same face of the double bond. For example, cyclopropanation of allylic alcohol **21** provided *syn*-addition product **22** as a single stereoisomer of the process (Scheme 2.6).[85]

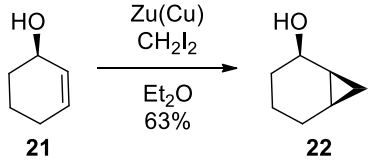

Scheme 2.6 Hydroxyl-directed Simmons-Smith cyclopropanation.

Many other auxiliary-based approaches have been developed over time for stereospecific Simmons-Smith cyclopropanation to synthesize enantiomerically pure

cyclopropyl derivatives, however most of them rely on the directing effect of allylic or homoallylic oxygenfunctional groups. Highly diastereoselective cyclopropanation of a range of tertiary aminesusing Simmons–Smithreagent was reported by the Aggarwal group in 2003 (Scheme 2.7).[86] This directing effect is caused by coordination of heteroatoms to organozinc reagent.

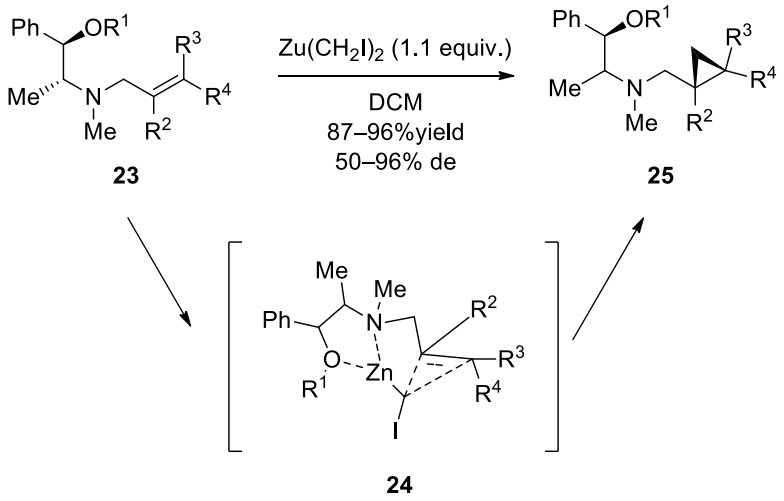

Scheme 2.7 Diastereoselective cyclopropanation of amino alcohols.

Use of a chiral catalyst can also assist in enantiocontrol of Simmons-Smiths cyclopropanation. In 2005, Charette and co-workers developed new family of chiral iodomethylzinc phosphate reagents **27** for the cyclopropanation of protected alcohols **26** (Scheme 2.8). Although typically used in stoichiometric amounts, the chiral phosphoric acid ligand could be employed in substoichiometric amounts in cases employing more complex ligands whose availability was limited.[87]

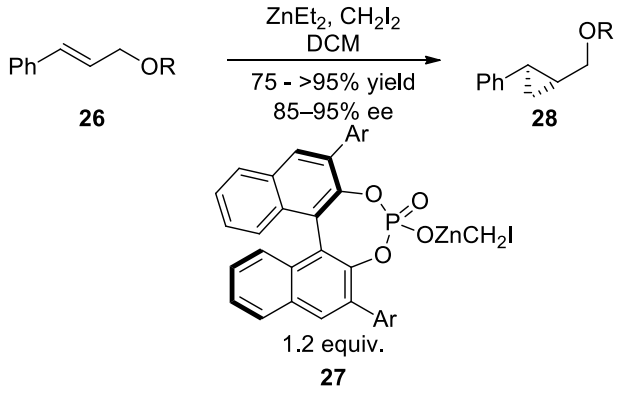

Scheme 2.8 Asymmetric cyclopropanation in the presence of chiral phosphoric acid.

In carbenoids of type MCH_2X, Zn, Sm and Al are the most commonly encountered metals.[84] For the generation of aluminum carbenoids, the most commonly employed trialkyl aluminum reagents are *i*-Bu_3Al and Et_3Al.

Compared to zinc analogues, samarium carbenoids exhibit superior chemoselective cyclopropanating properties of allylic alcohols in the presence of other alkenes; this could be demonstrated in chemoselective cyclopropanation of polyunsaturated allylic alcohol geraniol **29,** in which the remote alkene stayed intact while only the proximal alkene of the allylic alcohol underwent transformation (Scheme 2.9). High chemoselectivity is the result of the directing effect of Sm metal center which in turn is dictated by its high oxophilicity (E_{Sm-O} = 619 kJ/mol).[88]

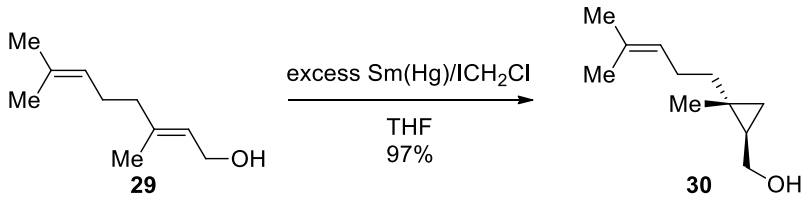

Scheme 2.9 Chemoselective cyclopropanation of geraniol with samarium carbenoid.

2.3.1 Aluminum Carbenoids in Cyclopropanation

In 1963 Collette's report about reaction of *i*Bu_3Al with CCl_4, involvement of an aluminum carbenoid was proposed to explain formation of *i*-Bu_2AlCl.[89] However, no

carbene trapping experiments were performed by Collette. In 1964, Miller experimentally confirmed carbene formation by its trapping in cyclopropanation of cyclohexene **19** when treating it with 1.5 equivalents of Et_3Al and 1 equivalent of CH_2I_2 to form norcarane **20** in 20% yield (Scheme 2.10).[90] This was the first example of cyclopropanation with aluminum carbenoid.

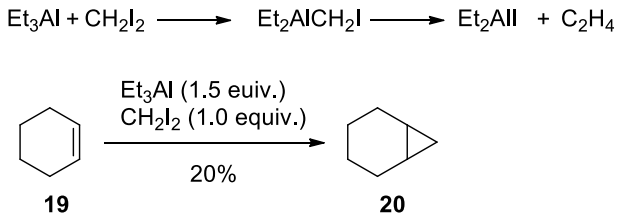

Scheme 2.10 First report of cyclopropanation using organoaluminum reagent.

However, Miller's protocol suffered from low yields. In 1985, Yamamoto and co-workers successfully cyclopropanated range of cyclic and acyclic olefins **32** using equimolar amount of trialkylaluminum reagent and CH_2I_2 as the source of aluminum carbenoid.[91] The use of excess amount of trialkylaluminum was causing decomposition of dialkyliodomethyl aluminum intermediate. The yields for all the substrates were satisfactory with the use of Me_3Al, Et_3Al or *i*-Bu_3Al reagents (Scheme 2.11).

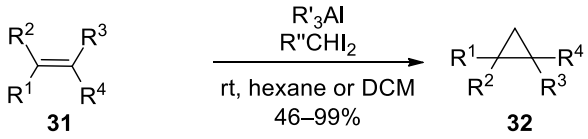

Scheme 2.11 Yamamoto's conditions for cyclopropanation with organoaluminum reagent.

In the same publication, the authors performed chemoselective cyclopropanation of geraniol **29**. Variation of metal centers in carbenoid species may affect chemoselectivity of cyclopropanation. Carbenoids generated on the basis of organoaluminum reagent showed the opposite selectivity from that observed with

samarium carbenoids in Scheme 2.9. On the example of the same alcohol **29**, cyclopropanation with organoaluminum reagent in the presence of CH_2I_2 took place on the unfunctionalized olefin, leaving allylic alcohol moiety untouched (Scheme 2.12) However, cyclopropanation of the terminal double bond was achievable only in the presence of allylic alcohols.[88]

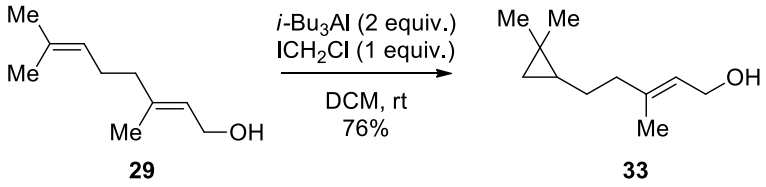

Scheme 2.12 Chemoselective cyclopropanation of geraniol with aluminum carbenoid.

2.4 Results and Discussion

In 1985 Yamamoto's report, one of the substrates successfully cyclopropanated with the aluminum-based carbenoid was a silyl enol ether which also was a suitable precursor for the optimized reaction conditions (Scheme 2.13).

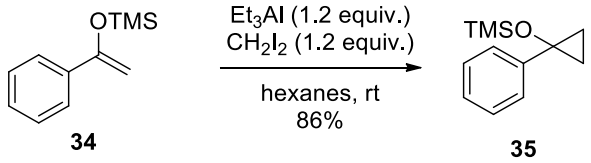

Scheme 2.13 Cyclopropanation of the silyl enol ether.

In 2013, the West group reported the use of triorganoaluminum reagents in Nazarov cyclization as Lewis acids to activate precursor divinyl ketones **1** where tetravalent trialkylaluminate could function as an internal source of alkyl group to accomplish nucleophilic trapping of reactive oxyallyl cation **36.**[92] We wondered whether the aluminum enolate **37** resulting from the nucleophilic trapping could participate in a subsequent aluminum-mediated Simmons-Smith cyclopropanation. Based on precedents of employing organoaluminum reagents in both Nazarov

cyclization and Simmons-Smith cyclopropanation, our former group member Yonghoon Kwon reasoned to implement this idea in the possible multistep domino sequence involving successive electrocyclization, methyl transfer, and cyclopropanation to afford bicyclo[3.1.0]hexanol scaffolds **39** (Scheme 2.14). The test of hypothesis by Kwon gave the positive result, however, even after some preliminary optimization the reaction was too sluggish (8 days).

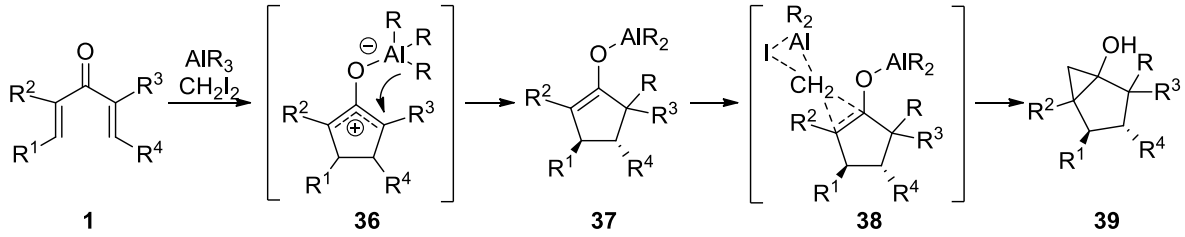

Scheme 2.14 The proposed idea of *in situ* cyclopropanation of Nazarov intermediates.

I tried to further improve the reaction outcome and investigate the substrate scope by subjecting dienone **1a** to $AlMe_3$ in the presence of excess CH_2I_2. Two products ensued from this reaction: the desired bicyclohexanol **40a** and minor amounts of truncated product **41a** resulting from methyl transfer with no subsequent cyclopropanation. Via examination of reaction parameters such as solvent, concentration, stoichiometry, and time the optimal reaction conditions were found to be 3 equiv. each of $AlMe_3$ and CH_2I_2 at -41 °C with no added solvent beyond that coming from the standard solution of the organoaluminum reagent, followed by warming to room temperature and stirring for 4 days. Quenching at -41 °C was crucial to avoid decomposition of the intermediatecyclopropanol **40a** (Scheme 2.15).

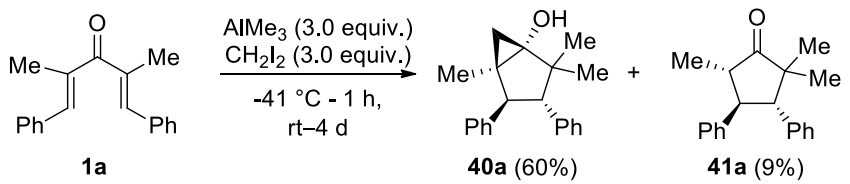

Scheme 2.15 Tandem Nazarov cyclization – Simmons-Smith cyclopropanation.

After establishing optimal conditions, we turned our attention to the generality of this methodology by exploring a series of differently substituted dienones. In the process of investigation, the bicyclic alcohols **40** were revealed to be labile towards aerobic decomposition pathways, which hindered our ability to fully purify and characterize these products and which affected chemical yields. We reasoned that acetylation of the hydroxyl groups of the crude cyclopropanol products *in situ* and then isolation and characterization of the resulting acetates **42** would be the rational solution to the problem (Table 2.1).

Table 2.1 Synthesis of bicyclic alcohols under optimized conditions.[a]

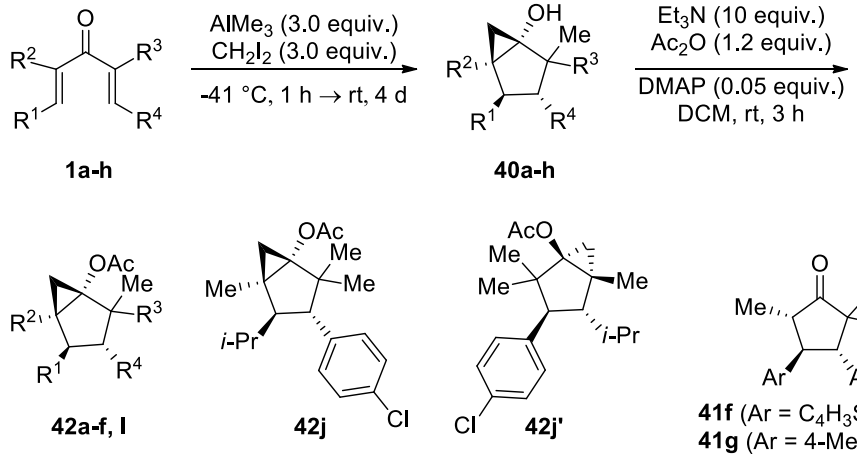

Entry	Substrate	R^1	R^4	R^2	R^3	Product (s)	Yield (%)[b]
1	**1a**	Ph/Ph		Me/Me		**42a**	66
2	**1b**	4-ClC_6H_4/4-ClC_6H_4		Me/Me		**42b**	81
3	**1c**	4-MeC_6H_4/4-MeC_6H_4		Me/Me		**42c**	55
4	**1d**	4-BrC_6H_4/4-BrC_6H_4		Me/Me		**42d**	50
5	**1e**	2-ClC_6H_4/2-ClC_6H_4		Me/Me		**42e**	44
6	**1f**	2-thienyl/2-thienyl		Me/Me		**42f/416f**	14/44[c]
7	**1g**	4-$MeOC_6H_4$/4-$MeOC_6H_4$		Me/Me		**41g**	76
8	**1h**	Me/Me		Me/Me		**--**	--[d]
9	**1i**	i-Pr/ i-Pr		Me/Me		**--**	--[d]
10	**1j**	4-ClC_6H_4	i-Pr	Me/Me		**42j/42j′**	74[e]
11	**1k**	Ph	H	Me/Me		**--**	--[f]
12	**1l**	Ph/Ph		n-Pr	Me	**42l**	42[g]

[a] Standard procedure: CH_2I_2 (3 equiv.) was added to **1** (0.5 mmol) and cooled to -41 °C. To the cooled reaction mixture $AlMe_3$ (2M in hexanes, 0.75 mL) was added and the reaction was stirred at -41 °C for 1 h, then at rt for 4 d. After aqueous work-up, crude product was dissolved in CH_2Cl_2 (5 mL) with Et_3N (10 equiv.) and cooled to 0 °C. DMAP (0.05 equiv.) and Ac_2O were added and the reaction was stirred for 3h while being allowed to warm to rt. [b] Yields are based on isolated acetylated product after chromatography. [c] 6 equiv. of $AlMe_3$ was used in this case. [d] Complex mixtures from which no discernible amounts of bicyclic acetates **42h** or **42i** could be isolated

were formed. [e] Formed as an inseparable mixture of two regioisomers (**42j:42j'**) in a 2.5:1; ratio determined via 1H NMR integration of benzylic proton). [f] Although desired product **42k** was detected in the crude product, it could not be purified to homogeneity. [g] Evidence for a minor amount of a regioisomeric product was seen by TLC and crude NMR analysis, but it was not possible to cleanly isolate and characterize this product.

First, we started examining symmetrical β,β′-aryl-substituted1,4-dien-3-ones for the substrate scope of this methodology (entries 1-6). Methyl migration after the cyclization step on the model substrate **1a**, was followed by cyclopropanation of the interrupted Nazarov intermediate with complete facial selectivity, acetylation of which afforded **42a** in good overall yield of 66% after two steps (entry 1). According to the key HMBC and NOE correlations of **40a**, cyclopropanation had occurred *syn* to the neighboring phenyl group (Figure 2.4). The X-ray crystallographic analysis of acetate **42a**[93] served as a confirmation of the originally performed assignment (Figure 2.5).

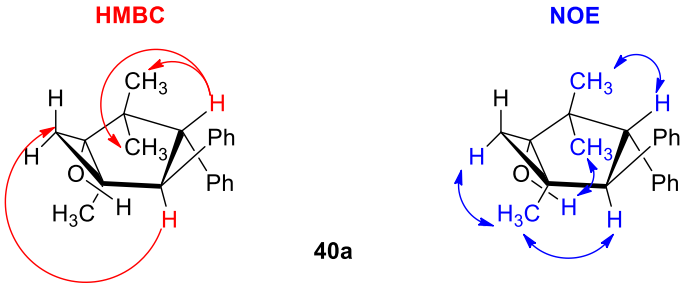

Figure 2.4 Key HMBC and NOE correlations of **40a**.

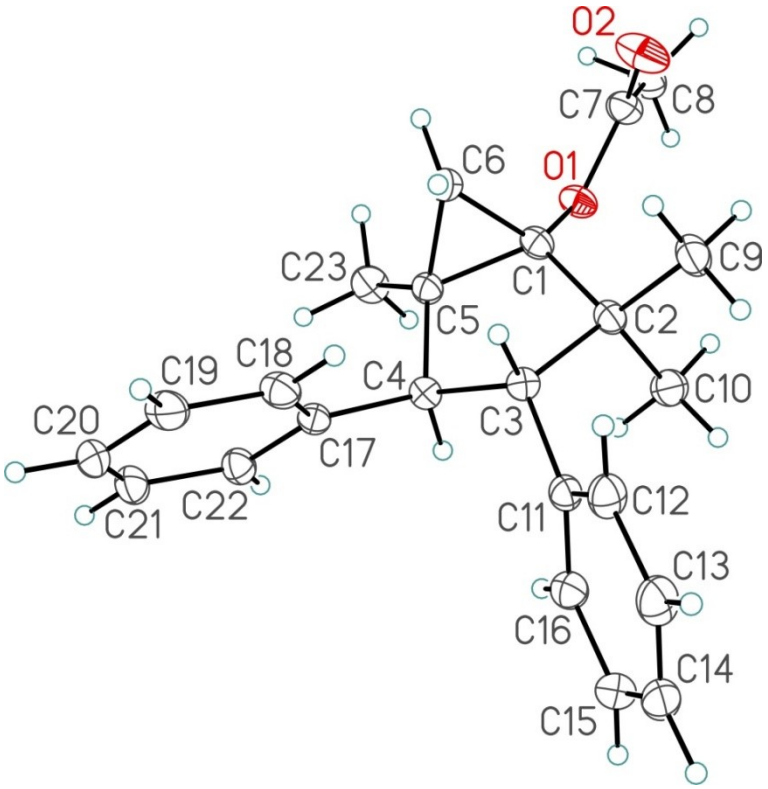

Figure 2.5 X-Ray crystal structure of bicyclic alcohol **42a.**

Substrate **1b** having 4-Cl-phenyl substituents at C-1 and C-5positions underwent desired double interrupted Nazarovcyclization/acetylation process to afford acetate **42b** as the major productin a yield of 81% (entry 2). Similarly, divinyl ketones **1c–e** with modified substituents at R^1/R^4 positions were converted to **42c–e** in moderate to good yields (entries 3–5). The substrate **1f** containing 2-thienyl groups at the dienone termini (entry 6), afforded the desired product **42f** in only 14% yield along with significant amount of methyl trapping product **41f,** while, substrate **1g** bearing 4-methoxyphenylsubstituents gave only the methyl trapping product **41g**, although in good yield (entry 7). These two examples indicate that substrates with electron releasing aryl substituents are not compatible with the Simmons-Smith conditions, although the initial methyl-transfer step was not affected.

Dienones with alkyl groups in both β-positions with furnished complex mixtures with no indications on desired acetates (entries 8 and 9). We also examined three unsymmetrical substrates (entries 10–12). Compound **1j**, with *i*-Pr group at C-5 position underwent the desired domino process in good overall yield. However, as the result of

methyl migration to both C-2 and C-4, with a preference for attack adjacent to the aryl substituent, regioisomeric acetylated cyclopropanols **42j** and **24j'** were obtained in a 2.5:1 ratio. Preferential formation of **42j** may be the result of methyl group migration from $AlMe_3$ to the sterically more accessible terminus of the oxyallyl cation, with consequent cyclopropanation of the more hindered aluminum enolate. Trisubstituted dienone **1k** lacking substitution at one terminus gave only traces of the desired product. From this outcome it could be deduced that incorporation of alkyl substituent in one of the β-termini can be tolerated as long the other terminus bears an aryl group. Finally, replacement of one of the C-2/C-4 methyl groups with *n*-Pr (entry 12) led to the predominant formation of **42l** in moderate yield, resulting from methyl transfer to the methylated C-4 position followed by cyclopropanation of the propyl-substituted enolate. The presence of minor amounts of the regioisomer analogous to **42j′** was evident; however it was impossible to isolate and characterize this component.

As already mentioned above, unprotected cyclopropanol **40a** was noticed to be labile. Storage under aerobic conditions caused this compound to autooxidize to furnish a 1:1 mixture of peroxides **43a**[94] and **43a'**. The cyclohexanone products formed upon oxidative cleavage of the ring-fusing cyclopropane bond are not accessible through Nazarov electrocyclization chemistry.[95] The Nazarov electrocyclization furnishes only 5-membered products, so a route to form cyclohexanones would expand the versatility of the interrupted Nazarov reaction. Therefore, we set out to examine and optimize this autooxidation reaction. To speed up the oxidation process we carried out the reaction in solution under an atmosphere of oxygen, which allowed us the convenient formation of **43a** and **43a′**in 59% yield overall. X-ray crystallography was a useful tool in analyzing relative configuration of **43a** to confirm the structure (Figure 2.6). We obtained diasteromeric β-hydroxycyclohexanones **44a** and **44a′** in excellent yields when reduced peroxides **43a** and **43a′** with triphenylphosphine (Scheme 2.16).[96]

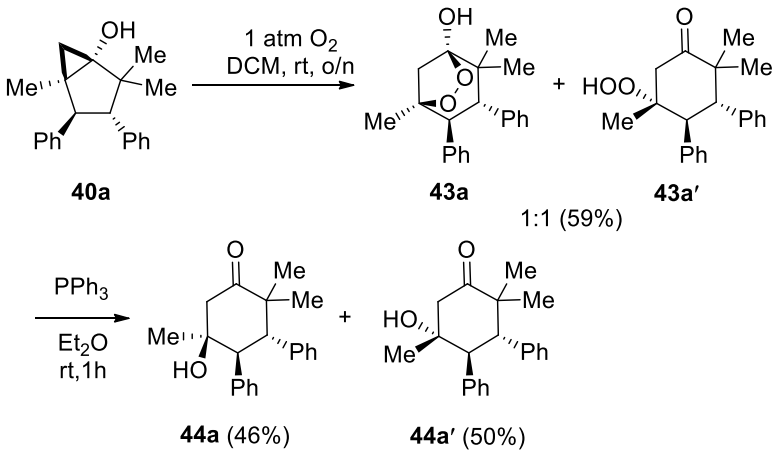

Scheme 2.16 Autooxidation of alcohol **40a** followed by reduction.

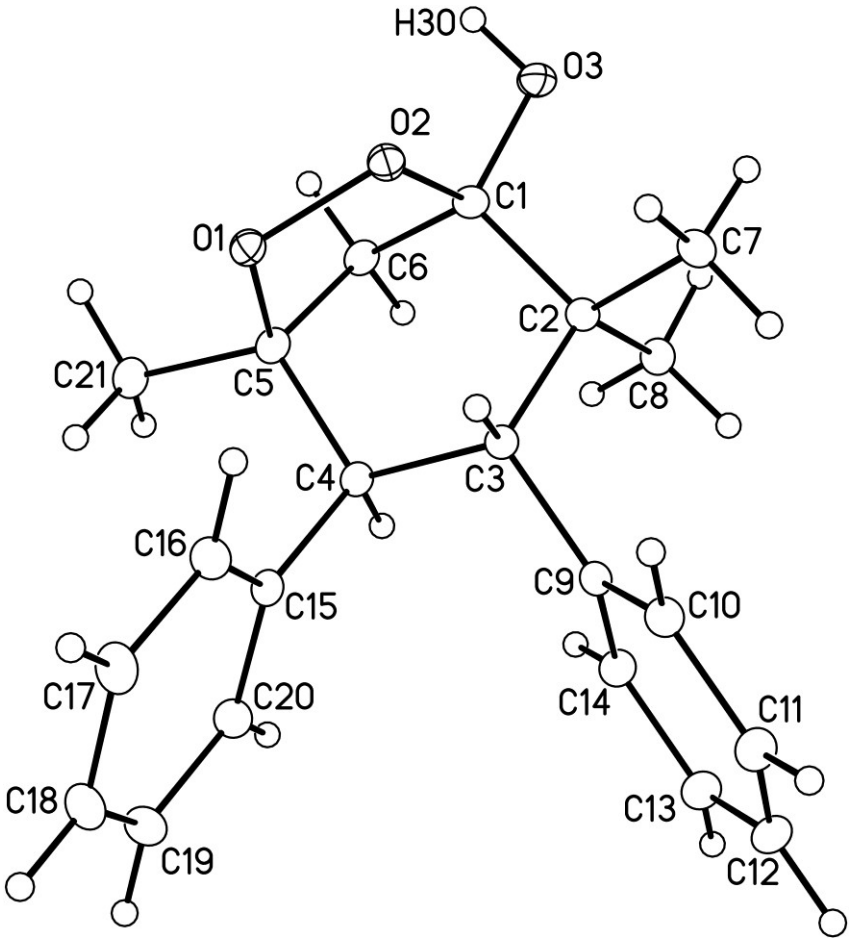

Figure 2.6 X-Ray crystal structure of bridged peroxide **43a**.

In contrast to Blanco's protocol, we did not need to use metal catalyst to accomplish the desired transformation. In 2001, Blanco and co-workers reported oxidation of bicycloalkanols into peroxides using copper catalyst.[97] In the presence of light and oxygen, catalytic amount of $Cu(acac)_2$ in ethanol could promote the oxidative rearrangement of bicyclo[*n*.1.0]alkan-1-ols **46** to form mixture of peroxides **47** and **47'**. The bicyclo[*n*.1.0]alkan-1-ols **46** were prepared from the corresponding silylated compounds **45** by adding 2 mol% TMSCl and then, in the same reaction pot, introduction of oxygen, light and the copper catalyst furnished the oxidation products (Scheme 2.17). The absence of either light or catalyst significantly affected the reaction time and the yield of the products.

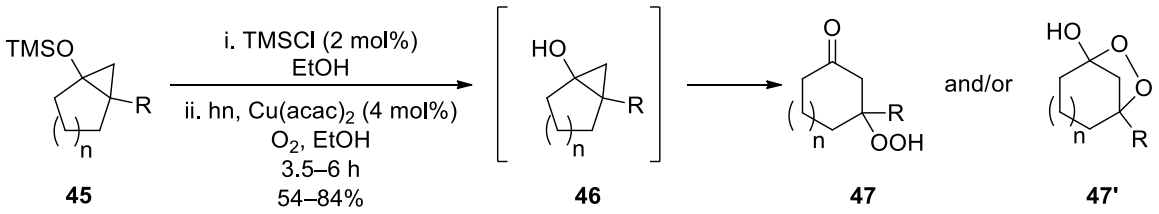

Scheme 2.17 Blanco's protocol for oxidation of bicyclo[*n*.1.0]alkan-1-ols.

The formation of peroxides **43a** and **43a'** proceeds via involvement of the alkoxy radical **48a** produced upon hydrogen abstraction by triplet oxygen from the bicyclic alcohol **40a**. The homolytic scission of the bridging C–C bond and recombination of the formed tertiary radical **49a** with the peroxy radical affords the mixture of epimers **50a** and **43a'**. The isomer **50a** cyclizes into the bridged product **43a** (Scheme 2.18).

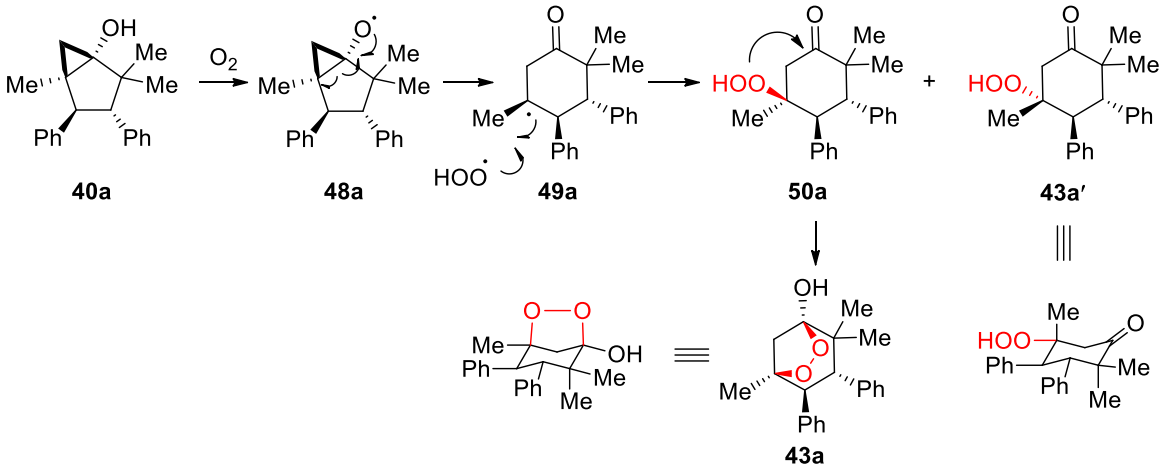

Scheme 2.18 Mechanistic proposal for oxidation of **40a** into peroxides.

The finding by DePuy and Gibson supports our mechanistic proposal.[98] When tetramethylcyclopropanone methyl hemiketal **51** in hexane reacted with atmospheric oxygen at room temperature, ring-opened β-hydroperoxy ester was formed as a sole product in 97% yield (Scheme 2.19).

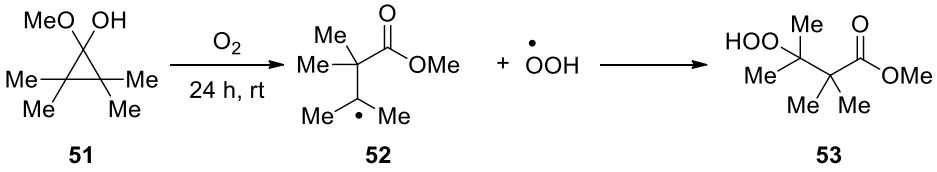

Scheme 2.19 Radical ring opening in cyclopropane.

To further diversify the labile alcohol **40a,** we treated it with an excess $FeCl_3$ in DMF toaffect the ring expansion. Thecrude mixture of β-chlorocyclohexanones formed upon ring expansion-halogen trapping was immediately treated with DBU to afford cyclohexenone **54a** (Scheme 2.20). To access cyclohexenones via Nazarov cyclization of 1,4-dien-3-ones (rather than the usualcyclopentenones) rendered new useful application of this tandem domino transformation.

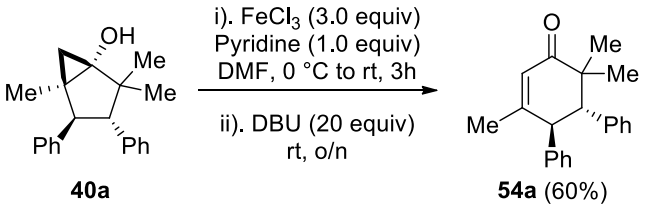

Scheme 2.20 $FeCl_3$ promoted ring-expansion of alcohol **40a**.

According to Saegusa and co-workers, the oxidation reaction of silyloxybicyclo[n .l.O]alkanes **55** with $FeCl_3$ under basic conditions led to the formation of the corresponding 2-cycloalkenones **59** via the 3-chlorocycloalkanone **58** in moderate to excellent yields.[99] The ring enlargement was explained by a mechanism involving an alkoxy radical intermediate **56,** which underwent homolytic cleavage of the bridging C–C bond and the subsequent abstraction of chlorine by the resulting carbon radical species **57** to give 3-chlorocycloalkanone **58**. Treatment of the chloro-derivative **58** under mild basic conditions delivered the desired enones **59** (Scheme 2.21).

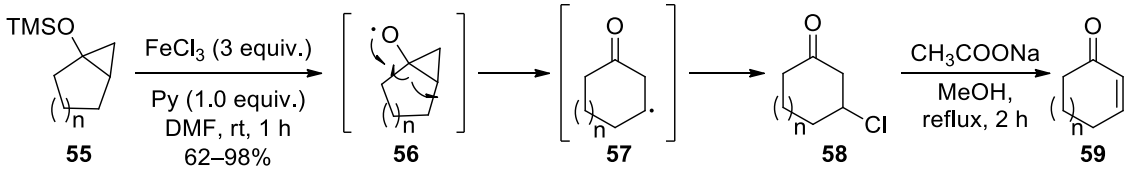

Scheme 2.21 Mechanism for $FeCl_3$ promoted ring expansion.

Finally, upon heating **40a** with conc. HCl at reflux in MeOH complementary cyclopropane fragmentation regiochemistry could be achieved. Tetramethylcyclopentanone **60a**[100] was obtained in high yield, presumably via protonolysis of the sterically most accessible cyclopropanol C–Cbond (Scheme 2.22).[101]

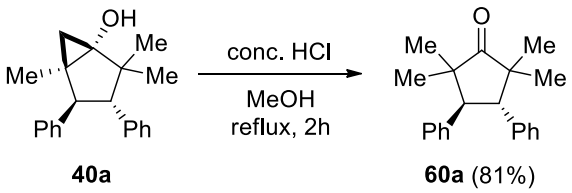

Scheme 2.22 Cyclopropane ring opening under strongly acidic conditions.

To confirm the idea of bond protonolysis in tetramethylcyclopentanone **60a**, the deuterium labelling study was conducted. First, the deuterated bicyclic alcohol ***d*$_2$-40a** was prepared via the reaction of dienone **1a** with deuterated diiodomethane. Treatment of ***d*$_2$-40a** with the strong acid gave the tetramethylcyclopentanone ***d*$_2$-60a** in which one of the methyl substituents resulting from the bond protonolysis, contained two deuterium atoms (Scheme 2.23).

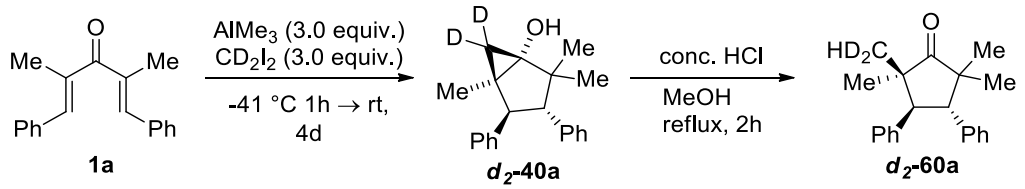

Scheme 2.23 Deuterium labelling study of the bond protonolysis.

2.5 Conclusion

In summary, we have developed the new protocol of "double interrupted" Nazarovcyclization to furnish bicyclo[3.1.0]hexanols, via the cascade of events of organoaluminum mediated Nazarov cyclization, nucleophilic trapping of reactive oxyallyl cation followed by Simmons-Smith type cyclopropanation. In this process, $AlMe_3$ played a triple role of Lewis acid activator, nucleophilic methyl source, and as part of the Simmons-Smith cyclopropanation reagent. We could achieve construction of two new rings in one pot, which in turn entails the formation of four new C-C bonds along with four new stereogenic centers via this transformation. The process was characterized with high diastereoselectivity and moderate to good regioselectivity. In addition, we have demonstrated the potential of the methodology to further reorganize the initial fused bicyclohexanol to obtain cyclohexanone or cyclohexenone derivatives, as well as tetramethyl-substituted cyclopentanone, thus expanding the repertoire of products accessible via the interrupted Nazarov reaction.

2.6 Future Directions

1. There have been numerous reports about generation of carbon centered radicals via d oxidative cleavage of cyclopropyl ethers in the presence of various metal catalysts (Cu, Fe, Mn). Booker-Milburn and co-workers in 1995 showcased that that treatment of cyclopropyl trimethylsilyl ether **61** with $FeCl_3$ in DMF could undergo cyclopropane ring opening, followed by cyclization/halogenation sequence to deliver chlorinated bicyclic structure **62** (Scheme 2.24).[102]

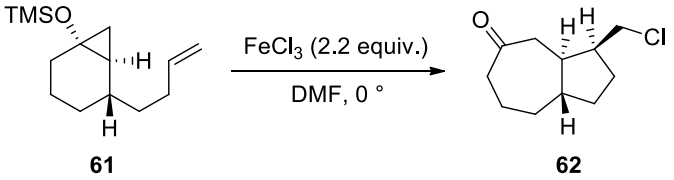

Scheme 2.24 $FeCl_3$ catalyzed cascade ring opening/cyclization/halogenation sequence.

The carbon centered radical generated upon cyclopropane ring opening can be intercepted by some external traps as well. In 2006, the Narasaka group reported generation of β-ketoradicals from cyclopropanols by means of a silver catalyst. They found that cyclopropanols **63** in the presence of Ag(I) species under mild reaction conditions can react with silyl enol ether **64** to produce diketones **65** (Scheme 2.25).[103]

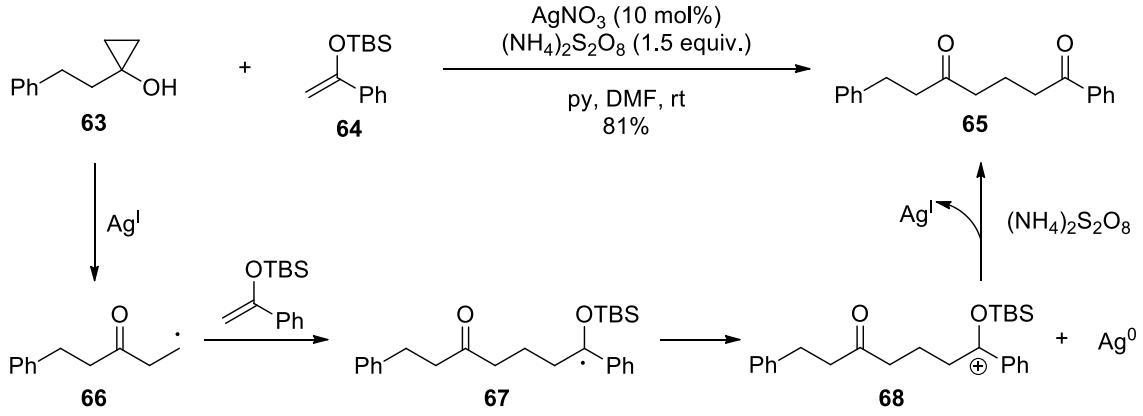

Scheme 2.25 Silver catalyzed generation of β-keto radicals.

Since we have already demonstrated the use of various ring opening strategies on our labile bicyclic alcohols, the above mentioned the silver catalyzed approach would be interesting to be tried on our substrates to form highly functionalized diketones (Scheme 2.26).

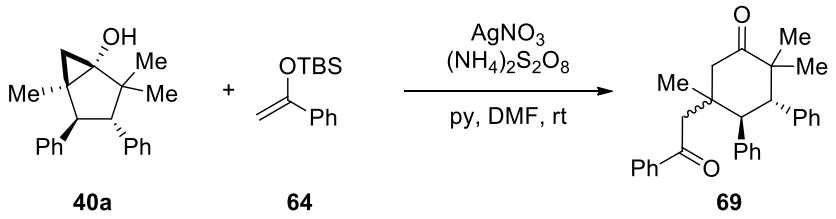

40a **64** **69**

Scheme 2.26 Tentative silver catalyzed ring expansion of **40a**.

2. There area large number of methods for aziridination of olefins as well as enolates employing nitrenes as electophilic trapping agents.[104] The method reported by Evans group in 1991 employs Cu(I) or Cu(II) catalysts and (N-(p-toluenesulfonyl)imino)phenyliodinane (PhI=NTs) as a nitrene precursor to aziridinate series of olefins (Scheme 2.27).[105] In some cases, Cu(II) was found to be superior than Cu(I) and CH_3NO_2 and CH_3CN were the best solvents to achieve products **71** at reasonable timescale to avoid decomposition of the nitrene precursor.

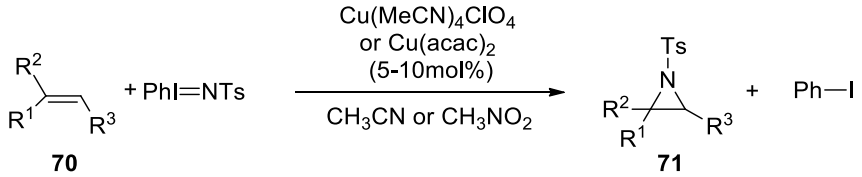

70 **71**

Scheme 2.27 Aziridination of olefins with nitrene source.

In the same work, silylenol ethers **72** as well were found to be compatible substrates for aziridination under Cu(I) catalysis. The products of the transformation were corresponding N-(*p*-toluenesulfonyl)-α-amino ketones **74** which were believed to form via ring opening of corresponding [(trimethylsilyl)oxy]aziridines **73** (Scheme 2.28).

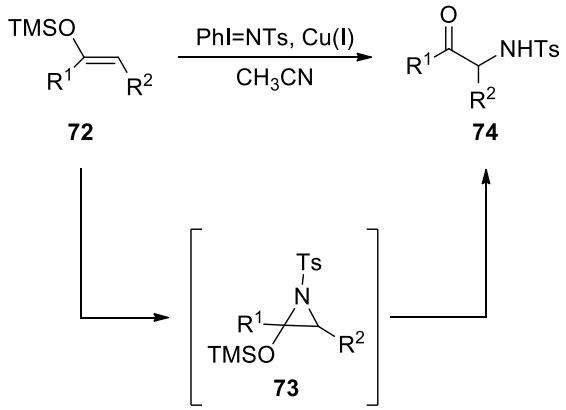

Scheme 2.28 Aziridination of silylenol ethers.

As it is well known, in the absence of nucleophilic trap, proton elimination takes place during Nazarov cyclization to form silyl enol ether **75**. It would be interesting to see if intermediate **75** could be intercepted with nitrenes and which double bond (depending on sterics and electronic effects) would show superior affinity towards aziridination. Even though there is no report of employing Cu(I) catalyst for initiation of Nazarov cyclization (probably due to its poor Lewis acidity), the reaction could be carried out with Cu(II) analogues or use of TMSOTf or any other Lewis acid potent enough to activate divinyl ketones **1** (Scheme 2.29).

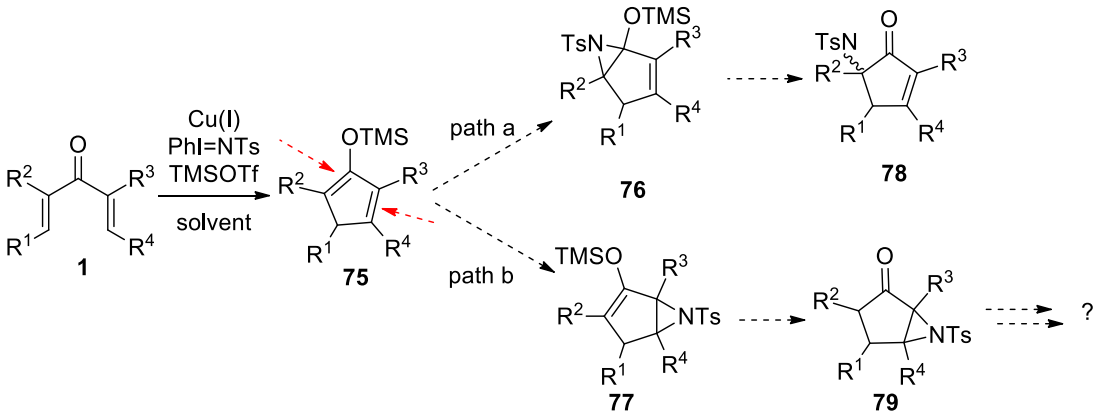

Scheme 2.29 Hypothetical aziridination of divinyl ketones.

2.7 Experimental

2.7.1 General Information

Reactions were carried out in flame-dried glassware under a positive nitrogen atmosphere unless otherwise stated. Transfer of anhydrous solvents and reagents was accomplished with oven-dried syringes or cannulae. Solvents were purified using LC Technology Solutions Inc. solvent purification system. Thin layer chromatography was performed on glass plates pre-coated with 0.25 mm Kieselgel 60 F254 (Merck). Flash chromatography columns were packed with 230-400 mesh silica gel (Silicycle). ^{1}H NMR and ^{13}C spectra were recordedusing Agilent/Varian DD2 MR two channel 400 MHz, Agilent/Varian Inova two-channel 400MHz, Agilent/Varian Inova four-channel 500 MHz, Agilent/Varian VNMRS two-channel 500 MHz, Agilent VNMRS four-channel, dual receiver 700 MHz at 400/500/700 and 100/125/175 MHz, respectively. NMR chemical shifts are reported relative to a TMS (0.00 ppm) or $CDCl_3$ (7.26 ppm) internal standard. Coupling constants (*J*) are reported in Hertz (Hz). Standard notation is used to describe the multiplicity of signals observed in 1H NMR spectra: broad(br), apparent (app), multiplet (m), singlet (s), doublet (d), triplet (t), etc. Carbon nuclear magnetic resonance spectra (^{13}C NMR) were recorded at 100 MHz, 125 MHz or 175 MHz and are reported in ppm relative to the center line of the triplet from $CDCl_3$. Infrared (IR) spectra were measured with a Mattson Galaxy Series FT-IR 3000 spectrophotometer. High resolution mass spectrometry (HRMS) data (APPI/ESI technique) were recorded using an Agilent Technologies 6220 oaTOF instrument. HRMS data (EI technique) were recordedusing a Kratos MS50 instrument.Dienones **1a**,[106] **1b**,[107] **1e–1f,**[106] **1g**,[108] **1h**,[109] **1i**,[110] **1k**,[111] and **1l**[108] were prepared via literature procedures.

2.7.2 General procedure A for the preparation of dienones 1c, 1d, and 1j:

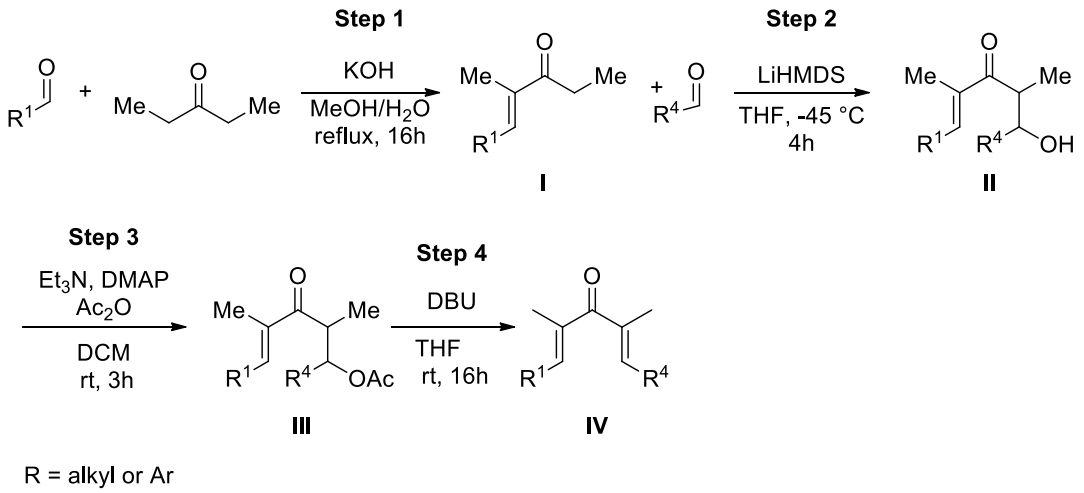

Step 1. Intermediate enone **I** was prepared via known literature procedure.[106]

Step2: To the flame dried 250 mL round bottom flask charged with nitrogen was added LiHMDS (1.5 equiv.) and diluted with THF (0.7 mL solvent for 1 mmol of reagent) and cooledto −45 °C. In a separate flame dried flask, intermediate **I** (1 equiv.) was dissolved in THF (0.2 M solution). The solution of intermediate **I** was added to the stirred solution of LiHMDS dropwise at −45 °C and stirred for 1 h while maintaining the temperature of −45 °C. After 1h, to the resulting solution was added solution of aldehyde **II** (1.3 equiv.) in THF (0.7 M solution) dropwise at −45 °C and stirring was continued for additional 3 h. The cold reactionmixture was quenched with sat. aqueous solution of NH_4Cl. Solution was extracted with EtOAc (3 x 50 mL). Combined organic layers were washed with water, brine, dried over $MgSO_4$ and concentrated in vacuo. The crude reaction mixture was purified using flash column chromatography (hexanes/EtOAc 8:1) to obtain mixture of alcohols **III**.

Step 3: In a round bottom flask, the mixture of alcohols **III** (1 equiv.) was dissolved in DCM (0.17 M solution). To the resulting solution was added Et_3N (10 equiv.). After cooling downto 0 °C, DMAP (0.05 equiv.) and Ac_2O (1.3 equiv.) were added to the solution and stirredfor 3 h at room temperature. Then it was neutralized with sat. aqueous solution of NH_4Cl. Extraction was performed with EtOAc (3 x 50 mL). Combined organic layers were washed with water, brine, dried over $MgSO_4$ and

concentrated in vacuo. The crude reaction mixture was purified using flash column chromatography (hexanes/EtOAc 10:1) to obtain themixture of acetates **IV**.

Step 4: To the solution of acetate **IV** (1 equiv.) in THF (0.8 M solution) was added DBU (1.5equiv.) and stirred at room temperature for 16 h. The solvent was removed by reduced pressure evaporation and the crude mixture was subjected to flash column chromatography (hexanes/EtOAc 20:1) to obtain pure dienone **V**.

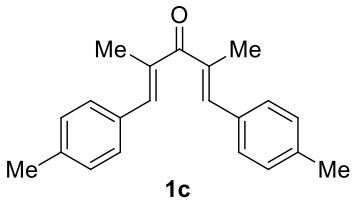

1c

Step 1. Intermediate enone **Ic** was prepared via known literature procedure[106] from 3-pentanone and *p*-tolualdehyde at 75 mmol scale. The reaction afforded 6.4g (45% yield) ofthe desired enone **Ic** as a white solid.

Step 2: To a flame dried 250 mL round bottom flask charged with nitrogen was added LiHMDS (1.0 M in THF, 12 mL, 12 mmol, 1.5 equiv.) and diluted with THF (0.7 mL solventfor 1 mmol of reagent) and cooled to −45 °C. In a separate flame dried flask, intermediate **Ic (**1.5 g, 8 mmol, 1 equiv**)** was dissolved in THF (0.2 M solution). The solution of intermediate **Ic** was added to the stirred solution of LiHMDS dropwise at −45 °C and stirred for 1 h while maintaining the temperature at −45 °C. After 1 h, to the resulting solution was added a solution of *p*-tolualdehyde (1.23 mL, 10.4 mmol, 1.3 equiv.) in THF (0.7 M solution) dropwise at −45 °C and stirring was continued for additional 3 h. The cold reaction mixture was quenched with sat. aqueous solution of NH_4Cl. The solution was extracted with EtOAc (x 3). The combined organic layers were washed with water, brine, dried over $MgSO_4$ and concentrated in vacuo. The crude reaction mixture was purified using flash column chromatography (hexanes/EtOAc 8:1) to obtain 1.66 g, (67% yield) of a diastereomeric mixture of alcohols **IIIc** as a yellow oil.

Step 3: In a round bottom flask, the mixture of alcohols **IIIc** (1.66 g, 5.4 mmol) was dissolved in DCM (0.17 M solution). To the resulting solution was added Et_3N (7.5 mL, 54 mmol, 10 equiv). After cooling down to 0 °C, DMAP (33 mg, 0.27 mmol, 0.05

equiv) and Ac_2O (0.66mL, 7.02 mmol, 1.3 equiv.) were added to the solution and stirred for 3 h at rt. Then it was neutralized with sat. aqueous solution of NH_4Cl. Extraction was performed with EtOAc (x 3).The combined organic layers were washed with water, brine, dried over $MgSO_4$ and concentrated in vacuo. The crude reaction mixture was purified using flash column chromatography (hexanes/EtOAc 10:1) to obtain 1.79 g (95% yield) the diastereomeric mixture of acetates **IVc** as a yellow oil.

Step 4: To a solution of the mixture of acetates **IVc** (1.79 g, 5.1 mmol) in THF (0.8 M solution) was added DBU (1.15 mL, 7.7 mmol, 1.5 equiv) and the reaction was stirred at rt for 16 h. The solvent was removed by reduced pressure evaporation and the crude mixture was subjected to flash column chromatography (hexanes/EtOAc 20:1) to obtain 1.24 g (84% yield) pure dienone **1c** as a white solid.

(*1E,4E*)-2,4-dimethyl-1,5-di-p-tolylpenta-1,4-dien-3-one (1c): R_f 0.45 **(**hexanes/EtOAc 30:1); mp 67–69 °C; IR (cast film), 3089, 3032, 2962, 2857, 1654, 1609, 1511, 1444 cm^{-1}. ^1H NMR (500 MHz, $CDCl_3$) δ 7.35 (d, J = 7.92 Hz, 4H), 7.22 (d, J = 7.92 Hz, 4H), 7.18 (s, 2H), 2.39 (s, 6H), 2.22 (s, 6H); ^{13}C NMR (125 MHz, $CDCl_3$) δ 202.2, 139.0, 138.4, 136.2, 133.2, 129.7, 129.2, 21.4, 15.0; HRMS (EI, M^+) for $C_{21}H_{22}O$ calcd. 290.1671, found: m/z 290.1671.

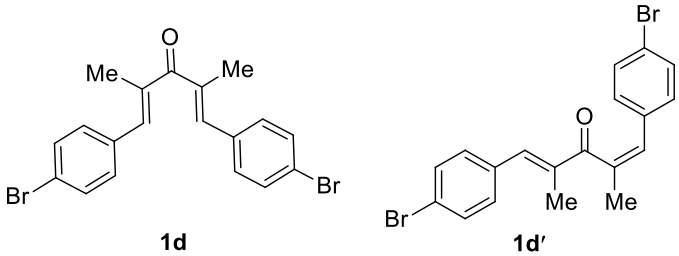

1d **1d′**

The mixture of dienones **1d** and **1d'** was prepared via known literature procedure[106] from 3-pentanone (5.17 g, 60 mmol, 6.4 mL) and 4-bromobenzaldehyde (11.1 g, 60 mmol). The reaction afforded 6 : 1 mixture of mono-adduct **Id** (6.33 g; 42% yield) and dienones **1d**/**1d'** (1.75 g, 7% yield). Attempts to carry the mixture through the general sequence (step 2 using LiHMDS and 4-bromobenzaldehyde) did not furnish the desired aldol adduct **IIId**. Therefore, 1.38 g of the crude mixture was subjected to careful

chromatographic separation to furnish 395 mg (6% yield) of a 5 : 1 isomeric mixture of dienones **1d** and **1d'** asa light yellow solid. NMR analysis was done on the mixture.

(*1E,4E*)-1,5-bis(4-bromophenyl)-2,4-dimethylpenta-1,4-dien-3-one (1d, major component): R_f 0.35 (hexanes/EtOAc 20:1); mp 48−54 °C; IR (film) 2972, 2936, 2876, 1713, 1664, 1585 cm^{-1}; ^1H NMR (500 MHz, $CDCl_3$) δ 7.54 (d, *J* = 8.0 Hz, 4H), 7.30 (d, *J* =8.0 Hz, 4H), 7.10 (s, 2H), 2.18 (s, 6H); ^{13}C NMR (125 MHz, $CDCl_3$) δ 201.2, 137.5, 137.4, 134.6, 131.6, 131.0, 122.5, 14.9; HRMS (EI, M^+) for $C_{19}H_{16}Br_2O$ calcd. 417.9568, found: m/z 419.9556.

(*1Z,4E*)-1,5-bis(4-bromophenyl)-2,4-dimethylpenta-1,4-dien-3-one (1d', minor component): R_f 0.35 (hexanes/EtOAc 20:1); mp 48–54 °C; IR (film) 2972, 2936, 2876, 1713, 1664, 1585 cm^{-1}; ^1H NMR (500 MHz, $CDCl_3$) δ 7.46 (d, *J* = 8.1 Hz, 2H), 7.34 (d, *J* = 8.1 Hz, 2H), 7.33 (s, 1H), 7.05 (d, *J* = 8.2 Hz, 2H), 6.98 (d, *J* = 8.2 Hz, 2H), 6.62 (s, 1H), 2.14 (s, 3H), 2.00 (s, 3H); ^{13}C NMR (125 MHz, $CDCl_3$) δ 202.8, 141.1, 138.6, 136.3, 135.4, 134.6, 134.4, 131.4, 131.0, 129.5, 128.8, 123.0, 121.3, 23.0, 12.5; HRMS (EI, M^+) for $C_{19}H_{16}Br_2O$ calcd. 417.9568, found: m/z 419.9556.

[**NOTE:** Compounds **1e** and **1f** were previously described in the literature;[106] however, their data were not included in that report, so we include them here.

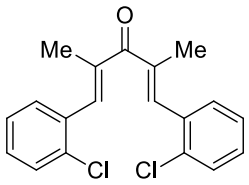

1e

(*1E,4E*)-1,5-bis(2-chlorophenyl)-2,4-dimethylpenta-1,4-dien-3-one (1e): product was obtained as awhite solid; R_f 0.41 (hexanes/EtOAc 30:1); mp 83−85 °C; IR (film) 3068, 2987, 2957, 2857, 1642, 1590, 1469 cm^{-1}; ^1H NMR (500 MHz, $CDCl_3$) δ 7.45 (dd, *J* = 7.5, 1.6 Hz, 2H), 7.42–7.40 (m, 4H), 7.33–7.28 (m, 4H), 2.08 (s, 6H); ^{13}C NMR (125 MHz, $CDCl_3$) δ 201.0, 138.3, 136.3, 134.6, 134.1, 130.3, 129.6, 129.3, 126.5, 14.6; HRMS (EI, M^+) for $C_{19}H_{16}Cl_2O$ calcd. 330.0578, found: m/z 330.0572.

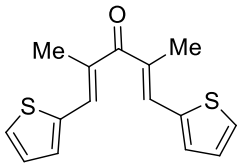

1f

(*1E,4E*)-2,4-dimethyl-1,5-di(thiophen-2-yl)penta-1,4-dien-3-one (1f): R_f 0.68 (hexanes/EtOAc 10:1); mp 88–90 °C; IR (film) 3094, 3081, 3028, 2940, 2911, 2843, 1789, 1628, 1609, 1540 cm^{-1}; ^1H NMR (500 MHz, $CDCl_3$) δ 7.53 (dd, *J* = 5.1, 0.4 Hz, 2H), 7.36 (qd, *J* = 1.3, 0.8 Hz, 2H), 7.26 (ddd, *J* = 3.7, 0.8, 0.4 Hz, 2H), 7.14 (dd, *J* = 5.1, 3.7 Hz, 2H), 2.29 (d, *J* = 1.3 Hz, 6H); ^{13}C NMR (125 MHz, $CDCl_3$) δ 200.8, 139.4, 133.7, 131.8, 131.3, 129.0, 127.4, 15.5; HRMS (EI, M^+) for $C_{15}H_{14}S_2O$ calcd. 274.0486, found: m/z 274.0484.

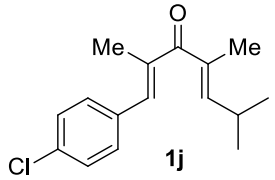

1j

Reaction performed under the **general procedure A**.

Step 1: Intermediate enone **Ij** was prepared via known literature procedure[106] from 3-pentanone and 4-chlorobenzaldehyde at 50 mmol scale. The intermediate **Ij** (2.34g; 23% yield) was isolated asa white solid.

Step2: To a flame dried 250 mL round bottom flask charged with nitrogen was added LiHMDS (1.0 M in THF, 12.0 mL, 12.0 mmol, 1.5 equiv.) and diluted with THF (0.7 mL solvent for 1 mmol of reagent) and cooled to –45 °C. In a separate flame dried flask the intermediate **Ij** (1.67 g, 8.0 mmol, 1 equiv.) was dissolved in THF (0.2 M solution). The solution of intermediate **Ij** was added to the stirred solution of LiHMDS dropwise at –45 °C and stirred for 1 h while maintaining the temperature of −45 °C. After 1 h, to the resulting solution was added a solution of isobutyraldehyde (0.90 mL, 10 mmol, 1.3 equiv.) in THF (0.7 M solution) dropwise at –45 °C and stirring was continued at this temperature for additional 3 h. The cold reaction mixture was quenched with sat. aqueous solution of NH_4Cl. The solution was extracted with EtOAc (3 x 50 mL). Combined organic layers were washed with water, brine, dried over $MgSO_4$ and

concentrated in vacuo. The crude reaction mixturewas purified using flash column chromatography (hexanes/EtOAc 8:1) to obtain 1.65 g,(74% yield) of a diastereomeric mixture of alcohols **IIIj** as a yellow oil.

Step 3: In a round bottom flask, the mixture of alcohols **IIIj** (1.65 g, 5.9 mmol) was dissolved in DCM (0.17 M solution). To the resulting solution was added Et_3N (.8.1 mL, 59.0 mmol, 10equiv). After cooling down to 0 °C, DMAP (36 mg, 0.3 mmol, 0.05 equiv) and Ac_2O (0.7 mL,7.6. 0 mmol, 1.3 equiv) were added to the solution and the reaction was stirred for 3 h at rt.Then it was neutralized with sat. aqueous solution of NH_4Cl. Extraction was performed with EtOAc (3 x 50 mL). Combined organic layers were washed with water, brine, dried over $MgSO_4$ and concentrated in vacuo. The crude reaction mixture was purified using flashcolumn chromatography (hexanes/EtOAc 10:1) to obtain 1.72 g (90% yield) the mixture of diastereomeric acetates **IVj** as a yellow oil.

Step 4: To the solution of mixture of acetates **IVj** (1.72 g, 5.3 mmol) in THF (0.8 M solution) was added DBU (1.2 mL, 7.95 mmol, 1.5 equiv) and the reaction was stirred at rt for 16 h.The solvent was removed by reduced pressure evaporation and the crude mixture was subjected to flash column chromatography (hexanes/EtOAc 20:1) to obtain 1.03 g (74% yield) pure dienone **1j** asa yellow solid.

(*1E,4E*)-1-(4-chlorophenyl)-2,4,6-trimethylhepta-1,4-dien-3-one (1j): R_f 0.45 (hexanes/EtOAc 20:1); mp 65–67 °C; IR (cast film) 3090, 2973, 29.54, 2866, 1660, 1623, 1492 cm^{-1}. ^1H NMR (400 MHz, $CDCl_3$) δ 7.39–7.35 (ddd, *J* = 8.7, 4.6, 2.8 Hz, 2H), 7.33–7.29 (ddd, *J* = 8.8, 4.6, 2.3 Hz, 2H), 6.95 (s, 1H), 6.11 (dq, *J* = 9.5, 1.6 Hz, 1H), 2.74 (dsept, *J* = 7.04, 1.6 Hz, 1H), 2.09 (d, *J* = 1.45 Hz, 3H), 1.91 (d, *J* = 1.42 Hz, 3H), 1.05 (d, *J* = 7.04,6H); ^{13}C NMR (175 MHz, $CDCl_3$) δ 201.7, 150.2, 137.6, 136.4, 134.5, 133.9, 133.5, 130.7, 128.6, 28.2, 22.1, 15.0, 12.7; HRMS (EI, M^+) for $C_{16}H_{19}ClO$ calcd. 262.1124, found: m/z262.1129.

Table 2.2 Optimization of $AlMe_3$ mediated double interrupted Nazarov cyclization.[a],[b]

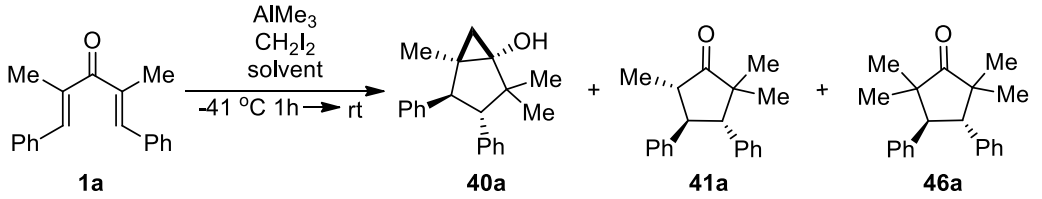

Entry	$AlMe_3$ (equiv.)	CH_2I_2 (equiv.)	Solvent	Time	Product Yield (%)
1	2.5 (2M in toluene)	2.5	DCM	2d	**41a** + complex mixture
2	2.5 (2M in toluene)	2.5	hexane	3 d	**40a** (25)
3	4.0 (2M in toluene)	2.5	hexane	2 d	**41a** + complex mixture
4	2.5 (2M in toluene)	4.0	hexane	7 d	**40a** (11) + **41a** (68)
5	3.0 (2 M in hexane)	2.0	hexane	7 d	**40a** (40) + **41a** (51)
6	3.0 (2 M in hexane)	3.0	hexane	7 d	**40a** (61)
7	3.0 (2 M in hexane)	4.0	hexane	7 d	**40a** (60)
8	3.0 (2 M in hexane)	3.0	hexane	8 d	**25a** (65)
9	3.0 (2 M in hexane)	3.0	hexane	8 d	**40a** (60) + **41a** (13) + **31a** (21)[c]
10	3.0 (2 M in hexane)	3.0	--[d]	1 d	**40a** (44) + **41a** (29)
11	3.0 (2 M in hexane)	3.0	--	2 d	**40a** (49) + **41a** (16)
12	3.0 (2 M in hexane)	3.0	--	3 d	**40a** (58) + **41a** (12)
13	3.0 (2 M in hexane)	3.0	--	4 d	**40a** (60)+**41a** (9)
14	3.0+2.0 (2 M in hexane)	3.0 + 2.0	--	2 d	**40a** (30)+**41a** (7)
15	3.0 (2 M in hexane)	3.0 + 2.0	--	2 d	**40a** (23)+complex mixture

Footnotes: [a] For entries 1–9 the reactions were performed at 0.09 M concentration. [b] Higher temperature (50 °C) even when under reflux, compromised the inertness of the reaction vessel, caused the loss of CH_2I_2, plus produced a lot of side products when

tracked by GC/MS [c] To avoid formation of **46a,** reaction needs to bequenched with 1M HCl at -41 °C.

Table 2.3 Screening of Lewis acids.

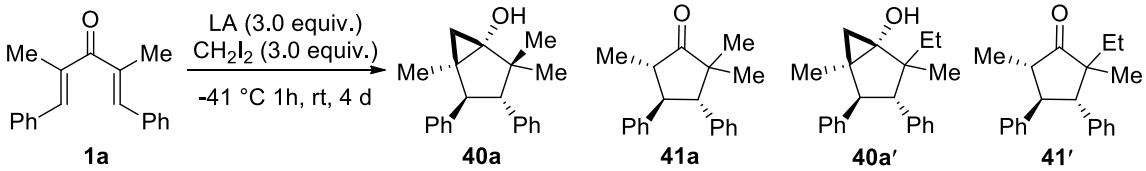

Entry	Lewis Acid	R	Time	Conc. (M)	Product Yield (%)
1	$AlPh_3$	-	7 d	0.09	No product, complex mixture
2	$AlEt_3$	Et	8 d	0.09	**40a'** (15)[a] + **41a′**(42) + **41aa′**(22)
3	$Al(Me)_2Cl$ (1 M in hexane)	Me	4 d	0.3	**41a** (31)+complex mixture
4	$ZnEt_2$	Et	4 d	0.3	**40a'**(27)[a]

[a] Poor purity after column chromatography based on NMR.

2.7.3 Representative procedure B for organoaluminum mediated double interrupted Nazarov cyclization (42a).

Step 1: To a flame dried round bottom flask charged with dienone **1a** (131 mg, 0.50 mmol) were added 3.0 equiv of CH_2I_2 (0.121 mL, 1.5 mmol, d = 3.325 g/mL) under N_2 atmosphere and cooled down to −41 °C. To the cooled mixture, 3.0 equiv of $AlMe_3$ (0.75 mL, 1.5 mmol, 2 M solution in hexanes) were added and stirring was continued at -41 °C. After 1 h thereaction mixture was allowed to warm up to room temperature and stirred for 4 days. The reaction was diluted with hexanes (15 mL), cooled to -41 °C, and quenched with 1 M aq. HCl (10 mL), then warmed up to rt. [**NOTE:** Significant heat is generated during quenching of $AlMe_3$ with 1 M HCl, and this can cause unwanted secondary reactions of the labile cyclopropanol intermediate, as exemplified by the formation of cyclopentanone **46a** from **40a** (see Scheme 2.18). Cooling to –41 °C via CH_3CN/dry ice bath was sufficient to suppress this undesired reactivity.] To the

quenched mixture was added 15 mL of DCM and after separation of layers, aqueous phase was extracted with DCM (2 x 15 mL). The combined organic layers were washed with water (2 x 20 mL), brine, dried over $MgSO_4$, filtered and concentrated by reduced pressure evaporation.

Step 2: The crude residue was subjected to acetylation conditions by dissolving it in DCM (5 mL) and adding 10 equiv. of NEt_3 (0.07 mL, d = 0.725 g/mL) at room temperature. The reaction mixture was cooled to 0 °C followed by addition of 0.05 equiv of DMAP (0.025 mmol,3.0 mg) and 1.2 equiv of Ac_2O (0.6 mmol, 0.06 mL, d = 1.08 g/mL). After stirring at room temperature for 3 h, the reaction mixture was quenched with saturated aq. solution of NH_4Cl (10 mL). The layers were separated and the aqueous layer was extracted with DCM (2 x15 mL). Combined organic layers were washed with water (20 mL), brine, dried over $MgSO_4$, filtered and concentrated in vacuo. Purification by flash column chromatography (hexane/EtOAc 50:1 → 20:1) afforded **42a** (110 mg, 66%).

2.7.4Spectral Data for Compounds 40a, 41a, 42a–42f, 41f, 42j,42j', and 42l

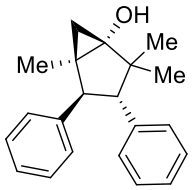

40a

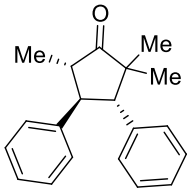

41a

Reaction performed under the **standard procedure B - Step 1.** Flash column chromatography (hexanes/EtOAc 20:1) gave **40a** (175 mg, 60%) as colorless oil and **41a** (25 mg, 9%) as a white solid.

(*1R*,3S*,4S*,5R)-2,2,5-trimethyl-3,4-diphenylbicyclo[3.1.0]hexan-1-ol (40a):** R_f 0.14 (hexanes/EtOAc 9:1); IR (cast film) 3411, 3028, 2963, 2926, 1450, 1146 cm^{-1}; ^1H NMR (400 MHz , $CDCl_3$) δ 7.27–7.12 (m, 10 H), 3.57 (d, *J* = 11.7 Hz, 1H), 2.56 (d, *J* = 11.7 Hz, 1H), 1.37 (d, *J* = 6.0 Hz, 1H), 1.30 (s, 3H), 1.10 (s, 3H), 0.83 (s, 3H), 0.54 (d, *J* = 6.0 Hz, 1H); ^{13}C NMR (175 MHz, $CDCl_3$) δ 141.2, 137.9, 129.8, 128.1, 127.8, 127.7, 126.4, 126.3, 69.8, 56.8, 50.9, 44.8, 32.4, 22.3, 19.3, 18.4, 16.2; HRMS (EI, M^+) for $C_{21}H_{24}O$ calcd. 292.1827, found: m/z 292.1834.

(*3S*,4R*,5S)-2,2,5-trimethyl-3,4-diphenylcyclopentan-1-one (41a):** product was obtained as awhite solid; R_f 0.45(hexanes/EtOAc 10:1); mp 118–120 °C; IR (cast film) 3064, 3003, 2971, 2927, 2872, 1727,1683, 1601, 1498 cm^{-1}. ^1H NMR (500 MHz, $CDCl_3$) δ 7.29–7.24 (m, 6H), 7.21–7.15 (m,4H), 3.38–3.30 (m, 2H), 2.44 (dd, *J* = 10.8, 7.0 Hz, 1H), 1.24 (s, 3H), 1.20 (d, *J* =, 7.0 Hz,3H), 0.76 (s, 3H); ^{13}C NMR (125 MHz, $CDCl_3$) δ 221.9, 140.6, 137.0, 129.1, 128.5, 128.0,127.6, 126.72, 126.68, 58.4, 51.9, 50.6, 49.7, 23.9, 20.1, 13.5; HRMS (EI, M^+) for $C_{20}H_{22}O$ calcd. 278.1671, found: m/z 278.1671.

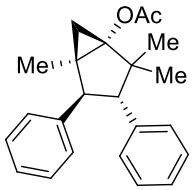

42a

The reaction was performed under the **standard procedure B**. Flash column chromatography (hexanes/EtOAc 50:1 → 10:1) gave **42a** (110 mg, 66%) as a white solid.

(*1R*,3S*,4S*,5R)-2,2,5-trimethyl-3,4-diphenylbicyclo[3.1.0]hexan-1-yl acetate (42a):** R_f 0.40 (hexanes/EtOAc 10:1); mp 157–159 °C; IR (film) 3087, 3064, 3003, 2966, 2869, 1752,1602, 1497, 1227 cm^{-1}; ^1H NMR (400 MHz, $CDCl_3$) δ 7.25–7.22 (m, 2H), 7.19–7.12 (m, 8H), 3.60 (d, *J* = 11.8 Hz, 1H), 2.62 (d, *J* = 11.8 Hz, 1H), 2.11 (s, 3H), 1.78 (d, *J* = 7.2 Hz, 1H), 1.23 (s, 3H), 1.09 (s, 3H), 0.80 (s, 3H), 0.77 (d, *J* = 7.2 Hz, 1H);^{13}C NMR (125 MHz, $CDCl_3$) δ 171.2, 140.8, 137.2, 130.0, 128.2, 127.8, 127.7, 126.6, 126.5, 71.6, 57.6, 50.6,45.4, 30.8, 23.8, 21.2, 20.1, 18.6, 17.0; HRMS (EI, M^+) for $C_{23}H_{26}O_2$ calcd. 334.1933, found: m/z 334.1938.

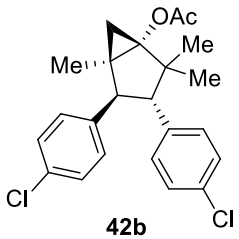

42b

The reaction was performed under the **standard procedure B**. Flash column chromatography (hexanes/EtOAc 50:1→10:1) gave **42b** (163 mg, 81%) as a white solid.

(*1R*,3S*,4S*,5R)-3,4-bis(4-chlorophenyl)-2,2,5-trimethylbicyclo[3.1.0]hexan-1-ylacetate (42b):** R_f 0.40 (hexanes/EtOAc 10:1); mp 106−107 °C; IR (film) 3032, 2967, 2927, 2870, 1753, 1493, 1266 cm^{-1}; ^1H NMR (400 MHz, $CDCl_3$) δ 7.22 (d, *J* = 8.5 Hz, 2H), 7.16 (d, *J* = 8.5 Hz, 2H), 7.09 (d, *J* = 8.5 Hz, 2H), 7.07 (d, *J* = 8.5 Hz, 2H), 3.48 (d, *J* = 11.9 Hz, 1H), 2.50 (d, *J* = 11.9 Hz, 1H), 2.10 (s, 3H), 1.72 (d, *J* = 7.3 Hz, 1H), 1.21 (s, 3H), 1.06 (s, 3H),0.79 (s, 3H), 0.78 (d, *J* = 7.3 Hz, 1H); ^{13}C NMR (125 MHz, $CDCl_3$) δ 171.1, 138.9, 135.5,132.7, 132.4, 131.1, 128.9, 128.5, 128.1, 71.2, 57.3, 50.4, 45.4, 30.6, 23.7, 21.2, 19.9, 18.5, 16.9; HRMS (EI, M^+) for $C_{23}H_{24}Cl_2O_2$ calcd. 402.1153, found: m/z 402.1147.

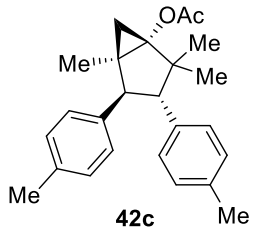

42c

The reaction was performed under the **standard procedure B.** Flash column chromatography (hexane/EtOAc 50:1 → 10:1) gave **42c** (100 mg, 55%) as a white solid.

(*1R*,3S*,4S*,5R)-2,2,5-trimethyl-3,4-di-p-tolylbicyclo[3.1.0]hexan-1-yl acetate (42c):** R_f 0.33 (hexanes/EtOAc 10:1); mp 113−115 °C; IR (film) 3051, 3010, 2965, 2925, 2888, 1753, 1647, 1515, 1223 cm^{-1}; ^1H NMR (400 MHz, $CDCl_3$) δ 7.08−7.04 (m, 6H), 7.00−6.98(m, 2H), 3.54 (d, *J* = 11.9 Hz, 1H), 2.56 (d, *J* = 11.9 Hz, 1H), 2.27 (s, 3H), 2.24 (s, 3H), 2.10 (s, 3H), 1.74 (d, *J* = 7.3 Hz, 1H), 1.22 (s, 3H), 1.07 (s, 3H), 0.78 (s, 3H), 0.73 (d, *J* = 7.3 Hz, 1H); ^{13}C NMR (125 MHz, $CDCl_3$) δ 171.2, 137.7, 136.0, 135.8, 134.2, 129.8, 128.9, 128.4, 127.6, 71.6, 57.0, 50.3, 45.3, 30.7, 23.8, 21.2, 21.0, 20.97, 20.96, 18.5, 17.0; HRMS (EI,M^+) for $C_{25}H_{30}O_2$ calcd. 362.2246, found: m/z 362.2249.

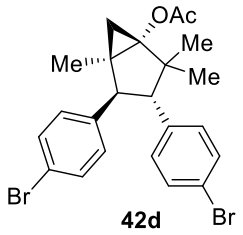

42d

The reaction was performed under the **standard procedure B.** Flash column chromatography (hexanes/EtOAc 50:1 → 10:1) gave **42d** (123 mg, 50%) as a white solid.

(*1R*,3S*,4S*,5R)-3,4-bis(4-bromophenyl)-2,2,5-trimethylbicyclo[3.1.0]hexan-1-ylacetate (42d):** R_f 0.25 (hexanes/EtOAc 10:1); mp 116–118 °C; IR (film) 3064, 2966, 2867, 1752, 15.90, 1490, 1227 cm^{-1}; ^1H NMR (400 MHz, $CDCl_3$) δ 7.37 (d, *J* = 8.4 Hz, 2H), 7.31 (d, *J* = 8.5 Hz, 2H), 7.03 (d, *J* = 7.8 Hz, 2H), 7.01 (d, *J* = 7.8 Hz, 2H), 3.48 (d, *J* = 11.9 Hz, 1H), 2.49 (d, *J* = 11.9 Hz, 1H), 2.10 (s, 3H), 1.72 (d, *J* = 7.3 Hz, 1H), 1.21 (s, 3H), 1.06 (s, 3H), 0.79 (s, 3H), 0.78 (d, *J* = 7.3 Hz, 1H); ^{13}C NMR (125 MHz, $CDCl_3$) δ 171.0, 139.4, 136.0, 131.5, 131.4, 131.0, 129.3, 120.8, 120.5, 71.1, 57.3, 50.4, 45.4, 30.6, 23.7, 21.2, 19.9, 18.5, 16.8; HRMS (EI, M^+) for $C_{23}H_{24}Br_2O_2$ calcd. 490.0143, found: m/z 492.0162.

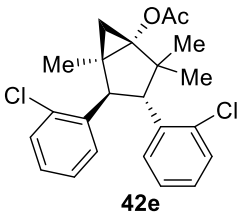

42e

The reaction was performed under the **standard procedure B.** Flash column chromatography (hexanes/EtOAc 50:1 → 10:1) gave **42e** (88 mg, 44%) asa white solid.

(*1R*,3R*,4R*,5R)-3,4-bis(2-chlorophenyl)-2,2,5-trimethylbicyclo[3.1.0]hexan-1-ylacetate (42e):** R_f 0.45 (hexanes/EtOAc 15:1); mp 122–124 °C; IR (film) 3069, 2969, 2869, 1754, 1671, 1647, 1557, 1226 cm^{-1}; ^1H NMR (400 MHz, $CDCl_3$) δ 7.44 (dd, *J* = 7.9, 1.6 Hz,1H), 7.40 (dd, *J* = 7.9, 1.6 Hz, 1H), 7.24 (ddd, *J* = 7.9, 0.9, 0.9 Hz, 2H), 7.19 (ddd, *J* = 7.9, 1.6. 1.6 Hz, 1H), 7.17 (ddd, *J* = 7.9, 1.6. 1.6 Hz, 1H), 7.07 (ddd, *J* = 7.9, 1.6. 0.4 Hz, 1H), 7.05 (ddd, *J* = 7.9, 1.6. 0.4 Hz, 1H), 4.34 (d, *J* = 12.3 Hz, 1H), 3.63 (d, *J* = 12.3 Hz, 1H), 2.11(s, 3H), 1.95 (d, *J* = 7.6 Hz, 1H), 1.21 (s, 3H), 1.16 (s, 3H), 0.97

(s, 3 H), 0.68 (d, J = 7.6 Hz, 1 H); ^{13}C NMR (125 MHz, $CDCl_3$) δ 171.1, 138.0, 135.9, 134.9, 134.6, 130.8, 129.6, 129.4,127.8, 127.7, 127.5, 127.1, 126.0, 71.3, 50.3, 46.5, 46.3, 32.8, 24.4, 21.2, 20.2, 18.1, 16.7; HRMS (EI, M^+) for $C_{23}H_{24}Cl_2O_2$ calcd. 402.1153, found: m/z 402.1146.

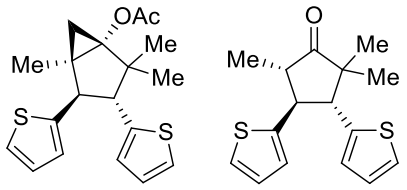

42f **41f**

The reaction was performed under the **standard procedure B.** Flash column chromatography (hexanes/EtOAc 50:1 → 10:1) gave **42f** (25 mg, 14%) as a light yellow oil and **41f** (65 mg,44%) as light yellow oil.

(*1R*,3R*,4R*,5R)-2,2,5-trimethyl-3,4-di(thiophen-2-yl)bicyclo[3.1.0]hexan-1-yl acetate (42f):** R_f 0.35 (hexanes/EtOAc 20:1); IR (film) 3069, 2964, 2869, 1757, 1643, 1606, 1228 cm^{-1}; ^{1}H NMR (400 MHz, $CDCl_3$) δ 7.17 (dd, J = 5.1, 1.1 Hz, 1 H), 7.07 (dd, J = 5.1, 1.1 Hz, 1 H), 6.94 (dd, J = 5.1, 3.5 Hz, 1 H), 6.86 (dd, J = 5.1, 3.5 Hz, 1 H), 6.84–6.80 (m,2 H), 3.72 (d, J = 11.2 Hz, 1 H), 2.79 (d, J = 11.2 Hz, 1 H), 2.10 (s, 3 H), 1.64 (d, J = 7.5 Hz,1 H), 1.29 (s, 3 H), 1.15 (s, 3 H), 0.85 (s, 3 H), 0.78 (d, J = 7.5 Hz, 1 H); ^{13}C NMR (125 MHz, $CDCl_3$) δ 170.9, 144.0, 140.9, 126.6, 126.3, 126.2, 124.7, 123.8, 123.2, 71.9, 55.1, 49.9, 45.4, 31.2, 23.7, 21.2, 20.5, 18.9, 16.6; HRMS (EI, M^+) for $C_{19}H_{22}O_2S_2$ calcd. 346.1046, found: m/z 346.1057.

(*3R*,4S*,5S)-2,2,5-trimethyl-3,4-di(thiophen-2-yl)cyclopentan-1-one (41f):** R_f 0.37(hexanes/EtOAc 20:1); ^{1}H NMR (500 MHz, $CDCl_3$) δ 7.18 (dd, J = 5.1, 1.1 Hz, 1H), 7.12 (dd, J = 4.1, 2.1 Hz, 1H), 6.96 (dd, J = 5.1, 3.5 Hz, 1H), 6.90–6.88 (m, 2H), 6.86 (d, J = 3.5Hz, 1H), 3.50 (d, J = 11.9 Hz, 1H), 3.48 (d, J = 11.9 Hz, 1H), 2.44 (qd, J = 7.0, 1.8 Hz, 1H),1.27 (d, J = 7.0 Hz, 3H), 1.27 (s, 3H), 1.25 (s, 3H); ^{13}C NMR (125 MHz, $CDCl_3$) δ 220.6,144.7, 140.3, 126.71, 126.69, 125.9, 125.0, 123.9, 123.5, 55.8, 52.4, 49.9, 48.4, 29.7, 23.6,20.4, 13.8; HRMS (EI, M^+) for $C_{16}H_{18}OS_2$ calcd. 290.0799, found: m/z 290.0796.

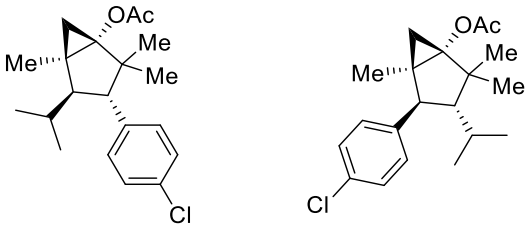

42j **42j′**

The reaction was performed under the **standard procedure B.** Flash column chromatography (hexane/EtOAc 50:1 → 10:1) gave an inseparable 2.5:1 mixture of regioisomers **42j** and**42j'** (124 mg, 74%) as a light yellow oil. To determine the structures and assign resonances 2D correlations such as HMBC, HSQC and TROESY were used (see below).

(*1R*,3S*,4R*,5R)-3-(4-chlorophenyl)-4-isopropyl-2,2,5-trimethylbicyclo[3.1.0]hexan-1-yl acetate (42j):** R_f 0.35 (hexanes/EtOAc 20:1); IR (film) 30.71, 2930, 2873, 1755, 1595,1494, 1227 cm^{-1}; ^1H NMR (500 MHz, $CDCl_3$) δ7.27–7.25 (m, 2H), 7.07–7.06 (m, 2H), 2.32(dd, *J* = 11.6, 3.5 Hz, 1H), 2.18 (d, *J* = 11.6 Hz, 1H), 2.07 (s, 3H), 1.64–162 (m, 1H), 1.43 (d, *J* =7.4 Hz, 1H), 1.28 (s, 3H), 0.97 (s, 3H), 0.86 (d, *J* = 7.0 Hz, 3H), 0.80 (d, *J* = 7.0 Hz, 3H),0.66 (d, *J* = 7.4 Hz, 1H), 0.66 (s, 3H); ^{13}C NMR (125 MHz, $CDCl_3$) δ 171.2, 137.9, 132.2, 128.3, 127.9, 71.3, 54.3, 50.4, 44.6, 29.4, 27.8, 23.8, 22.2, 21.2, 20.2, 20.1, 18.7, 18.4; HRMS (EI, M^+) for $C_{20}H_{27}ClO_2$ calcd. 334.1700, found: m/z 334.1704.

(*1R*,3R*,4S*,5R)-4-(4-chlorophenyl)-3-isopropyl-2,2,5-trimethylbicyclo[3.1.0]hexan-1-yl acetate (42j'):** product was obtained as alight yellow oil, R_f 0.35 (hexanes/EtOAc 20:1); IR (film) 3071, 2930, 2873,1755, 1595, 1494, 1227 cm^{-1}; ^1H NMR (500 MHz, $CDCl_3$) δ 7.27–7.25 (m, 2H), 7.17–7.15(m, 2H), 2.94 (d, *J* = 11.4 Hz, 1H), 2.07 (s, 3H), 1.73–1.71 (m, 1H), 1.54 (d, *J* = 7.2 Hz, 1H), 1.40 (dd, *J* = 11.4, 3.2 Hz, 1H), 1.14 (s, 3H), 1.01 (s, 3H), 1.00 (s, 3H), 0.76 (d, *J* = 7.0 Hz, 3H), 0.67 (d, *J* = 7.0 Hz, 3H), 0.51 (d, *J* = 7.2 Hz, 1H); ^{13}C NMR (125 MHz, $CDCl_3$) δ 171.0, 141.6, 132.0, 129.4, 127.9, 72.3, 54.5, 50.0, 45.5, 32.8, 26.6, 25.4, 24.6, 21.2, 20.7, 19.2, 18.3, 16.4; HRMS (EI, M^+) for $C_{20}H_{27}ClO_2$ calcd. 334.1700, found: m/z 334.1704.

Assignment of Regioisomers: The two regioisomeric Nazarov/methylation/Simmons-Smith trapping produces were distinguished via a combination of vicinal coupling, HMBC correlations, and TROESY correlations, as illustrated in the figure below.

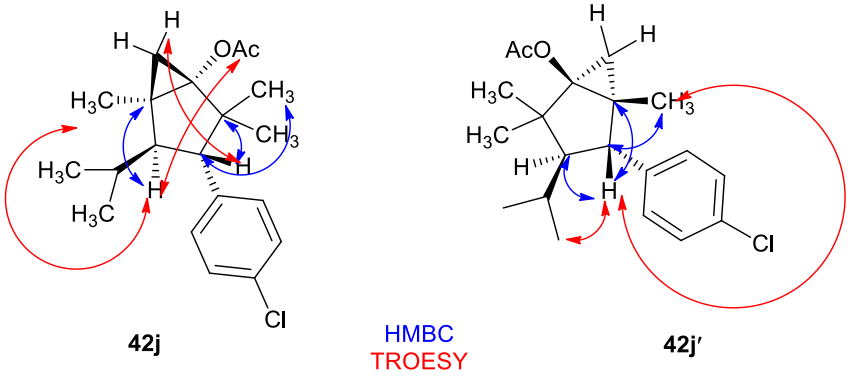

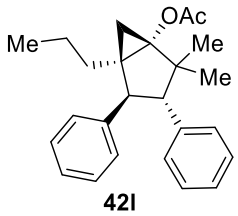

The reaction was performed under the **standard procedure B.** Flash column chromatography (hexanes/EtOAc 50:1 → 10:1) gave **42l** (76 mg, 42%) as a white solid. **(*1R*,3S*,4S*,5R**)-2,2-dimethyl-3,4-diphenyl-5-propylbicyclo[3.1.0]hexan-1-yl acetate(42l):** White solid, R_f 0.33 (hexanes/EtOAc 10:1); mp 118–120 °C; IR 3062, 3029, 2963, 2871, 1752, 1601, 1497, 1463, 1223 cm^{-1}; ^1H NMR (500 MHz, $CDCl_3$) δ 7.25–7.09 (m, 10H),3.75 (d, J = 11.7 Hz, 1H), 2.60 (d, J = 11.7 Hz, 1H), 2.10 (s, 3H), 1.87 (d, J = 7.4 Hz, 1H), 1.77–1.68 (m, 1H), 1.56–1.50 (m, 1H), 1.39–1.33 (m, 1H), 1.29–1.26 (m, 1H), 1.08 (s, 3H), 0.90 (t, J = 7.2 Hz, 3H), 0.84 (d, J = 7.4 Hz, 1H), 0.81 (s, 3H); ^{13}C NMR (125 MHz, $CDCl_3$) δ 171.2, 141.3, 137.3, 130.2, 128.1, 127.8, 127.7, 126.6, 126.4, 71.8, 57.9, 47.4, 45.1, 34.7, 33.6, 23.7, 21.3, 20.1, 19.8, 19.0, 14.6; HRMS (EI, $M+H)^+$) for $C_{25}H_{31}O_2$ calcd. 363.2324, found: m/z. 363.2325.

2.7.5 Oxidation of 40a to peroxides 43a and 43a'

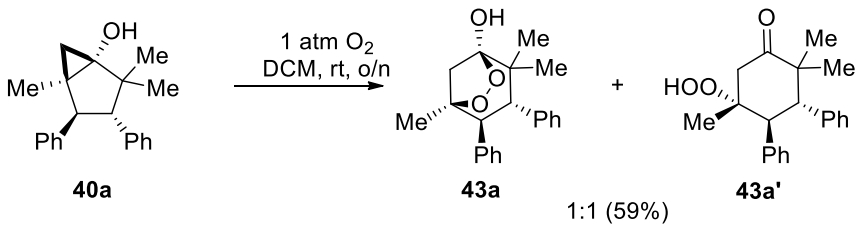

In the round bottom flask, alcohol **40a** (193 mg, 0.66 mmol) was dissolved in DCM (5 mL) and stirred at room temperature for 16 h under oxygen atmosphere. The solvent was removed by reduced pressure evaporation and the crude was purified by flash column chromatography (hexanes/EtOAc 8:1→5:1) to afford peroxides **43a** and **43a'** in 1:1 ratio (126 mg, 59%) as a white solid.

(*1R*,3S*,4S*,5S)-2,2,5-trimethyl-3,4-diphenyl-6,7-dioxabicyclo[3.2.1]octan-1-ol (43a):** R_f 0.26 (hexanes/EtOAc 8:2); mp 134–136 °C; IR (cast film) 3404, 3085, 3072, 2987, 2970, 2875, 1495, 1467 cm^{-1}; ^1H NMR (500 MHz, $CDCl_3$) δ 7.56 (d, *J* = 8.12 Hz, 1H), 7.18–6.94 (m, 8H), 6.75 (d, *J* = 8.3 Hz, 1H), 3.66 (d, *J* = 12.2 Hz, 1H), 3.15 (d, *J* = 12.5 Hz, 1H), 2.88(d, *J* = 11.8 Hz, 1H), 2.77 (s, 1H), 2.47 (d, *J* = 11.9 Hz, 1H), 1.02 (s, 6H), 0.99 (s, 3H); ^{13}CNMR (125 MHz, $CDCl_3$) δ 140.1, 138.4, 131.3, 128.3, 127.3, 126.9, 126.4, 126.2, 110.1,87.3, 54.6, 54.4, 50.2, 43.3, 21.4, 20.54, 20.51; HRMS (EI, $[M+Na]^+$) for $C_{21}H_{24}NaO_3$calcd.347.1618, found: m/z 347.1616.

(*3R*,4R*,5R)-5-hydroperoxy-2,2,5-trimethyl-3,4-diphenylcyclohexan-1-one (43a'):** R_f 0.24 (hexanes/EtOAc 8:2); mp 171–174 °C; IR (cast film) 3369, 3030, 2976, 1712, 1691, 1452, 1288 cm^{-1}; ^1H NMR (500 MHz, $CDCl_3$) δ 7.11–7.00 (m, 10H), 4.31 (d, *J* = 13.2 Hz, 1H), 3.68 (dq, *J* = 12.8, 1.0 Hz, 1H), 3.22 (d, *J* = 13.2 Hz, 1H), 2.63 (d, *J* = 12.8 Hz, 1H), 1.20 (s, 3H), 1.09 (d, *J* = 0.9 Hz, 3H), 1.02 (s, 3H); ^{13}C NMR (125 MHz, $CDCl_3$) δ 212.8,137.9, 137.4, 127.5, 127.4, 126.4, 126.4, 85.7, 52.3, 48.9, 48.1, 47.6, 23.4, 21.4, 18.8 (2 aromatic carbon resonances not detected, due to presumed spectral overlap); HRMS (ESI, $[M+Na]^+$) for $C_{21}H_{24}NaO_3$ calcd. 347.1618, found: m/z 347.1616.

2.7.6 Reduction of peroxides 43a and 43a' to alcohols 44a and 44a'

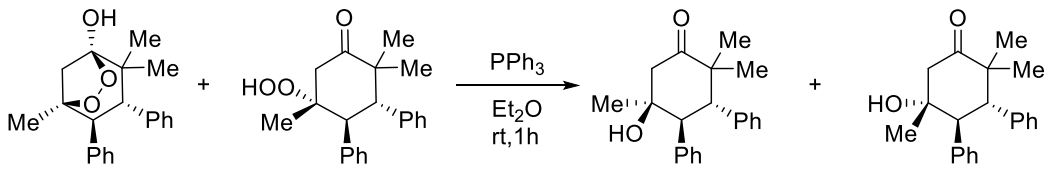

43a **43a′** **44a** (46%) **44a′** (50%)

In the round bottom flask, mixture of peroxides **43a** and **43a'** (126 mg, 0.39 mmol) was dissolved in diethyl ether (7 mL). To the reaction mixture triphenylphosphine was added (112 mg, 0.43 mmol) and stirred at room temperature for 1 h. The solvent was evaporated and the crude mixture was purified by column chromatography (hexanes/EtOAc 5:1) to afford alcohols **44a** (55 mg, 0.18 mmol) and **44a' (**60 mg, 0.2 mmol) as white solids.

(*3S*,4S*,5S)-5-hydroxy-2,2,5-trimethyl-3,4-diphenylcyclohexan-1-one (44a):** R_f 0.29 (hexanes/EtOAc 2:1); mp 168–170 °C; IR (cast film) 3459, 3030, 2972, 1708, 1452 cm^{-1}; ^1H NMR (400 MHz, $CDCl_3$) δ 7.21 (d, *J* = 8.1 Hz, 1H), 7.14–6.96 (m, 9H), 3.70 (d, *J* = 12.6Hz, 1H), 3.58 (d, *J* = 12.6 Hz, 1H), 3.07 (d, *J* = 14.0 Hz, 1H), 2.57 (d, *J* = 14.0 Hz, 1H), 1.50 (br s, 1H), 1.16 (s, 3H), 1.12 (s, 3H), 1.00 (s, 3H); ^{13}C NMR (100 MHz, $CDCl_3$) δ 212.8, 138.9, 138.2, 132.4, 129.5, 128.2, 127.6, 126.5, 126.2, 74.5, 52.9, 52.7, 51.2, 48.7, 30.3, 22.9, 21.2; HRMS (EI, $[M–H_2O]^+$) for $C_{21}H_{22}O$ calcd. 290.1671, found: m/z 290.1674.

(*3S*,4S*,5R)-5-hydroxy-2,2,5-trimethyl-3,4-diphenylcyclohexan-1-one (44a'):** R_f0.45(hexanes/EtOAc 2:1); mp 222–225 °C; IR (cast film) 3410, 2972, 1700, 1454 cm^{-1}; ^{1}HNMR (500 MHz, $CDCl_3$) δ 7.13–7.03 (m, 10H), 3.86 (d, *J* = 13.2 Hz, 1H), 3.24 (d, *J* = 13.1Hz, 1H), 3.17 (d, *J* = 13.2 Hz, 1H), 2.64 (d, *J* = 13.1 Hz, 1H), 1.67 (br s, 1H), 1.16 (s, 3H), 1.12 (s, 3H), 1.02 (s, 3H); ^{13}C NMR (175 MHz, $CDCl_3$) δ 212.2, 137.5, 137.4, 127.8, 127.4,126.8, 126.4, 73.6, 54.4, 52.6, 52.1, 49.0, 23.22, 23.17, 21.6; HRMS (EI, $[M−H_2O]^+$) for $C_{21}H_{22}O$ calcd. 290.1671, found: m/z 290.1672.

2.7.7 Preparation of (*1'R*,2'S**)-3',3',6'-trimethyl-2',3'-dihydro-[1,1':2',1''-terphenyl]-4'(1'H)-one (54a)

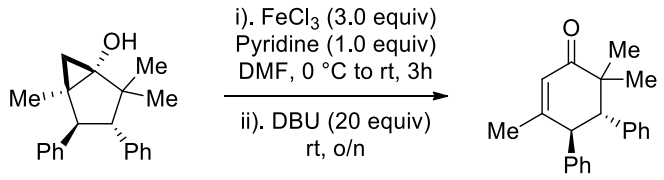

40a **54a**

In the round bottom flask, $FeCl_3$ (248 mg, 1.53 mmol) was dissolved in DMF (1.1 mL). In aseparate flask, to the solution of alcohol **40a** (150 mg, 0.51 mmol) in DMF (2.2 mL) was added pyridine (40.34 mg, 0.51 mmol). The solution of alcohol **40a** and pyridine was added to the solution of $FeCl_3$ dropwise over 15 min at 0 °C. The reaction mixture was stirred at 10 °C for 2 h and then at room temperature for 1 h followed by addition of DBU (1.53 mL, 10.2mmol). The stirring was continued overnight. The reaction mixture was poured into cold 1 M HCl (10 mL) and the aqueous phase was extracted with DCM (2 x 20 mL). Combined organiclayer was washed with water (20 mL), brine, dried over $MgSO_4$ and concentrated in vacuo. Purification by silica gel flash column chromatography (hexanes/EtOAc 10:1) afforded **54a** (88 mg, 0.30 mmol) as a white solid. R_f 0.32 (hexanes/EtOAc 10:1); mp 106–108 °C; IR (cast film) 3062, 3028, 2971, 2874, 1707, 1669, 1634, 1495 cm^{-1}; ^1H NMR (400 MHz, $CDCl_3$) δ 7.18–7.04 (m, 8H), 6.98–6.96 (m, 2H), 6.09 (q, *J* = 1.2 Hz, 1H), 3.95 (br d, *J* = 11.0 Hz, 1H), 3.22 (d, *J* = 11.0 Hz, 1H), 1.68 (app t, *J* = 1.1 Hz, 3H), 1.20 (s, 3H), 0.91 (s, 3H); ^{13}C NMR (125 MHz, $CDCl_3$) δ 204.8, 160.8, 141.0, 138.1, 128.2, 127.7, 126.6, 126.5, 126.3, 58.6, 50.4, 45.5, 23.1, 22.5, 20.6 (note: 2 signals missing due to spectral overlap); HRMS (EI, M^+) for $C_{21}H_{22}O$ calcd. 290.1671, found: m/z 290.1670.

2.7.8 Preparation of (*3S*,4S**)-2,2,5,5-tetramethyl-3,4-diphenylcyclopentan-1-one (60a)

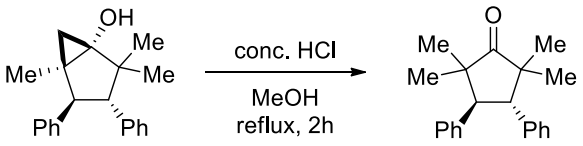

40a **60a**

In the round bottom flask, to the solution of alcohol **40a** (166 mg, 0.57 mmol) in methanol (18mL) was added conc. HCl (5.7 mL, 68 mmol) and heated at reflux for 2 h. After cooling downto room temperature, the reaction mixture was extracted with DCM (2 x 30 mL). Combinedorganic layers were washed with water (2 x 40 mL), brine, dried over $MgSO_4$ and concentrated in vacuo. Purification by silica gel flash column chromatography (hexanes/EtOAc 40:1) afforded **60a** (135 mg, 0.46 mmol) as a white solid. R_f 0.60 (hexanes/EtOAc 20:1); mp 128–130 °C; IR (cast film) 3028, 2959, 2929, 2866, 1736, 1601,1499 cm^{-1}; ^1H NMR (400 MHz, $CDCl_3$) δ 7.27–7.14 (m, 10H), 3.67 (s, *2*H), 1.28 (s, 6H), 0.76 (s, 6H); ^{13}C NMR (125 MHz, $CDCl_3$) δ 224.8, 137.3, 129.0, 128.0, 126.6, 52.6, 49.2, 24.7, 20.5; HRMS (EI, M^+) for $C_{21}H_{24}O$ calcd. 292.1827, found: m/z 292.1827.

2.7.9 Spectral data of d_2-40a and d_2-60a

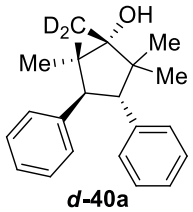

***d*-40a**

(*1R*,3S*,4S*,5R)-2,2,5-trimethyl-3,4-diphenylbicyclo[3.1.0]hexan-6,6-d2-1-ol (d_2-40a)** ^1H NMR (500 MHz, $CDCl_3$) δ 7.27–7.23 (m, 2H), 7.21–7.16 (m, 7H), 7.14–7.10 (m, 1H), 3.57 (d, *J* = 11.7 Hz, 1H), 2.56 (d, *J* = 11.7 Hz, 1H), 1.30 (s, 3H), 1.10 (s, 3H), 0.84 (s, 3H); ^{13}C NMR (125 MHz, $CDCl_3$) δ 141.3, 137.9, 129.8, 128.1, 127.8, 127.7, 126.4, 126.3, 69.6, 56.8, 50.8, 44.7, 32.2, 22.4, 19.3, 17.7 (quin, *J* = 23.1 Hz), 16.1; HRMS (EI, M^+) for $C_{21}H_{22}D_2O$ calcd. 294.1953, found: m/z 294.1952.

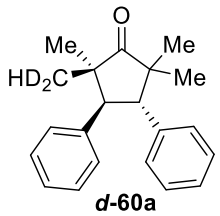

***d*-60a**

(*3S*,4S*,5R)-2,2,5-trimethyl-5-(methyl-d2)-3,4-diphenylcyclopentan-1-one (*d_2*-60a):** ^{1}H NMR (400 MHz, $CDCl_3$) δ 7.26–7.14 (m, 10H), 3.66 (s, 2H), 1.28 (s, 6H), 0.75 (s, 3H),0.72 (br s, 1H); ^{13}C NMR (125 MHz, $CDCl_3$) δ 224.9, 137.31, 137.30, 128.98, 128.97, 128.04, 126.6, 52.7, 52.6, 49.2, 49.1, 24.7, 24.6, 20.5, 20.0 (quin, J = 19.6 Hz); HRMS (EI, M^+) for$C_{21}H_{22}D_2O$ calcd 294.1953, found: m/z 294.1956.

Chapter 3

Synthesis of Cyclobutanes via Lewis Acid Mediated Formal Crossed [2+2] Cycloaddition of *o*-Styrenyl Chalcones

3.1 Introduction

Cyclobutane and its derivatives, being a commonly encountered basic structural unit in a large number of natural products and biologically active compounds, are of particular interest for synthetic and medicinal chemists.[112] Restricted spatial arrangement of substituents dictated by rigidity of this strained cyclic motif makes cyclobutane-containing molecules attractive targets for drug design[113] due to their promising therapeutic effects.[114] Their biological activity can span from anticancer, anti-inflamatory, analgesic, insect-repellant, phytotoxins to UV protective properties and more.[115] Figure 3.1 illustrates some representative examples of biologically active compounds containing the cyclobutane unit.[116,117]

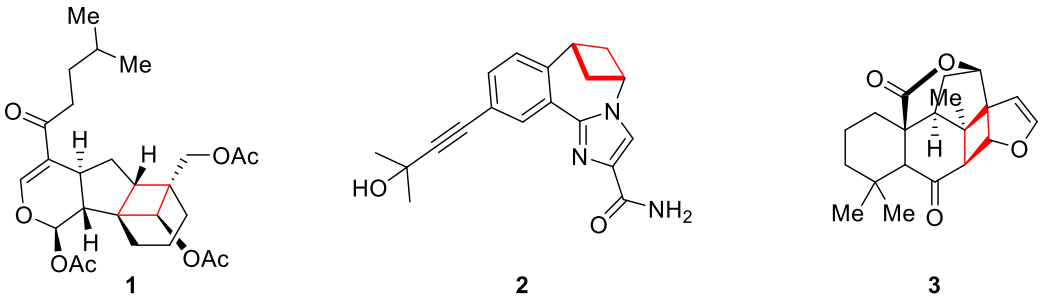

1
Plumisclerin A
(anticancer activity)

2
benzoimidazoazepine derivative
(antiinflammatory/anticancer activity)

3
Haplomitrin B
(phytotoxin)

Figure 3.1 Representative examples of cyclobutane-containing compounds.

As a small sized cyclic molecule, cyclobutane possesses the ring strain energy of 26.7 kcal/mol. To minimize the strain caused by eclipsing interactions, it adopts a puckered conformation, in which substituents can occupyaxial-like or equatorial-like positions (Figure 3.2).[118] For *cis*-1,3-disubstituted cyclobutanes, conformers **4b** with both substituents in equatorial-like positions are slightly favored over isomers **4a** in which both substituents adopt axial-like positions. For *gem*-dimethyl substituted

cyclobutanes, ring strain energy decreases by 8 kcal/mol compared to their substituted analogues due to the Thorpe–Ingold effect.

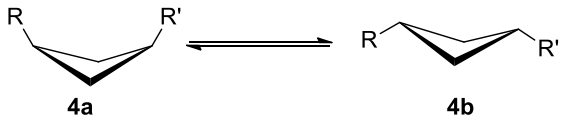

Figure 3.2 Conformations in cyclobutanes.

3.2 Mechanistic Fundamentals of Photochemical [2+2] Cycloadditions

A large number of methods allow access to cyclobutane derivatives. Among them, photochemical [2+2] cycloadditions are the most prevalent approaches owing to atom economy and environmental considerations. They involve two olefin partners, one of which must be excited by either UV or visible light, forming two new σ-bonds form at the expense of two π-bonds simultaneously.

There are several modes of inducing photochemical [2+2] cycloadditions. In the absence of any photosensitizer, the substrate is excited via direct absorption of a photon, thus moving from the ground state S_0 to its short-lived first excited S_1 singlet state.[119] Then, the excited olefin undergoes a subsequent addition to another π-partner or another identical molecule (Scheme 3.1a). For non-conjugated olefins with a high lying S_1 state, excitation with long wave light sources is not always successful. However, use of metal catalysts (mostly Cu(I) salts) can enable the excitation process by lowering the S_1 state via complexation of the metal to the olefin (Scheme 3.1b).[120]

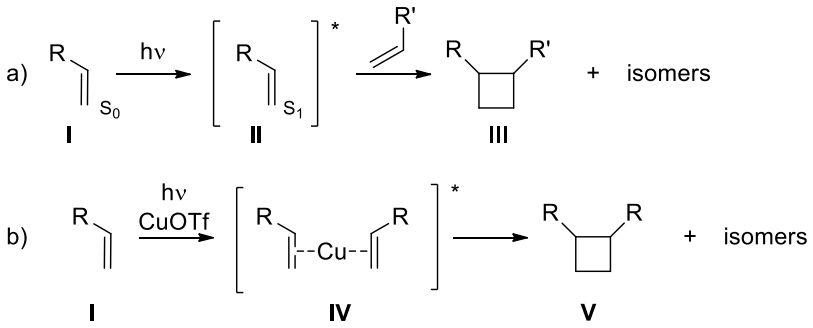

Scheme 3.1 Photochemical [2+2] cycloaditions via S_1 excited state.

The long-lived T_1 triplet excited state of olefins is lower in energy compared to S_1, and intersystem crossing is required to achieve a transition from S_1 to T_1 via spin flip. The lower energy of the T_1 state is the result of less repulsion of the unpaired electrons which in turn is because of the electrons to be spatially more far apart than in S_1 state.[121] In conjugated carbonyl compounds, which meet these criteria ideally, ISC is fast and facile (Scheme 3.2). 1,4-biradical species **VII** formed upon olefin attack on intermediate **VI** undergoes another ISC to singlet hypersurface, affording product **III**.[122]

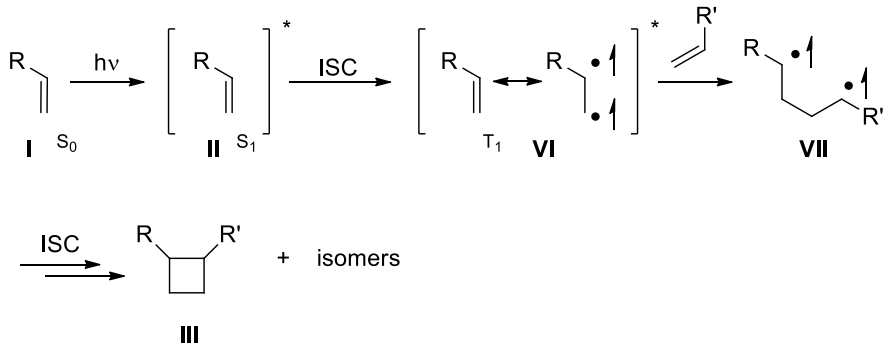

Scheme 3.2 Photochemical [2+2] cycloadditions via a T_1 excited state.

Direct excitation is not the only way of achieving the T_1 state. It could be done via photosensitization, which implies triplet energy transfer to olefin from another photoexcited molecule. An ideal candidate for photosensitization must have low lying S_1 and high lying T_1 states. For effective energy transfer, a close spatial arrangement of the photosensitizer and olefin molecules is required, and the olefin should have a lower energy T_1 state (VI) than the T_1 of the photosensitizer (Figure 3.3). Via this approach, excitation could be achieved at a longer wavelength than in the case of direct excitation to the olefin S_1 excited state (II).

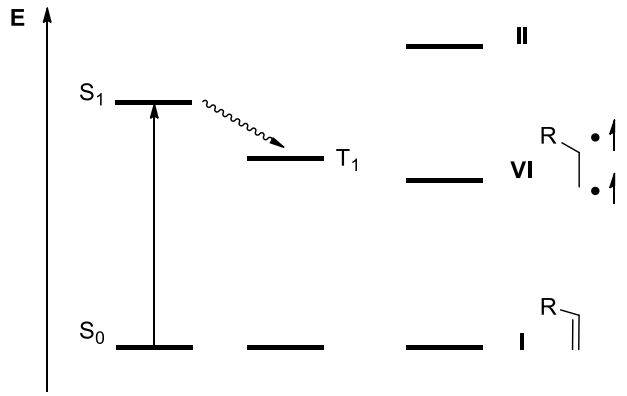

Figure 3.3 Photochemical [2+2] cycloadditions employing triplet sensitizers.

Except for photosensitization, [2+2] photocycloaddition also can be initiated by a single electron transfer from a redox catalyst (Scheme 3.3). In this transformation, the substrate gets reduced/or oxidized to the radical ion **VIII** before reacting with another olefin to form the radical ion **IX,** which cyclizes to **X** before back electron transfer. Scheme 3.3 represents the reductive process, while for the oxidative quench, the same sequence proceeds via involvement of radical cation species.

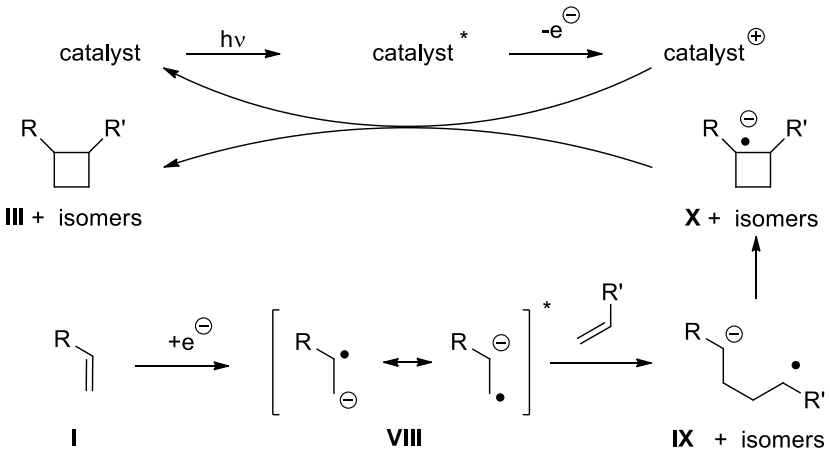

Scheme 3.3 Photochemical [2+2] cycloadditions mediated by single electron transfer.

3.3 Synthesis of Cyclobutanes via Photochemical [2+2] Cycloadditions

The first documented [2+2] cycloadditions were the photodimerization of identical olefins on exposure to sunlight to form a cyclobutane ring. The very first example of this process was described by Liebermann in 1877 when thymoquinone **5** underwent photodimerization in its solid state (Scheme 3.4).[123] Later, this reaction was shown to be possible in solution as well.[124] Since then, an overwhelming amount of work has been carried out on photoinduced [2+2] cycloadditions.

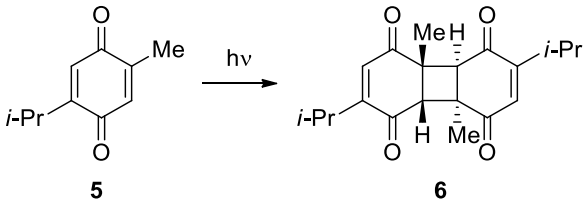

Scheme 3.4 Photodimerization of thymoquinone.

An interesting example of using direct excitation (strategy described in Scheme 3.1a) towards total synthesis of a natural product is the work by the Hsung group in 2003.[125] In the total synthesis of (±)-rhododaurichromanic acids A and B in six steps with an overall yield of 15%, one of the steps was the intramolecular photochemical [2+2] cycloadditionof methyl esters of daurichromenicacids **7** (racemic). Irradiation of **7** with a medium pressuremercury lamp (Pyrex filter) gave esters **8** of (±)-rhododaurichromanic acids A and B as a 50/50 mixture of epimers differing at the C12 carbon atom. Upon saponification, **8** delivered a racemic mixture of (±)-rhododaurichromanic acids A and B (**9)** (Scheme 3.5).

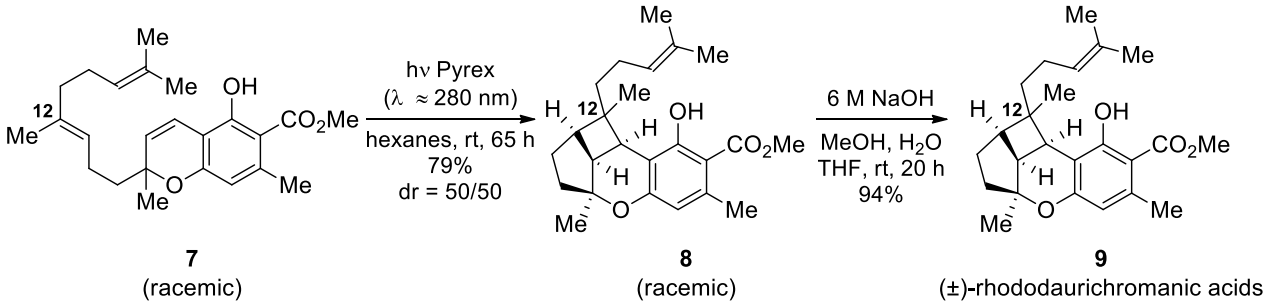

Scheme 3.5 [2+2] Cycloaddition via direct photo-excitation.

Enantiomerically pure natural products can be formed via [2+2] photocycloaddition when starting with enantiomerically pure precursors. Application of metal catalyst assisted direct excitation strategy (strategy described in Scheme 3.1b) can be exemplified in the work of Ghosh and co-workers.[126] The key step in the synthesis of marine diterpene bielschowskysin was the intramolecular stereoselective Cu(I)-catalyzed [2 + 2] photocycloaddition of glucose-derived 1,6-heptadiene **10** to construct a highly functionalized bicyclo[3.2.0]heptane moiety in high yield with excellent diastereoselectivity (Scheme 3.6).

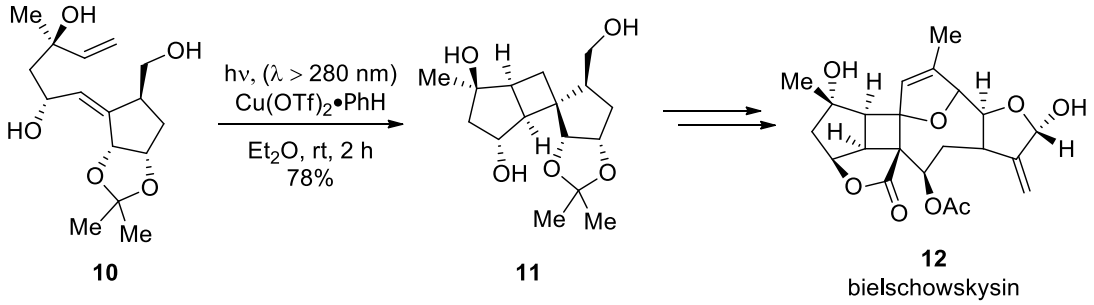

Scheme 3.6 Catalyst assisted direct photo-excitation.

Photoredox catalysis (strategy described in Scheme 3.3) is another powerful and useful strategy employed in [2+2] cycloadditions, along with direct excitation, Cu(I) catalysis, and energy transfer approaches. Photocatalysts' exclusive oxidative or reductive potential contribute to the main progress in this field. Both cationic and anionic pathways are equally realizable pathways en route to final products.

Yoon's 2008 work demonstrated the efficacy of $Ru(bpy)_3Cl_2$as a reductive photocatalyst to induce intramolecular [2+2] cycloaddition of different aryl and heteroaryl bis(enones) under visible light irradiation.[127] The necessity of each component in the reaction was confirmed by mechanistic studies. The base served as a reductive quencher to reduce the photoexcited $Ru(bpy)_3^{2+}$ to $Ru(bpy)_3^{+}$, while $LiBF_4$ was required to activate enone **13** before being reduced to the radical anion **14** by the excited catalyst. However, the protocol was limited to bis(enones) with aromatic substituents, and substitution with aliphatic groups proved unsuccessful (Scheme 3.7).

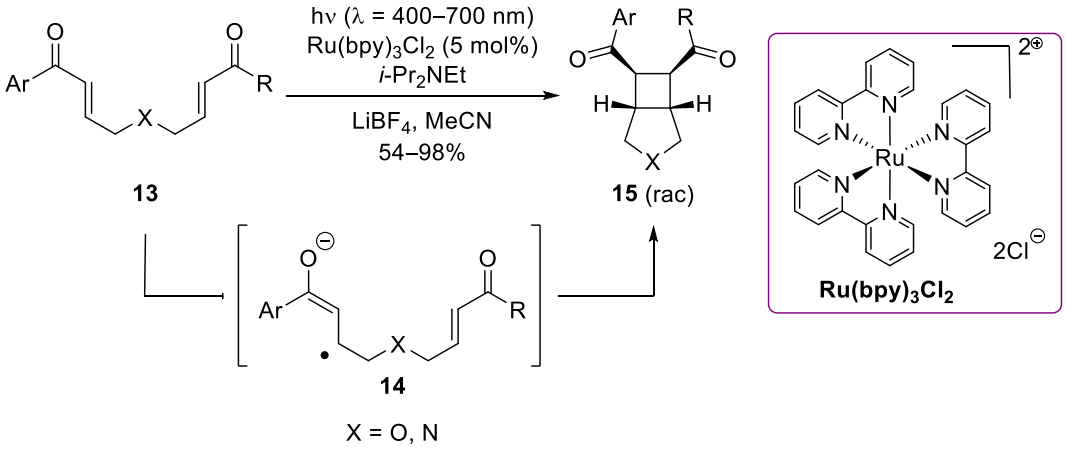

Scheme 3.7 Reductive photocycloaddition.

In later work by the same group (2010), the competence of a similar photocatalyst in visible light induced intramolecular oxidative [2+2] cycloaddition of bis(styrenes) was demonstrated.[128] The employed photocatalyst $Ru(bpy)_3(PF_6)_2$, depending on the appropriately chosen quencher, can reveal photooxidative as well as photoreductive reactivity. In combination with 15 mol% viologen (MV^{2+}) and 1 mol% $Ru(bpy)_3^{2+}$, electron-rich olefins **16** underwent [2+2] cycloaddition under ambient sunlight conditions. However, mechanistic studies revealed the necessity of an electron-donating methoxy-group at least on one of the termini of olefins for the key radical cation **17** formation to be facile (Scheme 3.8).

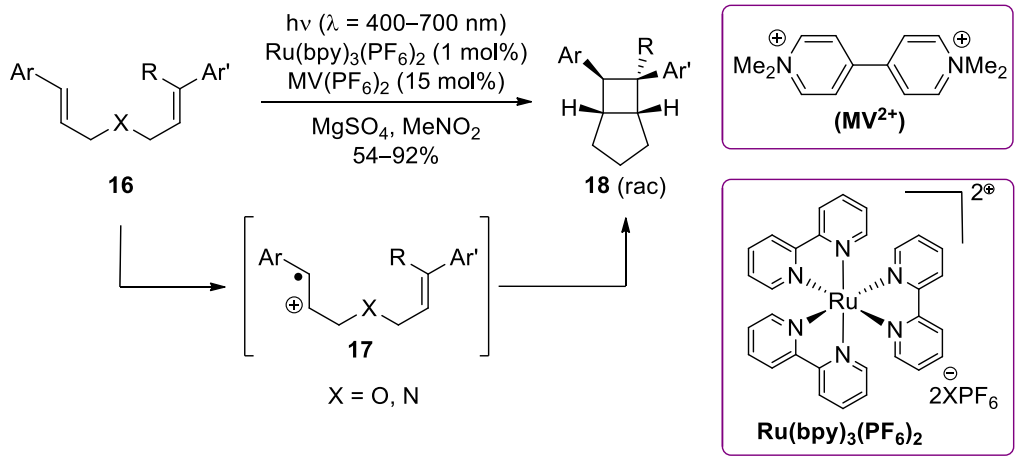

Scheme 3.8 Oxidative photocycloaddition.

3.3.1 Intramolecular [2+2] Photocycloaddition of Conjugated Enones: Straight vs Crossed Addition

As already mentioned above (Scheme 3.2), [2+2] cycloadditions with the participation of enones proceed through the T_1 excited state and are characterized with the fast ISC. For enones with olefin tethers, regiochemistry of a [2+2] ring closure event is governed more by the size of the formed ring than the electronics of the substituents. Olefins may undergo straight or crossed additions, forming two different regioisomers (Scheme 3.9). For enones with a tether length of 3 and 4 (in most cases), straight addition products **XII** are predominant. When n = 3, a 5-membered ring arises from cyclization, while for a tether with n = 4, a 6-membered ring formation is more advantageous. If the tether between reacting olefins only consists of two carbons, then the reaction yields crossed addition products **XIII**.

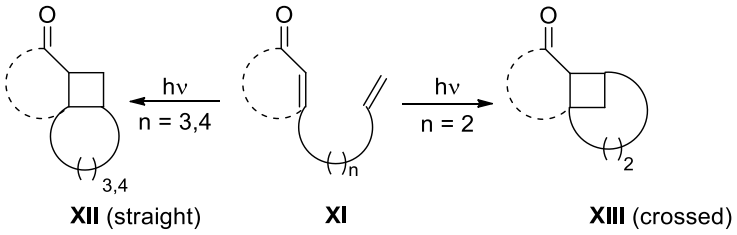

Scheme 3.9 Regiocontrol in [2+2] cycloadditions.

The regiochemistry of [2 + 2] photocycloaddition as well as the outcome of the reaction can be influenced or improved by the nature and length of the tether. A properly chosen tether can promote a high diastereoselectivity of the process.

An example of straight addition is the work published by Navarro and Reisman in 2012.[129] During the preparation of the aza-propellane core of acutumine, high degree of regioselectivity (forming straight product) as well as diastereoselectivity was observed. When **19** was irradiated at the wavelength of 350 nm in pentane, the cycloaddition product **20** was obtained in 54% yield with excellent regio- and diastereocontrol (Scheme 3.10).

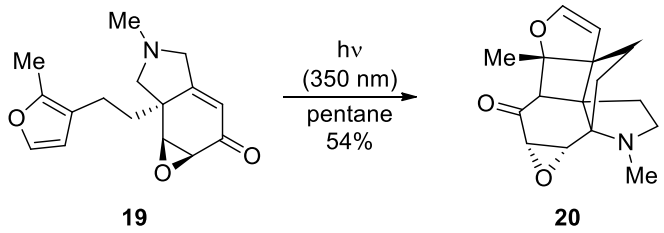

19 **20**

Scheme 3.10 Catalyst assisted direct photo-excitation.

An interesting example of crossed addition was published by Winkler and co-workers in 2009 (strategy described in Scheme 3.2).[130] The authors found that by irradiation through a uranium filter, benzenethiazoline tethered enone **21** could undergo desulfurative crossed [2+2] cycloaddition via the intermediacy of enecarbamate **22**. The reaction was postulated to proceed via the T_1 excited state of the enone (Scheme 3.11).

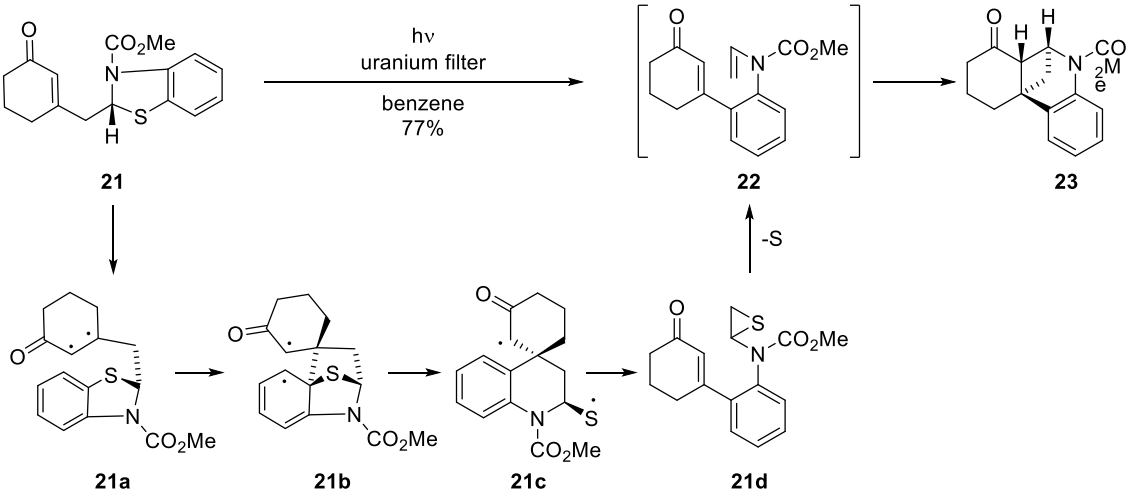

Scheme 3.11 Crossed [2+2] cycloaddition of enones.

Very recently (2017), Kwon's group reported visible light induced intramolecular crossed [2+2] cycloaddition of *o*-styrenyl enones **24** using polypyridyl Ir(III) catalyst as a triplet photosensitizer.[131] The reaction yielded bridged bicyclic structures **26** with high yields and excellent diastereoselectivities. Mechanistically, the reaction proceeded via energy transfer from the triplet sensitizer to enone **24,** which in the triplet state underwent cyclization to form the thermodynamically most stable biradical **25,** as predicted by computational studies. Upon second cyclization, bridged products were delivered in high yields with outstanding stereocontrol (Scheme 3.12).

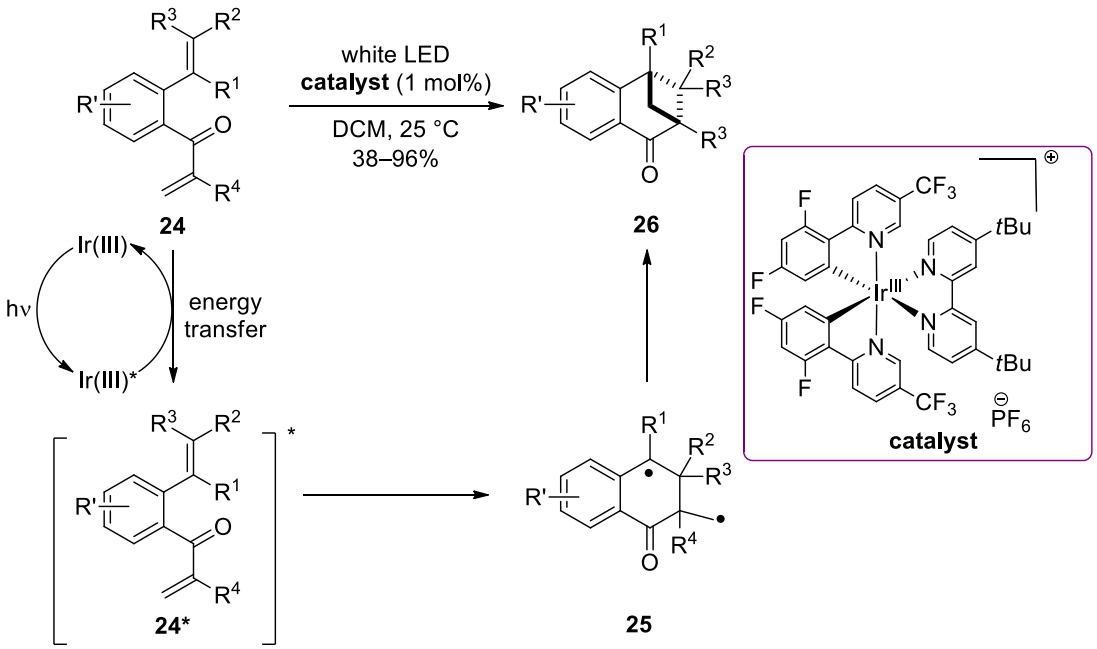

Scheme 3.12 Crossed [2+2] cycloaddition via energy transfer.

3.4 Lewis Acid Catalyzed Thermal [2+2] Cycloadditions

Even though non-photochemical methods for the generation of 4-membered carbocycles via Lewis or Brønsted acidactivation of olefin precursors do not require high energy irradiation or expensive catalysts, they are still less prominent. Thermal non-catalytic variants require heating, which in many cases can be disadvantageous in terms of substrate stability and product control. The use of polarized substrates in combination with Lewis acids would be justified to get better control of the reaction, and this approach has been investigated thoroughly towards catalytic [2+2] cycloadditions.[132]

Dimerization of alkenes under heating conditions is the most illustrative example of thermal [2+2] cycloadditions for constructing the cyclobutane skeleton. They were postulated to proceed via biradical intermediates that were recently proven byradical scavenging reactions and electron paramagnetic resonance.[133]

Based on the previous work by Engler et al.[134] on stereoselective [2+2] cycloaddition of styrenes and quinones in the presence of a stoichiometric amount of

Ti(IV) catalyst, Narasaka and co-workers in 1989 reported the first catalytic enantioselective [2+2] cycloaddition.[135] The chiral Ti-TADDOL complex could promote enantioselective [2+2] cycloaddition between unsaturated oxazolidinones **27** and alkenyl sulfide **28**, as well as related alkynyl or allenyl examples with high degrees of enantioselectivity (Scheme 3.13). A stepwise mechanism with the formation of dipolar intermediate **30** was proposed to explain the product formation (Scheme 3.14).

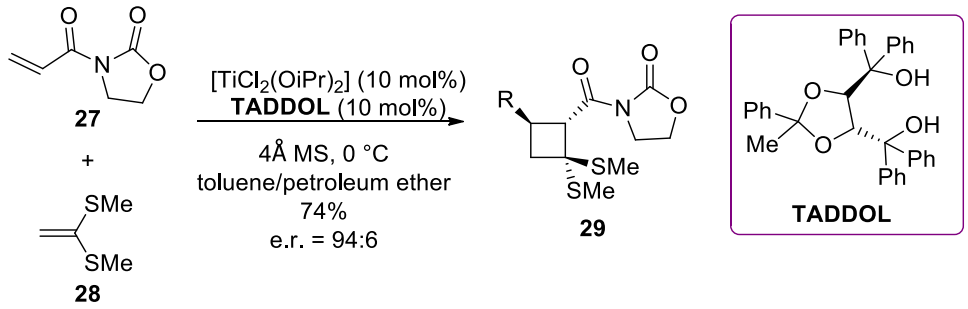

Scheme 3.13 Representative example of Ti(IV) catalyzed enantioselective [2+2] cycloaddition.

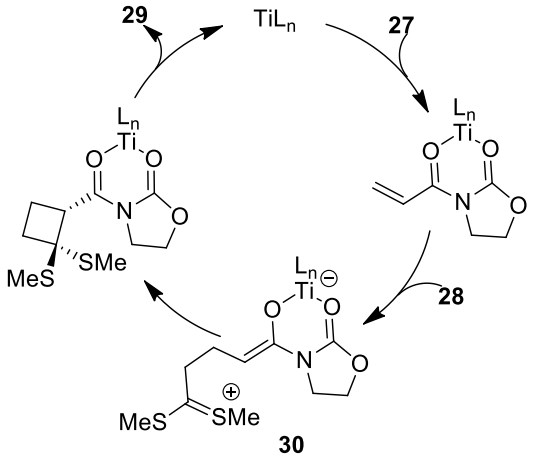

Scheme 3.14 Mechanistic proposal for stepwise [2+2] cycloaddition.

Recently (2015), Brown's group demonstrated that weakly or nonpolarized alkenes **31** in the presence of a chiral oxazaborolidine catalyst can undergo enantioselective [2+2] cycloadditions with allenoates **32**; however, the adducts were proposed to be formed via a concerted mechanism.[136] Oxazoborolidine **33** was found to

be the best catalyst for achieving high degrees of enantioselectivity, and an electron deficient aryl substituent on boron proved to be an effective promoter to achieve reasonable yields. A concerted mechanism was postulated based on the stereospecificity of the reaction, via involvement of the transition state **35** (Scheme 3.15).

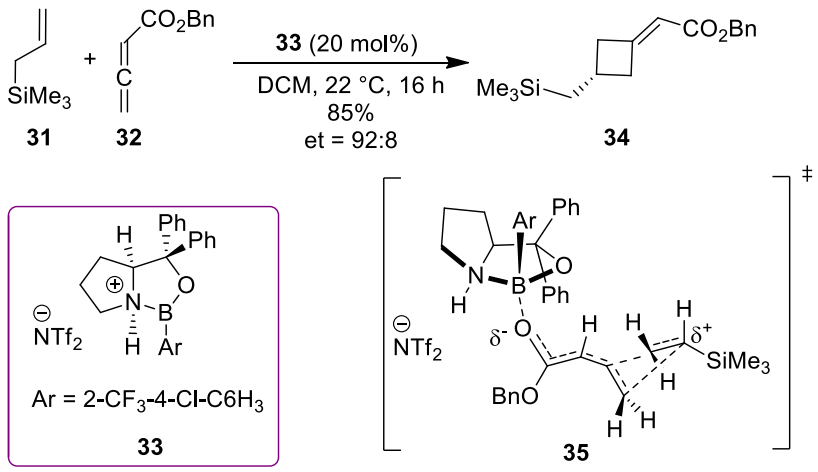

Scheme 3.15 Representative example of oxazoborolidine mediated [2+2] cycloaddition.

3.5 Lewis Acid Assisted Photo [2+2] Cycloadditions

In contrast to stereocontrolled thermal cycloaddition strategies, in most of the photochemical analogues, control of racemic background reactions for photoexcited substrates that are not bound to a catalyst remains challenging. Even though approaches using chiral auxiliary or other non-covalent directing groups have been developed to control the stereochemical outcome of the cycloadditions, these stereocontrollers were used in stoichiometric amounts, and the catalytic approaches were shown to be more challenging.

In 2014, the Yoon group reported a conceptually new dual-catalysis approach for enantioselective [2+2] cycloadditions of α,β-unsaturated ketones to the corresponding cyclobutanes by using a visible light-absorbing transition-metal photocatalyst and a stereocontrolling Lewis acid cocatalyst.[137] Lewis acid activated aryl enones underwent one-electron reduction by the Ru(I) complex generated by visible light irradiation of

$Ru(bpy)_3^{2+}$ in the presence of an amine donor. Two factors were responsible for diminishing the undesired background racemic reaction: first, under irradiation with the wavelength at which the ruthenium catalyst underwent photoexcitation (λ = 450 nm), enone substrates **36** remained inert; second, Lewis acid activation made enones prone to one-electron reduction. Use of 5 mol% $Ru(bpy)_3Cl_2$ as a photocatalyst and 10 mol% of a Lewis acid complex composed of a 1:2 ratio of $Eu(OTf)_3$ and chiral ligand **38** delivered adducts **39** in moderate to high yields with high enantiopurity (Scheme 3.16). Homodimerization of the aryl enone **36** was avoided by the use of five-fold excess of aliphatic enone **37**.

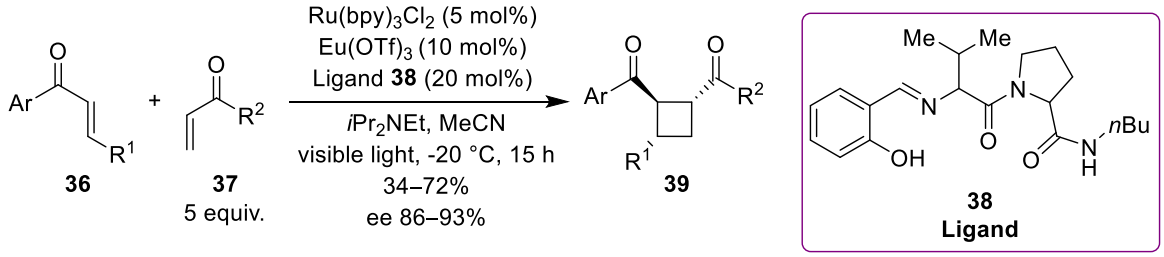

Scheme 3.16 Lewis acid assisted photochemical [2+2] cycloaddition.

A few years later, the same group reported highly enantioselective crossed photo [2+2] cycloadditions of 2′-hydroxychalconeswith a range of styrene coupling partners using Lewis acid catalyzed triplet sensitization.[138] Lewis acid coordination to chalcone derivatives significantly lowered the singlet-triplet gap (E_{ST} = 54 kcal/mol). This effect made energy transfer from the photosensitizer (E_{ST} = 45 kcal/mol) to the Lewis acid activated substrate (E_{ST} = 32 kcal/mol) thermodynamically feasible, and high levels of enantioselectivities could be achieved with chiral Lewis acids.[139] Use of 10 mol% $Sc(OTf)_3$, 15 mol% *t*-BuPybox, and 2.5 mol% $Ru(bpy)_3^{2+}$ asa triplet photosensitizer upon irradiation of 2′-hydroxychalcones **40** and styrenes **41** with a 23W compact fluorescent light (CFL) yielded cycloadducts **42** in high yields and with high degrees of enantioselectivity (Scheme 3.17).

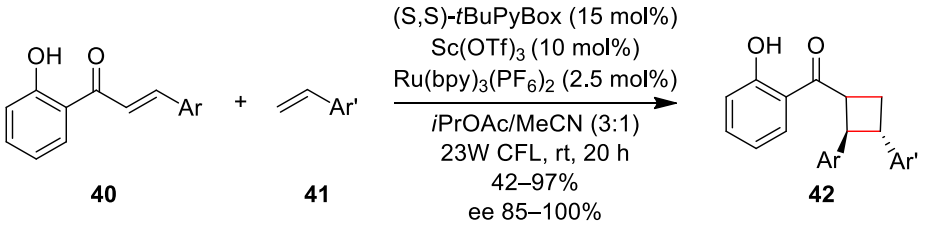

Scheme 3.17 Photochemical [2+2] cycloaddition by Lewis acid catalyzed triplet sensitization.

3.6 Formal [2+2] Cycloadditions

According to the Woodward–Hoffmann rules of conservation of orbital symmetry, concerted thermal [2+2] cycloadditions are symmetry disallowed and, therefore typically proceed via a stepwise mechanism. This phenomenon can account for the fact that photochemical approaches for [2+2] cycloaddition are more prevalent. However, during the stepwise process, long-lived intermediates get generated that are disadvantageous as some undesired side reactions can take place.

Yamamoto and co-workers in 2008 used an organoaluminum catalyst to promote a formal [2+2] cycloaddition between silyl enol ethers and α,β-unsaturated esters to get access to cyclobutane scaffolds.[140] Steric and electronic stabilization of reaction intermediates was believed to be a determining factor for avoiding undesired transformations. A sterically bulky but electronically strongly donating tris(trimethylsilyl)silyl group on enols **43** was found to be the proper substituent providing the desired results. Organoaluminum catalyst $Al(NTf_2)_3$ in 3 mol% loading was efficient, delivering products in excellent yields with high levels of diastereoselectivity (Scheme 3.18). The reaction was believed to proceed via a stepwise Michael-aldol type mechanism via a zwitterionic intermediate **49** (Scheme 3.19).

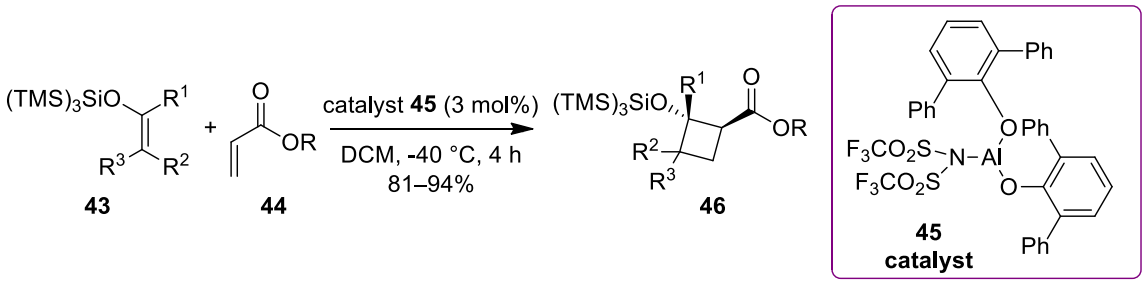

Scheme 3.18 Formal [2+2] cycloaddition via a Michael-aldol type reaction.

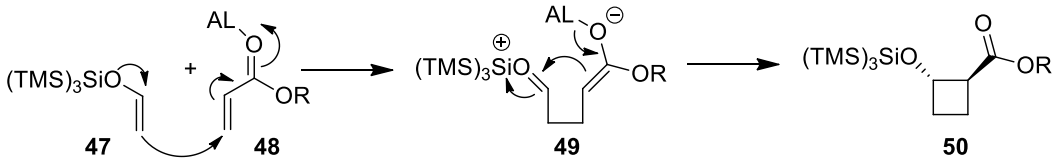

Scheme 3.19 Proposed mechanism for formal [2+2] cycloaddition.

During studies of the behaviour of highly conjugated stryryl chalcone systemsan interesting new nonphotochemical [2+2] cycloaddition process that was discovered serendipitously. The details of these studies will be describedbelow.

3.7 Results and Discussion

As already mentioned above, thermal approaches towards cyclobutane ring construction via [2+2] cycloaddition are scarce compared to their photochemical equivalents. In this context, development of efficient alternative strategies would give synthetic chemists better leverage to alleviatethe task.

The Nazarov cyclization is a matter of continuous interest in our group to build complex cyclic skeletons (see Chapter 1 for more details). Other substrates resembling the Nazarov precursors may well be potentially susceptible to similar electrocyclization processes to access different size ring systems.

Opatz's 2016 work[62] (more details in Chapter 1) prompted us to modify 4π cross-conjugated divinyl ketones into their 6π analogues by adding extra conjugation and converting them into substituted *o*-styrenyl chalcones. We were hopeful that this

modification could reveal novel electrocyclization reactivity, which could lead to 7-membered ring systems through a higher order electrocyclization pathway.

To our surprise, treatment of the new substrate **51a** with 1.2 equiv BF_3•OEt_2, a Lewis acid commonly employed in the Nazarov cyclization,[141] in DCM yielded two diastereomers **52a** and **52a′** as a product of formal crossed [2+2] cycloaddition (Scheme 3.20). X-ray crystallographic analysis played a crucial role in determining the structure and stereochemistry of **52a** (Figure 3.4).[142]

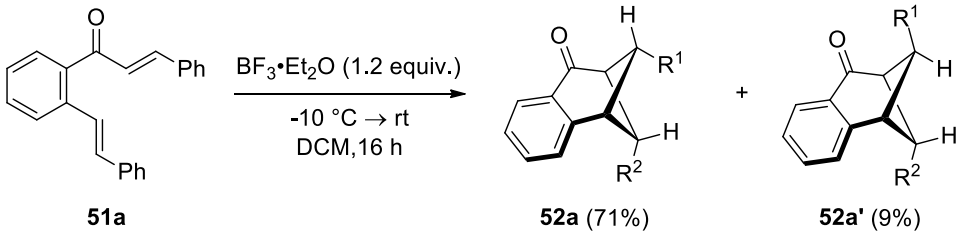

51a **52a** (71%) **52a'** (9%)

Scheme 3.20 Formal crossed [2+2] cycloaddition of *o*-styrenyl chalcone.

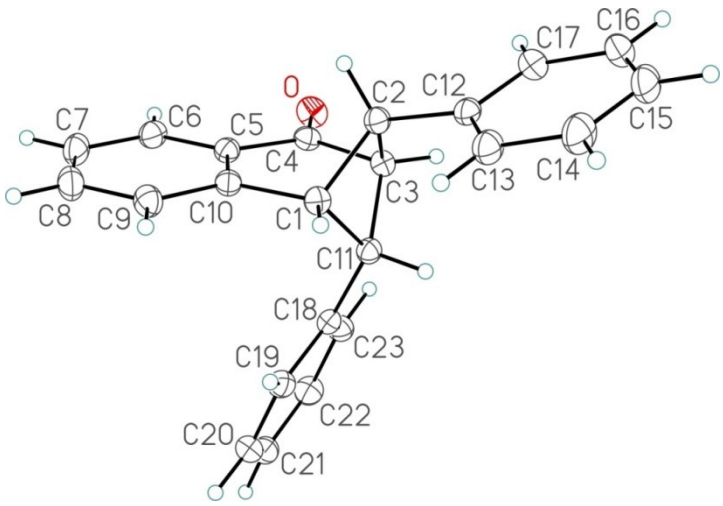

Figure 3.4 X-Ray crystal structure of **52a.**

This intriguing outcome inspired us to investigate the reaction conditions and screen various Lewis acids, along with other reaction parameters, on model substrate **51a** (Table 3.1). The use of 2.0 equiv. of BF_3·Et_2O slightly improved the yield of the products; this could be attributed to the full conversion of the starting material into the products (entry 1). Heating **51a** at reflux eroded the selectivity of the reaction,

delivering both diastereomers in comparable yields (entry 2). It is worth noting that whether the substrate **51a** was exposed to light or not, there was no significant change in the reaction outcome (entry 3). Irradiation with a blue light emitting diode (LED) in the absence of a Lewis acid gave no product (entry 4). However, due to decomposition of the starting material under irradiation with a UV lamp for 3 h, an uncharacterizable complex mixture was produced (entry 5). When other Lewis acids were used in catalytic amounts, no satisfactory results could be obtained. The inability of $Cu(OTf)_2$, $Sc(OTf)_2$, or $In(OTf)_3$ to trigger the reaction at room temperature was tackled with the application of heat; however, the isolated products were impure, or poor conversions were observed by crude NMR analysis (entries 6–9). Nor could a catalytic amount of TfOH fully convert the starting material into cycloadducts (entry 10). While a stoichiometric amount of organoaluminum reagent only delivered 1,2 and 1,4 methyl addition products with no traces of the desired product formation (entry 11), Al(III) chloride was too harsh and caused decomposition of the starting material (entry 12). A stoichiometric amount of TMSOTf as an activator produced an excess amount of impurities, which hampered isolation of the pure products (entry 13). Based on the observations, it was concluded that the optimal conditions for the desired transformation was the use of 2.0 equiv. of $BF_3{\cdot}Et_2O$ in DCM, while stirring at room temperature for 16 h.

Table 3.1 Finding optimal conditions for the formal [2+2] cycloaddition.

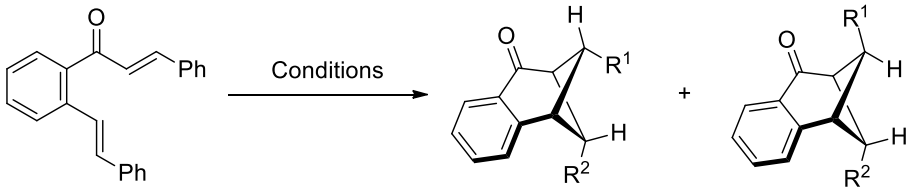

51a **52a** **52a'**

Entry	Acids (equiv.)	Solvent	T (°C)	Reaction time	Yield (%) (**52a**)[a]	Yield (%) (**52a′**)
1	2.0 $BF_3{\cdot}Et_2O$	DCM	-10 °C → rt	16h	74	10
2	2.0 $BF_3{\cdot}Et_2O$	DCE	-10 °C→reflux	16 h	46	34
3	2.0 $BF_3{\cdot}Et_2O$	DCM	-10 °C → rt	16 h	75[b]	6
4	Blue LED	DCM	rt	16 h	-	-
5	UV	DCM	rt	3 h	-[c]	-
6	0.2 $Cu(OTf)_2$	DCE	rt → 60 °C	16 h	-[d]→ -[e]	-
7	0.2 $Sc(OTf)_2$	DCE	rt → 60 °C	16 h	-[d]→ 9%(NMR)	-
8	0.1 $In(OTf)_3$	DCE	rt → 60 °C	16 h	-[d]→ 14%(NMR)	-
9	0.1 $In(OTf)_3$	MeCN	50 °C	16 h	6% (NMR)	-
10	0.1 TfOH	DCM	0 °C → rt	16 h	35%(NMR)	Trace (NMR)
11	1.2 $AlMe_3$	hexanes	-41 → 0 °C	2.5 h	-[f]	-
12	1.2 $AlCl_3$	DCM	-10 → rt	16 h	-[d]	-
13	1.2 TMSOTf	DCM	-10 → rt	16 h	-[g]	-

[a] Yields are based on isolated products after chromatography, unless otherwise stated. [b] The reaction was performed in the dark. [c] Due to decomposition of SM, a complex mixture was observed. [d] No reaction; only SM observed by crude NMR analysis. [e] The full conversion of SM was observed, but due to excess side product formation, isolation of the pure product proved to be impossible. [f] Only 1,2 and 1,4 methyl addition products were isolated with unsatisfactory NMR purity; no evidence for product formation was seen. [g] A complex mixture was observed on TLC, which impeded the isolation of pure products.

Our curiosity prompted us to investigate the substituent effect on the generality of the methodology. We alternated substituents on olefin and enone tethers as well as in the phenylene ring (Table 3.2). First, substrates with identical aryl groups on the ends of both olefin and enone chains were examined. To our delight, both electron-withdrawing as well as donating groups either in para- or ortho-positions were all well tolerated, delivering cycloadducts in high overall yields (entries 1–5). The structure and stereochemistry of the second diastereomer **52f′** were confirmed by X-ray crystallography (Figure 3.5).[142] Modification of the phenylene ring by placing a fluoro group in the 2nd or a methyl group in the 5th positions did not deteriorate the reaction yields (entries 6 and 7). Unfortunately, substrate **51i** with electron releasing groups furnished the products in diminished yields, probably due to the ability of the nitrogen free lone pair to coordinate to the Lewis acid and cause some undesired side reactions. Exposure of **51j** to standard reaction conditions delivered cycloadducts **52j** and **52j′** in low yields, along with a small amount of **53j** due to proton elimination from the benzyl cation formed uponthe cyclobutane ring opening (entry 9). Substrate **51k** witha methyl group in the α-position of the enone underwent smooth cyclization (entry 10).

Table 3.2 Generality of the formal [2+2] cycloaddition.

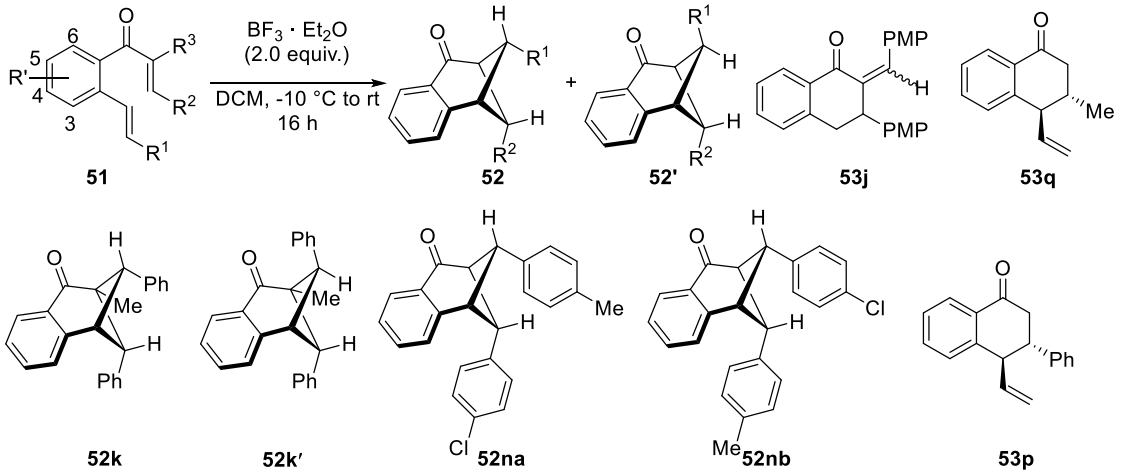

Entry	Substrate	R^1/R^2	R^3	R′	Products	Yield (%)[b]
1	**51b**	4-Cl-Ph/4-Cl-Ph	H	H	**52b/52b′**	62/25
2	**51c**	4-F-Ph/4-F-Ph	H	H	**52c/52c′**	63/18
3	**51d**	2-Cl-Ph/2-Cl-Ph	H	H	**52d/52d′**	68/17
4	**51e**	4-Tolyl/4-Tolyl	H	H	**52e/52e′**	41/39
5	**51f**	1-naphthyl/1-naphthyl	H	H	**52f/52f′**	67/23
6	**51g**	Ph/ Ph	H	5-F	**52g/52g′**	55/26
7	**51h**	Ph/ Ph	H	3-Me	**52h/52h′**	44/23
8	**51i**[c]	4-NMe_2-Ph/4-NMe_2-Ph	H	H	**52i/52i′**	28/28
9	**51j**[c]	4-OMe-Ph/4OMe-Ph	H	H	**52j/52j′/53j**	20/27/17
10	**51k**	Ph/ Ph	Me	H	**52k/52k′**	48/36
11	**51l**	4-Tolyl/4-CF_3-Ph	H	H	**52l/52l′**	55/30
12	**51m**	4-CF_3-Ph/4-Tolyl	H	H	**52m/52m′**	-[d]
13	**51n**	4-Tolyl/4-Cl-Ph	H	H	**52na/52nb/52n′**	23/4/44
14	**51o**	Ph/Me	H	H	**52o/52o′**	62/19
15	**51p**[e]	Me/Ph	H	H	**52p/52p′/53p**	0/0/32
16	**51q**[e]	Me/Me	H	H	**52q/52q′/53q**	0/0/22
17	**51r**	H/H	H	H	**52r/52r′**	-[f]

[a] The reaction was performed on a 0.3 mmol scale. If 0.3 mmol was under 100 mg by mass, the scale was raised to 100 mg of starting material. Standard procedure: a solution of *o*-styrenyl chalcone (0.3 mmol) in CH_2Cl_2 (4 mL) was added to the cooled solution (-

10 °C) of 2.0 equiv. of $BF_3{\cdot}Et_2O$ in CH_2Cl_2 (1 mL). After stirring at -10 °C for 0.5 h, the reaction mixture was warmed to room temperature, and stirring continued for 16 h. [b] Yields are based on isolated products after column chromatography. [c] 3.0 equiv. of Lewis acid was used. [d] No reaction happened either at rt or 55 °C; heating at 85°C caused the substrate to decompose. [e] The reaction required heating at 55 °C for cyclization to happen. [f] SM polymerized under standard reaction conditions.

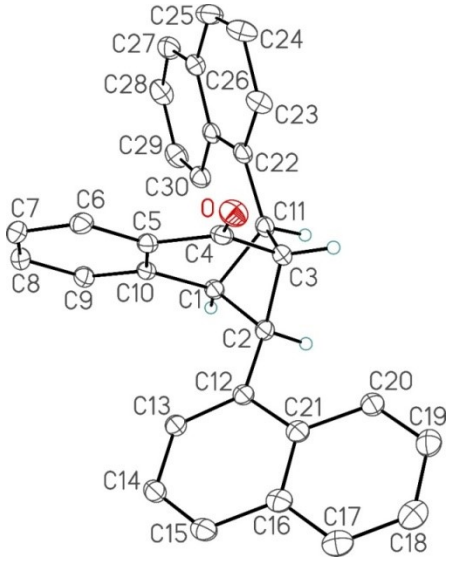

Figure 3.5 X-Ray crystal structure of **52f′.**

Next, we tried substrates with non-identical substituents at the two olefin termini. For the substrate **51l,** formation of only two major products was observed (entry 11). Fortunately, X-ray crystallography was a suitable option to confirm the stereochemistry of **52l** (Figure 3.6).[142] However, switching the positions of 4-tolyl and 4-CF_3-phenyl groups in **51m** made the substrate inert towards standard cyclization conditions, while heat only led to its decomposition (entry 12). Installation of the less electronically biased 4-Cl-phenyl group in the R^2 position of compound **51n** compared to 4-CF_3-phenyl in **51l** resulted in three diastereomeric cycloadducts (entry 13).

Finally, the influence of partial or full replacement of aromatic groups with aliphatic substituents was examined. Keeping R^1 aromatic while placing a methyl group as R^2 still enabled formation of cycloadducts in high overall yield (entry 14). However, depriving the olefin tether of aromaticity in substrate **51p** did not give any desired

product; proton elimination instead delievered **53p** in 32% yield (entry 15). A similar trend was observed for dimethylated substrate **51q,** producing **53q** in 22% yield when heated (entry 16). The unsubstituted *o*-styrenyl enone underwent polymerization, likely due to a combination of inefficient cyclization and facile addition to the olefin termini (entry 17).

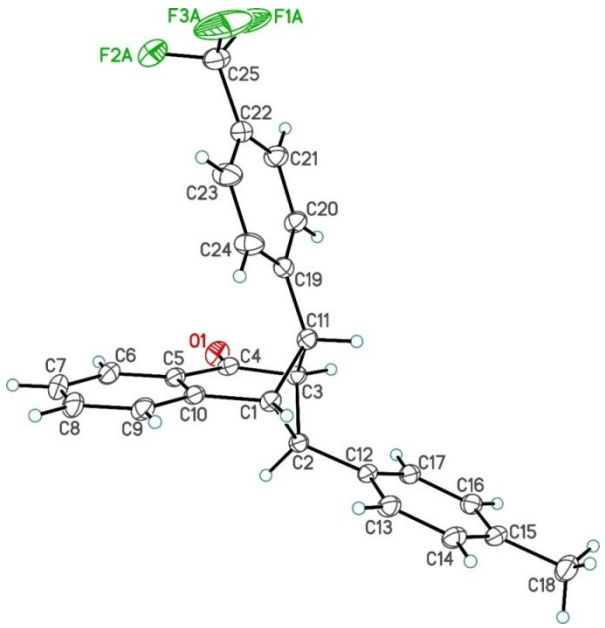

Figure 3.6 X-Ray crystal structure of **52l.**

Interestingly, use of BBr_3 as a Lewis acid during the optimization process delivered the two brominated epimers **54a** and **54a′** in 41% and 36% yields, respectively, instead of cycloadducts (Scheme 3.21a (i)). X-ray crystallography was a valuable toolin the determination of the relative stereochemistry of **54a** (Figure 3.7).[142] According to the 2D NMR analysis (TROESY), substituents in cyclohexenone are *trans* in both isomers which allows us to assume that they only differ by the stereochemistry of the brominated carbon center. Later, we found that with the same amount of the Lewis acid, the reaction could be completed in 1 h at -41 °C. However, at low temperature, the reaction turned out to be more selective yielding **52a** as the major product (Scheme 3.21a (ii)).

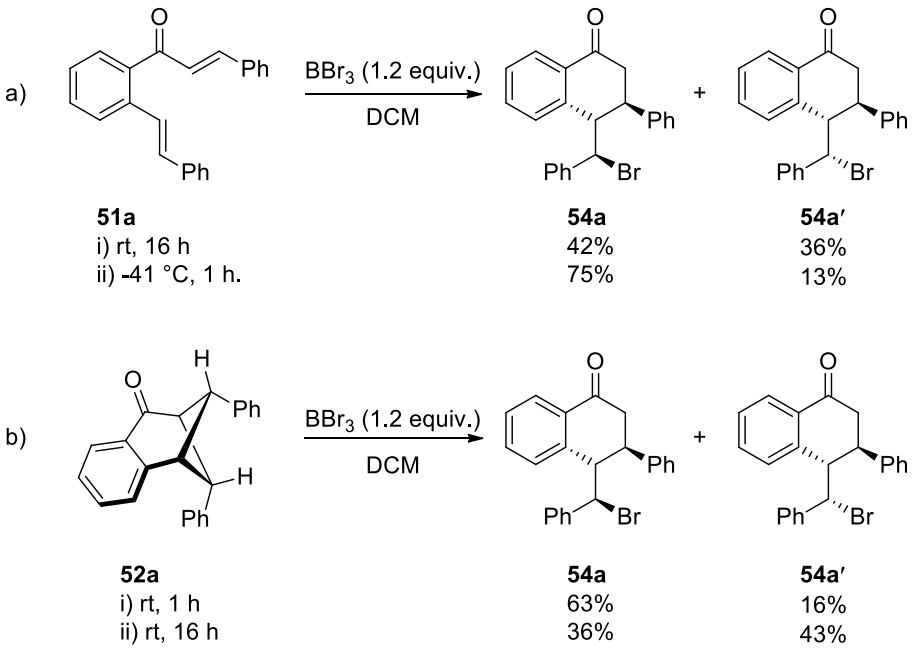

Scheme 3.21 Boron tribromide mediated cyclization.

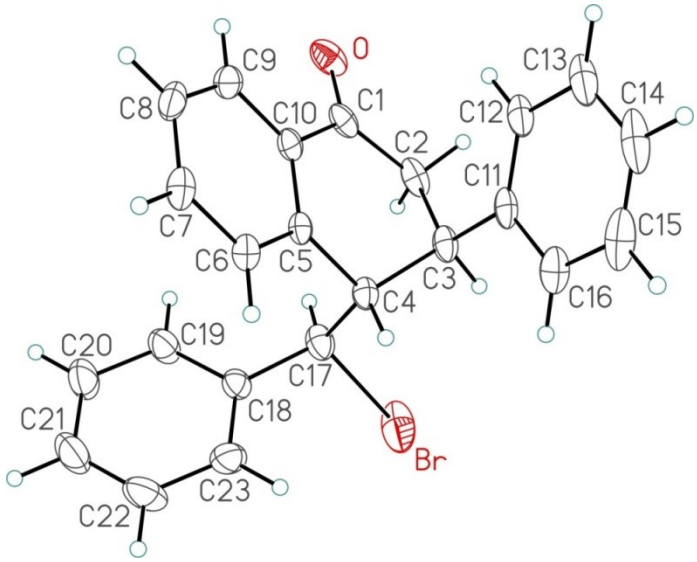

Figure 3.7 X-Ray crystal structure of **54a.**

Treatment of cycloadduct **52a** with 1.2 equiv. of BBr_3 in DCM delivered the same brominated products **54a** and **54a';** however, ring opening could be achieved only at room temperature. The time dependence of the product ratio was obvious; with a short time exposure to BBr_3, **54a** was formed as a major product (Scheme 3.21b (i)), while overnight stirring gave an almost equimolar mixture of diastereomers (Scheme 3.21b

(ii)). In a control experiment, after a 1 h treatment of substrate **51a** with BBr_3 at -41 °C the product ratio of **54a** to **54a′** byNMR analysis of the crude reaction mixture was 6.7:1. However, overnight stirring of the same reaction mixture at room temperature caused a change in product ratio to 1:1.1.

The results suggest that initial stereoselective cation-olefin cyclization of the Lewis acid activated chalcone moiety with the styrene furnishes an isolated benzylic cation intermediate **56**. Bromine migration from the tribromoborate then delivers the brominated products (Scheme 3.22). The temperature dependence of the product ratio clearly shows the kinetic control of the processwhich explains why **54a** forms predominantly at low temperature, while at room temperature it equilibrates with **54a′** via a debromination-brominationt sequence; this is a reason forthe deterioration of diastereoselectivity of the process. The stereochemical model **56**‡ depicted in Figure 3.8 shows the transition state of the bromine migration step, according to which the phenyl group prefers to stay out of the ring space to avoid steric repulsion.

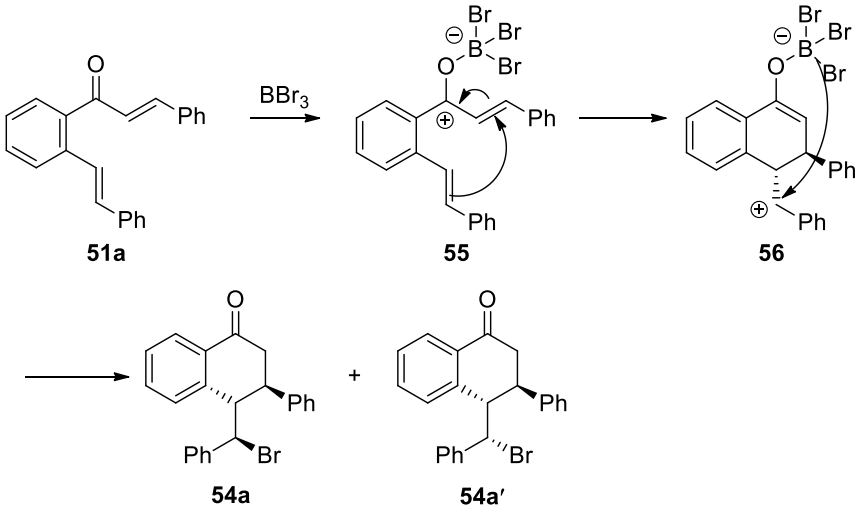

Scheme 3.22 Bromine trapping mechanism.

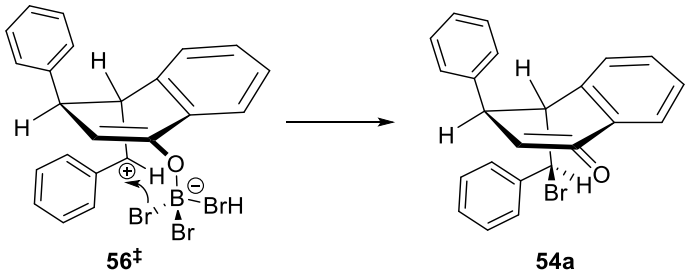

Figure 3.8 Stereochemical model for the predominant formation of **54a.**

Having a strained cyclobutane moiety in a bridged bicyclic skeleton of **52a** encouraged us to carry out other ring opening/rearrangement processes. First, we exposed **52a** to Beckman rearrangement conditions.[131] Ketoxime **57** was formed in 96% yield upon treatment of major cycloadduct **52a** with hydroxylamine hydrochloride and sodium acetate in methanol; next it underwent skeletal reorganization in the presence of thionyl chloride to yield lactam **58** in 61% yield (Scheme 3.23). Treatment of **52a** with a strong Brønsted acid under heating conditions led to a cyclobutane ring opening intermediate, which underwent rearomatization,producing 1-naphthol derivative **59** in 45% yield (Scheme 3.23).

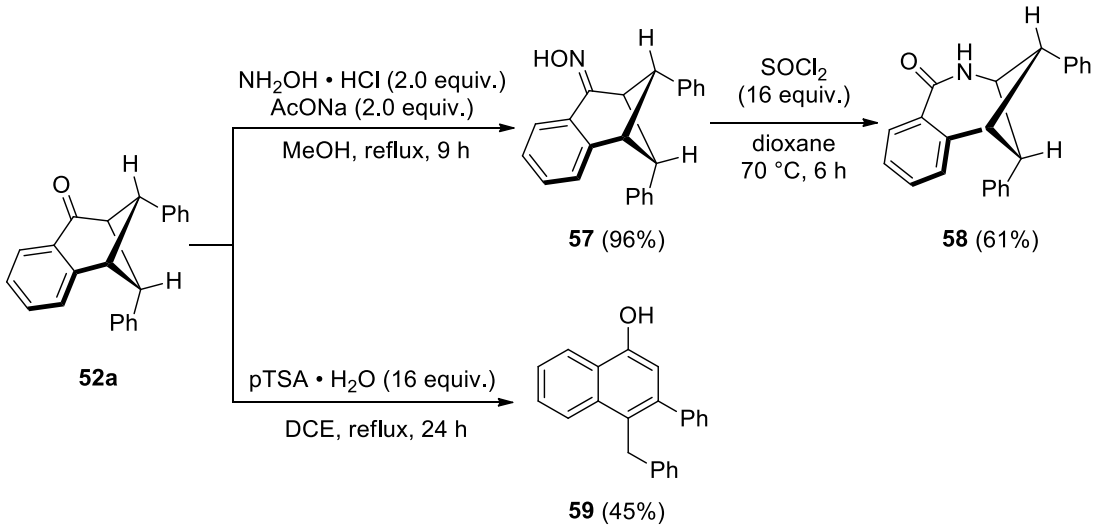

Scheme 3.23 Derivatization of cycloadduct **52a**.

The stepwise mechanism outlined in Scheme 3.24 was proposed as the most plausible route towards the product formation. A Michael-type addition of the

nucleophilic *o*-styrenyl olefin on the Lewis acid activated enone **60** establishes the first C—C bond to give cationic intermediate **61**. The second C—C bond in intermediates **62** and **62′**is formed viaenolate attack on the benzylic cation from either faces. In the presence of a Lewis acid, **62** and **62′**can undergo cyclobutane ring opening via the breakage of the C—C bond as shown in **64** and **64′**; free bond rotation in the latter one and the repetitious enolate collapse on the benzylic cation gives the mixture of other two isomers **65** and **65′**.

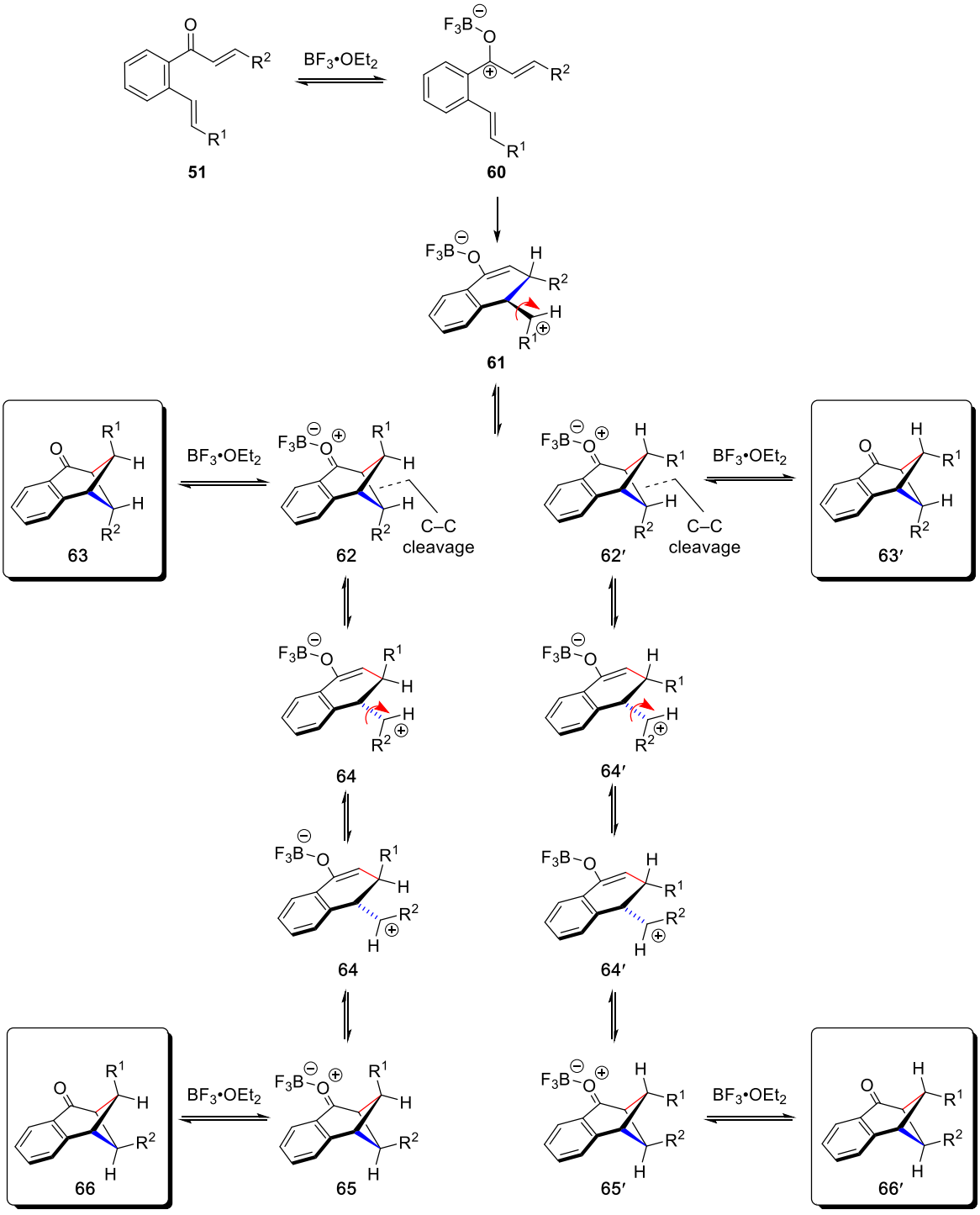

Scheme 3.24 Proposed mechanism of formal [2+2] cycloaddition.

The proposed mechanism clearly explainsthe formation of only two diastereomers from substrate **51l**; in the presence of a strongly electron withdrawing CF_3 group, ring

opening in cycloadducts **52l** and **52l'** is favored no longer due to poor stabilization of the benzylic cation. However, in the case of **51n**, weaker electron withdrawing *p*-chlorophenyl with a positive resonance effect could bias the ring openingslightly; therefore, three products form rather than two. The same phenomenon accounts for the formation of three products from **51j**. An exo olefin **53j** results from proton elimination in the cationic species formed after the originally established C—C bond cleavage in cyclobutane.

In order for cyclization to occur for substrates with aliphatic substituents on the olefin moiety, such as **51p** and **51q**, harsher conditions are required due to the lack of stabilization; with such destabilized intermediates, proton elimination can outcompete the second ring closing process. The complete absence of stabilizing groups in substrate **51r** is a determining factor for polymerization.

The ring opening of cycloadducts was confirmed via two separate control experiments, in which **52a** and **52a′** were treated with 2.0 equiv. of $BF_3{\cdot}Et_2O$. Even though no or negligible interconversion was observed at room temperature, overnight heating at 70 °C caused both substrates to equilibrate to a 1:1 mixture (Scheme 3.25)**.**

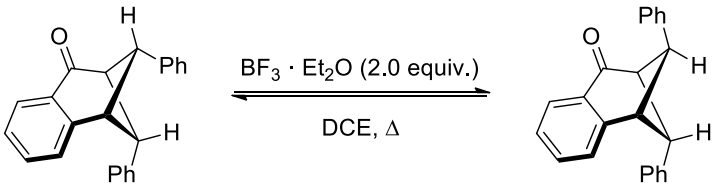

52a **52a′**

Scheme 3.25 Control experiments confirming cyclobutane ring opening under LA acidic conditions.

3.8 Conclusion

In summary, we have developed a formal crossed [2+2] cycloaddition reaction of *o*-styryl chalcones employing the inexpensive and readily available Lewis acid $BF_3{\bullet}OEt_2$, which to the best of our knowledge is the first intramolecular non-

photochemical example of generating cyclobutanes. The method features a wide substrate scope: in most cases, products are obtained in moderate to high overall yields with excellent mass balance from easily synthesized starting materials. In addition, a strain inherently present in the cyclobutane ring makes bridged products suitable precursors for ring opening and rearrangements to get access to 7-membered lactams, brominated tetralones as well as 1-naphthol derivatives under appropriate reaction conditions.

3.9 Future Directions

Except for synthesizing cyclobutanes via formal [2+2] cycloaddition, these highly conjugated systems can potentially allow an access to other ring systems. There are many interesting and unexplored directions to take this project in the future.

1) First of all, it would be interesting to see how a simple modification of *o*-styrenyl chalcones into 1,3-inverted enones by switching the carbonyl group two carbons away would affect the reaction outcome under similar reaction conditions (Scheme 3.26).

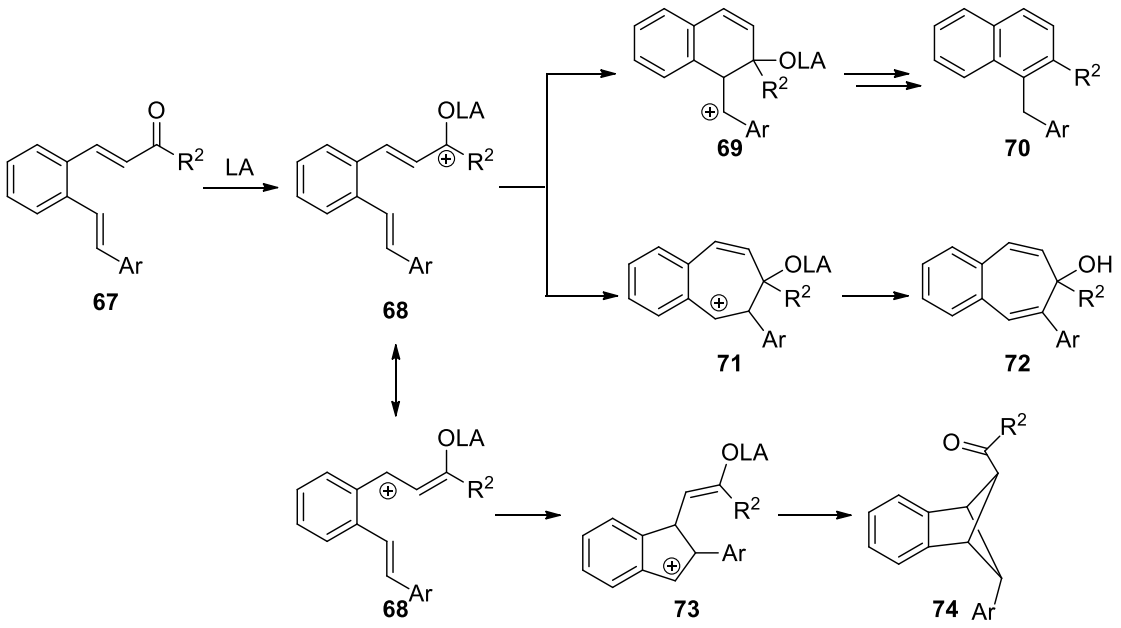

Scheme 3.26 Switching carbonyl group two carbons away.

2) In 1982, the Denmark group developed the concept of silicon-directed Nazarov cyclization (SDNC). Strategic placement of a trimethylsilyl group in the β-position of divinyl ketone could direct the introduction of the double bond to the less substituted (thermodynamically less stable) position due to the β-silicon effect.[143] The method proved to be very general for the series of β-silyl divinylketones **75** in the presence of 1.05 equiv. of $FeCl_3$ to produce 4,5-annulated 2-cyclopentenones **78** (Scheme 3.27).

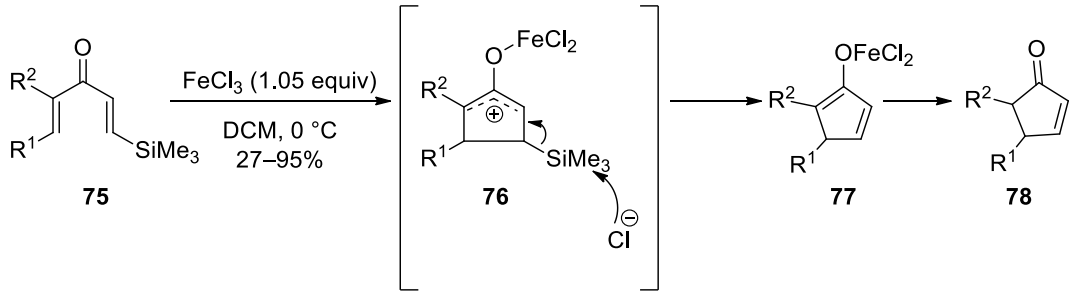

Scheme 3.27 Silicon-directed Nazarov cyclization.

In later reports, when the group was investigating the substituent effect on reaction rates as well as the compatibility of various functional groupswith SDNC, they found that divinyl ketones with vinyl appendages in the β-position (**79)** were also compatible for this protocol; however, skeletal rearrangement yielded unusual α-vinyl cyclopentenones **82** (Scheme 3.28).[144]

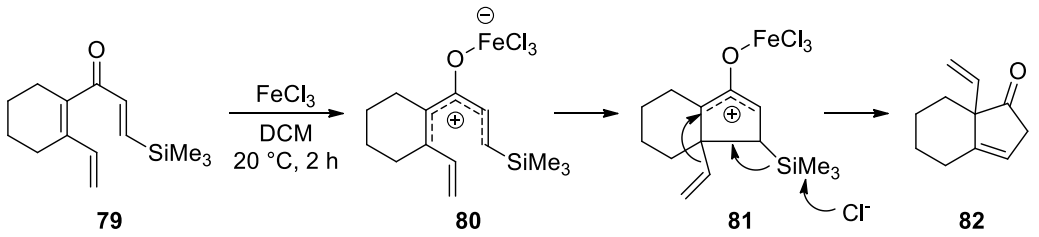

Scheme 3.28 β-Vinyl dienones in silicon-directed Nazarov cyclization.

These substrates resemble our *o*-styrenyl chalcones, except for having a non-aromatic bridging cycle. According to my hypothesis, attaching a silicon group to an

olefin tether in the *o*-position (**83**) could promote 7-endo-trig cyclization due to the β-stabilizing effect of silicon (**84**) (Scheme 3.29a), while in the case of 6-endo-trig cyclization, no similar effect could be expected (**87**) (Scheme 3.29b).[145] It is challenging to access larger size rings and having an approach towards their construction could be of a great value.

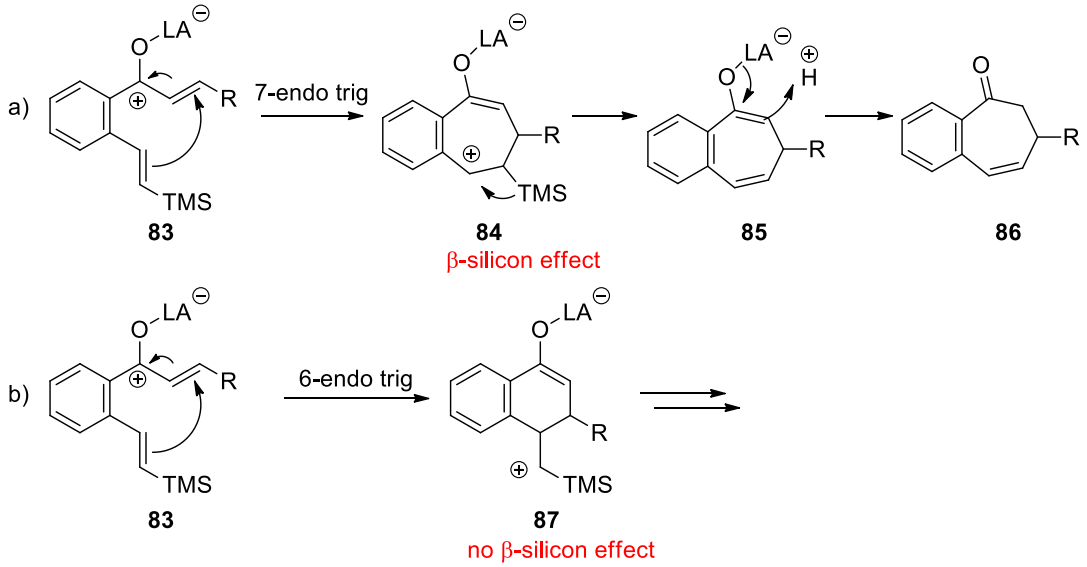

Scheme 3.29 Effect of silicon introduction into*o*-styrenyl chalcones.

3) Another interesting approach to build the 7-membered skeletons could be the replacement of the intervening aryl group with an olefin to help the desired electrocyclization to happen, since it will not involve the destruction of the aromaticity during the ring-closure (Scheme 3.30).

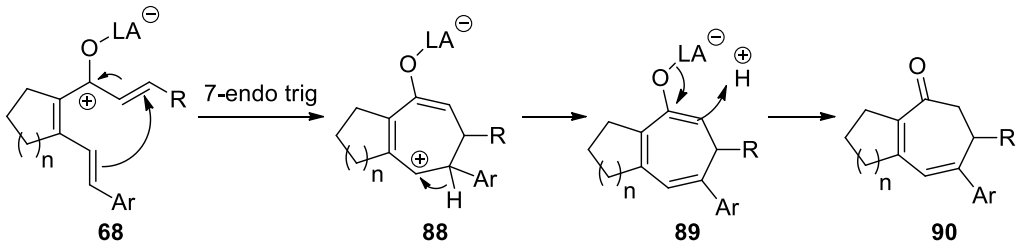

Scheme 3.30 Hypothetic 7-endo-trig cyclization of trienones.

3.10 Experimental

3.10.1 General Information

The reactions were carried out in flame-dried glassware under a positive nitrogen atmosphere, unless otherwise stated. Transfer of anhydrous solvents and reagents was accomplished with oven-dried syringes or cannulae. Solvents were purified using a LC Technology Solutions Inc. solvent purification system. Thin layer chromatography was performed on glass plates pre-coated with 0.25 mm Kieselgel 60 F254 (Merck). Flash chromatography columns were packed with 230–400 mesh silica gel (Silicycle). ^{1}H NMR, ^{13}C and ^{19}F spectra were recorded using Agilent/Varian DD2 MR two channel 400 MHz, Agilent/Varian Inova two-channel 400 MHz, Agilent/Varian Inova four-channel 500 MHz, Agilent/Varian VNMRS two-channel 500 MHz, Agilent VNMRS four-channel, Agilent/Varian VNMRS four-channel 600 MHz, and dual receiver 700 MHz at 400/500/600/700, 100/125/150/175 and 376/470 MHz, respectively. ^{1}H NMR chemical shifts are reported relative to a TMS (0.00 ppm) or $CDCl_3$ (7.26 ppm) internal standard. Coupling constants (*J*) are reported in Hertz (Hz). Standard notation is used to describe the multiplicity of signals observed in ^{1}H NMR spectra: broad (br), apparent (app), multiplet (m), singlet (s), doublet (d), triplet (t), etc. Carbon nuclear magnetic resonance spectra (^{13}C NMR) are reported in ppm relative to the center line of the triplet from $CDCl_3$. The carbon chemical shifts are reported to nearest 0.1 ppm and to the nearest 0.01 ppm when necessary to distinguish two close resonances. Fluorine nuclear magnetic resonance spectra (^{19}F NMR) were recorded at 376 and 470 MHz and are reported in ppm relative to a TFA (-76.55 ppm) internal standard. Infrared (IR) spectra were measured with a Mattson Galaxy Series FT-IR 3000 spectrophotometer. High resolution mass spectrometry (HRMS) data (APPI/ESI technique) were recorded using an Agilent Technologies 6220 oaTOF instrument. HRMS data (EI technique) were recorded using a Kratos MS50 instrument.

3.10.2 General Procedure 1 for the Preparation of 2-Substituted Benzoates (S2).

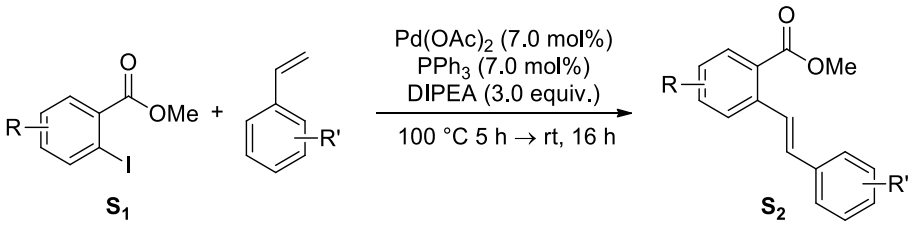

Methyl 2-iodobenzoate (**S1**) was prepared via a known literature procedure.[141]

2-substituted benzoates (S2) were prepared via modified literature procedure:[146] A mixture of methyl 2-iodo benzoate **S1** (1.0 equiv.), styrene (1.2 equiv.), N,N-diisopropylethylamine (3.0 equiv.), palladium acetate (0.07 equiv), and triphenylphosphine (0.07 equiv.) was heated at 100 °C for 5 h and then stirred at room temperature for 16 h. The reaction mixture was passed through Celite and diluted with DCM (3 mL for 1 mmol of starting material). The organic layer was washed with 2 M solution of HCl (5 mL for 1 mmol of starting material), water and brine, dried over $MgSO_4$, and concentrated in vacuo. The crude reaction mixture was purified by flash column chromatography.

Methyl (*E*)-2-styrylbenzoate (S2a)

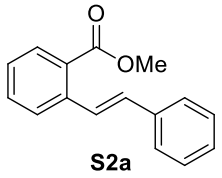

The product was obtained as a yellow oil (4.89 g, 20.5 mmol) in 68% yield from methyl 2-iodobenzoate (**S1**) (7.86 g, 30.0 mmol) and styrene. R_f 0.41 (hexanes/EtOAc 20:1); ^{1}H NMR (500 MHz, $CDCl_3$) δ 8.01 (d, *J* = 16.2 Hz, 1H), 7.95 (dd, *J* = 7.8, 1.2 Hz, 1H), 7.74 (d, *J* = 7.9 Hz, 1H), 7.57 (d, *J* = 7.8 Hz, 2H), 7.52 (t, *J* = 7.6 Hz, 1H), 7.38 (t, *J* = 7.6 Hz, 2H), 7.33 (t, *J* = 7.6 Hz, 1H), 7.30–7.28 (m, 1H), 7.03 (d, *J* = 16.2 Hz, 1H), 3.94 (s, 3H); ^{13}C NMR (125 MHz, $CDCl_3$) δ 167.8, 139.2, 137.4, 132.1, 131.4, 130.6, 128.6, 128.5, 127.8, 127.4, 127.1, 126.9, 126.8, 52.1; HRMS (EI, M^+) for $C_{16}H_{14}O_2$ calcd.

238.0994, found: m/z 238.0992. The spectroscopic data are in agreement with the literature.[146]

Methyl (*E*)-2-(4-chlorostyryl)benzoate (S2b)

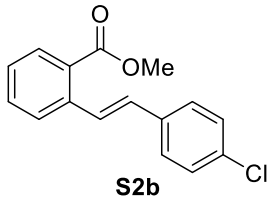

S2b

The product was obtained as a white solid (2.90 g, 10.7 mmol) in 71% yield from methyl 2-iodobenzoate (**S1**) (3.93 g, 15.0 mmol) and 4-chlorostyrene. R_f 0.39 (hexanes/EtOAc 10:1); mp 83–85 °C; ^{1}H NMR (500 MHz, $CDCl_3$) δ 7.98 (d, J = 16.2 Hz, 1H), 7.94 (ddd, J = 7.9, 1.1, 0.4 Hz, 1H), 7.70 (ddd, J = 8.0, 0.6, 0.6 Hz, 1H), 7.52 (dddd, J = 7.9, 7.9, 1.5, 0.6 Hz, 1H), 7.47 (d, J = 8.4 Hz, 2H), 7.35–7.31 (m, 3H), 6.95 (d, J = 16.2 Hz, 1H), 3.93 (s, 3H); ^{13}C NMR (125 MHz, $CDCl_3$) δ 167.8, 139.0, 135.9, 133.4, 132.2, 130.7, 130.1, 128.8, 128.5, 128.1, 128.0, 127.4, 127.0, 52.2; HRMS (EI, M^+) for $C_{16}H_{13}ClO_2$ calcd. 272.0604, found: m/z 272.0599. The spectroscopic data are in agreement with the literature.[146]

Methyl (*E*)-2-(4-fluorostyryl)benzoate (S2c)

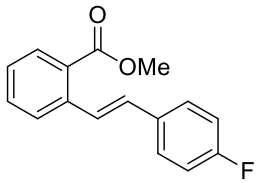

S2c

The product was obtained as an off-white solid (2.73 g, 10.6 mmol) in 71% yield from methyl 2-iodobenzoate (**S1**) (3.93 g, 15.0 mmol) and 4-fluorostyrene. R_f 0.30 (hexanes/EtOAc 15:1); mp 65–68 °C; ^{1}H NMR (400 MHz, $CDCl_3$) δ 7.94 (ddd, J = 7.9, 1.5, 0.3 Hz, 1H), 7.92 (d, J = 16.3 Hz, 1H), 7.70 (ddd, J = 7.9, 0.6, 0.6 Hz, 1H), 7.53–7.49 (m, 3H), 7.33 (td, J = 7.6, 1.2 Hz, 1H), 7.05 (app t, J = 8.8 Hz, 2H), 6.96 (d, J = 16.3 Hz, 1H), 3.93 (s, 3H); ^{13}C NMR (125 MHz, $CDCl_3$) δ 167.8, 162.5 (d, J = 248.0 Hz), 139.2, 133.6 (d, J = 3.1 Hz), 132.2, 130.7, 130.2, 128.4 (d, J = 8.3 Hz), 127.27,

127.26 127.2, 126.9, 115.6 (d, J = 21.7 Hz), 52.1; ^{19}F NMR (376 MHz, $CDCl_3$) δ -114.0; HRMS (EI, M^+) for $C_{16}H_{13}FO_2$ calcd. 256.0900, found: m/z 256.0895.

Methyl (*E*)-2-(4-methylstyryl)benzoate (S2d)

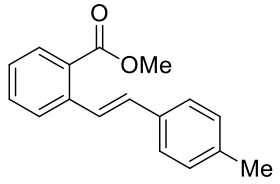

S2d

The product was obtained as a white solid (1.70 g, 6.7 mmol) in 58% yield from methyl 2-iodobenzoate (**S1**) (3.01 g, 11.5 mmol) and 4-methylstyrene. R_f 0.41(hexanes/EtOAc 25:1); mp 73–75 °C; ^{1}H NMR (500 MHz, $CDCl_3$) δ 7.94 (d, J = 16.2 Hz, 1H), 7.92 (ddd, J = 7.9, 1.5, 0.4 Hz, 1H), 7.72 (dt, J = 8.1, 0.6 Hz, 1H), 7.50 (dddd, J = 7.9, 7.4, 1.5, 0.6 Hz, 1H), 7.45 (d, J = 8.2 Hz, 2H), 7.31 (td, J = 7.6, 1.3 Hz, 1H), 7.17 (d, J = 7.7 Hz, 2H), 7.00 (d, J = 16.2 Hz, 1H), 3.93 (s, 3H), 2.37 (s, 3H); ^{13}C NMR (125MHz, $CDCl_3$) δ 167.9, 139.4, 137.8, 134.6, 132.1, 131.4, 130.6, 129.4, 128.5, 126.9, 126.83, 126.77, 126.3, 52.1, 21.3; HRMS (EI, M^+) for $C_{17}H_{16}O_2$ calcd. 252.1150, found: m/z 252.1150. The spectroscopic data are in agreement with the literature.[146]

Methyl (*E*)-2-(2-(naphthalen-1-yl)vinyl)benzoate (S2e)

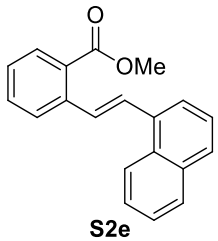

S2e

The product was obtained as a yellow oil (3.10 g, 10.7 mmol) in 71% yield from methyl 2-iodobenzoate (**S1**) (3.93 g, 15.0 mmol) and 1-vinylnaphthalene (1-vinylnaphthalene was prepared via a known literature procedur).[146] R_f 0.44 (hexanes/EtOAc 20:1); ^{1}H NMR (500 MHz, $CDCl_3$) δ 8.27 (d, J = 8.3 Hz, 1H), 8.04 (d, J = 15.9 Hz, 1H), 8.00 (d, J = 7.8 Hz, 1H), 7.90 (d, J = 8.2 Hz, 1H), 7.87 (d, J = 7.7 Hz, 2H), 7.84 (d, J = 8.2 Hz, 1H), 7.80 (d, J = 15.9 Hz, 1H), 7.60–7.52 (m, 4H), 7.38 (td, J = 7.6, 1.2 Hz, 1H), 3.95 (s, 3H); ^{13}C NMR (125 MHz, $CDCl_3$) δ 167.8, 139.5, 134.9, 133.7, 132.2, 131.4, 130.7,

130.5, 128.7, 128.6, 128.4, 128.2, 127.3, 127.2, 126.0, 125.73, 125.72, 124.2, 123.7, 52.1; HRMS (EI, M^+) for $C_{17}H_{16}O_2$ calcd. 288.1150, found: m/z 288.1151. The spectroscopic data are in agreement with the literature.[146]

Methyl (*E*)-3-methyl-2-styrylbenzoate (S2f)

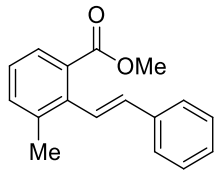

S2f

The product was obtained as a yellow oil (3.90 g, 15.4 mmol) in 80% yield from methyl 2-iodo-3-methylbenzoate (5.33 g, 19.3 mmol) and styrene. R_f 0.37 (hexanes/EtOAc 25:1); ^{1}H NMR (500 MHz, $CDCl_3$) δ 7.63 (d, *J* = 7.9 Hz, 1H), 7.52–7.50 (m, 2H), 7.41 (d, *J* = 16.5 Hz, 1H), 7.38–7.35 (m, 3H), 7.30–7.22 (m, 2H), 6.52 (d, *J* = 16.5 Hz, 1H), 3.84 (d, *J* = 0.6 Hz, 3H), 2.42 (s, 3H); ^{13}C NMR (125 MHz, $CDCl_3$) δ 169.4, 137.9, 137.4, 137.1, 133.4, 133.3, 131.2, 128.6, 127.7, 127.3, 126.8, 126.7, 126.5, 52.1, 20.9; HRMS (EI, M^+) for $C_{17}H_{16}O_2$ calcd. 252.1150, found: m/z 252.1152.

Methyl (*E*)-2-(4-methoxystyryl)benzoate (S2g)

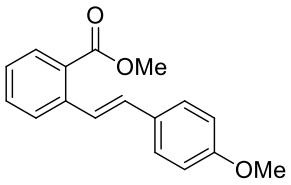

S2g

The product was obtained as a white solid (2.48 g, 9.2 mmol) in 62% yield from methyl 2-iodobenzoate (**S1**) (3.93 g, 15.0 mmol) and 4-vinylanisole. R_f 0.39 (hexanes/EtOAc 10:1); mp 76–78 °C; ^{1}H NMR (600 MHz, $CDCl_3$) δ 7.91 (dd, *J* = 7.9, 1.2 Hz, 1H), 7.86 (d, *J* = 16.2 Hz, 1H), 7.71 (d, *J* = 7.9 Hz, 1H), 7.51–7.48 (m, 3H), 7.29 (td, *J* = 7.6, 1.2 Hz, 1H), 6.98 (d, *J* = 16.2 Hz, 1H), 6.90 (d, *J* = 8.8 Hz, 2H), 3.93 (s, 3H), 3.84 (s, 3H); ^{13}C NMR (125 MHz, $CDCl_3$) δ 168.0, 159.5, 139.5, 132.1, 131.0, 130.6, 130.3, 128.3, 128.1, 126.73, 126.70, 125.2, 114.1, 55.3, 52.1; HRMS (EI, M^+) for $C_{17}H_{16}O_3$ calcd.

268.1099, found: m/z 268.1096. The spectroscopic data are in agreement with the literature.[146]

Methyl (*E*)-2-(2-chlorostyryl)benzoate (S2h)

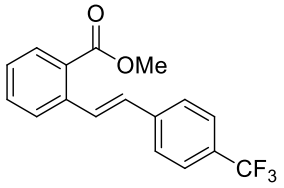

S2h

The product was obtained as a yellow oil (2.70 g, 8.7 mmol) in 73% yield from methyl 2-iodobenzoate (**S1**) (3.14 g, 12.0 mmol) and 4-(trifluoromethyl)styrene. R_f 0.31 (hexanes/EtOAc 25:1); ^{1}H NMR (500 MHz, $CDCl_3$) δ 8.10 (d, *J* = 16.2 Hz, 1H), 7.97 (dd, *J* = 8.0, 1.2 Hz, 1H), 7.72 (dt, *J* = 7.9, 0.6 Hz, 1H), 7.64 (d, *J* = 8.6 Hz, 2H), 7.61 (d, *J* = 8.6 Hz, 2H), 7.54 (ddd, *J* = 7.9, 1.5, 0.6 Hz, 1H),), 7.37 (td, *J* = 7.5, 1.3 Hz, 1H), 7.01 (d, *J* = 16.2 Hz, 1H), 3.94 (s, 3H); ^{13}C NMR (125 MHz, $CDCl_3$) δ 167.6, 140.9 (q, *J* = 1.5 Hz), 138.7, 132.3, 130.8, 130.2, 129.8, 129.5 (q, *J* = 32.5 Hz), 128.7, 127.7, 127.1, 126.9, 125.6 (q, *J* = 3.6 Hz), 124.2 (q, *J* = 271.7 Hz), 52.2; ^{19}F NMR (376 MHz, $CDCl_3$) δ -62.5; HRMS (EI, M^+) for $C_{17}H_{13}F_3O_2$ calcd. 306.0868, found: m/z 306.0871.

3.10.3 General Procedure 2 for the Preparation of 2-Substituted Acetophenones (S3).[146]

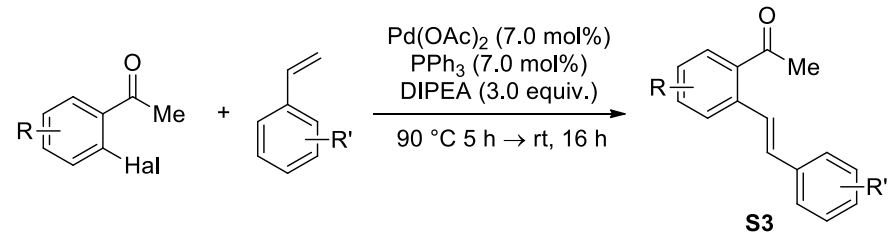

S3

Hal = I or Br

(*E*)-1-(2-(2-chlorostyryl)phenyl)ethan-1-one (S3a)

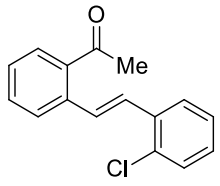

S3a

The product was obtained as a light yellow solid (1.28 g, 5.0 mmol) in 33% yield from 2′-bromoacetophenone (2.00 g, 15.0 mmol) and 2-chlorostyrene. R_f 0.37 (hexanes/EtOAc 20:1); ^{1}H NMR (500 MHz, $CDCl_3$) δ 7.77–7.71 (m, 3H), 7.65 (d, *J* = 16.1 Hz, 1H), 7.52 (td, *J* = 7.6, 1.3 Hz, 1H), 7.37–7.40 (m, 3H), 7.27 (dddd, *J* = 7.9, 7.3, 1.5, 0.6 Hz, 1H), 7.20 (td, *J* = 7.7, 1.7 Hz, 1H), 2.63 (s, 3H); ^{13}C NMR (175 MHz, $CDCl_3$) δ 201.8, 137.3, 137.2, 135.4, 133.5, 131.9, 130.2, 129.7, 129.2, 128.7, 127.8, 127.6, 127.4, 127.0, 127.0, 29.7; HRMS (EI, M^+) for $C_{16}H_{13}ClO$ calcd. 256.0655, found: m/z 256.0651.

(*E*)-1-(2-(4-(dimethylamino)styryl)phenyl)ethan-1-one (S3b)

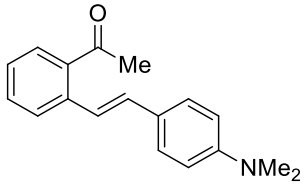

S3b

The product was obtained as a brown solid (1.40 g, 5.3 mmol) in 39% yield from 2′-bromoacetophenone (2.69 g, 13.5 mmol) and N,N-dimethyl-4-vinylaniline. R_f 0.30 (hexanes/EtOAc 10:1); mp 83–84 °C. ^{1}H NMR (600 MHz, $CDCl_3$) δ 7.70 (dd, *J* = 8.0, 0.7 Hz, 1H), 7.63 (dd, *J* = 7.8, 1.1 Hz, 1H), 7.50–7.43 (m, 4H), 7.28 (td, *J* = 7.5, 1.2 Hz, 1H), 6.97 (d, *J* = 16.1 Hz, 1H), 6.72 (d, *J* = 8.8 Hz, 2H), 2.99 (s, 6H), 2.61 (s, 3H); ^{13}C NMR (175 MHz, $CDCl_3$) δ 202.7, 150.3, 137.8, 137.3, 132.0, 131.3, 128.8, 127.9, 126.8, 126.2, 125.6, 122.5, 112.3, 40.3, 30.1; HRMS (ESI, $[M+H]^+$) for $C_{18}H_{20}NO$ calcd. 266.1545, found: m/z 266.1538.

(*E*)-1-(5-fluoro-2-styrylphenyl)ethan-1-one (S3c)

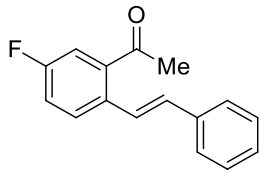

S3c

The product was obtained as a brown oil (1.70 g, 7.1 mmol) in 38% yield from 1-(5-Fluoro-2-iodophenyl)ethanone (5.00 g, 18.9 mmol) and styrene. R_f 0.30 (hexanes/EtOAc 10:1); ^{1}H NMR (600 MHz, $CDCl_3$) δ 7.67 (dd, *J* = 8.7, 5.4 Hz, 1H), 7.59 (d, *J* = 16.2 Hz, 1H), 7.52–7.51 (m, 2H), 7.38–7.34 (m, 3H), 7.28 (dt, *J* = 6.8, 1.2 Hz, 1H), 7.20 (ddd, *J* = 8.3, 8.1, 2.7 Hz, 1H), 6.92 (d, *J* = 16.2 Hz, 1H), 2.60 (s, 3H); ^{13}C NMR (125 MHz, $CDCl_3$) δ 200.7 (d, *J* = 2.1 Hz), 161.5 (d, *J* = 249.0 Hz), 138.7 (d, *J* = 5.7 Hz), 137.1, 133.4 (d, *J* = 3.6 Hz), 131.7 (d, *J* = 1.5 Hz), 129.3 (d, *J* = 7.2 Hz), 128.7, 127.9, 126.8, 126.2, 118.7 (d, *J* = 21.1 Hz), 115.6 (d, *J* = 22.7 Hz), 29.8; ^{19}F NMR (376 MHz, $CDCl_3$) δ -113.8; HRMS (EI, M^+) for $C_{16}H_{13}FO$ calcd. 240.0950, found: m/z 240.0947.

(*E/Z*)-1-(2-((E)-prop-1-en-1-yl)phenyl)but-2-en-1-ol (S4)

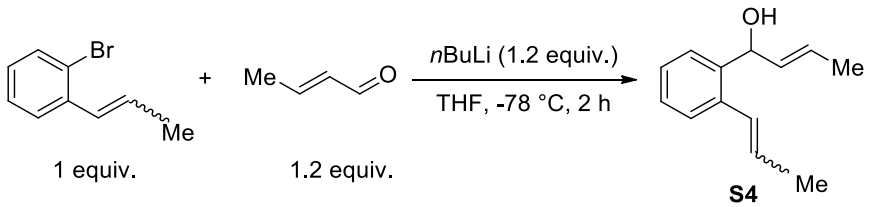

The mixture of alcohols **S4** was prepared from (*E/Z*)-1-bromo-2-(prop-1-en-1-yl)benzene following the known literature procedure.[131] To the cooled solution of bromides (3.79 g, 19.0 mmol) in THF (50 mL) at -78 °C was added *n*-BuLi (2.5M in hexanes, 9.12 mL, 22.8 mmol) dropwise and stirred at -78 °C for 1 h. Then, crotonaldehyde (1.9 mL, 22.8 mmol) diluted with THF (20 mL) was added and stirred at -78 °C for another 1 h. The reaction mixture was quenched with a sat. aqueous solution of NH_4Cl and extracted with DCM (2 x 30 mL). The combined organic layer was washed with water (2 x 30 mL) and brine, dried over $MgSO_4$, and concentrated in vacuo. The crude mixture of alcohols (2.90 g, 15.4 mmol) was used in the next step without further purification.

Substrate **51r** was prepared via a known literature procedure.[131]

3.10.4 General Procedure 3 for the Preparation of *o*-Styrenyl Chalcones 51a, 51b, 51c, 51e, 51f, 51h, 51j, 51k, 51l,[a] 51m, 51n, 51o[b] and 51p

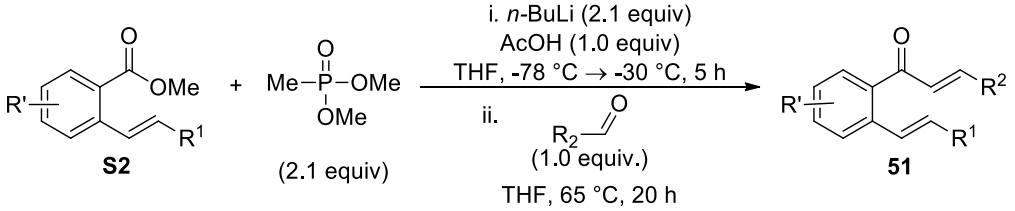

Chalchones **51a, 51b, 51c, 51e, 51f, 51h, 51j, 51k, 51l, 51m, 51n, and 51p** were prepared via a modified literature procedure:[147] 2.5 M hexane solution of *n*-BuLi (2.1 equiv.) was added dropwise to a stirred solution of dimethyl methylphosphonate (2.1 equiv.) in THF (0.4 M solution) at -78 °C under nitrogen and stirred for 30 min. 2-Substituted benzoates **(S2**) (1.0 equiv.) in THF (1.7 M) was added slowly and stirred at -78 °C for 30 min. Then, the reaction mixture was allowed to warm to -30 °C and the stirring was continued for 2 h. After addition of glacial acetic (1.0 equiv.) at -30 °C, the mixture was allowed to reach room temperature with continued stirring for 2 h. Aldehyde (1.0 equiv) was added to the reaction mixture and stirred at 65 °C for 20 h. Another portion of glacial acetic acid (1.0 equiv.) was added to quench the reaction. The solvent was evaporated, and the residue was dissolved in DCM (7.5 mL per 1 mmol of benzoate **S2**). The organic phase was washed with 5% ammonium hydroxide solution (4 mL per 1 mmol of benzoate **S2**), water and brine, dried over $MgSO_4$, and concentrated in vacuo. The crude reaction mixture was purified by flash column chromatography.

(*E*)-3-phenyl-1-(2-((*E*)-styryl)phenyl)prop-2-en-1-one (51a)

[a] Diethyl ethylphosphonate was used instead of dimethyl methylphosphonate
[b] Acetaldehyde was used in excess (2.0 equiv.) and no heat was applied; reaction mixture was stirred at room temperature for 16 h.

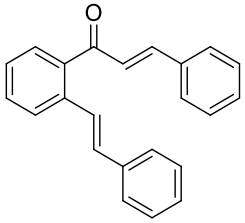

51a

The product was obtained as a yellow solid (6.15 g, 19.8 mmol) in 78% yield from **S2a** (6.02 g, 25.3 mmol) and benzaldehyde. R_f 0.33 (hexanes/EtOAc 30:1); mp 72–75°C; IR (cast film) 3059, 3025, 1663, 1640, 1598, 1575, 1495, 1448 cm^{-1}; ^1H NMR (500 MHz, $CDCl_3$) δ 7.79 (dd, *J* = 7.9, 0.4 Hz, 1H), 7.58–7.48 (m, 7H), 7.46 (d, *J* = 16.3 Hz, 1H), 7.40–7.36 (m, 4H), 7.32 (t, *J* = 7.5 Hz,2H), 7.26–7.24 (m, 1H), 7.20 (dd, *J* = 16.1, 0.7 Hz, 1H), 7.10 (d, *J* = 16.3 Hz, 1H); ^{13}C NMR (125 MHz, $CDCl_3$) δ 196.0, 146.0, 138.6, 137.1, 136.5, 134.5, 131.5, 130.8, 130.7, 128.9, 128.6, 128.5, 128.4, 127.9, 127.1, 126.9, 126.8, 126.4, 126.3; HRMS (EI, M^+) for $C_{23}H_{18}O$ calcd. 310.1358, found: m/z 310.1359.

(*E*)-3-(4-chlorophenyl)-1-(2-((*E*)-4-chlorostyryl)phenyl)prop-2-en-1-one (51b)

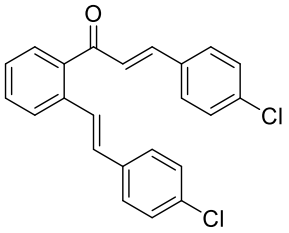

51b

The product was obtained as a yellow solid (470 mg, 1.24 mmol) in 54% yield from **S2b** (623 mg, 2.3 mmol) and 4-chlorobenzaldehyde. R_f 0.30 (hexanes/EtOAc 50:1); mp 134–136 °C; IR (cast film) 3061, 3026, 1664, 1641, 1601, 1566, 1491, 1445, 1405 cm^{-1}; ^1H NMR (500 MHz, $CDCl_3$) δ 7.76 (d, *J* = 7.9 Hz, 1H), 7.58 (dd, *J* = 7.8, 1.1 Hz, 1H), 7.53–7.47 (m, 4H), 7.42–7.38 (m, 4H), 7.36 (d, *J* = 8.6 Hz, 2H), 7.29 (d, *J* = 8.5 Hz, 2H), 7.15 (d, *J* = 16.1 Hz, 1H), 7.01 (d, *J* = 16.1 Hz, 1H); ^{13}C NMR (125 MHz, $CDCl_3$) δ 195.4, 144.4, 138.3, 136.7, 136.4, 135.6, 133.6, 133.0, 131.1, 130.2, 129.6, 129.3, 128.8, 128.6, 127.9, 127.4, 127.0, 126.9, 126.5; HRMS (EI, M^+) for $C_{23}H_{16}Cl_2O$ calcd. 378.0578, found: m/z 378.0574.

(*E*)-3-(4-fluorophenyl)-1-(2-((*E*)-4-fluorostyryl)phenyl)prop-2-en-1-one (51c)

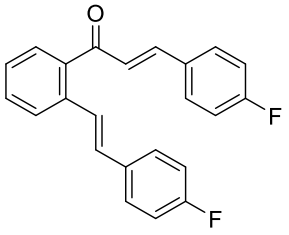

51c

The product was obtained as a yellow solid (1.71 g, 4.5 mmol) in 66% yield from **S2c** (2.61 g, 7.5 mmol) and 4-fluorobenzaldehyde. R_f 0.2 (hexanes/EtOAc 50:1); mp 108–110 °C; IR (cast film) 3061, 1663, 1639, 1599, 1509, 1477, 1415 cm^{-1}; ^1H NMR (600 MHz, $CDCl_3$) δ 7.76 (d, *J* = 7.9 Hz, 1H), 7.57–7.51 (m, 5H), 7.45–7.43 (m, 2H), 7.38–7.35 (m, 2H), 7.11 (d, *J* = 16.1 Hz, 1H), 7.09–6.99 (m, 5H); ^{13}C NMR (125 MHz, $CDCl_3$) δ 195.6, 164.2 (d, *J* = 252.1 Hz), 164.2 (d, *J* = 248.0 Hz), 144.6, 138.4, 136.5, 133.3 (d, *J* = 3.6 Hz), 130.9, 130.8 (d, *J* = 3.6 Hz), 130.4 (d, *J* = 8.8 Hz), 130.3 (d, *J* = 1.0 Hz), 128.6, 128.3 (d, *J* = 8.3 Hz), 127.2, 126.5 (d, *J* = 2.1 Hz), 126.4, 126.1 (d, *J* = 2.6 Hz), 116.2 (d, *J* = 21.7 Hz), 115.6 (d, *J* = 21.7 Hz); ^{19}F NMR (376 MHz, $CDCl_3$) δ -108.6, -113.7; HRMS (EI, M^+) for $C_{23}H_{16}F_2O$ calcd. 346.1169, found: m/z 346.1162.

(*E*)-1-(2-((*E*)-4-methylstyryl)phenyl)-3-(p-tolyl)prop-2-en-1-one (51e)

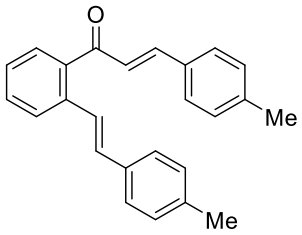

51e

The product was obtained as a yellow solid (1.0 g, 3.0 mmol) in 59% yield from **S2d** (1.26 g, 5.0 mmol) and *p*-tolualdehyde. R_f 0.24 (hexanes/EtOAc 50:1); mp 63–65 °C; IR (cast film) 3051, 3023, 2919, 2863, 1662, 1638, 1597, 1568, 1512, 1476, 1445, 1412 cm^{-1}; ^1H NMR (500 MHz, $CDCl_3$) δ 7.78 (d, *J* = 7.9 Hz, 1H), 7.54–7.44 (m, 5H), 7.40–7.33 (m, 4H), 7.19–7.12 (m, 5H), 7.07 (d, *J* = 16.1 Hz, 1H), 2.37 (s, 3H), 2.34 (s, 3H); ^{13}C NMR (125 MHz, $CDCl_3$) δ 196.3, 146.1, 141.2, 138.7, 137.8, 136.5, 134.4,

131.8, 131.3, 130.6, 129.7, 129.3, 128.5, 128.4, 126.9, 126.7, 126.2, 126.0, 125.2, 21.5, 21.2; HRMS (EI, M^+) for $C_{25}H_{22}O$ calcd. 338.1671, found: m/z 338.1663.

(*E*)-3-(naphthalen-1-yl)-1-(2-((*E*)-2-(naphthalen-1-yl)vinyl)phenyl)prop-2-en-1-one (51f)

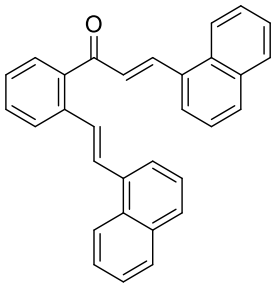

51f

The product was obtained as yellow solid (1.90 g, 4.6 mmol) in 52% yield from **S2e** (2.60 g, 9.0 mmol) and 1-naphthaldehyde. R_f 0.52 (hexanes/EtOAc 50:1); mp 115–117 °C; IR (cast film) 3058, 1715, 1660, 1597, 1509, 1477 cm^{-1}; ^1H NMR (500 MHz, $CDCl_3$) δ 8.43 (d, *J* = 15.7 Hz, 1H), 8.23–8.21 (m, 1H), 8.11–8.09 (m, 1H), 7.92 (d, *J* = 7.9 Hz, 1H), 7.89–7.84 (m, 4H), 7.78 (d, *J* = 7.7 Hz, 2H), 7.72 (d, *J* = 7.1 Hz, 1H), 7.69 (d, *J* = 7.9 Hz, 1H), 7.60 (t, *J* = 7.7 Hz, 1H), 7.54 (d, *J* = 15.9 Hz, 1H), 7.52–7.48 (m, 4H), 7.45 (t, *J* = 7.7 Hz, 1H), 7.40 (td, *J* = 7.7, 1.9 Hz, 2H), 7.30 (d, *J* = 15.7 Hz, 1H); ^{13}C NMR (125 MHz, $CDCl_3$) δ 195.8, 142.7, 138.9, 137.0, 134.7, 133.7, 131.9, 131.6, 131.4, 131.0, 130.9, 129.7, 129.4, 128.9, 128.8, 128.7, 128.6, 128.3, 127.5, 126.97, 126.95, 126.3, 126.2, 125.8, 125.7, 125.4, 125.3, 124.1, 123.7, 123.3, (one signal is missing due the overlap); HRMS (EI, M^+) for $C_{31}H_{22}O$ calcd. 410.1671, found: m/z 410.1662.

(*E*)-1-(3-methyl-2-((*E*)-styryl)phenyl)-3-phenylprop-2-en-1-one (51h)

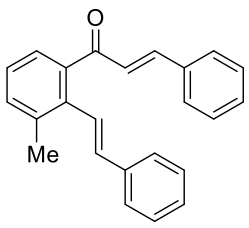

51h

The product was obtained as a yellow solid (3.54 g, 10.9 mmol) in 71% yield from **S2f** (3.89 g, 15.4 mmol) and benzaldehyde. R_f 0.38 (hexanes/EtOAc 50:1); mp 79–81 °C; IR (cast film) 3059, 3026 1666, 1645, 1602, 1495, 1449 cm^{-1}; ^1H NMR (500 MHz, $CDCl_3$) δ 7.45–7.43 (m, 2H), 7.41–7.25 (m, 12H), 7.23–7.20 (m, 1H), 6.95 (d, *J* = 16.2 Hz, 1H), 6.56 (d, *J* = 16.2 Hz, 1H), 2.45 (s, 3H); ^{13}C NMR (125 MHz, $CDCl_3$) δ 197.4, 143.7, 140.3, 137.2, 137.1, 136.5, 135.9, 134.8, 132.1, 130.3, 128.8, 128.6, 128.2, 128.0, 127.8, 127.1, 126.6, 126.2, 125.8, 20.4; HRMS (EI, M^+) for $C_{24}H_{20}O$ calcd. 324.1514, found: m/z 324.1510.

(*E*)-3-(4-methoxyphenyl)-1-(2-((*E*)-4-methoxystyryl)phenyl)prop-2-en-1-one (51j)

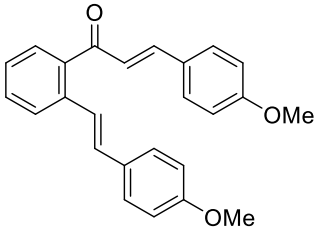

51j

The product was obtained as a yellow solid (1.30 g, 3.5 mmol) in 70% yield from **S2g** (1.34 g, 5.0 mmol) and 4-anisaldehyde. R_f 0.41 (hexanes/EtOAc 10:1); mp 76–79 °C; IR (cast film) 3054, 3031, 3005, 2957, 2934, 2837, 1659, 1634, 1593, 1511, 1463, 1422 cm^{-1}; ^1H NMR (500 MHz, $CDCl_3$) δ 7.75 (d, *J* = 8.1 Hz, 1H), 7.52–7.46 (m, 5H), 7.41 (d, *J* = 8.6 Hz, 2H), 7.32 (td, *J* = 7.5, 1.1 Hz, 1H), 7.28 (d, *J* = 16.1 Hz, 1H), 7.05 (d, *J* = 15.9 Hz, 1H), 7.04 (d, *J* = 16.1 Hz, 1H), 6.89 (d, *J* = 9.0 Hz, 2H), 6.85 (d, *J* = 9.0 Hz, 2H), 3.83 (m, 3H), 3.81 (m 3H); ^{13}C NMR (125 MHz, $CDCl_3$) δ 196.4, 161.8, 159.5, 145.9, 138.7, 136.6, 130.8, 130.5, 130.3, 130.0, 128.4, 128.0, 127.3, 126.7, 126.0, 124.9, 124.2, 114.4, 114.1, 55.4, 55.3; HRMS (EI, M^+) for $C_{25}H_{22}O_3$ calcd. 370.1569, found: m/z 370.1562.

(*E*)-2-methyl-3-phenyl-1-(2-((*E*)-styryl)phenyl)prop-2-en-1-one (51k)

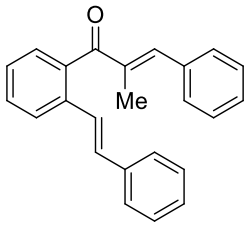

51k

The productwas obtained as a viscous yellow oil (589 mg, 1.8 mmol) in 74% yield from **S2a** (586 mg, 2.5 mmol) and benzaldehyde. [**NOTE**: for the phosphonate part, diethyl ethylphosphonate was used instead of dimethyl methylphosphonate]. R_f 0.30 (hexanes/EtOAc 50:1); IR (cast film) 3058, 3045, 2954, 2923, 1648, 1620, 1576, 1494, 1448 cm^{-1}; ^1H NMR (500 MHz, $CDCl_3$) δ 7.80 (d, *J* = 7.9 Hz, 1H), 7.52–7.47 (m, 3H), 7.34–7.41 (m, 9H), 7.29–7.20 (m, 3H), 7.10 (dq, *J* = 16.1, 1.3 Hz, 1H), 2.32 (q, *J* = 1.3 Hz, 3H); ^{13}C NMR (125 MHz, $CDCl_3$) δ 201.1, 145.0, 138.9, 138.3, 137.1, 136.0, 135.6, 131.1, 129.8, 129.7, 128.8, 128.6, 128.4, 128.3, 127.8, 126.9, 126.7, 125.9, 125.8, 13.3; HRMS (EI, M^+) for $C_{24}H_{20}O$ calcd. 324.1514, found: m/z 324.1510.

(*E*)-1-(2-((*E*)-4-methylstyryl)phenyl)-3-(4-(trifluoromethyl)phenyl)prop-2-en-1-one (51l)

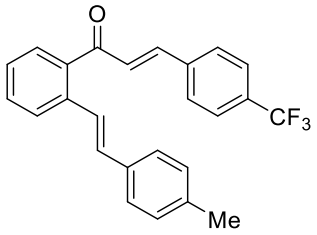

51l

The product was obtained as a yellow solid (2.00 g, 5.1 mmol) in 76% yield from **S2d** (1.70 g, 6.7 mmol) and 4-(trifluoromethyl)benzaldehyde. R_f 0.38 (hexanes/EtOAc 30:1); mp 83–85 °C; IR (cast film) 3060, 3019, 2923, 2858, 1665, 1636, 1607, 1577, 1514, 1477, 1445, 1413 cm^{-1}; ^1H NMR (500 MHz, $CDCl_3$) δ 7.77 (d, *J* = 7.9 Hz, 1H), 7.65–7.51 (m, 7H), 7.40–7.35 (m, 4H), 7.25 (d, *J* = 15.9 Hz, 1H), 7.12 (d, *J* = 8.1 Hz, 2H), 7.05 (d, *J* = 16.3 Hz, 1H), 2.34 (s, 3H); ^{13}C NMR (125 MHz, $CDCl_3$) δ 195.3, 143.3, 138.1, 138.0 (q, *J* = 2.0 Hz), 137.0, 134.2, 132.0 (q, *J* = 33.0 Hz), 131.9, 131.2, 129.4, 128.9, 128.6, 128.5, 127.0, 126.7, 126.6, 125.9 (q, *J* = 3.6 Hz), 125.2, 123.8 (q,

J= 272.2 Hz), 21.2 (one signal is missing due to the overlap); ^{19}F NMR (376 MHz, $CDCl_3$) δ -62.9; HRMS (EI, M^+) for $C_{25}H_{19}F_3O$ calcd. 392.1388, found: m/z 392.1385.

(*E*)-3-(p-tolyl)-1-(2-((*E*)-4-(trifluoromethyl)styryl)phenyl)prop-2-en-1-one (51m)

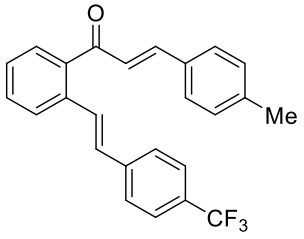

51m

The product was obtained as a yellow solid (1.97 g, 5.0 mmol) in 58% yield from **S2h** (2.66 g, 8.7 mmol) and 4-tolualdehyde. R_f 0.40 (hexanes/EtOAc 30:1); mp 84–85 °C; IR (cast film) 3056, 2925, 1663, 1597, 1569, 1512, 1477 cm^{-1}; ^{1}H NMR (500 MHz, $CDCl_3$) δ 7.79 (d, *J* = 7.9 Hz, 1H), 7.59 (dd, *J* = 7.6, 1.4 Hz, 1H), 7.56–7.51 (m, 7H), 7.46 (d, *J* = 8.4 Hz, 2H), 7.40 (td, *J* = 7.5, 1.2 Hz, 1H), 7.19 (d, *J* = 7.9 Hz, 2H), 7.15 (d, *J* = 15.9 Hz, 1H), 7.08 (d, *J* = 16.1 Hz, 1H), 2.38 (s, 3H); ^{13}C NMR (125 MHz, $CDCl_3$) δ 195.8, 146.5, 141.5, 140.3 (q, *J* = 1.5 Hz), 138.9, 135.9, 131.7, 130.8, 129.8, 129.6, 129.5 (q, *J* = 32.5 Hz), 129.0, 128.6, 128.5, 127.7, 126.9, 126.5, 125.7, 125.6 (q, *J* = 4.1 Hz), 124.2 (q, *J* = 272.2 Hz), 21.5; ^{19}F NMR (470 MHz, $CDCl_3$) δ -62.5; HRMS (EI, M^+) for $C_{25}H_{19}F_3O$ calcd. 392.1388, found: m/z 392.1392.

(*E*)-3-(4-chlorophenyl)-1-(2-((*E*)-4-methylstyryl)phenyl)prop-2-en-1-one (51n)

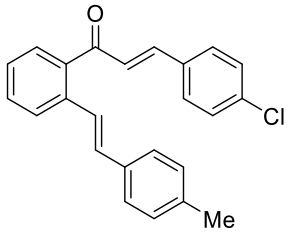

51n

The product was obtained as a yellow oil (728 mg, 2.0 mmol) in 60% yield from **S2d** (1.17 g, 3.4 mmol) and 4-chlorobenzaldehyde. R_f 0.40 (hexanes/EtOAc 30:1); IR (cast film) 3054, 3024, 2919, 1665, 1641, 1602, 1566, 1513, 1490, 1446, 1406 cm^{-1}; ^{1}H NMR (500 MHz, $CDCl_3$) δ 7.77 (d, *J* = 8.0 Hz, 1H), 7.55 (dd, *J* = 7.6, 1.3 Hz, 1H), 7.52–7.46

(m, 4H), 7.38–7.33 (m, 6H), 7.15 (d, J = 16.0 Hz, 1H), 7.12 (d, J = 7.9 Hz, 2H), 7.05 (d, J = 16.1 Hz, 1H), 2.34 (s, 3H); ^{13}C NMR (125 MHz, $CDCl_3$) δ 195.7, 144.1, 138.3, 138.0, 136.8, 136.6, 134.3, 133.1, 131.6, 130.9, 129.6, 129.4, 129.2, 128.5, 127.3, 127.0, 126.7, 126.4, 125.2, 21.3; HRMS (EI, M^+) for $C_{24}H_{19}ClO$ calcd. 358.1124, found: m/z 358.1122.

(*E*)-1-(2-((*E*)-styryl)phenyl)but-2-en-1-one (51o)

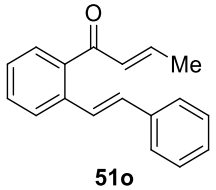

51o

The product was obtained as a yellow oil (2.40 g, 9.7 mmol) in 84% yield from **S2a** (2.74 g, 11.5 mmol) and acetaldehyde (2.0 equiv); [**NOTE**: no heat was applied after acetaldehyde addition; the reaction was stirred at room temperature for 20 h]. R_f 0.30 (hexanes/EtOAc 50:1); IR (cast film) 3059, 3024, 2967, 2936, 2912, 1671, 1649, 1619, 1597, 1563, 1495, 1477, 1446 cm^{-1}; ^{1}H NMR (500 MHz, $CDCl_3$) δ 7.74 (dd, J = 7.9, 0.4 Hz, 1H), 7.48 (d, J = 8.0 Hz, 2H), 7.44 (t, J = 6.9 Hz, 2H), 7.36–7.24 (m, 5H), 7.04 (d, J = 16.1 Hz, 1H), 6.78 (dq, J = 15.6, 6.9 Hz, 1H), 6.55 (dq, J = 15.6, 1.6 Hz, 1H), 1.94 (dd, J = 6.9, 1.6 Hz, 3H); ^{13}C NMR (125 MHz, $CDCl_3$) δ 196.5, 147.3, 138.5, 137.1, 136.2, 132.6, 131.1, 130.4, 128.6, 128.3, 127.8, 126.9, 126.7, 126.2, 126.1, 18.5; HRMS (EI, M^+) for $C_{18}H_{16}O$ calcd. 248.1201, found: m/z 248.1200.

(*Z/E*)-3-phenyl-1-(2-((*E*)-prop-1-en-1-yl)phenyl)prop-2-en-1-one (51p)

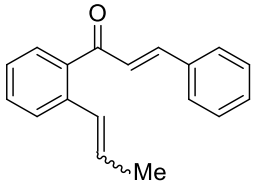

51p

The product was obtained as a yellow oil (mixture of *Z/E* isomers with the ratio 1.9:1 (*Z*-major, *E*-minor); 2.06 g, 8.3 mmol) in 57% yield from **methyl (*E/Z*)-2-(prop-1-en-1-yl)benzoate** (2.56 g, 14.5 mmol) and benzaldehyde. R_f 0.45 (hexanes/EtOAc 50:1);

IR (cast film) 3060, 3025, 2911, 1666, 1643, 1603, 1575, 1495, 1478, 1449, 1400 cm^{-1}; ^1H NMR (600 MHz, $CDCl_3$) δ 7.60–7.28 (m, 16H), 7.13 (d, *J* = 16.0 Hz, 1H, **major)**, 7.12 (d, *J* = 16.0 Hz, 1H, **minor**), 6.65 (d, *J* = 15.6 Hz, 1H, **major**), 6.63 (d, *J* = 11.6 Hz, 1H, **minor**), 6.21 (dq, *J* = 15.6, 6.7 Hz, 1H, **minor**), 5.84 (dq, *J* = 11.5, 7.1 Hz, 1H **major**), 1.86 (dd, *J* = 6.7, 1.8 Hz, 3H, **minor**) 1.77 (dd, *J* = 7.1, 1.8 Hz, 3H, **major**); ^{13}C NMR (125 MHz, $CDCl_3$) δ 196.5, 195.9, 145.7, 144.7, 139.4, 137.9, 136.7, 136.1, 134.7, 134.6, 130.6, 130.5, 130.2, 130.1, 129.0, 128.89, 128.88, 128.6, 128.5, 128.4, 128.3, 128.2, 128.0, 127.0, 126.6, 126.5, 126.41, 126.36, 18.7, 14.5; chemical shifts in ^{13}C are reported for both isomers together without specifying major and minor components; (two signals are missing due to the overlap); HRMS (EI, M^+) for $C_{18}H_{16}O$ calcd. 248.1201, found: m/z 248.1198

3.10.5 General Procedure 4 for the Preparation of *o*-Styrenyl Chalcones 51d, 51g, and 51i.

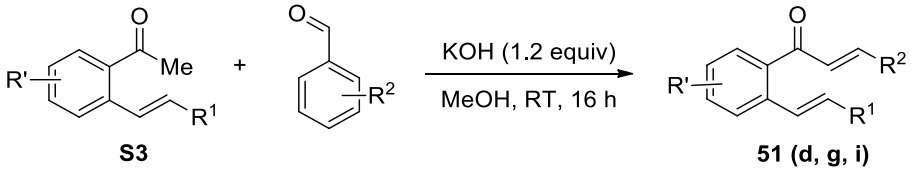

o-Styrenyl chalcones **51d, 51g,** and **51i** were prepared via a known literature procedure;[148] precursor (**S3**) (1.0 equiv) and the corresponding aldehyde (1.0 equiv.) were treated with methanolic solution of KOH (1.2 equiv. 30% solution) at 0 °C. The formation of precipitate was observed after about 5 min. The mixture was stirred at room temperature for 16 h for reaction completion. The solid was filtered off and washed with water until neutral pH. The crude product was recrystallized from methanol.

(*E*)-3-(2-chlorophenyl)-1-(2-((*E*)-2-chlorostyryl)phenyl)prop-2-en-1-one (51d)

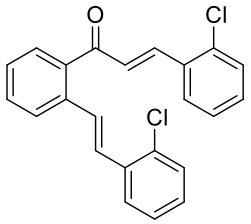

51d

The product was obtained as a yellow solid (1.04 g, 2.8 mmol) in 90% yield from **S3a** (789 mg, 3.1 mmol) and 2-chlorobenzaldehyde. R_f 0.23 (hexanes/EtOAc 30:1); mp 88–89 °C; IR (cast film) 3063, 3034, 1663, 1601, 1564, 1481, 1494 cm^{-1}; ^1H NMR (500 MHz, $CDCl_3$) δ 7.97 (d, *J* = 16.0 Hz, 1H), 7.83 (d, *J* = 7.9 Hz, 1H), 7.67 (dd, *J* = 7.8, 1.7 Hz, 1H), 7.65 (dd, *J* = 7.7, 1.7 Hz, 1H), 7.61 (dd, *J* = 7.7, 1.2 Hz, 1H), 7.55 (ddd, *J* = 7.6, 7.6, 1.2 Hz, 1H), 7.46 (d, *J* = 5.9 Hz, 2H), 7.42–7.39 (m, 2H), 7.37 (td, *J* = 7.8, 1.4 Hz, 1H), 7.32 (td, *J* = 7.7, 1.7 Hz, 1H), 7.27 (td, *J* = 7.6, 0.6 Hz, 1H),), 7.23–7.15 (m, 3H); ^{13}C NMR (175 MHz, $CDCl_3$) δ 195.5, 141.8, 138.2, 136.6, 135.5, 135.2, 133.5, 132.9, 131.3, 131.2, 130.3, 129.7, 129.1, 129.0, 128.8, 128.7, 127.8, 127.6, 127.5, 127.1, 127.0, 126.9 (two signals overlapping); HRMS (EI, M^+) for $C_{23}H_{16}Cl_2O$ calcd. 378.0578, found: m/z 378.0575.

(*E*)-1-(5-fluoro-2-((*E*)-styryl)phenyl)-3-phenylprop-2-en-1-one (51g)

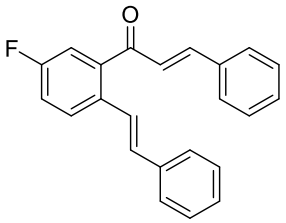

51g

The product was obtained as a yellow solid (606 mg, 1.9 mmol) in 51% yield from **S3c** (872 mg, 3.6 mmol) and benzaldehyde. R_f 0.45 (hexanes/EtOAc 25:1); mp 95–97 °C; IR (cast film) 3060, 3027, 1666, 1599, 1575, 1495, 1449, 1411 cm^{-1}; ^1H NMR (600 MHz, $CDCl_3$) δ 7.75 (dd, *J* = 8.7, 5.3 Hz, 1H), 7.56–7.54 (m, 3H), 7.46 (d, *J* = 7.3 Hz, 2H), 7.41–7.37 (m, 3H), 7.35–7.30 (m, 3H), 7.26–7.20 (m, 3H), 7.15 (d, *J* = 16.1 Hz, 1H), 7.01 (d, *J* = 16.1 Hz, 1H); ^{13}C NMR (125 MHz, $CDCl_3$) δ 194.6 (d, *J* = 2.1 Hz), 161.5 (d, *J* = 249.5 Hz), 146.7, 140.1 (d, *J* = 5.7 Hz), 136.9, 134.3, 132.7 (d, *J* = 3.6

Hz), 131.4 (d, J = 1.6 Hz), 131.0, 129.0, 128.7, 128.6, 128.4 (d, J = 7.7 Hz), 128.0, 126.7, 126.3, 125.2 (d, J = 1.0 Hz), 118.0 (d, J = 21.7 Hz), 115.2 (d, J = 22.7 Hz); ^{19}F NMR (376 MHz, $CDCl_3$) δ -113.8; HRMS (EI, M^+) for $C_{23}H_{17}FO$ calcd. 328.1263, found: m/z 328.1258.

(*E*)-3-(4-(dimethylamino)phenyl)-1-(2-((*E*)-4-(dimethylamino)styryl)phenyl)prop-2-en-1-one (51i)

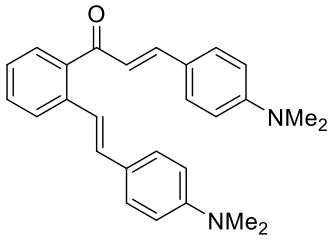

51i

The product was obtained as a reddish-brown solid (1.04 g, 2.6 mmol) in 50% yield from **S3b** (1.40 g, 5.3 mmol) and 4-(dimethylamino)benzaldehyde. R_f 0.3 (hexanes/EtOAc 3:1); mp 66–68 °C; IR (cast film) 2895, 2804, 1651, 1606, 1591, 1570, 1524, 1478, 1444 cm^{-1}; ^{1}H NMR (500 MHz, $CDCl_3$) δ 7.75 (dt, J = 7.9, 0.6 Hz, 1H), 7.47–7.41 (m, 5H), 7.36 (d, J = 8.6 Hz, 2H), 7.26 (td, J = 7.5, 1.3 Hz, 1H), 7.20 (d, J = 16.1 Hz, 1H), 7.03 (d, J = 16.1 Hz, 1H), 6.96 (d, J = 15.7Hz, 1H), 6.64 (td, J = 6.9, 2.3 Hz, 4H), 3.02 (s, 6H), 2.95 (s, 6H); ^{13}C NMR (125 MHz, $CDCl_3$) δ 196.9, 152.1, 150.2, 147.1, 139.2, 136.7, 131.0, 130.4, 130.0, 128.2, 127.9, 126.1, 125.8, 125.5, 122.41, 122.38, 121.9, 112.3, 111.8, 40.4, 40.1; HRMS (ESI, $[M+H]^+$) for $C_{27}H_{29}N_2O$ calcd. 397.2280, found: m/z 397.2273.

(*E*)-1-(2-((E)-prop-1-en-1-yl)phenyl)but-2-en-1-one (51q)

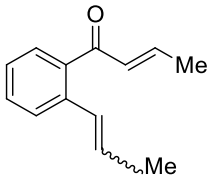

51q

The product was prepared from alcohol **S4** via a known literature procedure:[149] To the crude mixture of alcohol **S4** (2.79 g, 14.8 mmol) and pyridine (11.0 mL, 136.0 mmol) in

DCM (0.08M) was added Dess–Martin periodinane (6.59 g, 15.5 mmol) and stirred at room temperature for 1 h. The reaction mixture was quenched with a 3 M aqueous solution of NaOH (180 mL) and stirring continued for 10 min. The two layers were separated, and the aqueous layer was extracted with DCM (2 x 50 mL). The combined organic layer was washed with brine, dried over $MgSO_4$, and concentrated in vacuo. Flash column chromatography afforded the product as a yellow oil 2.5:1 mixture of E/Z isomers (1.90 g, 10.2 mmol) in 69% yield (*E*-major, *Z*-minor). R_f 0.3 (hexanes/EtOAc 50:1); IR (cast film) 3024, 2965, 2937, 2913, 2851, 1674, 1652, 1621, 1565, 1477, 1443 cm^{-1}; ^1H NMR (500 MHz, $CDCl_3$) δ 7.52 (d, *J* = 7.7 Hz, 1H), 7.44–7.22 (m, 3H), 6.76–6.68 (m, 1H), 6.58–6.46 (m, 2H), 6.17 (dq, *J* = 15.6, 6.7 Hz) and 5.81 (dq, *J* = 11.5, 7.1 Hz) (1H, 2.5:1 ratio), 1.94 (dd, *J* = 6.8, 1.6 Hz) and 1.92 (dd, *J* = 6.8, 1.5 Hz) (3H, 2.5:1 ratio), 1.86 (dd, *J* = 6.7, 1.7 Hz) and 1.73 (dd, *J* = 7.1, 1.8 Hz) (3H, 2.5:1 ratio); ^{13}C NMR (125 MHz, $CDCl_3$) **major** *E* isomer δ 197.1, 147.1, 137.8, 136.6, 132.7, 130.2, 128.6, 128.5, 127.93, 126.2, 126.1, 18.7, 18.5; **minor** *Z* isomer δ 196.4, 146.0, 139.2, 136.0, 132.1, 130.0, 129.9, 128.4, 128.0, 127.95, 126.4, 18.4, 14.5. HRMS (EI, M^+) for $C_{13}H_{14}O$ calcd. 186.1045, found: m/z 186.1044.

3.10.6 Representative Procedure 5 for the Preparation of Formal [2+2] Cycloadducts (52a/52a′)

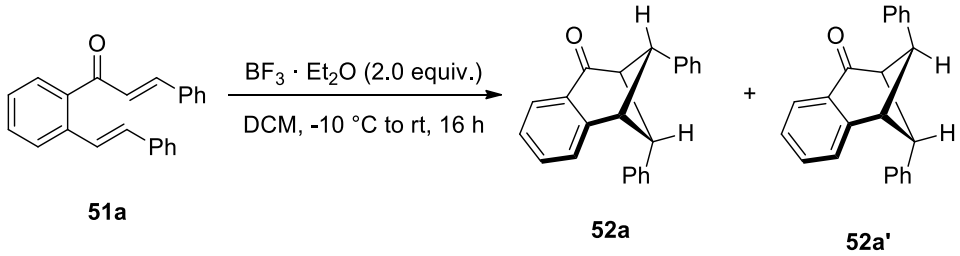

51a **52a** **52a'**

To a round bottom flask containing a cooled solution of $BF_3{\cdot}Et_2O$ (0.08 mL, 0.64 mmol) in DCM (1 mL) was added a solution of *o*-styrenyl chalcone **51a** (100 mg, 0.32 mmol) in DCM (4 mL) at -10 °C and stirred for 1 h. Then, the reaction mixture was allowed to warm to room temperature, and stirring was continued for 16 h, followed by quenching with a sat. aqueous solution of $NaHCO_3$. The layers were separated and the

aqueous layer was extracted with DCM (2 x 20 mL). The combined organic layer was washed with water (20 mL) and brine, dried over $MgSO_4$, and concentrated in vacuo. Flash column chromatography (hexanes/EtOAc 50:1) afforded **52a** (74 mg, 0.24 mmol) and **52a′** (10 mg, 0.032 mmol) in 74% and 10% yields, respectively.

3.10.7 Spectral Data for 52a/52a′–52l/52l′, 52na, 52nb, 52n′, 52o, 52o′, 53j, 53p, 53q

(*1R*,2S*,3R*,9S)-2,9-diphenyl-2,3-dihydro-1,3-methanonaphthalen-4(1H)-one (52a)**

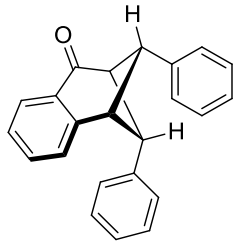

52a

The reaction was performed under the **representative procedure 5.** Flash column chromatography (hexanes/EtOAc 50:1) afforded **52a** (74 mg, 0.24 mmol) as an off-white solid in 74% yield.R_f 0.30 (hexanes/EtOAc 30:1); IR (cast film) 3054, 3026, 2961, 2899, 1693, 1603, 1497, 1461, 1447 cm^{-1}; ^1H NMR (500 MHz, $CDCl_3$) δ 7.79 (dt *J* = 7.6, 0.6 Hz, 1H), 7.54 (d, *J* = 8.1 Hz, 2H), 7.46 (t, *J* = 7.6 Hz, 2H), 7.41 (td, *J* = 7.3, 1.3 Hz, 1H), 7.37 (dd, *J* = 7.6, 1.1 Hz, 1H), 7.33 (t, *J* = 7.6 Hz, 1H), 7.21 (td, *J* = 7.4, 1.4 Hz, 1H), 7.05 (t, *J* = 7.6 Hz 2H), 6.97 (t, *J* = 7.6 Hz 1H), 6.85 (d, *J* = 7.6 Hz, 2H), 4.67 (t, *J* = 6.0 Hz, 1H), 4.10 (t, *J* = 6.0 Hz, 1H), 3.97 (t, *J* = 6.0 Hz, 1H), 3.91 (s, 1H); ^{13}C NMR (125 MHz, $CDCl_3$) δ 199.6, 147.8, 140.0, 139.2, 133.4, 130.3, 128.8, 128.0, 127.2, 127.1, 126.9, 126.6, 126.5, 126.2, 125.8, 57.3, 55.9, 52.5, 48.0; HRMS (EI, M^+) for $C_{23}H_{18}O$ calcd. 310.1358, found: m/z 310.1356.

(*1R*,2R*,3S*,9S)-2,9-diphenyl-2,3-dihydro-1,3-methanonaphthalen-4(1H)-one (52a′)**

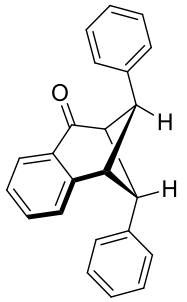

52a′

The reaction was performed under the **representative procedure 5.** Flash column chromatography (hexanes/EtOAc 50:1) afforded **52a′** (10 mg, 0.032 mmol) as an off-white solid in 10% yield. R_f 0.20 (hexanes/EtOAc 30:1); IR (cast film) 3060, 3027, 2963, 2897, 1686, 1604, 1496, 1448, 1300 cm^{-1}; ^1H NMR (500 MHz, $CDCl_3$) δ 7.41 (dt, *J* = 7.6, 0.6 Hz, 1H), 7.29–7.24 (m, 3H), 7.11–7.07 (m, 4H), 7.02–6.93 (m, 6H), 4.49 (t, *J* = 5.7 Hz, 2H), 4.34 (q, *J* = 5.7 Hz, 1H), 4.20 (q, *J* = 5.7 Hz, 1H); ^{13}C NMR (125 MHz, $CDCl_3$) δ198.8, 143.9, 138.3, 133.4, 130.7, 128.1, 127.8, 127.0, 126.9, 125.9, 125.0, 56.8, 53.0, 47.7; HRMS (EI, M^+) for $C_{23}H_{18}O$ calcd. 310.1358, found: m/z 310.1360.

(*1R*,2S*,3R*,9S)-2,9-bis(4-chlorophenyl)-2,3-dihydro-1,3-methanonaphthalen-4(1H)-one (52b)**

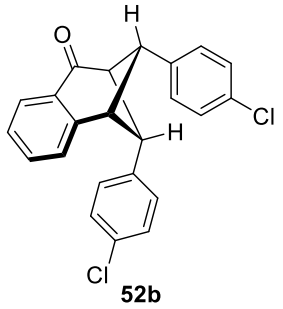

52b

The reaction was performed under the **representative procedure 5.** Flash column chromatography (hexanes/EtOAc 50:1) afforded **52b** (70 mg, 0.19 mmol) as a pale yellow solid in 62% yield. R_f 0.30 (hexanes/EtOAc 30:1); IR (cast film) 3050, 2954, 2917, 1693, 1603, 1492, 1461, 1401, 1349, 2184 cm^{-1}; ^1H NMR (500 MHz, $CDCl_3$) δ 7.79 (dt, *J* = 7.5, 0.7 Hz, 1H), 7.46–7.41(m, 5H), 7.36 (dd, *J* = 7.5, 0.7 Hz, 1H), 7.25 (td, *J* = 7.5, 1.3 Hz, 1H), 7.03 (d, *J* = 8.4 Hz, 2H), 6.77 (dd, *J* = 8.6, 0.9 Hz, 2H), 4.55 (t, *J* = 6.0 Hz, 1H), 4.03 (t, *J* = 6.0 Hz, 1H), 3.89 (t, *J* = 6.0 Hz, 1H), 3.85 (s, 1H); ^{13}C

NMR (125 MHz, $CDCl_3$) δ 198.8, 147.1, 138.2, 137.4, 133.7, 132.9, 131.8, 130.0, 129.0, 128.4, 128.3, 128.0, 127.6, 126.5, 126.4, 57.2, 55.1, 51.9, 47.9; HRMS (EI, M^+) for $C_{23}H_{16}Cl_2O$ calcd. 378.0578, found: m/z 378.0576.

(*1R*,2R*,3S*,9S)-2,9-bis(4-chlorophenyl)-2,3-dihydro-1,3-methanonaphthalen-4(1H)-one (52b′)**

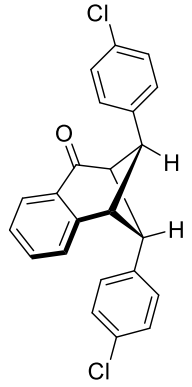

52b′

The reaction was performed under the **representative procedure 5.** Flash column chromatography (hexanes/EtOAc 50:1) afforded **52b′** (28 mg, 0.07 mmol) as a pale yellow solid in 25% yield. R_f 0.20 (hexanes/EtOAc 30:1); IR (cast film) 3032, 2958, 2905, 1694, 1608, 1492, 1462, 1399, 1296, 1204 cm^{-1}; ^1H NMR (500 MHz, $CDCl_3$) δ 7.43 (dt, *J* = 7.5, 0.6 Hz, 1H), 7.30 (td, *J* = 7.3, 1.3 Hz, 1H), 7.26 (dd, *J* = 7.3, 1.5 Hz, 1H), 7.06 (d, *J* = 8.6 Hz, 4H), 7.02 (td, *J* = 7.3, 1.3 Hz, 1H), 6.87 (dd, *J* = 8.6, 0.9 Hz, 4H), 4.42 (t, *J* = 5.7 Hz, 2H), 4.29 (q, *J* = 5.7 Hz, 1H), 4.14 (q, *J* = 5.7 Hz, 1H); ^{13}C NMR (125 MHz, $CDCl_3$) δ 198.2, 143.2, 136.6, 133.8, 131.9, 130.4, 128.4, 128.3, 127.8, 127.4, 125.3, 56.6, 52.3, 47.6; HRMS (EI, M^+) for $C_{23}H_{16}Cl_2O$ calcd. 378.0578, found: m/z 378.0573.

(*1R*,2S*,3R*,9S)-2,9-bis(4-fluorophenyl)-2,3-dihydro-1,3-methanonaphthalen-4(1H)-one (52c)**

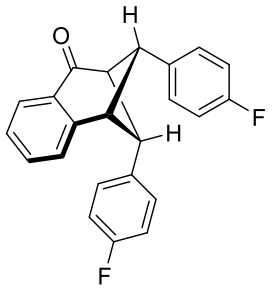

52c

The reaction was performed under the **representative procedure 5.** Flash column chromatography (hexanes/EtOAc50:1) afforded **52c** (65 mg, 0.19 mmol) as an off-white solid in 63% yield. R_f 0.30 (hexanes/EtOAc 30:1); mp 100–102 °C; IR (cast film) 3070, 3044, 2958, 2915, 1695, 1605, 1510, 1462 cm^{-1}; ^1H NMR (500 MHz, $CDCl_3$) δ 7.79 (dt, *J* = 7.6, 0.6 Hz, 1H), 7.50–7.47 (m, 2H), 7.43 (td, *J* = 7.4, 1.4 Hz, 1H), 7.36 (dd, *J* = 7.4, 0.6 Hz, 1H), 7.24 (td, *J* = 7.4, 1.2 Hz, 1H), 7.15–7.13 (m, 2H), 6.81–6.78 (m, 2H), 6.76–6.73 (m, 2H), 4.58 (t, *J* = 6.0 Hz, 1H), 4.03 (t, *J* = 6.0 Hz, 1H), 3.89 (t, *J* = 6.0 Hz, 1H), 3.86 (s, 1H); ^{13}C NMR (125 MHz, $CDCl_3$) δ 199.1, 161.7 (d, *J* = 241.6 Hz), 161.0 (d, *J* = 244.9 Hz), 147.3, 135.5 (d, *J* = 3.1 Hz), 134.7 (d, *J* = 3.1 Hz), 133.6, 130.2, 128.6 (d, *J* = 8.0 Hz), 128.1 (d, *J* = 8.0 Hz), 127.5, 126.5, 126.3, 115.7 (d, *J* = 20.9 Hz), 115.0 (d, *J* = 21.5 Hz), 57.3, 55.0, 51.8, 48.1; ^{19}F NMR (469 MHz, $CDCl_3$) δ -115.5, -116.5; HRMS (EI, M^+) for $C_{23}H_{16}F_2O$ calcd. 346.1169, found: m/z 346.1168.

(*1R*,2R*,3S*,9S)-2,9-bis(4-fluorophenyl)-2,3-dihydro-1,3-methanonaphthalen-4(1H)-one (52c′)**

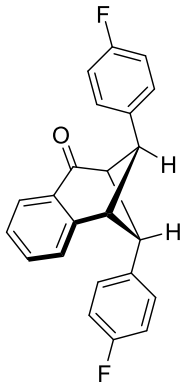

52c′

The reaction was performed under the **representative procedure 5.** Flash column chromatography (hexanes/EtOAc50:1) afforded **52c′** (19 mg, 0.05 mmol) as an off-white solid in 18% yield. R_f 0.20 (hexanes/EtOAc 30:1); decomposes at 110 °C; IR (cast film) 3039, 2948, 1694, 1608, 1511, 1463, 1407 cm^{-1}; ^1H NMR (500 MHz, $CDCl_3$) δ 7.43 (dt, *J* = 7.6, 0.6 Hz, 1H), 7.29 (td, *J* = 7.3, 1.3 Hz, 1H), 7.27–7.25 (m, 1H), 7.00 (td, *J* = 7.6, 1.6 Hz, 1H), 6.92–6.87 (m, 4H), 6.80–6.74 (m, 4H), 4.43 (t, *J* = 5.7 Hz, 2H), 4.29 (q, *J* = 5.7 Hz, 1H), 4.14 (q, *J* = 5.7 Hz, 1H); ^{13}C NMR (125 MHz, $CDCl_3$) δ 198.5, 161.0 (d, *J* = 244.3 Hz), 143.4, 133.9 (d, *J* = 3.7 Hz), 133.7, 130.6, 128.6 (d, *J* = 7.3 Hz), 127.8, 127.2, 125.2, 115.1 (d, *J* = 21.3 Hz), 56.8, 52.2, 47.3; ^{19}F NMR (469 MHz, $CDCl_3$) δ -116.4; HRMS (EI, M^+) for $C_{23}H_{16}F_2O$ calcd. 346.1169, found: m/z 346.1168.

(*1R*,2S*,3R*,9S)-2,9-bis(2-chlorophenyl)-2,3-dihydro-1,3-methanonaphthalen-4(1H)-one (52d)**

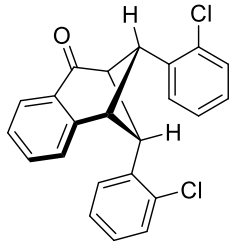

52d

The reaction was performed under the **representative procedure 5.** Flash column chromatography (hexanes/EtOAc50:1) afforded **52d** (77 mg, 0.20 mmol) as an off-white solid in 68% yield. R_f 0.20 (hexanes/EtOAc 30:1); mp 118–121 °C; IR (cast film) 3068, 2979, 2912, 1695, 1603, 1474, 1462, 1440, 1287 cm^{-1}; ^1H NMR (500 MHz, $CDCl_3$) δ 7.86 (dd, *J* = 7.3, 0.4 Hz, 1H), 7.70 (d, *J* = 7.5 Hz, 1H), 7.49 (dd, *J* = 7.8, 1.2 Hz, 1H), 7.43–7.38 (m, 3H), 7.31 (td, *J* = 7.5, 1.5 Hz, 1H), 7.27–7.22 (m, 1H), 7.13–7.09 (m, 1H), 6.99–6.93 (m, 3H), 4.63 (t, *J* = 6.0 Hz, 1H), 4.33 (t, *J* = 6.0 Hz, 1H), 4.03 (t, *J* = 6.0 Hz, 1H), 3.99 (s, 1H); ^{13}C NMR (175 MHz, $CDCl_3$) δ 199.2, 147.0, 137.0, 136.5, 135.3, 133.5, 133.0, 130.1, 129.8, 129.4, 129.1, 128.5, 127.9, 127.4, 127.1, 127.0, 126.6, 126.3, 126.1, 55.3, 54.9, 51.8, 48.0; HRMS (EI, M^+) for $C_{23}H_{16}Cl_2O$ calcd. 378.0578, found: m/z 378.0572.

(*1R*,2R*,3S*,9S)-2,9-bis(2-chlorophenyl)-2,3-dihydro-1,3-methanonaphthalen-4(1H)-one (52d′)**

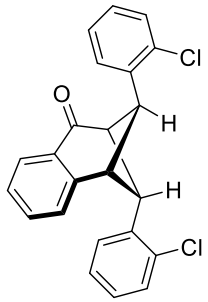

52d′

The reaction was performed under the **representative procedure 5.** Flash column chromatography (hexanes/EtOAc50:1) afforded **52d′** (19 mg, 0.05 mmol) as an off-white solid in 17% yield. R_f 0.30 (hexanes/EtOAc 30:1); IR (cast film) 3060, 2915, 1701, 1604, 1472, 1441, 1362, 1302, 1257 cm^{-1}; ^1H NMR (600 MHz, $CDCl_3$) δ 8.19 (dt, *J* = 7.6, 0.8 Hz, 1H), 7.57 (td, *J* = 7.5, 1.5 Hz, 1H), 7.50 (d, *J* = 7.5, Hz, 1H), 7.49 (td, *J* = 7.5, 1.5 Hz, 1H), 7.34 (dd, *J* = 7.9, 1.0 Hz, 2H), 7.04 (td, *J* = 7.5, 1.5 Hz, 2H), 6.75 (td, *J* = 7.5, 1.0 Hz, 2H), 6.68 (dd, *J* = 7.6, 1.3 Hz, 2H), 4.26 (d, *J* = 6.6 Hz, 1H), 4.15 (d, *J* = 6.6 Hz, 1H), 3.88 (s, 2H); ^{13}C NMR (125 MHz, $CDCl_3$) δ 199.7, 152.1, 136.9, 134.2, 133.4, 129.6, 129.5, 128.4, 127.80, 127.76, 127.72, 125.7, 125.1, 56.4, 54.3, 45.9; HRMS (EI, M^+) for $C_{23}H_{16}Cl_2O$ calcd. 378.0578, found: m/z 378.0572.

(*1R*,2S*,3R*,9S)-2,9-di-p-tolyl-2,3-dihydro-1,3-methanonaphthalen-4(1H)-one (52e)**

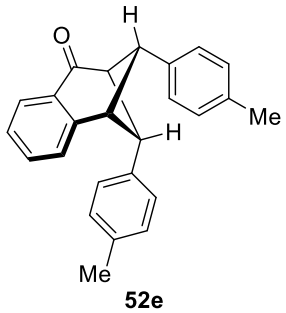

52e

The reaction was performed under the **representative procedure 5.** Flash column chromatography (hexanes/EtOAc50:1) afforded **52e** (42 mg, 0.12 mmol) as a yellow oil

in 41% yield. R_f 0.40 (hexanes/EtOAc25:1); IR (cast film) 3023, 2949, 2919, 1693, 1604, 1515, 1461, 1287, 1216 cm^{-1}; ^1H NMR (500 MHz, $CDCl_3$) δ 7.79 (dt, *J* = 7.6, 0.7 Hz, 1H), 7.42–7.39 (m, 3H), 7.36 (d, *J* = 7.3 Hz, 1H), 7.25 (d, *J* = 8.1 Hz, 2H), 7.21 (td, *J* = 7.5, 1.3 Hz, 1H), 6.85 (d, *J* = 8.1 Hz, 2H), 6.73 (d, *J* = 8.1 Hz, 2H), 4.63 (t, *J* = 6.0 Hz, 1H), 4.04 (t, *J* = 6.0 Hz, 1H), 3.91 (t, *J* = 6.0 Hz, 1H), 3.85 (s, 1H), 2.39 (s, 3H), 2.14 (s, 3H); ^{13}C NMR (125 MHz, $CDCl_3$) δ 199.8, 148.0, 137.1, 136.5, 136.1, 135.2, 133.4, 130.4, 129.5, 128.7, 127.1, 127.0, 126.5, 126.4, 126.1, 57.4, 55.7, 52.4, 48.1, 21.1, 21.0; HRMS (EI, M^+) for $C_{25}H_{22}O$ calcd. 338.1671, found: m/z 338.1667.

(*1R*,2R*,3S*,9S)-2,9-di-p-tolyl-2,3-dihydro-1,3-methanonaphthalen-4(1H)-one (52e′)**

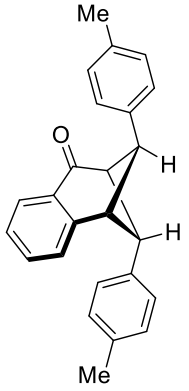

52e′

The reaction was performed under the **representative procedure 5.** Flash column chromatography (hexanes/EtOAc 50:1) afforded **52e′** (40 mg, 0.118 mmol) as an off-white solid in 39% yield. R_f 0.33 (hexanes/EtOAc 25:1); mp 162–164 °C; IR (cast film) 3049, 3024, 2944, 2920, 2887, 1693, 1607, 1516, 1458, 1408, 1370, 1297, 1265, 1216 cm^{-1}; ^1H NMR (500 MHz, $CDCl_3$) δ 7.42 (dq, *J* = 7.5, 0.9 Hz, 1H), 7.27–7.26 (m, 2H), 6.96 (ddd, *J* = 7.6, 4.7, 3.5 Hz, 1H), 6.88 (d, *J* = 8.1 Hz, 4H), 6.83 (d, *J* = 8.1 Hz, 4H), 4.43 (t, *J* = 5.5 Hz, 2H), 4.28 (q, *J* = 5.7 Hz, 1H), 4.14 (q, *J* = 5.7 Hz, 1H), 2.16 (s, 6H); ^{13}C NMR (125 MHz, $CDCl_3$) δ 199.1, 144.1, 135.3, 135.2, 133.3, 130.8, 128.8, 127.8, 126.9, 126.8, 125.0, 56.8, 52.9, 47.7, 21.0; HRMS (EI, M^+) for $C_{25}H_{22}O$ calcd. 338.1671, found: m/z 338.1668.

(*1R*,2S*,3R*,9S)-2,9-di(naphthalen-1-yl)-2,3-dihydro-1,3-methanonaphthalen-4(1H)-one (52f)**

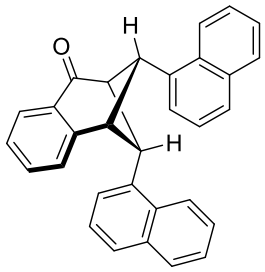

52f

The reaction was performed under the **representative procedure 5.** Flash column chromatography (hexanes/EtOAc 50:1) afforded **52f** (82 mg, 0.20 mmol) as an off-white solid in 67% yield. R_f 0.53 (hexanes/EtOAc 25:1); mp 222 °C (decomposes); IR (cast film) 3049, 2960, 2918, 1689, 1600, 1474, 1461, 1398 cm^{-1}; ^1H NMR (600 MHz, $CDCl_3$) δ 7.98 (m, 1H), 7.91–7.88 (m, 3H), 7.86–7.83 (m, 2H), 7.70 (dd, *J* = 7.9, 1.1 Hz, 1H), 7.62 (t, *J* = 8.2, Hz, 1H), 7.59 (m, 2H), 7.53 (d, *J* = 8.4, Hz, 1H), 7.43 (td, *J* = 8.4, 1.5 Hz, 1H), 7.39 (td, *J* = 8.1, 1.3 Hz, 1H), 7.28 (td, *J* = 7.4, 1.4 Hz, 1H), 7.24 (dd, *J* = 7.4, 0.7 Hz, 1H), 7.21 (td, *J* = 7.4, 1.3 Hz, 1H), 7.18 (d, *J* = 8.2 Hz, 1H), 7.11 (dd, *J* = 7.1, 1.3 Hz, 1H), 5.21 (t, *J* = 6.0 Hz, 1H), 4.46 (t, *J* = 6.0 Hz, 1H), 4.44 (s, 1H), 4.31 (t, *J* = 6.0 Hz, 1H); ^{13}C NMR (175 MHz, $CDCl_3$) δ 200.1, 147.1, 135.2, 134.8, 134.2, 133.5, 133.4, 131.7, 131.3, 130.3, 129.2, 128.8, 128.1, 127.4, 127.2, 126.6, 126.3, 126.2, 126.1, 125.9, 125.8, 125.5, 125.4, 124.9, 123.7, 123.5, 123.2, 56.3, 55.2, 52.5, 50.0; HRMS (EI, M^+) for $C_{31}H_{22}O$ calcd. 410.1671, found: m/z 410.1665.

(*1R*,2R*,3S*,9S)-2,9-di(naphthalen-1-yl)-2,3-dihydro-1,3-methanonaphthalen-4(1H)-one (52f′)**

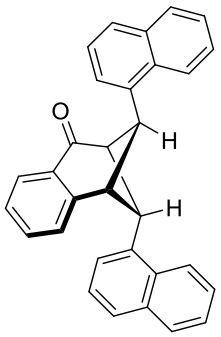

52f′

The reaction was performed under the **representative procedure 5.** Flash column chromatography (hexanes/EtOAc50:1) afforded **52f′** (28 mg, 0.07 mmol) as an off-white solid in 23% yield. R_f 0.35 (hexanes/EtOAc25:1); mp 228 °C (decomposes); IR (cast film) 3049, 2959, 2923, 1687, 1604, 1510, 1462, 1399 cm^{-1}; ^1H NMR (600 MHz, $CDCl_3$) δ 8.18 (d, *J* = 8.3 Hz, 2H), 7.75 (d, *J* = 8.1 Hz, 2H), 7.59–7.55 (m, 4H), 7.46 (app t, *J* = 7.3 Hz, 3H), 7.17 (t, *J* = 7.3 Hz, 2H), 7.13 (d, *J* = 7.3 Hz, 2H), 6.99–6.96 (m, 2H), 6.85 (td, *J* = 7.6, 2.4 Hz, 1H), 5.05 (t, *J* = 5.3 Hz, 2H), 4.98 (q, *J* = 5.3 Hz, 1H), 4.58 (q, *J* = 5.3 Hz, 1H); ^{13}C NMR (176 MHz, $CDCl_3$) δ 199.6, 142.6, 133.7, 133.6, 133.3, 131.7, 130.4, 128.9, 127.4, 127.3, 126.9, 126.4, 125.9, 125.5, 124.9, 124.6, 123.8, 58.1, 53.9, 51.9; HRMS (EI, M^+) for $C_{31}H_{22}O$ calcd. 410.1671, found: m/z 410.1670.

(*1R*,2S*,3R*,9S)-6-fluoro-2,9-diphenyl-2,3-dihydro-1,3-methanonaphthalen-4(1H)-one (52g)**

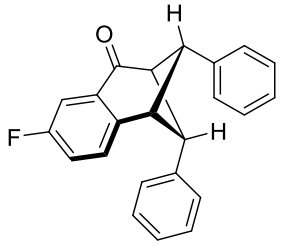

52g

The reaction was performed under the **representative procedure 5.** Flash column chromatography (hexanes/EtOAc 50:1) afforded **52g** (54 mg, 0.16 mmol) as a white solid in 55% yield. R_f 0.48 (hexanes/EtOAc 25:1); mp 135–137 °C; IR (cast film) 3058, 3029, 2948, 2907, 1698, 1602, 1488, 1433, 1352, 1270 cm^{-1}; ^1H NMR (500 MHz, $CDCl_3$) δ 7.54–7.52 (m, 2H), 7.47–7.44 (m, 3H), 7.36–7.32 (m, 2H), 7.12–7.06 (m, 3H), 7.00 (app t, *J* = 7.5 Hz, 1H), 6.84 (app d, *J* = 8.1 Hz, 2H), 4.68 (t, *J* = 6.0 Hz, 1H), 4.10 (t, *J* = 6.0 Hz, 1H), 3.97 (t, *J* = 6.0 Hz, 1H), 3.89 (s, 1H); ^{13}C NMR (125 MHz, $CDCl_3$) δ 198.4 (d, *J* = 2.1 Hz), 161.8 (d, *J* = 246.4 Hz), 143.6 (d, *J* = 3.1 Hz), 139.7, 138.9, 132.0 (d, *J* = 6.2 Hz), 128.9, 128.2 (d, *J* = 7.1 Hz), 128.1, 127.03, 127.01, 126.6, 126.0, 120.2 (d, *J* = 22.2 Hz), 112.8 (d, *J* = 22.2 Hz), 57.0, 56.0, 52.6, 47.2; ^{19}F NMR

(376 MHz, $CDCl_3$) δ -113.9; HRMS (EI, M^+) for $C_{23}H_{17}FO$ calcd. 328.1263, found: m/z 328.1265.

(*1R*,2R*,3S*,9S)-6-fluoro-2,9-diphenyl-2,3-dihydro-1,3-methanonaphthalen-4(1H)-one (52g′)**

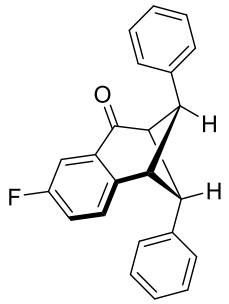

52g′

The reaction was performed under the **representative procedure 5.** Flash column chromatography (hexanes/EtOAc 50:1) afforded **52g′** (26 mg, 0.08 mmol) as a white solid in 26% yield. R_f 0.29 (hexanes/EtOAc25:1); IR (cast film) 3060, 3027, 2959, 2899, 1695, 1602, 1488, 1435, 1342, 1301, 1270 cm^{-1}; ^1H NMR (500 MHz, $CDCl_3$) δ 7.27 (dd, *J* = 8.2, 4.8 Hz, 1H), 7.14–7.10 (m, 5H), 7.06–7.03 (m, 2H), 6.98–6.95 (m, 5H), 4.52 (td, *J* = 5.7, 0.6 Hz, 2H), 4.37 (q, *J* = 5.7 Hz, 1H), 4.23 (q, *J* = 5.7 Hz, 1H); ^{13}C NMR (125 MHz, $CDCl_3$) δ 197.7 (d, *J* = 2.1 Hz), 161.5 (d, *J* = 246.4 Hz), 139.6 (d, *J* = 3.1 Hz), 138.0, 132.3 (d, *J* = 6.7 Hz), 129.4 (d, *J* = 7.2 Hz), 128.2, 127.0, 126.1, 120.1 (d, *J* = 22.2 Hz), 111.8 (d, *J* = 22.2 Hz), 56.4 (d, *J* = 1.0 Hz), 53.0 (d, *J* = 1.0 Hz), 47.0; ^{19}F NMR (376 MHz, $CDCl_3$) δ -114.1; HRMS (EI, M^+) for $C_{23}H_{17}FO$ calcd. 328.1263, found: m/z 328.1260.

(*1R*,2S*,3R*,9S)-8-methyl-2,9-diphenyl-2,3-dihydro-1,3-methanonaphthalen-4(1H)-one (52h)**

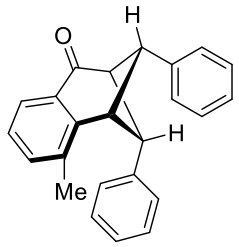

52h

The reaction was performed under the **representative procedure 5.** Flash column chromatography (hexanes/EtOAc50:1) afforded **52h** (43 mg, 0.13 mmol) as an off-white solid in 44% yield. R_f 0.35 (hexanes/EtOAc 25:1); IR (cast film) 3060, 3025, 2917, 1696, 1596, 1498, 1448, 1358, 1284 cm^{-1}; ^1H NMR (500 MHz, $CDCl_3$) δ 7.67 (dt, *J* = 7.5, 0.6 Hz, 1H), 7.56 (d, 7.8 Hz, 2H), 7.49 (t, *J* = 7.6 Hz, 2H), 7.36 (t, *J* = 7.6 Hz, 1H), 7.26 (dd, *J* = 7.5 Hz, 1H), 7.11–7.05 (m, 3H), 6.97 (ddd, *J* = 7.5, 7.5, 0.9 Hz, 1H), 6.84 (app d, *J* = 7.4 Hz, 2H), 4.70 (t, *J* = 6.0 Hz, 1H), 4.33 (t, *J* = 6.0 Hz, 1H), 3.98 (t, *J* = 6.0 Hz, 1H), 3.86 (s, 1H), 2.50 (s, 3H); ^{13}C NMR (125 MHz, $CDCl_3$) δ 199.9, 145.9, 140.3, 139.4, 135.0, 133.8, 130.4, 128.8, 128.1, 127.1, 126.9, 126.6, 126.3, 125.8, 124.2, 57.0, 55.4, 52.2, 43.7, 19.1; HRMS (EI, M^+) for $C_{24}H_{20}O$ calcd. 324.1514, found: m/z 324.1514.

(*1R*,2R*,3S*,9S)-8-methyl-2,9-diphenyl-2,3-dihydro-1,3-methanonaphthalen-4(1H)-one (52h′)**

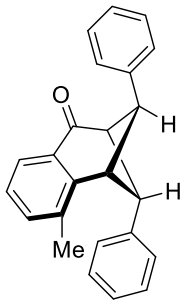

52h′

The reaction was performed under the **representative procedure 5.** Flash column chromatography (hexanes/EtOAc50:1) afforded **52h′** (22 mg, 0.07 mmol) as an off-white solid in 23% yield. R_f 0.46 (hexanes/EtOAc 25:1); IR (cast film) 3060, 3026, 2972, 2910, 1693, 1597, 1497, 1476, 1447, 1287 cm^{-1}; ^1H NMR (500 MHz, $CDCl_3$) δ 8.03 (dt, *J* = 7.5, 0.6 Hz, 1H), 7.43 (dq, *J* = 7.5, 0.7 Hz, 1H), 7.34 (t, *J* = 7.5, Hz, 1H),

7.08–7.03 (m, 8H), 7.02–6.98 (m, 2H), 4.40 (d, J = 6.4 Hz, 1H), 4.06 (d, J = 6.4 Hz, 1H), 3.86 (s, 2H), 2.58 (s, 3H); ^{13}C NMR (125 MHz, $CDCl_3$) δ 201.1, 150.8, 140.0, 134.9, 132.4, 130.1, 127.8, 126.9, 126.8, 125.8, 125.5, 58.0, 57.0, 44.0, 19.1; HRMS (EI, M^+) for $C_{24}H_{20}O$ calcd. 324.1514, found: m/z 324.1513.

(*1R*,2S*,3R*,9S)-2,9-bis(4-(dimethylamino)phenyl)-2,3-dihydro-1,3-methanonaphthalen-4(1H)-one (52i)**

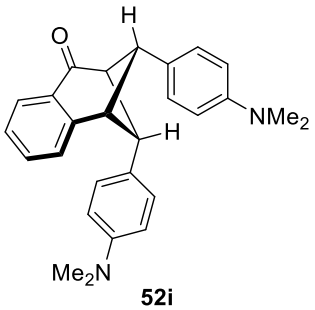

52i

The reaction was performed under the **representative procedure 5.** Flash column chromatography (hexanes/EtOAc50:1) afforded **52i** (33 mg, 0.08 mmol) as a yellow solid in 28% yield. R_f 0.41 (hexanes/EtOAc 3:1); IR (cast film) 2946, 2894, 2802, 1691, 1614, 1523, 1460, 1349, 1281 cm^{-1}; ^{1}H NMR (500 MHz, $CDCl_3$) δ 7.79 (d, J = 7.4 Hz, 1H), 7.40–7.37 (m, 3H), 7.34 (d, J = 7.1 Hz, 1H), 7.20 (td, J = 7.4, 1.0 Hz, 1H), 6.81 (d, J = 8.7 Hz, 2H), 6.70 (d, J = 8.3 Hz, 2H), 6.43 (d, J = 8.7 Hz, 2H), 4.63 (t, J = 6.0 Hz, 1H), 3.96 (t, J = 6.0 Hz, 1H), 3.85 (t, J = 6.0 Hz, 1H), 3.80 (s, 1H), 2.98 (s, 6H), 2.78 (s, 6H); ^{13}C NMR (125 MHz, $CDCl_3$) δ 200.5, 149.5, 148.5, 133.2, 130.6, 128.0, 127.8, 127.3, 127.2, 126.9, 126.4, 126.0, 112.8, 112.4, 57.6, 55.7, 52.2, 48.3, 40.7, 40.5 (one signal is missing due to overlap); HRMS (ESI, $[M+H]^+$) for $C_{27}H_{29}N_2O$ calcd. 397.2280, found: m/z 397.2274.

(*1R*,2R*,3S*,9S)-2,9-bis(4-(dimethylamino)phenyl)-2,3-dihydro-1,3-methanonaphthalen-4(1H)-one (52i′)**

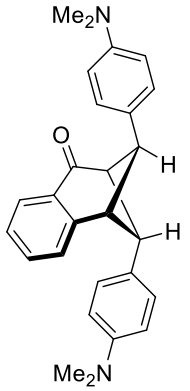

52i′

The reaction was performed under the **representative procedure 5.** Flash column chromatography (hexanes/EtOAc 50:1) afforded **52i′** (33 mg, 0.08 mmol) as a yellow solid in 28% yield. R_f 0.25 (hexanes/EtOAc 3:1); IR (cast film) 3071, 2875, 2801, 1690, 1606, 1532, 1479, 1462, 1363, 1305, 1228 cm^{-1}; ^1H NMR (500 MHz, $CDCl_3$) δ 7.47 (d, *J* = 7.6 Hz, 1H), 7.29–7.26 (m, 2H), 6.98 (ddd, *J* = 7.6, 6.3, 2.2 Hz, 1H), 6.82 (d, *J* = 8.2 Hz, 4H), 6.48 (d, *J* = 8.8 Hz, 4H), 4.40 (t, *J* = 5.6 Hz, 2H), 4.24 (q, *J* = 5.6 Hz, 1H), 4.04 (q, *J* = 5.6 Hz, 1H), 2.81 (s, 12H); ^{13}C NMR (125 MHz, $CDCl_3$) δ 199.8, 148.6, 144.4, 133.2, 131.1, 127.8, 127.7, 126.6, 126.4, 124.8, 112.4, 57.0, 52.9, 47.9, 40.5; HRMS (ESI, $[M+H]^+$) for $C_{27}H_{29}N_2O$ calcd. 397.2280, found: m/z 397.2273.

(*1R*,2S*,3R*,9S)-2,9-bis(4-methoxyphenyl)-2,3-dihydro-1,3-methanonaphthalen-4(1H)-one (52j)**

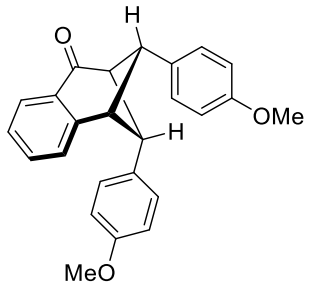

52j

The reaction was performed under the **representative procedure 5.** Flash column chromatography (hexanes/EtOAc 30:1) afforded **52j** (22 mg, 0.06 mmol) as a yellow solid in 20% yield. R_f 0.38 (hexanes/EtOAc 10:1); IR (cast film) 2954, 2835, 1692, 1610, 1582, 1513, 1461, 1296, 1248, 1178, 1111 cm^{-1}; ^1H NMR (500 MHz, $CDCl_3$)

δ7.79 (dt, *J* = 7.6, 0.6 Hz, 1H), 7.44 (dd, *J* = 8.8, 0.9 Hz, 2H), 7.40 (td, *J* = 7.3, 1.3 Hz, 1H), 7.35 (dd, *J* = 7.5, 0.7 Hz, 1H), 7.22 (td, *J* = 7.5, 1.3 Hz, 1H), 6.98 (d, *J* = 8.8 Hz, 2H), 6.75 (dd, *J* = 8.8, 1.0 Hz, 2H), 6.59 (d, *J* = 8.8 Hz, 2H), 4.61 (t, *J* = 6.0 Hz, 1H), 4.00 (t, *J* = 6.0 Hz, 1H), 3.87 (t, *J* = 6.0 Hz, 1H), 3.85 (s, 3H), 3.83 (s, 1H), 3.65 (s, 3H); ^{13}C NMR (125 MHz, $CDCl_3$) δ 199.9, 158.5, 157.5, 148.0, 133.4, 132.1, 131.2, 130.4, 128.1, 127.7, 127.2, 126.5, 126.1, 114.2, 113.5, 57.5, 55.38, 55.37, 55.0, 52.1, 48.2; HRMS (EI, M^+) for $C_{25}H_{22}O_3$ calcd. 370.1569, found: m/z 370.1575.

(*1R*,2R*,3S*,9S)-2,9-bis(4-methoxyphenyl)-2,3-dihydro-1,3-methanonaphthalen-4(1H)-one (52j′)**

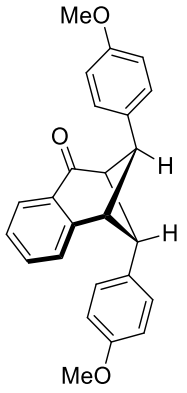

52j′

The reaction was performed under the **representative procedure 5.** Flash column chromatography (hexanes/EtOAc 30:1) afforded **52j′** (30 mg, 0.08 mmol) as an off-white solid in 27% yield. R_f 0.26 (hexanes/EtOAc 10:1); IR (cast film) 2956, 2899, 2835, 1690, 1607, 1582, 1514, 1462, 1414, 1299, 1248, 1177, 1132 cm^{-1}; ^{1}H NMR (500 MHz, $CDCl_3$) δ 7.43 (dt, *J* = 7.7, 0.6 Hz, 1H), 7.29–7.24 (m, 2H), 6.98 (ddd, *J* = 7.6, 6.6, 2.2 Hz, 1H), 6.85 (dd, *J* = 8.8, 0.9 Hz, 4H), 6.62 (d, *J* = 8.8 Hz, 4H), 4.42 (t, *J* = 5.7 Hz, 2H), 4.26 (q, *J* = 5.7 Hz, 1H), 4.10 (q, *J* = 5.7 Hz, 1H), 3.66 (s, 6H); ^{13}C NMR (125 MHz, $CDCl_3$) δ 199.2, 157.6, 144.0, 133.4, 130.9, 130.4, 128.1, 127.8, 126.8, 124.9, 113.5, 56.9, 55.0, 52.6, 47.8; HRMS (EI, M^+) for $C_{25}H_{22}O_3$ calcd. 370.1569, found: m/z 370.1563.

(*Z*)-2-(4-methoxybenzylidene)-3-(4-methoxyphenyl)-3,4-dihydronaphthalen-1(2H)-one (53j).

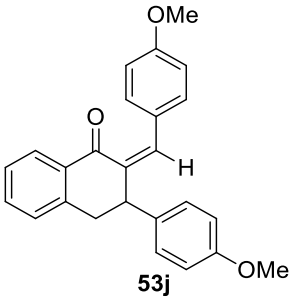

53j

The reaction was performed under the **representative procedure 5.** Flash column chromatography (hexanes/EtOAc 30:1) afforded **53j** (19 mg, 0.05 mmol) as a yellow oil in 17% yield. R_f 0.33 (hexanes/EtOAc 10:1); IR (cast film) 2929, 2837, 1663, 1603, 1510, 1457, 1301, 1254, 1178 cm^{-1}; ^1H NMR (500 MHz, $CDCl_3$) δ 8.10 (dd, *J* = 7.8, 1.3 Hz, 1H), 8.04 (s, 1H), 7.37 (td, *J* = 7.4, 1.4 Hz, 1H), 7.31 (d, *J* = 8.5 Hz, 2H), 7.28 (dt, *J* = 7.7, 1.0 Hz, 1H), 7.12 (dd, *J* = 8.3, 0.6 Hz, 2H), 7.07 (d, *J* = 7.6 Hz, 1H), 6.86 (d, *J* = 8.8 Hz, 2H), 6.75 (d, *J* = 8.8 Hz, 2H), 4.76 (dd, *J* = 3.6, 1.6 Hz, 1H), 3.81 (s, 3H), 3.72 (s, 3H), 3.51 (dd, *J* = 15.8, 5.4 Hz, 1H), 3.20 (dd, *J* = 15.8, 2.3 Hz, 1H); ^{13}C NMR (125 MHz, $CDCl_3$) δ 188.0, 160.3, 158.1, 140.3, 138.7, 135.4, 134.5, 133.5, 133.4, 131.8, 129.1, 128.8, 128.6, 128.0, 127.7, 127.0, 114.1, 55.3, 55.1, 41.4, 36.7; HRMS (EI, M^+) for $C_{25}H_{22}O_3$ calcd. 370.1569, found: m/z 370.1561.

(*1S*,2R*,3S*,9R)-3-methyl-2,9-diphenyl-2,3-dihydro-1,3-methanonaphthalen-4(1H)-one (52k)**

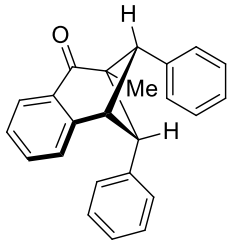

52k

The reaction was performed under the **representative procedure 5.** Flash column chromatography (hexanes/EtOAc 50:1) afforded **52k** (47 mg, 0.14 mmol) as a white solid in 48% yield. R_f 0.45 (hexanes/EtOAc 25:1); IR (cast film) 3061, 3026, 2962, 2923, 1688, 1603, 1497, 1447, 1378, 1295, 1200 cm^{-1}; ^1H NMR (500 MHz, $CDCl_3$) δ 7.85 (dt, *J* = 7.7, 0.6 Hz, 1H), 7.46–7.42 (m, 4H), 7.37 (td, *J* = 7.3, 1.4 Hz, 1H),

7.35–7.32 (m, 1H), 7.31 (dd, *J* = 7.3, 0.6 Hz, 1H), 7.21 (td, *J* = 7.5, 1.3 Hz, 1H), 7.04 (app t, *J* = 7.1 Hz, 2H), 6.97 (app t, *J* = 7.3 Hz, 1H), 6.87–6.85 (app d, *J* = 8.2 Hz, 2H), 4.59 (d, *J* = 6.0 Hz, 1H), 4.24 (d, *J* = 6.0 Hz, 1H), 3.75 (s, 1H), 1.26 (s, 3H); ^{13}C NMR (125 MHz, $CDCl_3$) δ 201.4, 148.4, 139.3, 138.0, 133.0, 130.1, 128.6, 128.4, 128.0, 127.1, 127.0, 126.7, 126.4, 126.2, 125.9, 61.1, 59.5, 57.1, 43.8, 17.0; HRMS (EI, M^+) for $C_{24}H_{20}O$ calcd. 324.1514, found: m/z 324.1514.

(*1S*,2R*,3S*,9S)-3-methyl-2,9-diphenyl-2,3-dihydro-1,3-methanonaphthalen-4(1H)-one (52k′)**

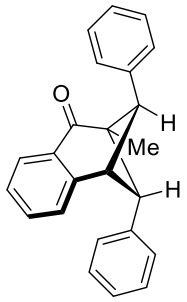

52k′

The reaction was performed under the **representative procedure 5.** Flash column chromatography (hexanes/EtOAc 50:1) afforded **52k′** (35 mg, 0.11 mmol) as a white solid in 36% yield. R_f 0.35 (hexanes/EtOAc 25:1); IR (cast film) 3087, 3060, 3027, 2959, 2926, 1685, 1603, 1497, 1447, 1375, 1309, 1199 cm^{-1}; ^{1}H NMR (500 MHz, $CDCl_3$) δ 7.51 (dt, *J* = 7.5, 0.6 Hz, 1H), 7.24–7.20 (m, 2H), 7.06 (t, *J* = 7.4 Hz, 4H), 7.00–6.91 (m, 7H), 4.33 (t, *J* = 5.9 Hz, 1H), 4.25 (d, *J* = 5.9 Hz, 2H), 1.93 (s, 3H); ^{13}C NMR (125 MHz, $CDCl_3$) δ 200.1, 144.7, 138.4, 133.1, 131.0, 128.0, 127.7, 127.0, 126.6, 126.0, 125.1, 60.4, 59.9, 46.9, 21.1; HRMS (EI, M^+) for $C_{24}H_{20}O$ calcd. 324.1514, found: m/z 324.1515.

(*1S*,2S*,3R*,9S)-2-(p-tolyl)-9-(4-(trifluoromethyl)phenyl)-2,3-dihydro-1,3-methanonaphthalen-4(1H)-one (52l)**

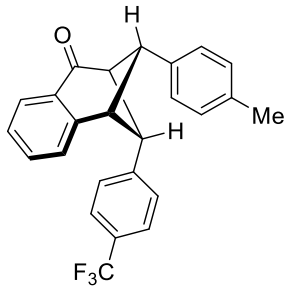

52l

The reaction was performed under the **representative procedure 5.** Flash column chromatography (hexanes/EtOAc 50:1) afforded **52l** (65 mg, 0.16 mmol) as a yellow solid in 55% yield. R_f 0.36 (hexanes/EtOAc 25:1); IR (cast film) 2972, 2918, 2845, 1695, 1619, 1515, 1461, 1411, 1328 cm^{-1}; ^1H NMR (500 MHz, $CDCl_3$) δ 7.79 (dd, *J* = 7.6, 1.3 Hz, 1H), 7.45–7.41 (m, 3H), 7.38 (dd, *J* = 7.4, 1.2 Hz, 1H), 7.31 (d, *J* = 8.1 Hz, 2H), 7.27 (d, *J* = 8.1 Hz, 2H), 7.24 (td, *J* = 7.5, 1.2 Hz, 1H), 6.96 (d, *J* = 8.0 Hz, 2H), 4.65 (t, *J* = 6.0 Hz, 1H), 4.09 (t, *J* = 6.0 Hz, 1H), 3.96 (t, *J* = 6.0 Hz, 1H), 3.89 (s, 1H), 2.40 (s, 3H); ^{13}C NMR (125 MHz, $CDCl_3$) δ 199.2, 147.4, 146.3 (q, *J* = 1.0 Hz), 136.8, 136.6, 133.7, 130.0, 129.6, 128.1 (q, *J* = 32.5 Hz), 127.5, 127.0, 126.9, 126.5, 126.4, 125.0 (q, *J* = 3.6 Hz), 124.0 (q, *J* = 272.2 Hz), 57.4, 55.7, 52.4, 48.0, 21.1; ^{19}F NMR (376 MHz, $CDCl_3$) δ -62.6; HRMS (EI, M^+) for $C_{25}H_{19}F_3O$ calcd. 392.1388, found: m/z 392.1389.

(*1S*,2R*,3R*,9S)-2-(p-tolyl)-9-(4-(trifluoromethyl)phenyl)-2,3-dihydro-1,3-methanonaphthalen-4(1H)-one (52l′)**

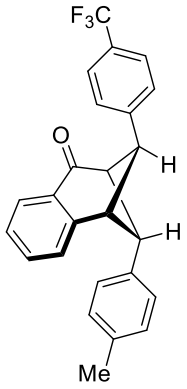

52l′

The reaction was performed under the **representative procedure 5.** Flash column chromatography (hexanes/EtOAc 50:1) afforded **52l′** (36 mg, 0.09 mmol) as a yellow solid in 30% yield. R_f 0.17 (hexanes/EtOAc 25:1); IR (cast film) 3047, 3026, 2957, 2923, 1692, 1606, 1517, 1462, 1410, 1327 cm^{-1}; ^1H NMR (500 MHz, $CDCl_3$) δ 7.42 (d, *J* = 7.6 Hz, 1H), 7.34 (d, *J* = 8.1 Hz, 2H), 7.29 (d, *J* = 4.1 Hz, 2H), 7.06 (d, *J* = 8.1 Hz, 2H), 7.03–6.95 (m, 1H), 6.89 (d, *J* = 7.9 Hz, 2H), 6.83 (d, *J* = 7.9 Hz, 2H), 4.48 (t, *J* = 5.6 Hz, 2H), 4.34 (q, *J* = 5.6 Hz, 1H), 4.20 (q, *J* = 5.6 Hz, 1H), 2.16 (s, 3H); ^{13}C NMR (125 MHz, $CDCl_3$) δ 198.4, 143.4, 142.6 (q, *J* = 1.0 Hz), 135.6, 134.7, 133.7, 130.5, 128.8, 128.2 (q, *J* = 32.5 Hz), 127.8, 127.4, 127.2, 126.9, 125.2, 125.0 (q, *J* = 3.6 Hz), 124.0 (q, *J* = 271.7 Hz), 56.8, 52.8, 52.7, 47.6, 21.0; ^{19}F NMR (376 MHz, $CDCl_3$) δ -62.6; HRMS (EI, M^+) for $C_{25}H_{19}F_3O$ calcd. 392.1388, found: m/z 392.1386.

(*1S*,2S*,3R*,9S)-2-(4-chlorophenyl)-9-(p-tolyl)-2,3-dihydro-1,3-methanonaphthalen-4(1H)-one (52na)**

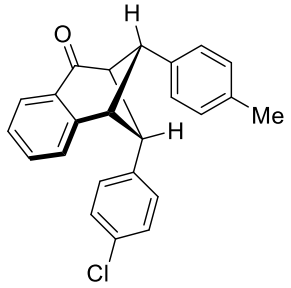

52na

The reaction was performed under the **representative procedure 5.** Flash column chromatography (hexanes/EtOAc 50:1) afforded **52na** (26 mg, 0.07 mmol) as a colorless oil in 23% yield. R_f 0.45 (hexanes/EtOAc 25:1); IR (cast film) 3026, 2920, 1693, 1604, 1493, 1461, 1400, 1349, 1287, 1183 cm^{-1}; ^1H NMR (600 MHz, $CDCl_3$) δ 7.79 (dt, *J* = 7.7, 0.7, Hz, 1H), 7.44 (td, *J* = 7.5, 1.3 Hz, 1H), 7.43 (d, *J* = 7.8 Hz, 2H), 7.38 (dd, *J* = 7.6, 0.7 Hz, 1H), 7.28 (d, *J* = 7.8 Hz, 2H), 7.26 (td, *J* = 7.5, 1.3 Hz, 1H), 7.43 (d, *J* = 8.4 Hz, 2H), 6.80 (dd, *J* = 8.7, 1.0 Hz, 2H), 4.61 (t, *J* = 5.9 Hz, 1H), 4.06 (t, *J* = 5.9 Hz, 1H), 3.93 (t, *J* = 5.9 Hz, 1H), 3.89 (s, 1H), 2.41 (s, 3H); ^{13}C NMR (125 MHz, $CDCl_3$) δ 199.4, 147.6, 137.9, 136.73, 136.71, 133.6, 131.6, 130.2, 129.5, 128.2,

128.0, 127.4, 126.9, 126.5, 126.3, 57.3, 55.6, 52.0, 48.0, 21.1; HRMS (EI, M^+) for $C_{24}H_{19}ClO$ calcd. 358.1124, found: m/z 358.1124.

(*1R*,2S*,3S*,9S)-2-(4-chlorophenyl)-9-(p-tolyl)-2,3-dihydro-1,3-methanonaphthalen-4(1H)-one (52nb)**

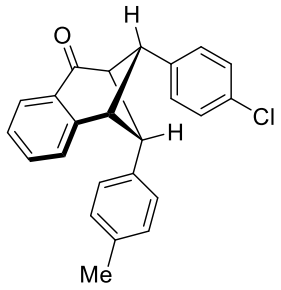

52nb

The reaction was performed under the **representative procedure 5.** Flash column chromatography (hexanes/EtOAc 50:1) afforded **52nb** (5 mg, 0.01 mmol) as a white solid in 4% yield. R_f 0.35 (hexanes/EtOAc 25:1); IR (cast film) 3024, 2956, 2925, 2854, 1694, 1604, 1516, 1492, 1461, 1402 cm^{-1}; ^1H NMR (600 MHz, $CDCl_3$) δ 7.79 (dt, *J* = 7.7, 0.7 Hz, 1H), 7.46 (dd, *J* = 8.7, 0.7 Hz, 2H), 7.43–7.40 (m, 3H), 7.36 (dd, *J* = 7.6, 0.7 Hz, 1H), 7.22 (td, *J* = 7.5, 1.3 Hz, 1H), 6.86 (d, *J* = 7.9 Hz, 2H), 6.72 (d, *J* = 7.6 Hz, 2H), 4.58 (t, *J* = 6.0 Hz, 1H), 4.02 (t, *J* = 6.0 Hz, 1H), 3.89 (t, *J* = 6.0 Hz, 1H), 3.84 (s, 1H), 2.14 (s, 3H); ^{13}C NMR (125 MHz, $CDCl_3$) δ 199.3, 147.6, 138.6, 135.7, 135.4, 133.5, 132.8, 130.2, 129.0, 128.8, 128.5, 127.3, 126.6, 126.4, 126.2, 57.3, 55.3, 52.3, 48.0, 20.9; HRMS (EI, M^+) for $C_{24}H_{19}ClO$ calcd. 358.1124, found: m/z 358.1119.

(*1R*,2R*,3S*,9S)-2-(4-chlorophenyl)-9-(p-tolyl)-2,3-dihydro-1,3-methanonaphthalen-4(1H)-one (52n′)**

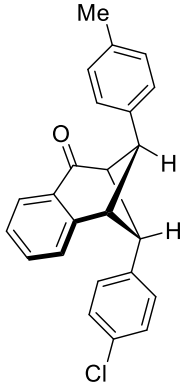

52n′

The reaction was performed under the **representative procedure 5.** Flash column chromatography (hexanes/EtOAc 50:1) afforded **52n′** (51 mg, 0.14 mmol) as a white solid in 44% yield. R_f 0.20 (hexanes/EtOAc 25:1); mp 170–172 °C; IR (cast film) 3044, 2943, 2892, 1691, 1608, 1516, 1491, 1460, 1399 cm^{-1}; ^1H NMR (400 MHz, $CDCl_3$) δ 7.42 (d, *J* = 7.6 Hz, 1H), 7.29–7.25 (m, 2H), 7.04 (d, *J* = 8.5 Hz, 2H), 7.00–6.94 (m, 1H), 6.87 (dd, *J* = 8.1, 2.8 Hz, 4H), 6.82 (d, *J* = 8.1 Hz, 2H), 4.44 (t, *J* = 5.6 Hz, 1H), 4.41 (t, *J* = 5.6 Hz, 1H), 4.29 (q, *J* = 5.6 Hz, 1H), 4.14 (q, *J* = 5.6 Hz, 1H), 2.15 (s, 3H);^{13}C NMR (125 MHz, $CDCl_3$) δ 198.6, 143.6, 136.9, 135.4, 134.9, 133.5, 131.7, 130.6, 128.8, 128.4, 128.2, 127.8, 127.0, 126.8, 125.1, 56.7, 52.7, 52.4, 47.6, 20.9; HRMS (EI, M^+) for $C_{24}H_{19}ClO$ calcd. 358.1124, found: m/z 358.1119.

(*1S*,2R*,3R*,9R)-2-methyl-9-phenyl-2,3-dihydro-1,3-methanonaphthalen-4(1H)-one (52o)**

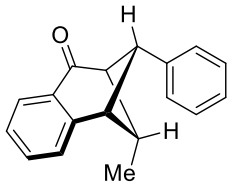

52o

The reaction was performed under the **representative procedure 5.** Flash column chromatography (hexanes/EtOAc 50:1) afforded **52o** (62 mg, 0.25 mmol) as a yellow oil in 62% yield. R_f 0.48 (hexanes/EtOAc 25:1); IR (cast film) 3060, 3023, 2964, 1692, 1604, 1497, 1461, 1381, 1297 cm^{-1}; ^1H NMR (500 MHz, $CDCl_3$) δ 8.04 (dt, *J* = 7.9, 0.6 Hz, 1H), 7.52 (td, *J* = 7.5, 1.4 Hz, 1H), 7.45–7.39 (m, 5H), 7.33 (dd, *J* = 7.5, 0.9 Hz,

1H), 7.31–7.27 (m, 1H), 3.76 (s, 1H), 3.61 (t, *J* = 6.0 Hz, 1H), 3.51 (app. hept, *J* = 6.8 Hz, 1H), 3.42 (t, *J* = 6.0 Hz, 1H), 0.77 (d, *J* = 6.8 Hz, 3H); ^{13}C NMR (125 MHz, $CDCl_3$) δ 200.3, 147.8, 140.3, 133.5, 130.9, 128.6, 127.3, 127.1, 126.6, 126.5, 125.8, 58.1, 56.2, 48.5, 45.4, 13.1; HRMS (EI, M^+) for $C_{18}H_{16}O$ calcd. 248.1201, found: m/z 248.1203.

(*1S*,2R*,3R*,9S)-2-methyl-9-phenyl-2,3-dihydro-1,3-methanonaphthalen-4(1H)-one (52o′)**

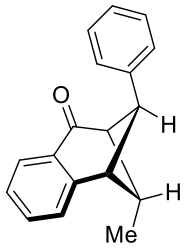

52o′

The reaction was performed under the **representative procedure 5.** Flash column chromatography (hexanes/EtOAc 50:1) afforded **52o′**(19 mg, 0.07 mmol) as a yellow oil in 19% yield. R_f 0.33 (hexanes/EtOAc 25:1); IR (cast film) 3060, 3027, 2958, 1690, 1605, 1496, 1461, 1447, 1305, 1208 cm^{-1}; ^{1}H NMR (500 MHz, $CDCl_3$) δ 7.65 (dt, *J* = 7. 6, 0.8 Hz, 1H), 7.36 (td, *J* = 7.4, 1.4 Hz, 1H), 7.22 (d, *J* = 7. 3 Hz, 1H), 7.14 (td, *J* = 7.5, 0.8 Hz, 1H), 7.05 (t, *J* = 7.6, Hz, 2H), 6.97 (app t, *J* = 7.5, Hz, 1H), 6.87 (app d, *J* = 8.1 Hz, 2H), 4.26 (t, *J* = 5.7 Hz, 1H), 3.83 (q, *J* = 5.6 Hz, 1H), 3.63 (q, *J* = 5.6 Hz, 1H), 3.30 (app. hept, *J* = 6.7 Hz, 1H), 0.87 (d, *J* = 6.9 Hz, 3H); ^{13}C NMR (125 MHz, $CDCl_3$) δ 199.7, 143.9, 138.7, 133.5, 131.3, 127.9, 127.8, 127.0, 126.9, 125.7, 124.6, 57.6, 53.4, 48.4, 45.9, 12.3; HRMS (EI, M^+) for $C_{18}H_{16}O$ calcd. 248.1201, found: m/z 248.1202.

(*3S*,4R)-3-phenyl-4-vinyl-3,4-dihydronaphthalen-1(2H)-one (53p)**

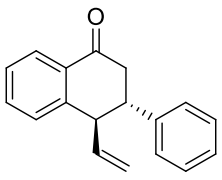

53p

The reaction was performed under the **representative procedure 5.** Flash column chromatography (hexanes/EtOAc 50:1) afforded **53p** (35 mg, 0.14 mmol) as a brown oil

in 32% yield. R_f 0.43 (hexanes/EtOAc 25:1); IR (cast film) 3062, 3028, 2887, 1684, 1634, 1601, 1497, 1453, 1410, 1288, 1263, 1223, 1158 cm^{-1}; ^1H NMR (500 MHz, $CDCl_3$) δ 8.13 (dd, *J* = 7.9, 1.5 Hz, 1H), 7.55 (td, *J* = 7.5, 1.5 Hz, 1H), 7.42–7.36 (m, 3H), 7.30–7.24 (m, 4H), 5.76 (ddd, *J* = 17.2, 10.4, 6.1 Hz, 1H), 5.09 (dt, *J* = 10.4, 1.3 Hz, 1H), 4.55 (dt, *J* = 17.2, 1.3 Hz, 1H), 3.93 (m, 1H), 3.77 (dt, *J* = 14.1, 3.8 Hz, 1H), 3.15 (dd, *J* = 17.0, 14.1 Hz, 1H), 2.83 (ddd, *J* = 17.0, 3.8, 1.3 Hz, 1H); ^{13}C NMR (125 MHz, $CDCl_3$) δ 197.9, 145.1, 141.1, 135.9, 133.7, 132.0, 129.6, 128.5, 127.7, 127.4, 127.3, 127.0, 118.9, 49.5, 43.2, 38.7; HRMS (EI, M^+) for $C_{18}H_{16}O$ calcd. 248.1201, found: m/z 248.1208.

(*3S*,4R)-3-methyl-4-vinyl-3,4-dihydronaphthalen-1(2H)-one (53q)**

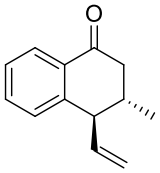

53q

The reaction was performed under the **representative procedure 5.** Flash column chromatography (hexanes/EtOAc 50:1) afforded **53q** (25 mg, 0.13 mmol) as a yellow oil in 22% yield. R_f 0.43 (hexanes/EtOAc 25:1); IR (cast film) 3073, 2960, 2876, 1686, 1634, 1600, 1453, 1413, 1379, 1288, 1227 cm^{-1}; ^1H NMR (600 MHz, $CDCl_3$) δ 8.04 (dd, *J* = 7.9, 1.5 Hz, 1H), 7.50 (td, *J* = 7.5, 1.5 Hz, 1H), 7.33 (td, *J* = 7.6, 1.3 Hz, 1H), 7.24 (dddd, *J* = 7.7, 1.3, 0.6, 0.6 Hz, 1H), 5.97 (ddd, *J* = 17.1, 10.2, 8.0 Hz, 1H), 5.20 (ddd, *J* = 10.2, 1.7, 0.8 Hz, 1H), 4.97 (dt, *J* = 17.0, 1.2 Hz, 1H), 3.59 (dd, *J* = 8.1, 3.4 Hz, 1H), 2.58–2.51 (m, 3H), 1.10 (d, J = 6.4 Hz, 3H); ^{13}C NMR (125 MHz, $CDCl_3$) δ 198.3, 145.7, 136.3, 133.6, 131.8, 129.4, 127.1, 127.0, 118.3, 49.0, 42.7, 33.1, 18.3; HRMS (EI, M^+) for $C_{13}H_{14}O$ calcd. 186.1045, found: m/z 186.1045.

3.10.8 Preparation of Brominated Products 54a and 54a′

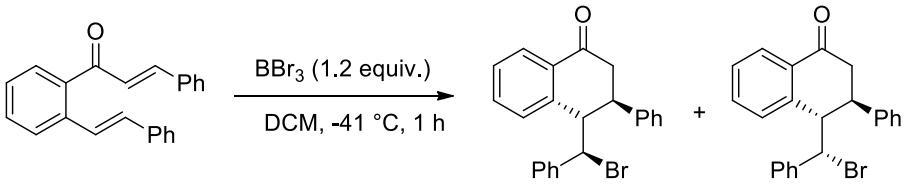

51a **54a** **54a′**

To a round bottom flask charged with BBr_3 (0.4 mL, 0.38 mmol, 1M in DCM) and cooled to -41 °C was added a solution of *o*-styrenyl chalcone **51a** (100 mg, 0.32 mmol) in DCM (4 mL) and stirred for 1 h. The reaction mixture was quenched with a sat. aqueous solution of $NaHCO_3$. The layers were separated, and the aqueous layer was extracted with DCM (2 x 20 mL). The combined organic layer was washed with water (20 mL) and brine, dried over $MgSO_4$, and concentrated in vacuo. Flash column chromatography (hexanes/EtOAc: 50:1) was performed to obtain products **54a** and **54a′.**

(*3R*,4S)-4-((R*)-bromo(phenyl)methyl)-3-phenyl-3,4-dihydronaphthalen-1(2H)-one (54a)**

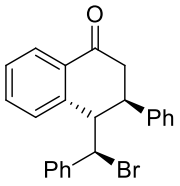

54a

The product was obtained as colorless crystals (94 mg, 0.24 mmol) in 75% yield. R_f 0.37 (hexanes/EtOAc 30:1); mp 105–108 °C; IR (cast film) 3062, 3029, 2923, 1680, 1599, 1485, 1452, 1288, 1248 cm^{-1}; ^1H NMR (500 MHz, $CDCl_3$) δ 8.00 (dd, *J* = 7.8. 1.4 Hz, 1H), 7.23–7.15 (m, 8H), 7.12–7.08 (m, 1H), 7.06–7.04 (m, 2H), 6.97 (td, *J* = 7.5, 1.5 Hz, 1H), 6.20 (d, *J* = 7.4 Hz, 1H), 5.10 (d, *J* = 10.7 Hz, 1H), 4.51 (d, *J* = 6.2 Hz, 1H), 3.72 (d, *J* = 10.7 Hz, 1H), 3.32 (dd, *J* = 19.2, 6.2 Hz, 1H), 3.09 (dt, *J* = 19.2, 1.4 Hz, 1H); ^{13}C NMR (125 MHz, $CDCl_3$) δ 196.6, 143.1, 140.1, 139.7, 133.1, 132.4, 131.3, 128.5, 128.4, 128.35, 128.27, 127.8, 127.4, 126.9, 126.5, 59.2, 54.4, 42.2, 37.8; HRMS (EI, M^+) for $C_{23}H_{19}BrO$ calcd. 390.0619, found: m/z 392.0595.

(*3R*,4S)-4-((R*)-bromo(phenyl)methyl)-3-phenyl-3,4-dihydronaphthalen-1(2H)-one (54a′)**

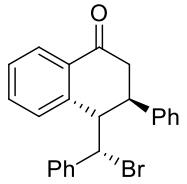

54a′

The product was obtained as colorless crystals (16 mg, 0.04 mmol) in 13% yield. R_f 0.33 (hexanes/EtOAc 30:1); mp 64–64 °C; IR (cast film) 3060, 3029, 2920, 1680, 1600, 1495, 1453, 1289, 1247 cm^{-1}; ^1H NMR (500 MHz, $CDCl_3$) δ 8.07 (dd, *J* = 7.7. 1.5 Hz, 1H), 7.53 (d, *J* = 7.6 Hz, 2H), 7.50–7.36 (m, 6H), 7.14–7.06 (m, 3H), 6.90–6.88 (m, 2H), 5.12 (d, *J* = 9.7 Hz, 1H), 3.91 (dd, *J* = 9.6, 2.1 Hz, 1H), 3.45 (dt, *J* = 6.3, 2.4 Hz, 1H), 2.92 (dd, *J* = 19.1, 6.3 Hz, 1H), 2.81 (ddd, *J* = 19.1, 2.2, 0.9 Hz, 1H); ^{13}C NMR (125 MHz, $CDCl_3$) δ 196.7, 142.9, 141.5, 140.4, 133.2, 132.4, 132.2, 129.3, 129.0, 128.5, 128.2, 127.3, 127.1, 127.0, 126.6, 59.6, 53.5, 40.4, 38.0; HRMS (EI, M^+) for $C_{23}H_{19}BrO$ calcd. 390.0619, found: m/z 392.0605.

(*1R*,2S*,3R*,9S*,Z*)-2,9-diphenyl-2,3-dihydro-1,3-methanonaphthalen-4(1H)-one oxime (57a)

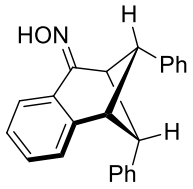

57a

Compound **57a** was prepared via a modified literature procedure:[131] The product was obtained as a single isomer, however, the geometry of the oxime cannot be determined. The solution of **52a** (100 mg, 0.32 mmol), $NH_2OH{\cdot}HCl$ (27 mg, 0.38 mmol) and AcONa (32 mg, 0.38 mmol) in MeOH (3 mL) was heated under reflux for 9 h. The solvent was removed by reduced pressure evaporation, and the crude residue was subjected to flash column chromatography (hexanes/EtOAc 10:1) to obtain **57a** (100 mg, 0.31 mmol) as colorless crystals in 96% yield. R_f 0.45 (hexanes/EtOAc 10:1); mp

165 °C (decomposes); IR (cast film) 3267, 3059, 3025, 2922, 1602, 1497, 1446, 1352, 1311, 1265, 1185 cm^{-1}; ^1H NMR (600 MHz, $CDCl_3$) δ 8.30 (br s, 1H), 7.69 (ddd, *J* = 7.7, 0.6, 0.6 Hz, 1H), 7.57 (d, *J* = 8.1 Hz, 2H), 7.44 (dd, *J* = 7.7, 7.7 Hz, 2H), 7.31 (t, *J* = 7.4 Hz, 1H), 7.28 (d, *J* = 7.4 Hz, 1H), 7.21 (td, *J* = 7.4, 1.2 Hz, 1H), 7.10 (td, *J* = 7.8, 1.5 Hz, 1H), 7.06 (t, *J* = 7.6 Hz, 2H), 6.97 (t, *J* = 7.6 Hz, 1H), 6.87 (d, *J* = 7.8 Hz, 2H), 4.96 (t, *J* = 6.0 Hz, 1H), 4.39 (t, *J* = 6.0 Hz, 1H), 3.97 (t, *J* = 6.0 Hz, 1H), 3.52 (s, 1H); ^{13}C NMR (150 MHz, $CDCl_3$) δ 157.5, 143.8, 140.7, 139.8, 129.2, 128.7, 128.5, 127.8, 127.3, 126.9, 126.8, 126.6, 126.5, 125.5, 122.9, 51.7, 48.1, 47.4, 40.9; HRMS (ESI, $[M+H]^+$) for $C_{23}H_{20}NO$ calcd. 326.1545, found: m/z 326.1542.

(*3S*,4R*,5S*,10R)-4,10-diphenyl-2,3,4,5-tetrahydro-1H-3,5-methanobenzo[c]azepin-1-one (58a)**

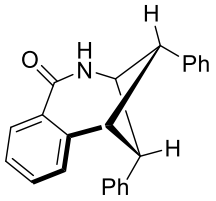

58a

Compound **(58a)** was prepared via a literature procedure.[131] A solution of thionyl chloride (0.36 mL, 4.9 mmol) in dioxane (1.5 mL) was added dropwise to the solution of oxime **57a** (99 mg, 0.31 mmol) in dioxane (3 mL) at 0 °C. The resulting solution was stirred at 70 °C for 6 h. The mixture was concentrated under reduced pressure to remove solvent and the crude residue was diluted with DCM (15 mL). Water was added to the organic phase and pH was adjusted to 7 with a sat. aqueous solution of $NaHCO_3$. The organic layer was washed with water and brine, dried over $MgSO_4$, and concentrated in vacuo. Flash column chromatography (hexanes/EtOAc 1:1) afforded **58a** (61 mg, 0.19 mmol) as a white solid in 61% yield. R_f 0.33 (hexanes/EtOAc 1:1); mp 238–240 °C; IR (cast film) 3286, 3171, 3024, 2944, 1645, 1598, 1570, 1485, 1445, 1419, 1366, 1335, 1277, 1257, 1186 cm^{-1}; ^1H NMR (400 MHz, $CDCl_3$) δ 8.32 (dd, *J* = 7.9, 0.9 Hz, 1H), 7.49–7.38 (m, 6H), 7.34–7.25 (m, 2H), 7.10 (t, *J* = 7.2 Hz, 2H), 7.02 (t, *J* = 7.2 Hz, 1H), 6.84 (d, *J* = 7.6 Hz, 2H), 6.73 (br d, *J* = 7.1 Hz, 1H), 4.44–4.35 (m, 2H), 4.21 (dd, *J* = 7.1, 4.9 Hz, 1H), 3.47 (s, 1H); ^{13}C NMR (125 MHz, $CDCl_3$) δ 167.8, 143.1, 140.2,

137.1, 133.3, 132.1, 130.3, 130.1, 129.0, 128.1, 128.0, 126.9, 126.7, 126.5, 125.8, 57.4, 52.2, 50.3, 39.2; HRMS (ESI, $[M+H]^+$) for $C_{23}H_{20}NO$ calcd. 326.1545, found: m/z 326.1537.

4-benzyl-3-phenylnaphthalen-1-ol (59a)

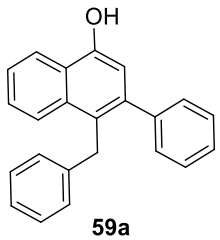

59a

The solution of **52a** (100 mg, 0.32 mmol) and *p*-toluenesulfonic acid monohydrate (122 mg, 0.64 mmol) in DCE (3 mL) was heated under reflux for 24 h. The reaction mixture was quenched with a sat. aqueous solution of $NaHCO_3$ (15 mL). The layers were separated and the aqueous layer was extracted with DCM (2 x 10 mL). The combined organic layer was washed with water and brine, dried over $MgSO_4$ and concentrated in vacuo. Flash column chromatography (hexanes/EtOAc 40:1) afforded **59a** (45 mg, 0.14 mmol) in 45% yield as a yellow oil. R_f 0.25 (hexanes/EtOAc 25:1); IR (cast film) 3524, 3398, 3060, 2925, 2848, 1652, 1624, 1597, 1495, 1452, 1389, 1232, 1138 cm^{-1}; ^1H NMR (500 MHz, $CDCl_3$) δ 8.26 (d, *J* = 8.2 Hz, 1H), 7.85 (d, *J* = 8.4 Hz, 1H), 7.48 (t, *J* = 7.7 Hz, 1H), 7.43 (td, *J* = 7.4, 1.4 Hz, 1H), 7.36–7.30 (m, 5H), 7.20 (t, *J* = 7.4 Hz, 2H), 7.13 (t, *J* = 7.2 Hz, 1H), 7.03 (d, *J* = 7.3 Hz, 2H), 6.83 (s, 1H), 5.24 (br s, 1H), 4.36 (s, 2H); ^{13}C NMR (125 MHz, $CDCl_3$) δ 149.9, 142.1, 142.0, 140.4, 133.8, 129.1, 128.3, 128.1 (two signals overlapping), 127.0, 126.9, 125.6, 125.5, 125.1, 124.9, 124.3, 122.0, 111.1, 35.0; HRMS (EI, M^+) for $C_{23}H_{18}O$ calcd. 310.1358, found: m/z 310.1362.

Chapter 4

Development of the New Family of Calcium Sensitizers to Target Cardiac Troponin C[150]

4.1 Introduction

The final stage of almost all cardiac diseases is a failing heartthat is no longer able to pump a sufficient amount of blood to satisfy the metabolic demands of the body. Cardiovascular diseases (CVDs) are the most common cause of death all over the world. People dead from CVDs represent 31% of all global deaths.[151] More than 75% of these deaths resulted from a malfunctioning heart and strokes.

Heart failure (HF) is the prevalent health issue in the United States. Usually, risk factors contributing to the development of the condition include aging, male gender, ethnicity, and low socioeconomic status.[152] Over 6.5 million Americans are affected by HF each year. The estimated direct and indirect cost of CVD for 2012 to 2013 was estimated to be $316.1 billion according to theAmerican Heart Association Report.[153] There is an increased prevalence of the disease in elderly patients over 75 years of age in Europe as well.[154] The most common cause of heart failure is coronary heart disease (ischemia); however, many other underlying conditions, such as hypertension, diabetes, hyperthyroidism, etc can contribute to its induction. Along with all the risk factors listed above, smoking is the largest preventable cause of heart failure and premature death in the United States.

Despite all the advances in understanding the concept of heart failure and therapeutic improvements, there is a big gap between the knowledge about fundamental cardiac physiology and its application to patients' care, which showcases in still extremely high rates of unplanned hospitalization and mortality, with up to 50% of cases culminating with sudden death.[155]

4.2. Definition and Classification of Heart Failure

Heart failure can be defined physiologically as a complex clinical syndrome characterized by an abnormality of cardiac structure or function, causing insufficient delivery of oxygen to the tissues to satisfy their metabolic demands, accompanied by a number of symptoms, such as shortness of breath, elevated heart rates, etc. The condition results in reduced quality of life and life expectancy.[154]

Systolic heart failure (SHF) and diastolic heart failure (DHF) are two broad categories by which chronic heart failure can be classified.[156] In a healthy heart, normal systolic or diastolic heart performance is related to the ability of the left ventricle to eject or fill blood. To quantify the ability of the left ventricle to contract, the term *emptying fraction* or *ejection fraction* is used, which indicates the ratio of blood stroke volume to end diastolic volume. For systolic left ventricular dysfunction, a reduced ejection fraction is characteristic. Over time, ineffective contraction leads to the chamber dilation, which even further impairs the contractile ability of the heart and its cardiac output.

For the proper functioning of the left ventricle as a pump, proper blood filling is as important as its ejection. During diastolic dysfunction, *preserved ejection fraction* prevents the left ventricle from being filled efficiently, leading to a small and stiff muscular chamber, known as concentric hypertrophy, which further impairs adequate filling. In this situation, normal systolic properties are maintained, but with dominant abnormalities in diastolic properties. Systolic and diastolic heart failures are not mutually exclusive; whether heart failure results from a systolic or diastolic dysfunction of the left ventricle, it might be manifested heterogeneously, meaning that patients with systolic heart failure may suffer from abnormalities in the dilation and vice versa.[157]

4.3 Mechanismof the Cardiac Contraction

4.3.1 Structure of a Cardiac Muscle Cell

In order to have a proper approach towards heart failure therapy, it is vital to understand the structure of the cardiac muscle and the mechanism of the contractile apparatus. A highly organized arrangement of a series of repeating basic structural units of sarcomeres create myofibrils, elements of striated human cardiac muscle cells.[158] A sarcomere, in turn, is composed of two parallel filaments, which due to their appearance under the microscope are referred to as thin and thick filaments (Figure 4.1). Thin filaments from adjacent sarcomeric units are bound together by Z-discs. An M-line protein at the center of a sarcomere connects thick filaments together. Heart muscle contraction is a result of sarcomere length shortening caused by the sliding of these two filaments along each other. The process is dependent on intracellular calcium concentration, which triggers and regulates the number of protein–protein interactions that finally assist in the cross-bridge formation between the two filaments.

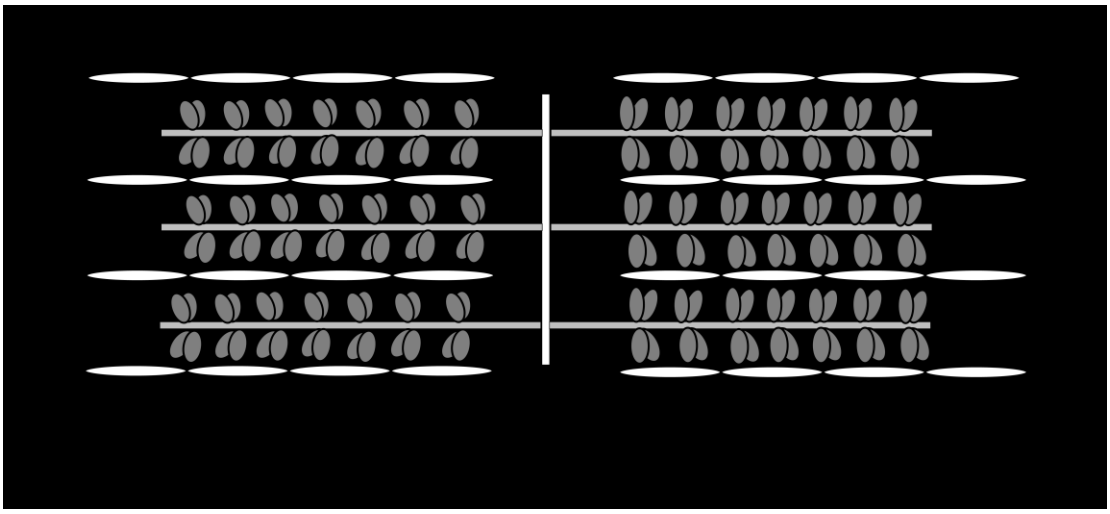

Figure 4.1 Schematic image of a sarcomere structure.

A polymeric thick filament of the sarcomere consists of monomer units of myosin molecules (Figure 4.2). There are two heavy and four light chains in myosin. A multitude of myosin heavy chains creates the backbone of the thick filament. Globular

heads (**S1**) of a myosin heavy chain that point out of the thick filament interact with the thin filament, forming cross-bridges to provide the basis for sarcomere contraction.[159] Some additional scaffolding proteins keep myosin molecules together and contribute to sarcomere elasticity.

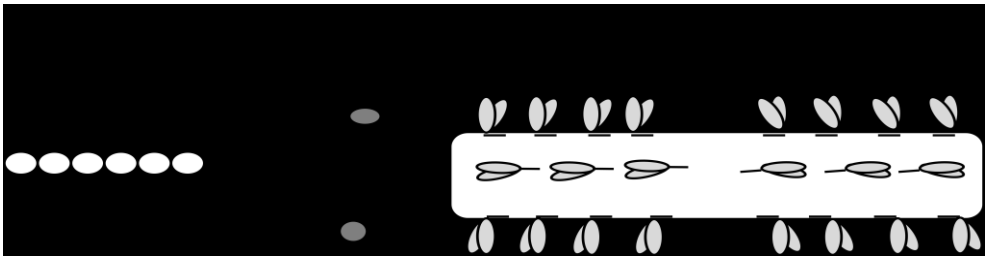

Figure 4.2 Cartoon representation of a myosin structure.

A polymeric twisted double-stranded helix of thin filament is composed of globular actin monomers (G-actin), which consist of two equal-sized domains available for integration with myosin (Figure 4.3).[160] A number of regulatory proteins on the thin filament regulate the interaction between thin and thick filaments. The most elongated of them, tropomyosin (Tm) rolls over the surface of the thin filament, depending on the intracellular calcium concentration, thus affecting the myosin head (S1) binding to actin.

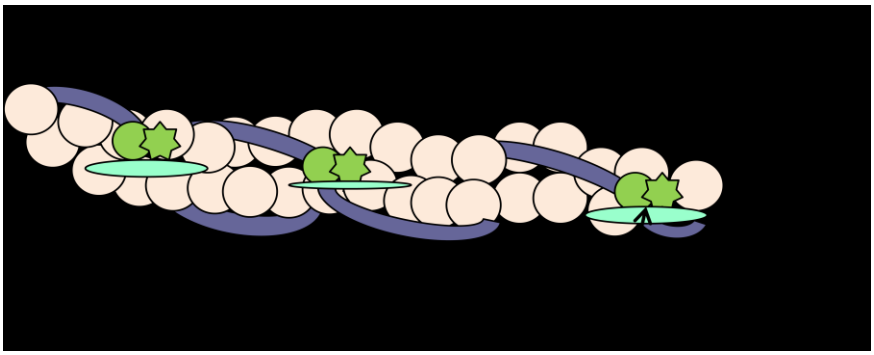

Figure 4.3 A thin filament with regulatory proteins.

4.3.2 Troponin Complex and Cardiac Contraction Mechanism

Every tropomyosin is associated with a troponin complex, a heterotrimeric protein assembly that consists of three components: calcium binding sub-unit troponin C (TnC); actomyosin ATP-ase inhibitory unit troponin I (TnI); and elongated troponin T (TnT), which binds the whole complex to tropomyosin (Tm) (Figure 4.4).[161]

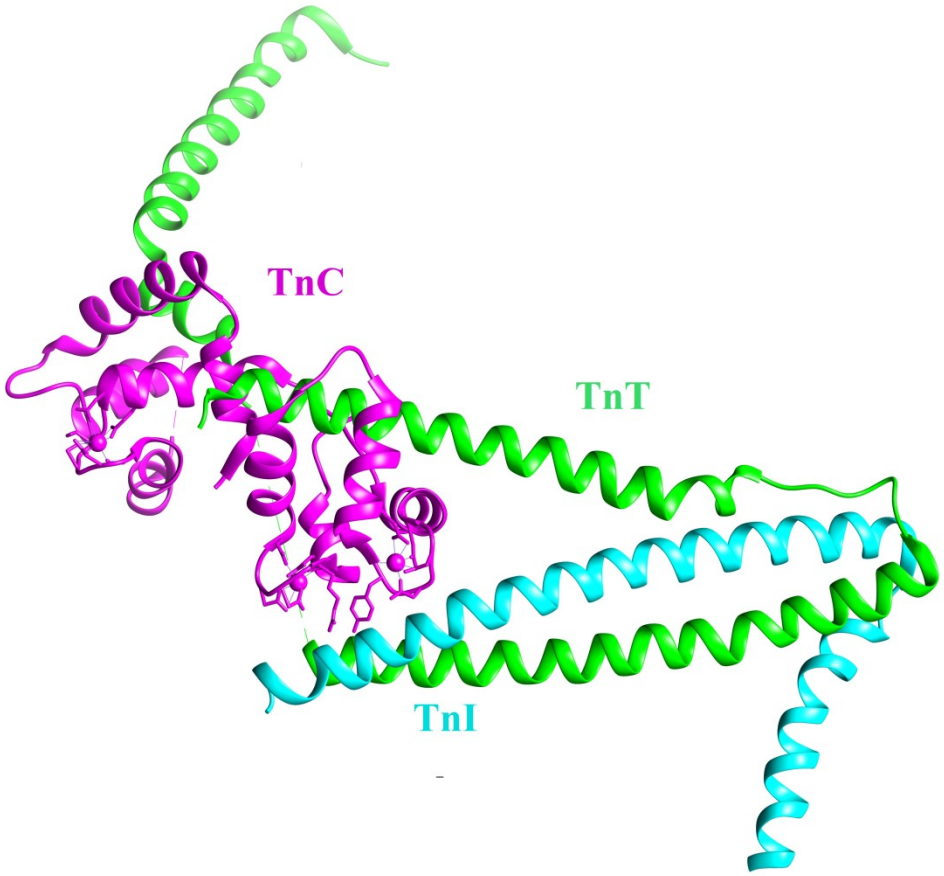

Figure 4.4 Ribbon representation of the troponin complex.

The cardiac muscle contracts involuntarily and is calcium dependent. In the resting muscle, when the intracellular concentration is low (10^{-7}M), the "*switch region*" of $TnI_{128–147}$ binds to actin/Tm and inhibits the ATPase activity of actomyosin (Figure 4.5).[162] At this point, tropomyosin (Tm), being in the "blocked" position, sterically

hinders the myosin approach towards actin (prevents cross-bridge formation). After calcium release from sarcoplasmic reticulum (SR), a calcium storing organelle in myocytes, calcium binds to TnC due to its increased concentration (10^{-5}M). Calcium saturation allows TnC to undergo conformational changes and bind to the inhibitory region of $TnI_{128–147}$ ("*switch region*"), thus removing it from actin.[163] At this point, Tm moves from its "blocked" state to its "closed" position and allows weak interaction between actin and myosin.[164] This causes conformational changes in Tm and pushes it to its "open" state.[165] Exposure of myosin binding sites to actin enables cross-bridge formation, which causes two filaments to slide along each other, and the whole process translates into muscle contraction. For relaxation to occur, the intracellular calcium concentration must decrease, and Ca^{2+} must dissociate from TnC. For each heart beat, the amount of extruded Ca^{2+} during relaxation must be the same as the amount entering the cell for the cell to be in a steady state.[166] ATP hydrolysis provides the energy for the entire process.

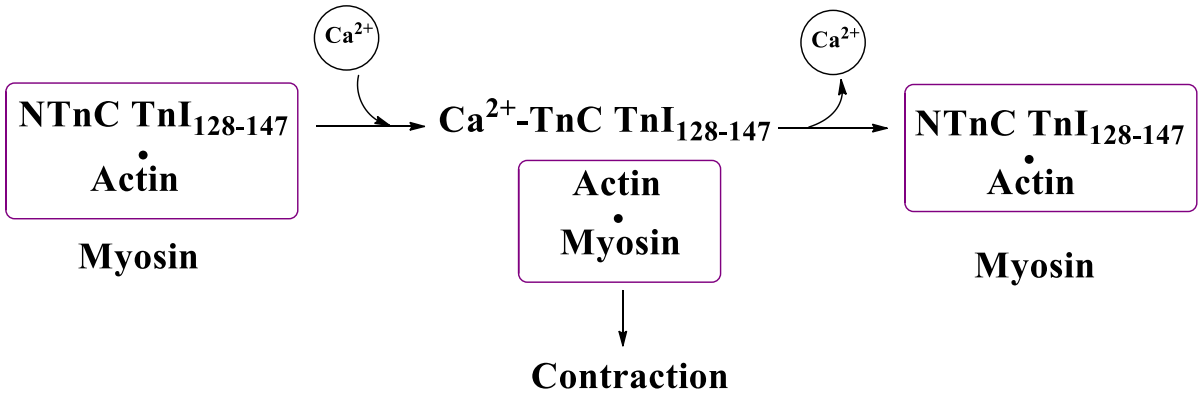

Figure 4.5 The mechanism of heart contraction.

4.3.2.1 Calcium Binding Protein Troponin C

TnC is an elongated, α-helical, dumbbell-shaped acidic protein of 18 kDa (Figure 4.6).[167] It consists of two globular N and C domains interconnected with a flexible linker. The N-regulatory domain (NTnC) is composed of helices A, B, C, and D, it has

two Ca^{2+} binding sites, and is responsible for contraction, while helices E, F, G, and H form a structural C domain (CTnC) with one Ca^{2+} binding unit that attaches TnC to the rest of the troponin complex. The linker keeps the two domains apart at the optimal distance from the target sites on TnI.[168]

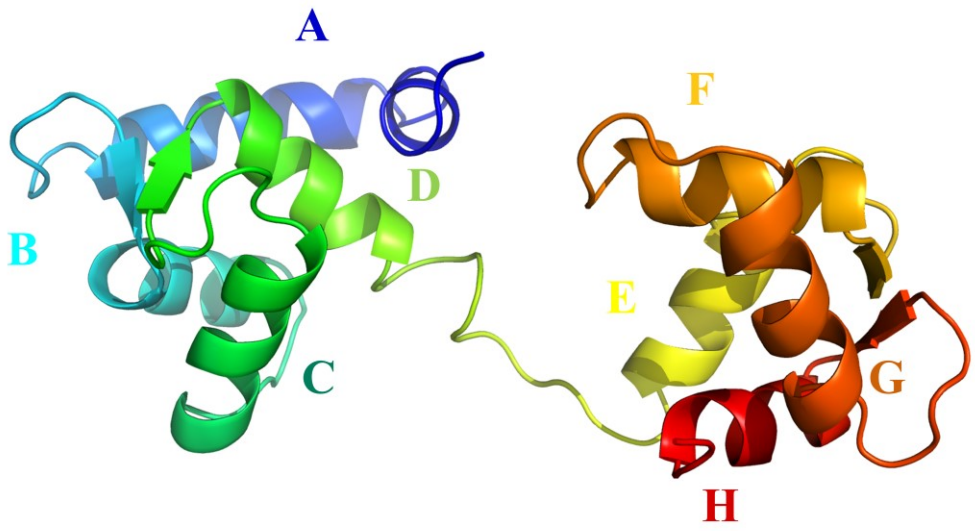

Figure 4.6 Ribbon representation of N- and C-domains of TnC.

Calcium binding to the N-regulatory domain of TnC during Ca^{2+} influx into the cytoplasm is a key event that triggers muscle contraction. N-regulatory domain has two Ca^{2+} binding sites with an affinity for calcium of $K_{Ca}=2\times10^{5}M^{-1}$.[169] Due to conformational changes caused by Ca^{2+} binding, NTnC exposes its hydrophobic pocket for binding tothe inhibitory region of TnI and removes it from its binding site on actin.[170] The driving force for calcium binding to the N domain of TnC is the higher stability of the metal-bound form compared to the apo state, and binding itself is electrostatic in nature.[171] The N-domain in its Ca^{2+} bound state is mostly in a closed conformation; however, a dynamic equilibrium between the closed and open forms exists. Binding of TnI to the hydrophobic pocket of NTnC stabilizes its open form, thus increases its Ca^{2+} binding affinity.[172] When the cardiac muscle is relaxed, TnI is bound

more tightly to actin/Tm than to TnC where it inhibits ATPase activity. However, interaction with TnC becomes stronger when the latter is bound to Ca^{2+} (contraction phase). Thus, TnI is moving back and forth between two states in accordance with the phases of the muscle contraction–relaxation cycle.[173]

In the C domain of TnC, there are also two Ca^{2+} binding sites with higher affinity ($K_{Ca}=2\times10^{7}M^{-1}$) and some sites with lower affinity towards Mg^{2+} ions ($K_{Mg}=5\times10^{3}$ M^{-1}). It is believed that under normal physiological conditions these sites are occupied always by either ion type. Since Mg^{2+} is chemically similar to Ca^{2+}, it competes for binding in both the muscle cells are pH sensitive; in an ischemic heart with low pH levels, due to the competition between H^{+} and Ca^{2+} ions, the affinity of TnC to Ca^{2+} decreases, resulting in decreased contractile force.[174]

Besides regulating myofilament activation via intracellular Ca^{2+} concentration fluctuation, phosphorylation of TnI also can affect cardiac contractility. As a response to β-adrenergic receptor stimulation, multiple kinase phosphorylation sites on TnI can get phosphorylated, this results in structural changes and affects the interaction of TnI with TnC.[175]

4.4 Calcium Sensitizers

Regulation of cardiac contraction via Ca^{2+} signaling can be divided into three different pathways of inotropic (drugs that enhance heart contraction)[176] intervention: in the first approach – upstream mechanism – intracellular Ca^{2+} concentration is increased, while in the second pathway – central mechanism – stabilization of Ca^{2+}-bound open conformation of TnC is a goal. The third process – downstream mechanism– is Ca^{2+} independent and aims at enhancement of cross-bridge formation between thin and thick filaments.[177]

As already discussed above, calcium binding to NTnC promotes interaction between NTnC and TnI, which translates into heart contraction through the sequence of events. For the treatment of cardiac insufficiency, manipulation of Ca^{2+} signaling pathways by increasing intracellular calcium concentration is an effective strategy.

However, this approach is characterized by some side effects, such as a higher demand for oxygen and energy to deal with elevated calcium levels. For the malfunctioning heart, this condition further aggravates the energy disbalance, which along with arrhythmias caused by a high calcium load, can result in fatality.[178]

In the 1980s, a new idea of calcium sensitization was introduced.[179] A positive inotropic effect on muscle contraction via increasing myofilament response to calcium without changing intracellular calcium concentration could be achieved by certain types of drugs uniformly denoted as calcium sensitizers.

In a healthy heart, there is a fine balance between contraction and relaxation, which is directly related to Ca^{2+} binding–dissociation to and from NTnC. Similarly, dissociation of an ideal calcium sensitizer from NTnC should be synchronized with Ca^{2+}detachment. At the same time, inertness towards other proteins regulating heart contraction–relaxation is an important feature. Therefore, knowledge of the structure to activity relationship (SAR) between drug and protein is crucial for rational drug design.

To achieve calcium sensitivity, the affinity of NTnC towards Ca^{2+} must be increased. However, it may result in poor relaxation due to slow dissociation of Ca^{2+} from NTnC. Therefore, stabilizing the interaction between NTnC and TnI and prolonging the lifetime of the active form is a competing alternative.

Among a number of compounds with some binding affinities towards cardiac TnC, levosimendan has been studied most widely and is used as a positive inotrope for the treatment of systolic heart failure in some South American and European countries (Figure 4.7). It has shown some promising results in terms of contractility improvement and symptomatic relief; however, some undesirable side effects, such as arrhythmias and hypotension, along with no improvement in overall mortality, make it a less than ideal drug candidate.[180,181] Although a model for levosimendan's binding to NTnC has been suggested,[182] there is no certainty about its binding. Furthermore, its mechanism of action is not fully understood and remains controversial.[170,183] It has been shown that along with binding with NTnC, levosimendan can influence the activity of other proteins, including type 3 phosphodiesterase[184] and ATP sensitive potassium channels.[185] There is no TnC·levosimendan complex crystal structure available for structural analysis.

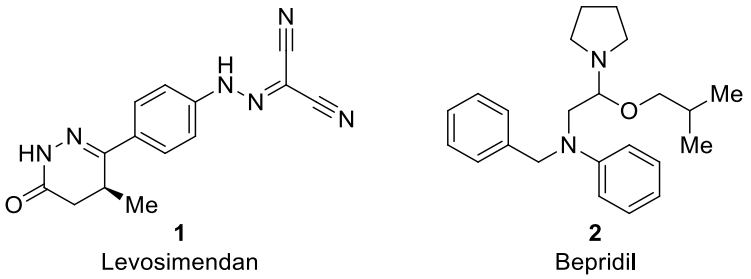

Figure 4.7 Small molecules with some calcium sensitizing effect.

Another compound, which showed an increase in Ca^{2+} sensitivity of myofilaments, actomyosin ATP activity, and cardiac contraction, is bepridil, the drug originally used as an anti-anginal agent (Figure 4.7).[186] An X-ray crystal structure of a complex of three bepridil molecules bound with the three Ca^{2+} bound form of TnC, generated by Li and co-workers (2000), confirmed its binding to the desired protein.[187] The results of analysis indicated that the calcium sensitizing effect of bepridil was arising from stabilization of the open form of NTnC by the drug (Figure 4.8). It was shown that the drug was binding to the hydrophobic pockets of both domains of troponin C; however, decreased binding of TnI with TnC was observed due to displacement of certain residues on TnI by bepridil since it could better fit into the hydrophobic pocket of the targeted protein.[188]

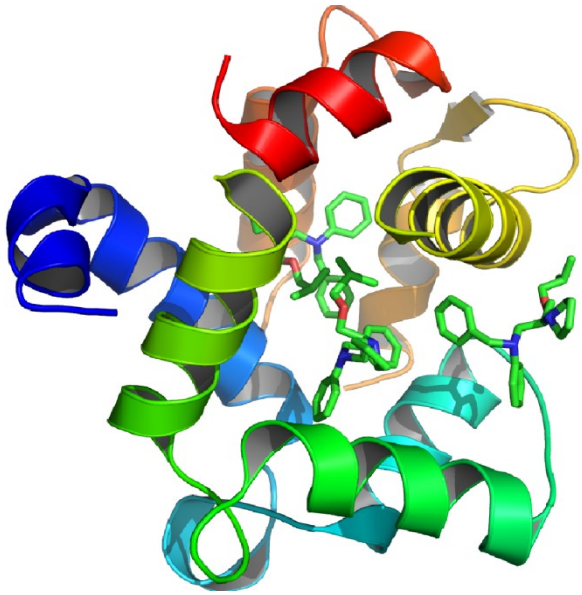

Figure 4.8 Three bepridil molecules complexed with TnC.

There are many other compounds under investigation that also show binding affinities towards different domains of cardiac TnC, however, more research needs to be done before they can be licensed as market drugs. In the upcoming chapter will be discussed our attempts to synthesize the library of small molecules which would exhibit good binding affinities towards troponin C and improve contractile performance without causing side effects associated with current drugs on the market.

4.5 Results and Discussion

As already mentioned positive inotropes currently used for treatment of decompensated heart failure suffer from some undesired side effect and show no mortality benefits. Our collaborator, Drs. Peter Hwang and Brian Sykes, proposed to develop a new family of calcium sensitizer drugs that would be more specific for binding to TnC and would have a larger positive inotropic effect without the negative side effects associated with the use of levosimendan. They would be expected to be useful for acute systolic heart failure caused by ischemia since the result of this condition is acidosis, which leads to calcium desensitization. Our task, as synthetic organic chemists, was to find efficient routes towards the synthesis of these target molecules.

For the design of the drugs, a complex of bepridil (**2**) bound to NTnC·TnI was taken as a starting point due to its calcium sensitizing effect. According to solution NMR titration data, the key binding groups in bepridil (**2**) are two aromatic rings that fits snuggly into the hydrophobic pocket of NTnC (K_D = 80 μM). Based on structural similarities with bepridil (**2**), our collaborators tested the binding of compound **3** that mimics two aromatic rings of bepridil (Figure 4.9) with NTnC·TnI chimera which was found to bind with K_D = 150 μM. The chimeric protein was created by fusing regulatory N-domain of cardiac troponinC (cNTnC) with the switch region of cardiac troponin I (cTnI), to mimic the key binding that turnson muscle contraction.[189]

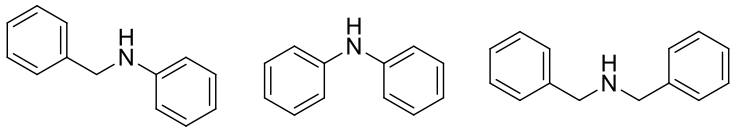

3 K_D 150 μM

4 K_D 120 μM

5 no binding

Figure 4.9 Binding affinities of commercially available aromatic secondary amines to NTnC·TnI chimera.

To test if the relative positions of aromatic rings were optimal, they further tested diphenylamine **4** and dibenzylamine **5,** with the former one showing improvement in dissociation constant (K_D = 120 μM), while the addition of an extra methylene carbon in **5** led to complete loss of binding. This effect was attributed to the lengthening of the molecule as well as to the increase of partial positive charge on the nitrogen atom due to the increased pKa of aliphatic amines as compared with anilines. Even though diphenylamine **4** (DPA) binds with slightly lower affinity than bepridil, its molecular weight is barely half that of bepridil; therefore, it was taken as a lead compound for further modifications to improve binding affinity.

The structure of $TnC{\cdot}TnI_{[147\text{-}163]}$▪bepridil complex (Figure 4.8) indicates a high hydrophobicity of binding sites; however, the entire volume of this hydrophobic pocket is not fully occupied, suggesting that addition of substituents would improve the van der Waals interaction between drug and protein further. However, an increase in hydrophobicity could compromise the solubility; therefore, our first approach involved attaching an aliphatic carbon chain of different length with polar amine or amide groups at the chain terminus to enhance aqueous solubility. Scheme 4.1 describes the synthetic strategy for the installation of a two-carbon chain. Reaction of diphenylamine **2** with chloroacetyl chloride delivered amide **6**,[190] which upon reduction with $NaBH_4$ could smoothly be converted into amine **7**.[191] The synthesis of the key intermediate **9** from chloride **7** was accomplished by following the detailed protocol for Gabriel synthesis.[192]

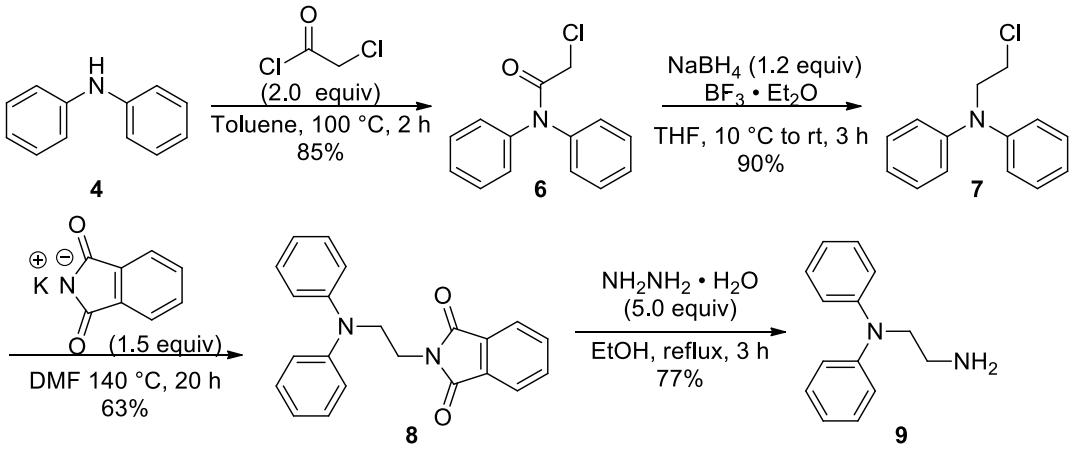

Scheme 4.1 Synthesis of a two-carbon long tether.

To increase the solubility of amine **9**, it was converted to its corresponding HCl salt **10** by treating it with a solution of HCl in ether. However, to see the effect of a two-carbon chain in non-charged species, amides **11** and **12** were made by treating **9** with acetyl chloride and propionyl chloride, respectively (Scheme 4.2).

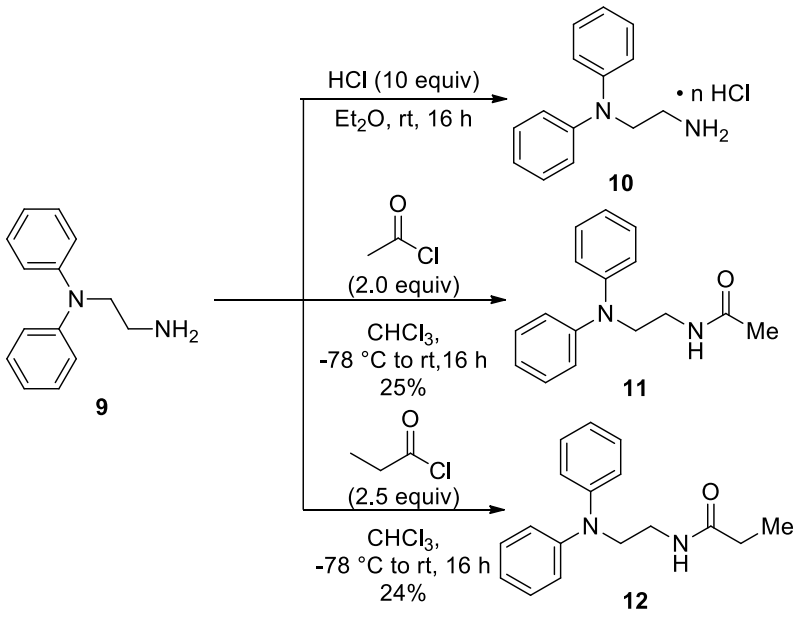

Scheme 4.2 Derivatization of the tether.

The three-carbon chain homologue **13** was synthesized in an analogous fashion using chloropropionyl chloride as a counter partner with diphenylamine **9**. However,

none of the diphenylamine derivatives showed any improvement in binding, presumably due to the attached tether inserting into the hydrophobic pocket and displacing the aryl groups from their original binding location (Figure 4.10).

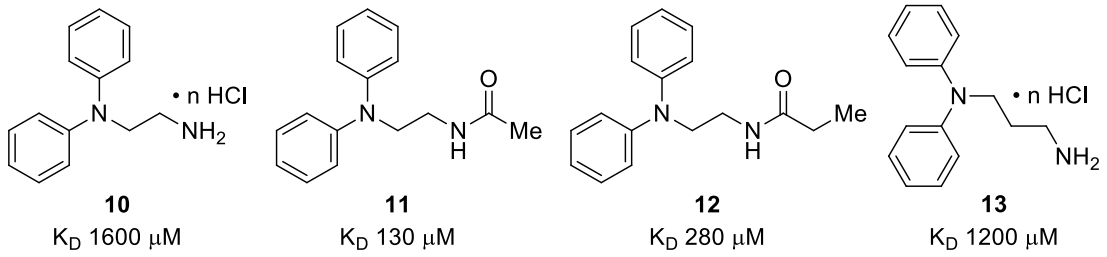

Figure 4.10 NMR titration data for derivatized diphenylamine.

In preliminary screening of a series of methyl substituteddiphenylamine scaffolds by our collaborators, it was found that the placement of one or more methyl groups on phenyl rings caused the dissociation constants to decrease further (Figure 4.11a). We decided to implement this idea into our tethered substrates (Figure 4.11b). Compounds **18** and **19** were prepared in an analogous way as the tethered substrates in Figure 4.10 starting from the corresponding starting materials. Unfortunately, these substrates turned out to be extremely insoluble in water, which precluded any binding with protein.

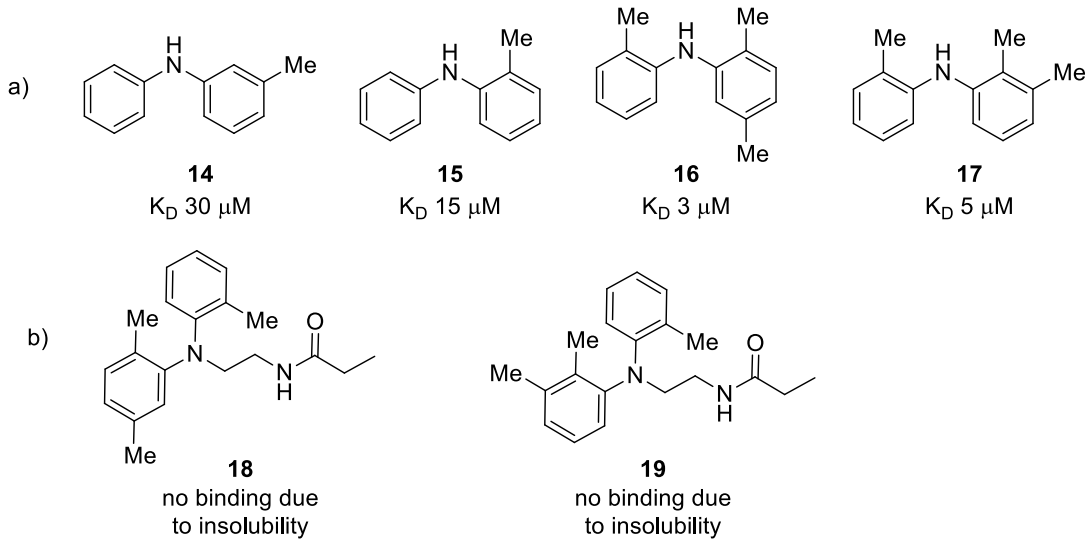

Figure 4.11 Methylated diphenylamine derivatives.

Our next approach involved keeping just one methyl substituent and at the same time moving a flexible tether into the aromatic ring (compounds **30** and **33**). This way, we hoped one of the phenyl rings would be able to burrow deeply into the hydrophobic pocket, while the tether would provide adequate solubility. Scheme 4.3 describes the synthetic pathway towards the common intermediate **27,** which was obtained from 1-bromo-4-iodobenzene **20** in six steps. The Jeffery condition of the Heck reaction afforded aldehyde **22** from 1-bromo-4-iodobenzene **20** and allyl alcohol **21**.[193] Reduction of the aldehyde **22** to the corresponding alcohol **23** and subsequent mesylation afforded intermediate **24,**[194] which was easily converted into amine **26** via nucleophilic substitution with cyanide,[194] followed by nitrile **25** reduction.[195] Treatment with Boc_2O delivered the corresponding *t*-Butyl carbamate **27**.[196]

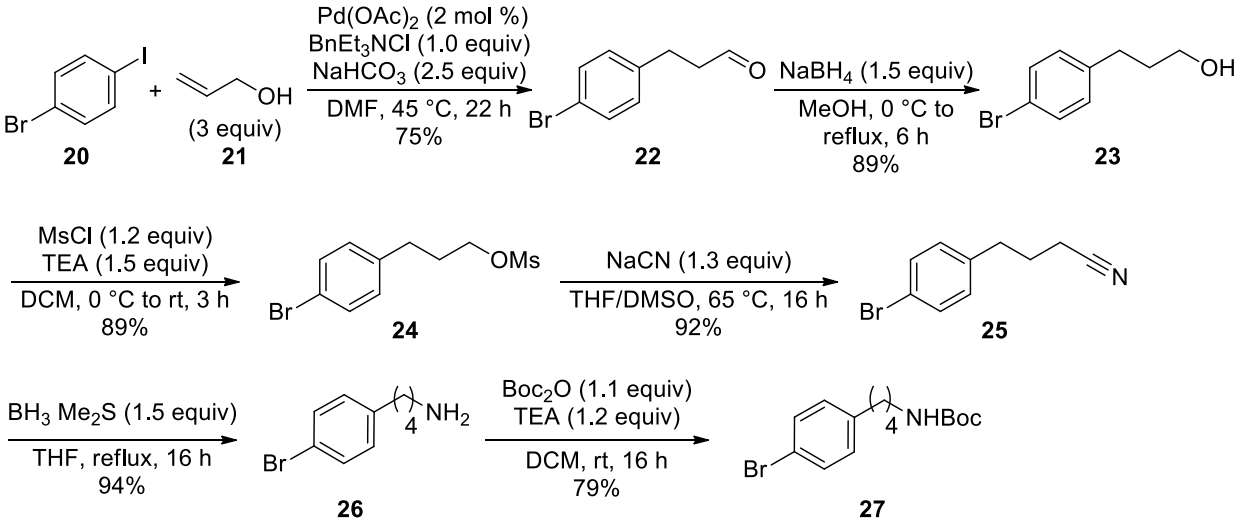

Scheme 4.3 Preparation of common intermediate **27**.

Carbamate **27** was used as an intermediate for the coupling with m- and *o*-toluidines **28** and **31** under Buchwald–Hartwig amination conditions (Scheme 4.4).[197] Subsequent deprotection of the amino group with TFA led to the formation of the corresponding TFA salts **30** (Scheme 4.4a) and **33** (Scheme 4.4b).

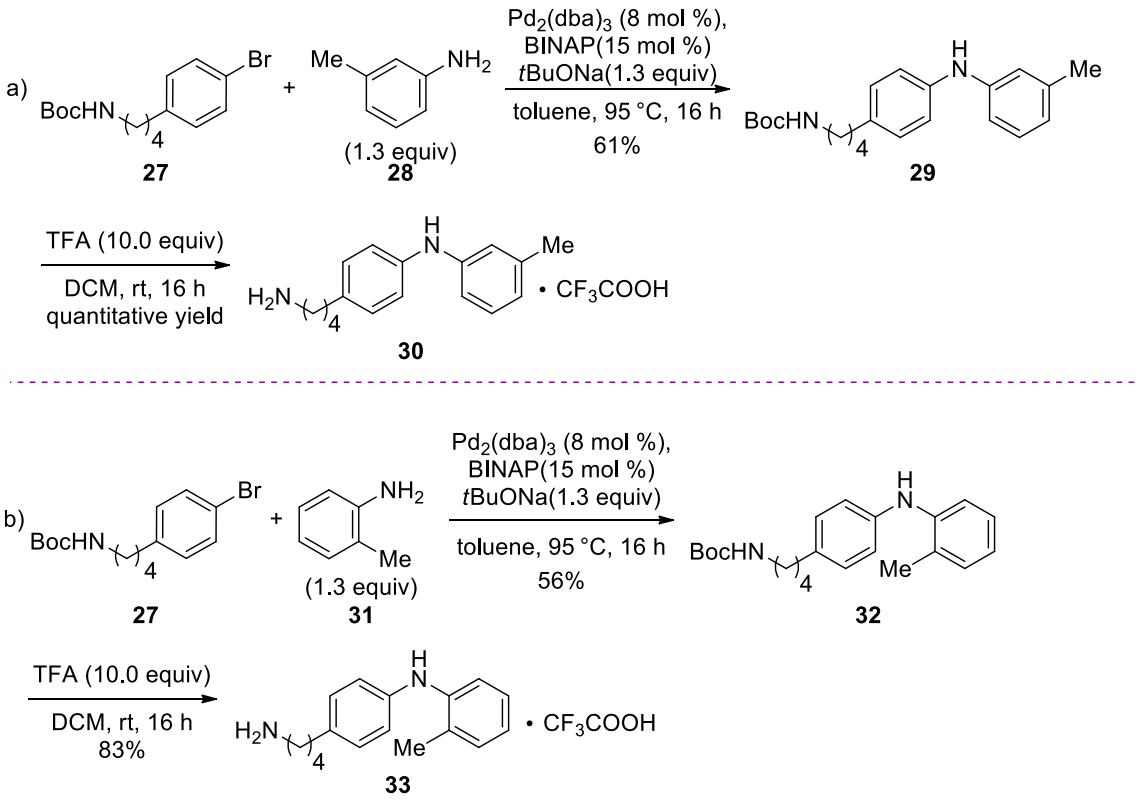

Scheme 4.4 Preparation of compounds **30** and **33**.

To our disappointment, compounds **30** and **33** displayed no measurable binding by NMR titration. As already known, one the phenyl rings fits well into the deep binding pocket of the protein, and introduction of an extra steric bulk deteriorates binding. Therefore, we reasoned that it would be more appropriate to preserve one phenyl ring unsubstituted and introduce substituents only on the second one to improve van der Waals interaction. Since flexibility of the linker showed a negative effect on binding, we decided to restrain it into a cyclic form. With this idea in mind, a series of amino-substituted aromatics were prepared in which different cyclic amines were incorporated into phenyl rings (Figure 4.12).

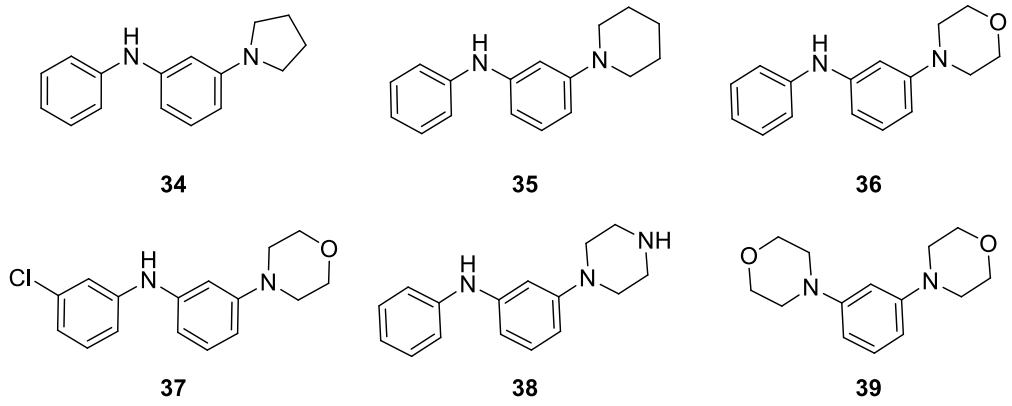

Figure 4.12 Diphenylamine derivatives with cyclic amines.

Compounds **34–37** were synthesized via a two step procedure starting with copper catalyzed amination of 3-bromoiodobenzene with corresponding secondary cyclic amines,[198] followed by palladium catalyzed Buchwald–Hartwig amination of intermediate aryl bromides with aniline derivatives.[197] A representative synthetic route is depicted in Scheme 4.5.

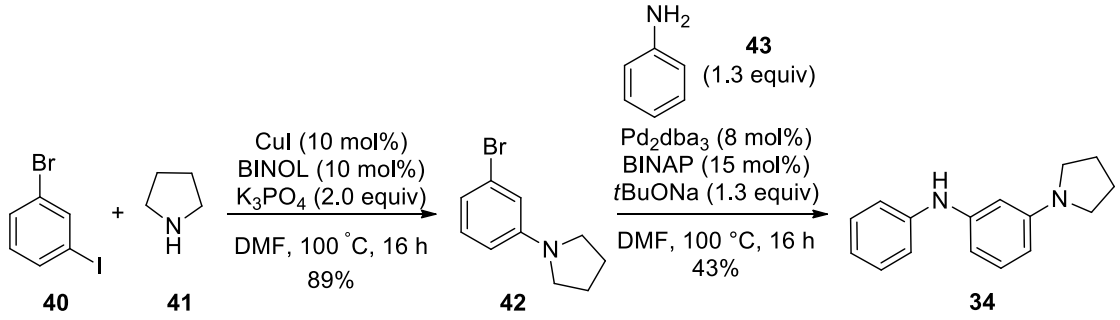

Scheme 4.5 Cyclic amine derivatives: representative procedure.

A similar approach was used to synthesize compound **38**, applying N-Boc-protected piperazine as a starting material. 1,3-Diiodobenzene and morpholine were used to obtain compound **39** in a single step under palladium catalyzed conditions.

In one of the substrates such as **51**, the central nitrogen atom was confined into the cyclic skeleton to see how a further increase in rigidity would influence binding. phenylenediamine **44** was converted into 3,4-dihydroquinoxalin-2(1H)-one **46,**[199] followed by reduction of the amide group with $LiAlH_4$ (Scheme 4.6).[200]

Monoprotection of diamine **47** with Boc group was achieved according to established literature protocol.[196] Coupling of Boc-protected tetrahydroquinoxaline **48** with 4-iodopyridine **49** under palladium catalyzed conditions delivered **50,** which upon treatment with TFA was converted into the corresponding salt **51**.[196]

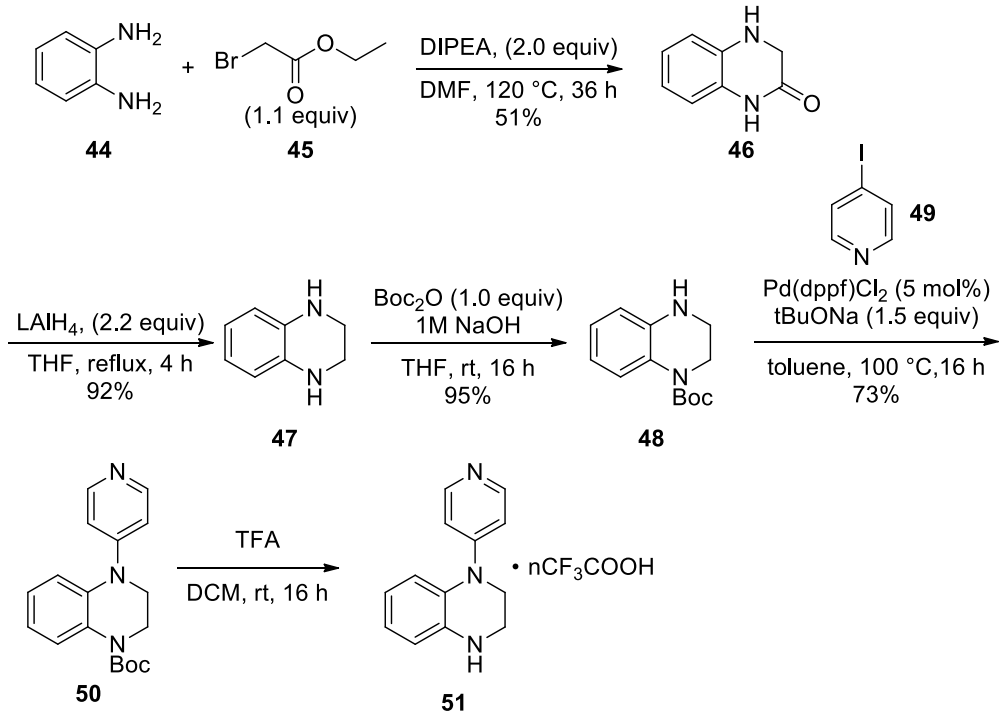

Scheme 4.6 Synthetic procedure for the preparation of **51**.

This strategy did not turn out to be successful, with the substrates exhibiting weak or no binding to the desired protein (Figure 4.13). Obviously, rigidifying diphenylamine scaffolds did not give satisfying results. Unfortunately, we have no reasonable rationale to explain this poor outcome at the moment.

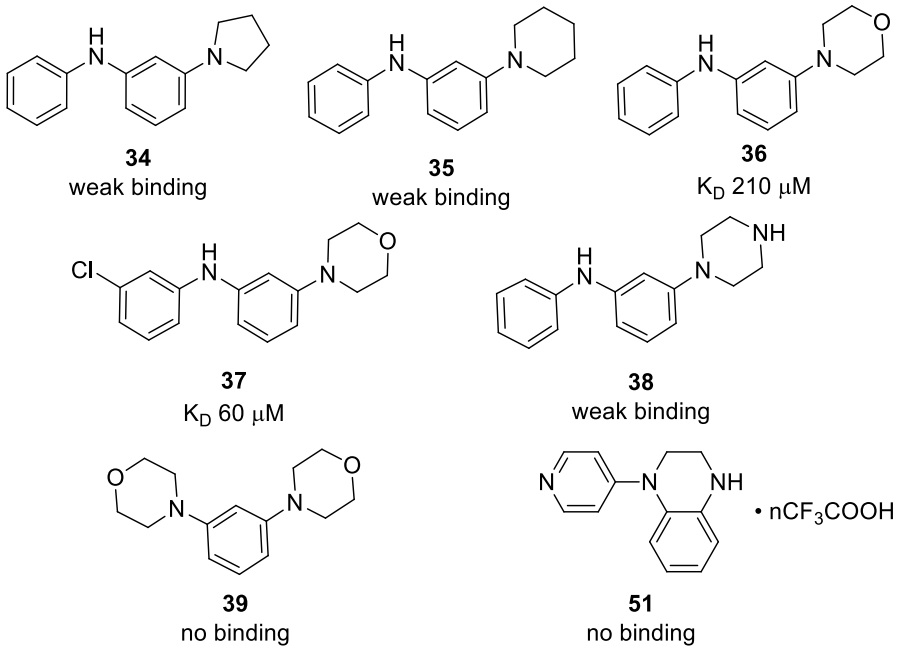

Figure 4.13 Binding affinities of rigid cyclic structures.

4.6 Conclusion

In order to develop calcium sensitizers with a larger inotropic effect than currently exists on the market drugs, our task was to synthesize a library of small molecules that would show high binding affinities towards cardiac troponin C (preferably in nanomolar concentrations).

A diphenylamine scaffold was chosen to be modified as a simplified model of bepridil, due to its high affinity to TnC (K_D = 80 μM). To increase the van der Waals interaction between drug and protein, in our first approach, we tried to incorporate an aliphatic two-, three-, or four-carbon tether either on the central atom of nitrogen or in one of the aromatic rings. In order not to compromise solubility, amine (charged species) and amide (neutral species) functionalities on the other termini of the carbon chain were chosen as solubilizing groups. In some cases, along with carbon-chains, aliphatic methyl groups were introduced in the aromatic ring of diphenylamine.

In another approach, more rigid cyclic amine groups were incorporated into aryl groups; in some cases, the central nitrogen atom of the main scaffold was constrained into the cyclic skeleton, hoping that a decrease of flexibility in the appendix would help to improve binding.

Unfortunately, none of these approaches furnished the desired results in terms of obtaining dissociation constants in the nanomolar range; however, based on discrepancies in binding between different classes of molecules, some common trends could be observed. These could be considered as a step forward towards better understanding of the properties of the hydrophobic pocket.

4.7 Experimental

4.7.1 General Information

Reactions were carried out in flame-dried glasswareunder a positive nitrogen atmosphere, unless otherwise stated. Transfer of anhydrous solvents and reagents was accomplished with oven-dried syringes. 4Å molecular sieves were stored in the oven and flame-dried before use. Solvents were distilled before use: methylene chloride from calcium hydride, tetrahydrofuran and toluene from sodium/benzophenone ketyl. Thin layer chromatography was performed on glass plates pre-coated with 0.25 mm Kiesel gel 60 F254 (Merck). Flash chromatography columns were packed with 230–400 mesh silica gel (Silicycle). ^{1}H and ^{13}C spectra were recorded using Agilent/Varian DD2 MR two channel 400 MHz, Agilent/Varian Inova two-channel 400 MHz, Agilent/Varian Inova four-channel 500 MHz, Agilent/Varian VNMRS two-channel 500 MHz, and Agilent VNMRS four-channel, at 400/500 and 100/125 MHz. ^{1}H NMR chemical shifts are reported relative to a TMS (0.00 ppm) or $CDCl_3$ (7.26 ppm) internal standard. Coupling constants (*J*) are reported in Hertz (Hz). Standard notation is used to describe the multiplicity of signals observed in ^{1}H NMR spectra: broad (br), apparent (app), multiplet (m), singlet (s), doublet (d), triplet (t), etc. Carbon nuclear magnetic resonance spectra (^{13}C NMR) were recorded at 100 MHz and 125 MHz and are reported in ppm

relative to the center line of the triplet from $CDCl_3$.High resolution mass spectrometry (HRMS) data (APPI/ESI technique) were recorded using an Agilent Technologies 6220 oaTOF instrument. HRMS data (EI technique) were recorded using a Kratos MS50 instrument.

4.7.2 Characterization of Compounds 10, 11, 12, 13, 18, 19, 30, 33, 34, 35, 36, 37, 38, 39, 51.

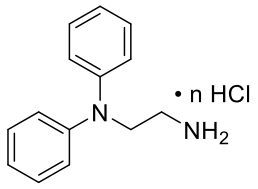

10

Precursors **6**,[190] **7**,[191] **8**–**9**[192] were prepared via the known literature procedure.

N,N-diphenylethane-1,2-diamine hydrochloride (10): In a round bottom flask, to the solution of *N,N*-diphenylethane-1,2-diamine **9** (0.200 g, 0 94 mmol) in ether (25 mL) was added hydrogen chloride (2 M in Et_2O, 5 mL, 10 mmol) and stirred at room temperature overnight. The formed precipitate was collected by filtration, washed with ether and dried. The product was obtained as off-white solid (0.190 g). ^{1}H NMR (400 MHz, DMSO-d_6) δ 7.95 (br s, 3H), 7.28–7.33 (m, 4H), 6.97–7.04 (m, 6H), 3.93 (t, J = 7.4 Hz, 2H), 2.94–2.99 (m, 2H); ^{13}C NMR (125 MHz, D_2O) δ 148.7, 130.8, 123.8, 122.6, 50.0, 38.1.

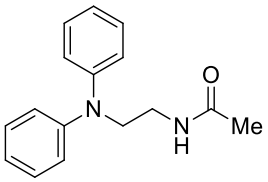

11

N-(2-(diphenylamino)ethyl)acetamide (11): In a round bottom flask, to the solution of *N,N*-diphenylethane-1,2-diamine **9** (0.2 g, 0. 94 mmol) in chloroform (0.5 mL) at -78 °C was added acetyl chloride (0.13 mL, 1.88 mmol). The reaction mixture was allowed to warm up from -78 °C to room temperature and stirred for 15 h. The solvent was removed by reduced pressure evaporation and the residue was purified by silica gel

flash column chromatography (hexanes/EtOAc 1:1) to afford product as beige powder (0.061 g, 0.24 mmol, 26% yield). ^{1}H NMR (400 MHz, $CDCl_3$) δ 7.26–7.31 (m, 4H), 7.02–7.05 (m, 4H), 6.97 (t, *J* = 7.23 Hz, 2H), 5.58 (br s, 1H), 3.91 (t, *J* = 6.5 Hz, 2H), 3.51 (q, *J* = 6.3Hz, 2H), 1.92 (s, 3H).

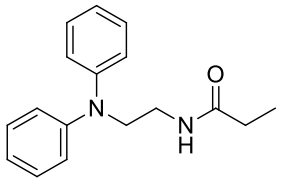

12

N,N-(2-(diphenylamino)ethyl)propionamide (12): To the solution of *N*,*N*-diphenylethane-1,2-diamine **9** (0.350 g, 1.65 mmol) in chloroform (1.0 mL) at -78 °C was added propionyl chloride (0.36 mL, 4.13 mmol). The reaction mixture was allowed to warm up from -78 °C to room temperature and stirred for 15 h. The solvent was removed by reduced pressure evaporation and the residue was purified by silica gel flash column chromatography (hexanes/EtOAc 1:1) to afford beige powder (0.105 g, 0.39 mmol, 24% yield). ^{1}H NMR (400 MHz, $CDCl_3$) δ 7.26–7.31 (m, 4H), 7.02–7.05 (m, 4H), 6.98 (tt, *J* = 7.35, 1.19 Hz, 2H), 5.56 (br s, 1H), 3.91 (t, *J* = 6.4 Hz, 2H), 3.53 (q, *J* = 6.3Hz, 2H), 2.14 (q, *J* = 7.6Hz, 2H), 1.11 (t, *J* = 7.5Hz, 2H); ^{13}C NMR (125 MHz, $CDCl_3$) δ 174.0, 147.8, 129.5, 121.7, 121.0, 51.1, 37.8, 29.6, 9.7.

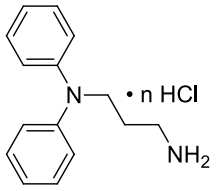

13

N,N-diphenylpropane-1,3-diamine (13) was prepared in an analogous way as **10** from the corresponding starting materials. The product was obtained as a beige solid; ^{1}H NMR (400 MHz, DMSO-d_6) δ 7.91 (br s, 2H), 7.28–7.25 (m, 4H), 6.97–6.92 (m, 6H), 3.75 (t, *J* = 8.3 Hz, 2H), 2.83 (tq, *J* = 15.9, 5.6 Hz, 2H), 1.85 (quint, *J* = 7.5 Hz, 2H).

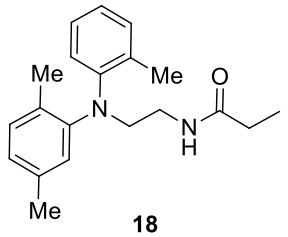

18

N-(2-((2,5-dimethylphenyl)(o-tolyl)amino)ethyl)propionamide (18) was prepared in an analogous way as **12** from the corresponding amine precursor. The product was obtained as a beige solid; ^{1}H NMR (400 MHz, $CDCl_3$) δ 7.15–7.10 (m, 2H), 7.04–6.91 (m, 3H), 6.81–6.78 (m, 2H), 5.72 (br s, 1H), 3.59 (t, *J* = 6.5 Hz, 2H), 3.49 (q, *J* = 6.1 Hz, 2H), 2.25 (s, 3H), 2.15 (q, *J* = 7.7 Hz, 2H), 2.08 (s, 3H), 2.04 (s, 3H), 1.12 (t, *J* = 7.7 Hz, 3H); ^{13}C NMR (125 MHz, $CDCl_3$) δ 173.8, 147.9, 147.7, 136.2, 133.1, 131.7, 131.6, 129.9, 126.6, 124.3, 123.7, 123.4, 123.0, 51.6, 37.8, 29.7, 21.2, 18.8, 18.3, 9.7.

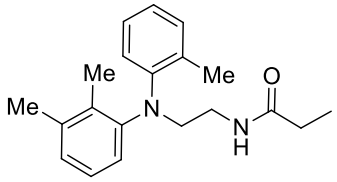

19

N-(2-((2,3-dimethylphenyl)(o-tolyl)amino)ethyl)propionamide (19) was prepared in an analogous way as **12** from the corresponding amine precursor. The product was obtained as a pale yellow oil; ^{1}H NMR (400 MHz, $CDCl_3$) δ 7.13 (d, *J* = 7.5 Hz, 2H), 7.03–6.95 (m, 3H), 6.91 (d, *J* = 7.9 Hz, 1H), 6.79 (d, *J* = 7.9 Hz, 1H), 5.93 (t, *J* = 6.2 Hz, 1H), 3.47 (t, *J* = 6.5 Hz, 2H), 3.47 (q, *J* = 6.0 Hz, 2H), 2.27 (s, 3H), 2.17 (q, *J* = 7.8 Hz, 2H), 2.12 (s, 3H), 2.04 (s, 3H), 1.12 (t, *J* = 7.9 Hz, 3H); ^{13}C NMR (125 MHz, $CDCl_3$) δ 174.0, 148.2, 148.1, 138.4, 132.9, 132.1, 131.8, 126.5, 125.8, 125.6, 123.1, 122.3, 121.6, 51.9, 37.9, 29.6, 20.7, 18.9, 14.3, 9.8.

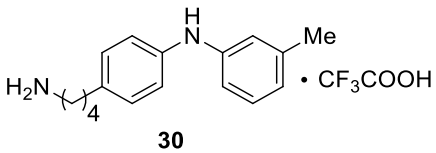

30

Precursors **22**,[193] **23–25**,[194] **26**,[195] **27**[196] and **29**[197] were prepared via the known literature procedure.

N-(4-(aminomethyl)phenyl)-3-methylaniline 2,2,2-trifluoroacetate (30): In the round bottom flask, to the solution of compound **29** (0.086 g, 0.22 mmol) in DCM (5 mL) was added TFA (0.18 mL, 2.4 mmol) and stirred at room temperature for 16 h. The solvent was evaporated and product was obtained as a brown oil (0.084 g, 0.22 mmol, quantitative yield). ^{1}H NMR (400 MHz, CD_3OD) δ 7.07–7.03 (m, 3H), 6.99 (d, *J* = 9.0 Hz, 2H), 6.84–6.80 (m, 2H), 6.63 (d, *J* = 7.0 Hz, 1H), 4.91 (br s, 2H), 2.90 (t, *J* = 7.0 Hz, 2H), 2.60 (t, *J* = 7.0 Hz, 2H), 2.25 (s, 3H), 1.69–1.65 (m, 4H); ^{13}C NMR (125 MHz, CD_3OD) δ 145.5, 143.3, 139.9, 134.6, 130.1, 129.9, 121.8, 119.0, 118.8, 115.2, 40.7, 35.5, 29.4, 28.1, 21.6; HRMS (ESI, $[M+H]^+$) for $C_{17}H_{23}N_2$ calcd. 255.1861, found: m/z 255.1857.

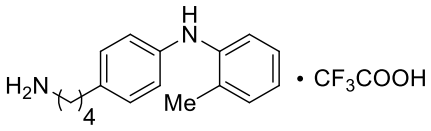

33

N-(4-(aminomethyl)phenyl)-2-methylaniline 2,2,2-trifluoroacetate (33) was prepared in an analogous way as **30** from the corresponding precursor **32**. The product was obtained as a brown oil; ^{1}H NMR (400 MHz, CD_3OD) δ 7.14–6.98 (m, 5H), 6.86–6.78 (m, 3H), 4.88 (br s. 2H), 2.88 (t, *J* = 7.1 Hz, 2H), 2.57 (td, *J* = 7.4, 2.7 Hz, 2H), 2.18 (s, 3H), 1.66–1.63 (m, 4H); ^{13}C NMR (125 MHz, CD_3OD) δ 144.7, 143.4, 133.8, 131.8, 130.5, 130.0, 127.5, 122.9, 120.6, 118.3, 40.7, 35.5, 39.5, 28.1, 18.1; HRMS (ESI, $[M+H]^+$) for $C_{17}H_{23}N_2$ calcd. 255.1861, found: m/z 255.1857.

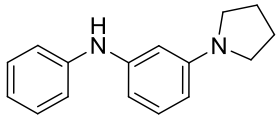

34

N-phenyl-3-(pyrrolidin-1-yl)aniline (34) was prepared via the known literature procedure.[197,198] The product was obtained as a reddish oil; ^{1}H NMR (400 MHz, $CDCl_3$) δ 7.32–7.26 (m, 2H), 7.18 (d, *J* = 8.4 Hz, 1H), 7.15–7.12 (m, 2H), 6.99 (tt, *J* = 1.2 Hz,

1H), 6.47 (ddd, *J* = 7.9, 2.2, 0.8 Hz, 1H), 6.35 (t, *J* = 2.3 Hz, 1H), 6.26 (ddd, *J* = 8.2, 2.2, 0.8 Hz, 1H), 5.68 (br s, 1H), 3.33–3.29 (m, 4H), 2.05–2.01 (m, 4H); ^{13}C NMR (125 MHz, $CDCl_3$) δ 149.1, 143.9, 143.8, 129.9, 129.3, 120.4, 117.7, 106.0, 105.4, 101.6, 47.7, 25.5; HRMS (ESI, $[M+H]^+$) for $C_{16}H_{19}N_2$ calcd. 239.1548, found: m/z 239.1539.

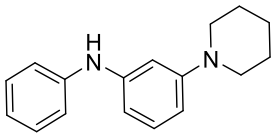

35

N-phenyl-3-(piperidin-1-yl)aniline (35) was prepared via the known literature procedure.[197,198] The product was obtained as a yellow oil; ^{1}H NMR (400 MHz, $CDCl_3$) δ 7.29–7.26 (m, 2H), 7.16 (d, *J* = 8.3 Hz, 1H), 7.09 (dd, *J* = 8.6, 1.2 Hz, 2H), 6.93 (tt, *J* = 7.3, 1.4 Hz, 1H), 6.68 (t, *J* = 2.3 Hz, 1H), 6.58 (dt, *J* = 7.9, 1.8 Hz, 2H), 5.67 (br s, 1H), 3.17 (dd, *J* = 5.8, 5.4 Hz, 4H), 1.72 (quint, *J* = 5.4 Hz, 4H), 1.63–1.56 (m, 2H); ^{13}C NMR (125 MHz, $CDCl_3$) δ 153.4, 143.8, 143.6, 129.8, 129.3, 120.6, 117.7, 109.7, 109.2, 106.3, 50.6, 25.8, 24.4.

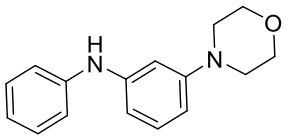

36

3-morpholino-N-phenylaniline (36) was prepared via the known literature procedure.[197,198] The product was obtained as an orange solid; ^{1}H NMR (400 MHz, $CDCl_3$) δ 7.31–7.26 (m, 2H), 7.18 (t, *J* = 8.0 Hz, 1H), 7.11–7.09 (m, 2H), 6.94 (tt, *J* = 7.4, 1.2 Hz, 1H), 6.62 (ddd, *J* = 7.8, 2.2, 0.9 Hz, 2H), 6.53 (ddd, *J* = 8.3, 2.2, 0.9 Hz, 1H), 3.87–3.84 (m, 4H), 3.17–3.14 (m, 4H), no signal detected for NH; ^{13}C NMR (125 MHz, $CDCl_3$) δ 152.5, 144.1, 143.2, 130.0, 129.3, 120.7, 118.0, 109.9, 108.7, 105.1, 66.9, 49.3; HRMS (ESI, $[M+H]^+$) for $C_{16}H_{19}N_2O$ calcd. 255.1497, found: m/z 255.1488.

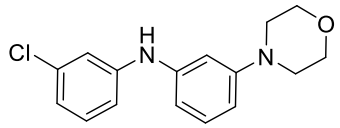

37

3-chloro-N-(3-morpholinophenyl)aniline (37) was prepared via the known literature procedure.[197,198] The product was obtained as an orange oil; ^{1}H NMR (400 MHz, $CDCl_3$) δ 7.25–7.15 (m, 2H), 7.05 (t, *J* = 2.1 Hz, 1H), 6.91 (ddd, *J* = 8.1, 2.1, 0.9 Hz, 1H), 6.88 (ddd, *J* = 7.8, 2.1, 0.9 Hz, 1H), 6.66-6.63 (m, 2H), 6.61–6.58 (m, 1H), 5.74 (br s, 1H), 3.89–3.86 (m, 4H), 3.18–3.15 (m, 4H); ^{13}C NMR (125 MHz, $CDCl_3$) δ 152.5, 145.0, 143.0, 135.0, 130.3, 130.1, 120.4, 116.9, 115.3, 110.8, 109.7, 106.4, 66.9, 49.2; HRMS (ESI, $[M+H]^+$) for $C_{16}H_{18}ClN_2O$ calcd. 289.1108, found: m/z 289.1102.

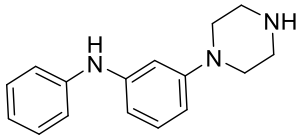

38

N-phenyl-3-(piperazin-1-yl)aniline (38) was prepared via the known literature procedure.[197,198] The product was obtained as abrown oil**;** ^{1}H NMR (400 MHz, $CDCl_3$) δ 7.25–7.29 (m, 2H), 7.16 (dd, *J* = 8.1, 8.1 Hz, 1H), 7.08 (dd, *J* = 8.5, 0.9 Hz, 2H), 6.93 (dd, *J* = 7.3, 7.3 Hz, 1H), 6.60–6.65 (m, 2H), 6.53 (dd, *J* = 8.2, 1.9 Hz, 1H), 5.73 (br s, 1H), 3.78 (br s, 1H), 3.19 (m, 4H), 3.08 (m, 4H); ^{13}C NMR (125 MHz, $CDCl_3$) δ 152.7, 144.1, 143.3, 130.0, 129.4, 120.9, 118.0, 109.9, 109.3 105.8, 49.8, 45.7; HRMS (ESI, $[M+H]^+$) for $C_{16}H_{20}N_3$ calcd. 254.1657, found: m/z 254.1648.

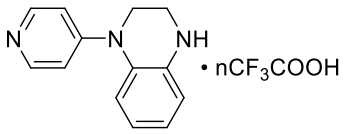

51

Precursors **46**,[199] **47**,[200] **48**–**50**[196] were prepared via the known literature procedure.

1-(Pyridin-4-yl)-1,2,3,4-tetrahydroquinoxaline trifluoroacatate (51)was prepared via the known literature procedure from the corresponding Boc-protected amine precursor.[196] Product was obtained as a brown oil; ^{1}H NMR (400 MHz, CD_3OD) δ 8.13

(d, J = 4.4 Hz, 2H), 7.35 (d, J = 6.8 Hz, 2H), 7.15 (dd, J = 8.1, 1.3 Hz, 1H), 6.99 (ddd, J = 8.3, 7.2, 1.3 Hz, 1H),6.72 (dd, J = 8.2, 1.3 Hz, 1H), 6.59 (ddd, J = 8.1, 7.3, 1.3 Hz, 1H), 3.88−3.90 (m, 2H), 3.42−3.44 (m, 2H); ^{13}C NMR (125 MHz, CD_3OD) δ 157.7, 141.7, 141.4, 128.8, 124.0, 123.8, 117.0, 116.9, 111.5, 45.4, 42.7; HRMS (ESI, $[M+H]^+$) for $C_{13}H_{14}N_3$ calcd. 212.1188, found: m/z 212.1182.

References:

[1] M. Bian, L. Li, H. Ding, *Synthesis,* **2017**, *49*, 4383–4413.

[2] F. A. Carey, R. J. Sundberg, Structure and Mechanisms, in *Advanced Organic Chemistry*, Part A, 5th edition, Springer: New York, **2007**, pp. 833–951.

[3] a) R. B. Woodward, R. Hoffmann, *The Conservation of Orbital Symmetry*; Verlag Chemie: Weinheim, **1970**; b) R. B. Woodward, R. Hoffmann*, Angew. Chem. Int. Ed.* **1969**, *8*, 781–853; *Angew. Chem.* **1969**, *81*, 797–869.

[4] J. L. Vicario, D. Badia, *ChemCatChem*. **2010**, *2*, 375–378.

[5] D. J. Kerr, B. L. Flynn, *Org. Lett.* **2012**, *14*, 1740–1743.

[6]Z. Q. Ren, Y. Hao, X. D. Hu, *Org. Lett.* **2016**, *18*, 4958–4961.

[7] W. H. Zhang, J. M. Ready, *J. Am. Chem. Soc.* **2016**, *138*, 10684–10692.

[8] R. Willstätter, von W. Schmaedel, *Ber. Deutsch. Chem. Ges.* **1905**, *38*, 1992–1995.

[9] W. R. Dolbier, H. Koroniak, N. Houk, C. Sheu, *Acc. Chem. Res.* **1996,** *29,* 471–477.

[10] E. Vogel, *Angew. Chem.* **1954**, *66*, 640–641.

[11] W. Cooper, W. D. Walters, *J. Am. Chem. Soc.* **1958**, *80,* 4220–4224.

[12] E. L. Myers, D. Trauner, Selected Diastereoselective Reactions: Electrocyclizations, in *Comprehensive Chirality*. Vol. 2, Elsevier Ltd, **2012**, 563–606.

[13] E. J. Corey, J. Streith, *J. Am. Chem. Soc*. **1964**, 86, 950–951.

[14] F. Frebault, M. Luparia, M. T. Oliveira, R. Goddard, N. Maulide, *Angew. Chem. Int. Ed*. **2010**, *49*, 5672–5676; *Angew. Chem.* **2010***, 122,* 5807–5811.

[15] a) M. Hübler, *Arch. Pharm*. **1865**, *171*, 205; b) H. Struve, *Z. Anal. Chem*. **1873**, *12*, 164; c) W. Jacobi, *Arch. Exp. Path. Pharmak*. **1890**, *27*, 129.

[16] D. Macht, *Science*, **1927**, *66*, 653–654.

[17] E. J. Forbes, *J. Chem. Soc*. **1955**, 3864–3870.

[18]M. Murakami, S. Ashida, T. Matsuda, *J. Am. Chem. Soc*. **2004**, *126*, 10838–10839.

[19] A. M. Pansuriya, M. M. Savant, C. V. Bhuva, J. Singh, N. Kapuryia, Y. T. Naliapara, *J. Heterocycl. Chem*. **2010**, *47*, 513–516.

[20] B. A. Boon, A. G. Green,P. Liu, K. N. Houk, C. A. Merlic, *J. Org. Chem*. **2017**, *82*, 4613–4624.

[21] N. Deno, C. U. Pittman, *J. Am. Chem. Soc.* ***1964,*** *86*, 1871–1872.

[22] R. Bladek, T. S. Sorensen, *Can. J. Chem*. **1972**, *50*, 2806–2816.

[23] T. S. Sorensen, *Can. J. Chem*. **1964**, *42*, 2781–2790.

[24] T. N. Grant, C. J. Rieder, F. G. West, *Chem. Commun*. **2009**, 5676–5688.

[25] D. Vorländer, G. Schroedter, *Ber. Dtsch. Chem. Ges*. **1903**, *36*, 1490–1497.

[26] C. F. H. Allen, J. A. Van Allan, J. F. Tinker, *J. Org. Chem*. **1955**, *20*, 1387–1391.

[27] I. N. Nazarov, I. I. Zaretskaya, *Izv. Akad. Nauk. SSSR, Ser. Khim*. **1941**, 211–224.

[28] E. A. Braude, J. A. Coles, *J. Chem. Soc.* **1952**, 1430–1433.

[29] Book chapter: F. G. West, O. Scadeng, Y.-K. Wu, R. J. Fradette and S. Joy, The Nazarov Cyclization, in *Comprehensive Organic Synthesis, 2nd Edition*, Vol. 5 (Eds: G. A. Molander, P. Knochel), Elsevier: Oxford, **2014**, pp. 827–866.

[30]J. A. Bender, A. E. Blize, C. C. Browder, S. Giese, F. G. West, *J. Org. Chem*. **1998**, *63*, 2430–2431.

[31] R. William,S. Wang,A. Mallick, X.-W. Liu, *Org. Lett*. **2016**, *18*, 4458–4461.

[32] H.-F. Cui, K.-Y. Dong, G.-W. Zhang, L. Wang, J.-A. Ma, *Chem. Commun.* **2007**, 2284–2286.

[33] H. Zhang, B. Cheng, Z. Lu, *Org. Lett.* **2018**, *20*, 4028–4031.

[34] Y. Kwon, O. Scadeng, R. McDonald. F. G. West, *Chem. Commun.* **2014**, *50*, 5558–5560.

[35] D. J. Schatz, Y. Kwon, T. W. Scully, F. G. West, *J. Org. Chem.* **2016**, *81*, 12494–12498.

[36] J. A. Barltrop, A. C. Day, C. J. Samuel, *J. Am. Chem. Soc.* **1979**, *101*, 7521–7528.

[37] F. Churruca, M. Fousteris, Y. Ishikawa, M. von Wantoch Rekowski, C. Hounsou, T. Surrey, A. Giannis, *Org. Lett*. **2010**, *12*, 2096–2099.

[38] S. Cai, Z. Xiao, Y. Shi, S. Gao*, Chem. Eur. J.* **2014**, *20*, 8677–8681.

[39] G. Liang, Y.-Xu, I. B. Seiple, D. Trauner, *J. Am. Chem. Soc.* **2006**, *128*, 11022–11023.

[40] V. A. Bakulev, *Russ. Chem. Rev.* **1995**, *64*, 99–124.

[41] a) R. J. Srinivasan, *Am. Chem. Soc*. **1960**, *82*, 5063–5066; c) K. E. Lewis, H. Steiner, *J. Chem. Soc.* **1964**, 3080–3092.

[42] D. Trauner, R. Webster, 1,3-Cyclohexadiene Formation Reactions: 6π and Higher-Order Electrocyclizations, in *Comprehensive Organic Synthesis II,* Vol.5, Elsevier Ltd, **2014**, 783–826.

[43]a) J. D. Evanseck, B. E. Thomas IV, D. C. Spellmeyer, K. N. Houk, *J. Org. Chem*. **1995**, *60*, 7134–7141; b) V. Guner, K. N. Houk, I. W. Davies, *J. Org.Chem*. **2004**, *69*, 8024–8028; c) L. Bishop, J. Barbarow, R. G. Bergman, D. Trauner, *Angew. Chem. Int. Ed*. **2008**, *47*, 8100–8103.

[44] O. N. Faza, C. Silva-Lopez, R. Alvarez, A. R. de Lera, *Chem. Eur. J.* **2009**, *15*, 1944–1956.

[45] a) L. Tietze, L. F. *Chem. Rev.* **1996**, *96*, 115–136. b) A de Meijere, P.V. Zezschwitz, S. Bräse, *Acc. Chem. Res.* **2005**, *38*, 413–422; c) M. Hussain, T. V. Sung, P. Langer, *Synlett,* **2012**, *23*, 2735–2744.

[46] L. Y. Zhu, R. B. Tong, *J. Antibiot.* **2016**, *69*, 280–286.

[47] M. Yang, X. W. Yang, H. B. Sun, A. *Angew. Chem. Int. Ed.* **2016**, *55*, 2851–2855; *Angew. Chem.* **2016**, *128*, 2901–2905.

[48] C. Dialer, D. Imbri, S. P. Hansen, T. Opatz, *J. Org. Chem.* **2015**, *80*, 11605–11610.

[49] a) T.-Q. Yu, Y. Fu, L. Liu, Q.-X. Guo, *J. Org. Chem*. **2006**, *71*, 6157–6164; c) T. J. Greshock, R. L. Funk, *J. Am. Chem. Soc*. **2006**, *128*, 4946–4947.

[50] V. A. Guner, K. N. Houk, I. W. Davies, *J. Org. Chem*. **2004**, *69*, 8024–8028.

[51] L. M. Bishop, J. E. Barbarow, R. G. Bergman, D. Trauner, *Angew. Chem. Int. Ed*. **2008**, *47*, 8100–8103; *Angew. Chem.* **2008**, *120*,8220–8223.

[52] S. L. Brandänge, H. Leijonmarck, *Chem. Commun*. **2004**, 292–293.

[53] N. A. Magomedov, P. L. Ruggiero, Y. Tang, *Org. Lett*. **2004**, 6, 3373–3375.

[54] R. Hayashi, J. B. Feltenberger, R. P. Hsung, *Org. Lett*. **2010**, *12*, 1152–1155.

[55] R. Wang, S.-C. Lu, Y.-M. Zhang, Z.-J. Shi, W. Zhang, *Org. Biomol. Chem*. **2011**, *9*, 5802–5808.

[56] a) A. Rescifina, M. A. Chiacchio, A. Corsaro, E. De Clercq, D. Iannazzo, A. Mastino, A. Piperno, G. Romeo, R. Romeo, V. Valveri, *J. Med. Chem*. **2006**, *49*, 709−715; b) L. H. Mejorado, T. R. R. Pettus, *J. Am. Chem. Soc*. **2006**, *128*, 15625−15631 c); A. N. Lowell, M. W. Fennie, M. C. Kozlowski, *J. Org. Chem.* **2008**, *73*, 1911−1918.

[57] W.-M. Liu,Y. L. Tnay, K. P. Gan, Z.-H. Liu, W. H. Tyan, K. Narasaka, *Helv. Chim. Act*. **2012**, 95, 1953−1969.

[58] G.-Q. Chen, G. Kehr, C. G. Daniliuc, C. Mück-Lichtenfeld, G. Erker, *Angew. Chem. Int. Ed*. **2016**, *55*, 5526−5530; *Angew. Chem.* **2016**, *128,* 5616−5620.

[59] S. S. Giri, R.-S. Liu, *Chem. Sci*. **2018**, *9*, 2991−2995;

[60] C. J. Rieder, K. J. Winberg, F. G. West, *J. Am. Chem. Soc*. **2009**, *131*, 7504−7505.

[61] a) D. V Patil, L. H. Phun, S. France, *Org. Lett*. **2010**, *12*, 5684−5687; b) L. H. Phun, D. V. Patil, M. A. Cavitt, S. France, *Org. Lett*. **2011**, *13*, 1952−1955.

[62] S. Pusch, D. Kowalczyk, T. Opatz, *J. Org. Chem*. **2016**, *81*, 4170−4178.

[63] C. C. Fu, Y. B. Zhang, J. Xuan, C. L. Zhu, B. N. Wang, H. F. Ding, *Org. Lett.* **2014**, *16*, 3376−3379.

[64] A. Shvartsbart, A. B. Smith, *J. Am. Chem. Soc*. **2015**, *137*, 3510−3519.

[65] Z. Y. Lu, Y. Li, J. Deng, A. Li, *Nat. Chem.* **2013**, *5*, 679−684.

[66] Part of this chapter has been published as: S. Gelozia, Y. Kwon, R. McDonald, F. G. West, *Chem. Eur. J*. **2018**, *24*, 6052−6056.

[67] Recent reviews: a) C. E. Sleet, U. K. Tambar, P. Maity, *Tetrahedron*, **2017**, *73*, 4023−4038; b) M. G. Vinogradov, O. V. Turova, S. G. Zlotin *Org. Biomol. Chem*. **2017**, *15*, 8245−8269; c) S. P. Simeonov, J. P. M. Nunes, K. Guerra, V. B. Kurteva, C. A. M. Afonso, *Chem. Rev*. **2016**, *116*, 5744−5893; d) D. R. Wenz, J. Read de Alaniz, *Eur. J. Org. Chem*. **2015**, 23−37; e) L. Barriault, M. Morin, *Cross Conj*. **2016**, 59−78.

[68] Recent Examples: a) T. D. R. Morgan, L. M. LeBlanc, G. H. Ardagh, R. J. Boyd, D. J. Burnell, *J. Org. Chem*. **2015**, *80*, 1042−1051; b) V. Z. Shirinian, A. G. Lvov, A. V. Yadykov, L. V. Yaminova, V. V. Kachala, A. I. Markosyan, *Org. Lett*. **2016**, *18*, 6260−6263; c) E. Grenet, J. Martinez, X. J. Salom-Roig, *Chem. Eur. J*. **2016**, *22*,

16770−16773; d) K. Fuchibe, R. Takayama, T. Yokoyama, J. Ichikawa, *Chem. Eur. J.* **2017**, *23*, 2831−2838; e) H. Liao, W.-L. Leng, K. L. M. Hoang, H. Yao, J. He, A. Y. H. Voo, X.-W. Liu, *Chem. Sci.* **2017**, *8*, 6656−6661.

[69] Recent reviews: a) T. Vaidya, R. Eisenberg, A. J. Frontier, *ChemCatChem.* **2011**, *3*, 1531−1548; b) N. Shimada, C. Stewart, M. A. Tius, *Tetrahedron,* **2011**, *67*, 5851−5870.

[70] Recent examples: a) T. Mietke, Thomas, T. Cruchter, V. A. Larionov, T. Faber, H. Klaus, E. Meggers, *Adv. Synth. Catal*. **2018**, 360, 2093−2100; b) R. Volpe, B. L. Flynn, R. J. Lepage, E. H. Krenske, J. M. White, *Chem. Sci*. **2018**, *9*, 4644−4649; c) J. Congmon, M. A. Tius, E. *J. Org. Chem*. **2018**, *23*, 2926−2930; d) L. Süsse, M. Vogler, M. Mewald, B. Kemper, E. Irran, M. Oestreich, *Angew. Chem. Int. Ed*. **2018**, *57*, 11441−11444; *Angew. Chem.* **2018,** *130,*11612−11615;e) A. Jolit, C. F. Dickinson, K. Kitamura, P. M. Walleser, G. P. A. Yap, M. A. Tius, *E. J. Org. Chem*. **2017**, *40*, 6067−6076; f) C.-S. Wang, J.-L. Wu, C. Li, L.-Z. Li, G.-J. Mei, F. Shi*, Adv. Synth. Catal*. **2018**, 360, 846−851.

[71] Recent examples: a) B. Aegurla, R. K. Peddinti, *Org. Biomol. Chem.* **2017**, *15*, 9643−9652; b) M. J. Riveira, L. A. Marsili, M. P. Mischne, *Org. Biomol. Chem*. **2017**, *15*, 9255−9274; c) R. William, W. L. Leng, S. Wang, X.-W. Liu, *Chem. Sci.* **2016,** *7*, 1100−1103; d) M. A. Tius, *Chem. Soc. Rev.* **2014**, *43*, 2979−3002; e) S. A. Bonderoff, T. N. Grant, F. G. West, M. Tremblay, *Org. Lett*. **2013**, *15*, 2888−2891.

[72] a) M. Liu, K. Gao, Y. Y. Fan, X. Guo, J. Wu, X. Meng, H. Hou, *Chem. Eur. J.***2018**, 24, 1416−1424; b) Y. Thigulla, S. Ranga, S. Ghosal, J. Subbalakshmi, A. Bhattacharya, *Chem. Select*, **2017**, *2*, 9744−9750; c) Y.-K. Wu, F. G. West, *Org. Lett*. **2014**, *16*, 2534–2537; d) J. H. Chaplin, K. Jackson, J. M. White, B. L. Flynn, *J. Org. Chem*. **2014**, *79*, 3659–3664; e) R. William, S. Wang, F. Ding, E. N. Arviana, X.-W. Liu, *Angew. Chem. Int. Ed.* **2014**, *53*, 10742−10746; *Angew. Chem*. **2014**, *126*, 10918–10922; f) Y.-K. Wu, C. R. Dunbar, R. McDonald, M. J. Ferguson, F. G. West, *J. Am. Chem. Soc*. **2014**, *136*, 14903−14911.

[73] Y. Naganawa, K. Maruoka, *Topics in Organometallic Chemistry*, Vol. 41 (Eds: S. Woodward, S. Dagorne), Springer-Verlag Berlin Heidelberg, **2013**, pp. 187–214.

[74] A. J. Lundeen, A. C. Oehlschlager, *J. Organomet. Chem*. **1970**, *25*, 337–344.

[75] E. C. Ashby, S. Yu, *Chem. Comm*. **1971**, *0*, 351–352.

[76] E. C. Ashby, J. T. Laemmle, H. M. Neumann, *J. Amer. Chem. Soc*. **1968**, *90*, 5179–5188.

[77] Y. Takemoto, S. Kuraoka, N. Hamaue, C. Iwata, *Tetrahedron*, **1996**, *7*, 14177–14188.

[78] C. R. Emschwiller, Hebd. *Séance. Acad*. *Sci*. **1929**, *188*, 1555.

[79] a) H. E. Simmons, R. D. Smith, *J. Am. Chem. Soc*. **1958**, *80*, 5323–5324; b) H. E. Simmons, R. D. Smith, *J. Am. Chem. Soc*. **1959**, *81*, 4256–4264.

[80] J. Mareda, N. G. Rondan, K. N. Houk, T. Clarc, P. R. Schleyer, *J. Am. Chem. Soc*. **1983,** *105*, 6997–6999.

[81] G. Wittig, K. Schwarzenbach, *Angew. Chem*. **1959**, *71*, 652; b) G. Wittig, K. Schwarzenbach, *J. Lieb.Ann. Chem*. **1962**, *650*, 1–20; c) G. Wittig, F. Wingler, F. *J. Lieb. Ann. Chem*. **1962**, 656, 18–21; d) G. Wittig, F. Wingler, *Chem. Ber*. **1964**, *97*, 2146−2164; e) G. Wittig, M. Jautelat, *Lieb. Ann. Chem*. **1967**, *702*, 24–37.

[82] a) J. Furukawa, N. Kawabata, J. Nishimura, *Tet. Lett.***1966**, *7*, 3353–3354; b) J. Furukawa, N. Kawabata, J. Nishimura, *Tetrahedron,* **1968**, *24*, 53–58.

[83] S. E. Denmark, J. P. Edwards, *J. Org. Chem*. **1991**, *56*, 6974−6981.

[84] A. B. Charette, A. Beauchemin in *Organic Reactions*, Vol. 58 (Ed.: L. E. Overman et al.), John Wiley and Sons, Inc. **2001**, pp. 1–415.

[85] A. B. Charette, J.-F. Macroux, *Synlett*, **1996**, 1197–1207.

[86] V. K. Aggarwal, G. Y. Fang, G. Meek, *Org. Lett*. **2003**, *5*, 4417–4420.

[87] M. C. Lacasse, C. Poulard, A. B. Charette, *J. Am. Chem. Soc*. **2005**, *127*, 12440–12441.

[88] G. A. Molander and L. S. Harring, *J. Org. Chem*. **1989**, *54*, 3525–3532.

[89] J. W. Collette, *J. Org. Chem.* **1963**, *28*, 2489–2490.

[90] D. B. Miller, *Tet. Lett.* **1964**, *17*, 989–991.

[91] K. Maruoka, Y. Fukutani, H. Yamamoto, *J. Org. Chem.* **1985**, *50*, 4412–4414.

[92] Y. Kwon, R. McDonald, F. G. West, *Angew. Chem. Int. Ed.* **2013**, *52*, 8616–8619; *Angew. Chem.* **2013**, *125*, 8778–8781.

[93] CCDC 1586723 (**42a**) and 1586722 (**43a**), contain the supplementary crystallographic data for this chapter. These data can be obtained free of charge from The Cambridge Crystallographic Data Centre via www.ccdc.cam.ac.uk/data_request/cif. **43a** was obtained by Dr. Yonghoon Kwon.

[94] In solution, **43a** equilibrates with its open form which complicates NMR analysis. Thus, for structure elucidation, only the X-ray crystal structure is presented.

[95] Cyclohexanones are accessible via the formal homo-Nazarov reaction of vinyl cyclopropyl ketones, although this process is generally thought to proceed through a stepwise mechanism: a) F. De Simone, T. Saget, F. Benfatti, S. Almeida, J. Waser, *Chem. Eur. J.* **2011**, *17*, 14527–14538; b) M. D. Martin, R. Shenje, S. France, *Isr. J. Chem.* **2016**, *56*, 499–511; c) S. Takada, N. Takaki, K. Yamada, Y. Nishii, *Org. Biomol. Chem.* **2017**, *16*, 2443–2449.

[96] G. Suss-Fink, S. Stanislas, G. B. Shul'pin, G. V. Nizova, H. Stoeckli-Evans, A. Neels, C. Bobillier S. J. Claude, *J. Chem. Soc. Dalton Trans.* **1999**, 3169–3175; b) R. Hiatt, R. J. Smythe, C. McColeman, *Can. J. Chem.* **1971**, *49*, 1707–1711.

[97] J.-P. Barnier, V. Morisson, L. Blanco, *Synth. Commun*. **2001**, *31*, 349–357.

[98] D. H. Gibson, C. H. DePuy, *Tetrahedron Lett*. **1969**, *10*, 2203–2206.

[99] Y. Ito, S. Fujii, T. Saegusa, *J. Org. Chem.* **1976***, 41,* 2073–2074.

[100] a) B. R. Davis, G. W. Rewcastle, P. D. Woodgate, *J. Chem. Soc. Perkin Trans. 1,* **1979**, 2820–2825; b) L. A. Paquette, R. J. Ross, Y. J. Shi, *J. Org. Chem.* **1990**, *55*, 1589–1598.

[101] For related transformations of bicycle[3.1.0]hexanols and their derivatives, see: (a) V. Morisson, J. P. Barnier, L. Blanco, *Tetrahedron,* **1998**, *54*, 7749–7764; (b) J. Tallineau, G. Bashiardes, J.-M. Coustard, F. Lecornue, *Synlett.* **2009**, 2761–2764.

[102] K. I. Booker-Milburn, D. F. Thompson, *J. Chem. Soc. Perkin Trans. I,* **1995**, 2315–2321.

[103] S. Chiba, Z. Cao, S. A. A. El Bialy, K. Narasaka, Chem. Lett. **2006**, *35*, 18−19.

[104] For recent reviews see: a) L. Degennaro, P. Trinchera, R. Luisi, *Chem. Rev*. **2014**, *114,* 7881−7929; b) Y. Zhu, Q. Wang, R. G. Cornwall, Y. Shi, *Chem. Rev*. **2014**, *114*, 8199−8256.

[105] a) D. A. Evans, M. M. Faul, M. T. Bilodeau, *J. Org. Chem*. **1991**, *56*, 6744−6746; b) D. A. Evans, M. M. Fad, M. T. Bilodeau, *J. Am. Chem. Soc*. **1994**, *116*, 2742−2153.

[106] Z. Daneshfar, A. Rostami, *RSC Adv*. **2015**, *5*, 104695−104707.

[107] C. J. Rieder, K. J. Winberg, F. G. West, *J. Org. Chem.* **2011**, *76*, 50−56.

[108] O. Scadeng, M. J. Ferguson, F. G. West, *Org. Lett*. **2011**, *13*, 114−117.

[109] C. J. Hastings, M. D. Pluth, R. G. Bergman, K. N. Raymond, *J. Am. Chem. Soc.* **2010**, *132*, 6938−6940.

[110] S. Giese, F. G. West, *Tetrahedron,* **2000**, *56,* 10221−10228.

[111] Y. Wang, B. D. Schill, A. M. Arif, F. G. West, *Org. Lett*. **2003**, *5*, 2747−2750.

[112] a) T. Seiser, T. Saget, D. N. Tran, N. Cramer, *Angew. Chem. Int. Ed*. **2011**, *50*, 7740–7752; *Angew. Chem*.**2011**, *123*, 7884−7896.

[113] a) E. M. Carreira, T. C. Fessard, *Chem. Rev*. **2014**, *114*, 8257−8322; b) C. M. Marson, *Chem. Soc. Rev*. **2011**, *40*, 5514–5533; c) K. A. Brameld, B. Kuhn, D. C. Reuter, M. Stahl, *J. Chem. Inf. Model*. **2008**, *48*, 1−24.

[114] a) G. M. Castanedo, et al. *J. Med. Chem*. **2017**, *60*, 627−640; b) D. C. Blakemore et al. *Bioorg. Med. Chem. Lett*. **2010**, *20*, 461−464; c) J. P. Vilaine, C. Thollon, N. Villenueve, J. L. Peglion, *Eur. Heart J. Suppl*. **2003**, *5*, G26−G35.

[115] R. M. Ortuno, A. G. Moglioni, G. Y. Moltrasio, *Curr. Org. Chem.* **2005**, *9*, 237. b) Y.-Y. Fan, X.-H. Gao, J.-M. Yue. *Sci. China Chem.* **2016**, *59*, 1126−1141.

[116] M. J. Martín, R. Fernández, A. Francesch, P. Amade, S.S. de Matos-Pita, F. Reyes, C. Cuevas, *Org Lett*, **2010**, *12,* 912−914.

[117] a) S. Staben, G. M. Castanedo, C. Montalbetti, J. Feng, Tricyclic Compounds and Methods of Use Therefor. U.S. Patent 9,034,866 B2, May 19, **2015**; b) G. M. Castanedo, N. Blaquiere, M Beresini, B. Bravo, H. Brightbill, J. Chen, H.-F. Cui, C. Eigenbrot, C. Everett, J. Feng, et al. *J. Med. Chem*. **2017**, *60*, 627−640.

[118] a) A. C. Legon, *Chem. Rev.* **80**, 1980, 231−262; b) N. L. Allinger, L. A. Tushaus, *J. Org. Chem*. **1965**, *30*, 1945−1951.

[119] S. Poplata, A. Tröster, Y.-Q. Zou, T. Bach, *Chem. Rev*. **2016**, *116*, 9748−9815.

[120] S. Ghosh, Copper(I)-Catalyzed Inter- and Intramolecular [2 + 2]-Photocycloaddition Reactions of Alkenes. In *CRC Handbook of Photochemistry and Photobiology,* 2nd ed.; (Eds. W. M. Horspool, F. Lenci), CRC Press: Boca Raton, **2004**; pp 18-1−18-24.

[121] F. Rioux, *J. Chem. Edu*. **2007,** *84*, 358−360.

[122] J. P. Hehn, C. Müller, T. Bach, Formation of a Four-Membered Ring: From a Carbonyl-Conjugated Alkene. *In Handbook ofSynthetic Photochemistry*, (Eds by A. Albini, M. Fagnoni), Wiley-VCH: Weinheim, **2010**; pp 171−215.

[123] C. Liebermann, *Ber. Dtsch. Chem. Ges*. **1877**, *10*, 2177−2179.

[124] C. Liebermann, M. Ilinski, *Ber. Dtsch. Chem. Ges*. **1885**, *18*, 3193−3201.

[125] A. V. Kurdyumov, R. P. Hsung, K. Ihlen, J. Wang, *Org. Lett*. **2003**, *5*, 3935−3938.

[126] A. Jana, S. Mondal, S. Ghosh*, Org. Biomol. Chem*. **2015**, *13*, 1846−1859.

[127] M. A. Ischay, M. E. Anzovino, J. Du, T. P. Yoon, *J. Am. Chem. Soc.* **2008**, *130*, 12886−12887.

[128] M. A. Ischay, Z. Lu, T. P. Yoon, *J. Am. Chem. Soc*. **2010**, *132*, 8572−8574.

[129] R. Navarro, S. E. Reisman, *Org. Lett*. **2012**, *14*, 4354−4357.

[130] H. Jo, M. E. Fitzgerald, J. D. Winkler, *Org. Lett.* **2009**, *11*, 1685−1687.

[131] J. Zhao, J. L. Brosmer, Q. Tang, Z. Yang, K. N. Houk, P. L. Diaconescu, O. Kwon, *J. Am. Chem. Soc*, **2017,** 139, 9807−9810.

[132] Y. Xu, M. L. Conner, M. K. Brown, *Angew. Chem. Int. Ed*. **2015**, *127*, 11918−11828; *Angew. Chem.***2015**, *54*, 12086−12097.

[133] J. Liese, N. Hampp, *J. Phys. Chem*. **2011**, *115*, 2927−2932; b) W. E. von Doering, J. L. Ekmanis, K. D. Belfield, F.-G. Klärner, B. J. Krawczyk, *J. Am. Chem. Soc*. **2001**, *123*, 5532−5541.

[134] T. A. Engler, M. A. Letavic, R. Iyengar, K. O. LaTessa, J. P. Reddy, *J. Org. Chem*. **1999**, *64*, 2391−2405.

[135] Y. Hayashi, K. Narasaka, *Chem. Lett*. **1989**, 793−796.

[136] M. L. Conner, Y. Xu, M. K. Brown, *J. Am. Chem. Soc.* **2015**, *137*, 3482–3485.

[137] J. Du, K. L. Skubi, D. M. Schultz, T. P. Yoon, *Science*, **2014**, *344*, 392–396.

[138] Z. D. Miller, B. J. Lee, T. P. Yoon, *Angew. Chem. Int. Ed.* **2017***, 56,* 11891–11895*; Angew. Chem.* **2017***, 129,* 12053–12057.

[139] T. B. Blum, Z. D. Miller, D. M. Bates, I. A. Guzei, T. P. Yoon, *Science*, **2016**, *354*, 1391–1395.

[140] M. B. Boxer, H. Yamamoto, *Org. Lett*. **2005**, *7*, 3127–3129.

[141] a) N. Ghavtadze, R. Narayan, B. Wibbeling, E.-U. Würthwein,*J. Org. Chem.* **2011**, 76, 5185–5197; b) C. C. Browder, F. P. Marmsäter, F. G. West, *Org. Lett.***2001**, *3*, 3033–3035; c) J. A. Bender, A. E. Blize, C. C. Browder, S. Giese, F. G. West, *J. Org. Chem*. **1998**, 63, 2430–2431.

[142] For the X-ray data of compounds **50a**, **50f′**, **50l** and **52a** see appendixes **IV, V, VI** and **VII**.

[143] S. E. Denmark, T. K. Jones*, J. Am. Chem. Soc*. **1982**, *104*, 2642–2645.

[144] a) S. E. Denmark*, K. L. Habermas, G. A. Hite, Helv. Chim. Acta*, **1988**, *71*, 168–194; b) S. E. Denmark*, G. A. Hite, Helv. Chim. Acta*, **1988**, *71*, 195–208.

[145] G. Majetich, Y. Zhang, *J. Am. Chem. Soc.* **1994**, 116, 4979–4980.

[146] S. A. Shahzad, C. Vivant, T. Wirth, *Org. Lett.* **2010**, *12*, 1364–1367.

[147] E. Wenkert, M. K. Schorp, *J. Org. Chem*. **1994**, *59*, 1943–1944.

[148] J. Dieker, R. Fröhlich, E-U Würthwein, *Eur. J. Org. Chem.* **2006**, 5339–5356.

[149] G. Liang, S. N. Gradl, D. Trauner, *Org. Lett.* **2003**, 5, 4931–4934.

[150] Part of this chapter has been published as: F. Cai, M. X. Li, S. E. Pineda-Sanabria, S. Gelozia, S. Lindert, F. G. West, B. D. Sykes, P. M. Hwang, *J. Mol. Cell. Cardiol*. **2016**, *101*, 134–144.

[151] http://www.who.int/en/news-room/fact-sheets/detail/cardiovascular-diseases-(cvds) (Link accessed on August 3, **2018**).

[152] P. A. Heidenreich, N. M. Albert, L. A. Allen, et al. *Circ. Heart Fail*. **2013**, *6*, 606–619.

[153] E. J. Benjamin, M. J. Blaha, S. E. Chiuve, et al. *Circulation,* **2017**, *135*, e146–e603.

[154] A. Mosterd, A. W. Hoes, *Heart*, **2007**, *93*, 1137–46.

[155] J. C. Fang, G. A. Ewald, L. A. Allen, et al. *J. Card. Fail*. **2015**, *21*, 519–534.

[156] F. H. Fukuta, W. C. Little, in *Diastology: clinical approach to diastolic heart failure,* 1st edition, (Eds. A. L. Klein, M. J. Garcia), Saunders Elsevier: Philadelphia, **2008**, pp 63–72.

[157] S. Brucks, W. C. Little, T. Chao, et al. *Am. J. Cardiol*. **2005**, *95*, 603–606.

[158] T. Sorsa, P. Polleselo, R. J. Solaro, *Molecular and Cellular Biochemistry*, **2004**, 266, 87–107.

[159] J. C. Haselgrove, H. E. Huxley, *J. Mol. Biol.* **1973**, 77, 549–568.

[160] K. C. Holmes, D. Popp, W. Gebhard, W. Kabsch, *Nature*, **1990**, *347*, 44–49.

[161] File was downloaded from Protein Data Bank, entry 1J1E, and generated with PyMOL, https://www.rcsb.org/3d-view/1J1E.

[162] a) M. C. Schaub, S. V. Perry, *Biochem. J.* **1969**, *115*, 993–1004; b) J. D. Potter, J. Gergely, *Biochemistry*, **1974**, *13*, 2697–2703; c) S. E. Hitchcock, *Eur. J. Biochem*. **1975,** *52*, 255–263.

[163] R. A. Weeks, S. V. Perry, *Biochem. J.* **1978***, 173*, 449–457.

[164] a) M. Rosol, W. Lehman, R. Craig, C. Landis, C. Butters, L. S. Tobacman, *Biophys. J.* **2000**, *78*, 908–917; b) L. S. Tobacman, C. A. Butters, *J. Biol. Chem*. **2000**, *275,* 27587–27593.

[165] W. Lehman, M. Rosol, L. S. Tobacman, R. Craig, *J. Mol. Biol.* **2001**, *307,* 739–744.

[166] D. M. Bers, *Nature*, **2002**, *415*, 198–205.

[167] File was downloaded from Protein Data Bank, entry 1AJ4, and generated with PyMOL, https://www.rcsb.org/structure/1AJ4.

[168] a) Z. L. Sheng, J. M. Francois, S. E. Hitchcock-DeGregori, J. D. Potter, *J. Biol. Chem.* **1991**, *266*, 5711–5715; b) A. Babu, V. G. Rao, H. Su, J. Gulati, *J. Biol. Chem*. **1993,** *268,* 19232–19238; c) S. Ramakrishnan, S. E. Hitchcock-DeGregori, *Biochemistry*, **1995**, *34*, 16789–16796.

[169] J. D. Potter, J. Gergely, *J. Biol. Chem*. **1975**, *250*, 4628–4633; b) H. G. Zot, J. D. Potter, *J. Biol. Chem.* **1982**, *257*, 7678–7683.

[170] M. X. Li, P. M. Hwang, *Gene*, **2015**, *571*, 153–166.

[171] J. L. Gifford, M. P. Walsh, H. J. Vogel, *Biochem. J.* **2007**, *405*, 199–221.

[172] S. B. Tikunova, J. P. Davis, *J. Biol. Chem*. **2004**, *279*, 35341–35352.

[173] S. V. Perry, *Rev. Mol. Cell. Biochem.* **1999**, *190*, 9–32.

[174] A. Fabiato, F. Fabiato, *J. Physiol*. **1978**, *276*, 233–255.

[175] a) A. J. Moir, R. J. Solaro, S. V. Perry, *Biochem. J.* **1980**, *185*, 505–513; b) R. Zhang, J. Zhao, J. D. Potter, *J. Biol. Chem.***1995**, 270, 30773–30780; c) W. J. Dong, M. Chandra, J. Xing, M. She, R. J. Solaro, H. C. Cheung, *Biochemistry*, **1997**, *36*, 6754–6761.

[176] G. S. Francis, J. A. Bartos, S. Adatya, *J. Am. Coll. Cardiol*. **2014**, *63*, 2069–2078.

[177] M. Endoh, *Circ. J.* **2008,** *72,*1915–1925.

[178] H. Kusuoka, Y. Koretsune, V. P. Chacko, M. L. Weisfeldt, E. Marban, *Circ. Res.* **1990**, *66*, 1268–1276.

[179] a) J. W. Herzig, K. Feile, H. Ihrig, J. C. Rüegg, *Pflügers Arch. Eur. J. Physiol*. **1980**, 384, R1. b) R. J. Solaro, J. C. Rüegg, *Circ. Res*. **1982**, *51*, 290–294.

[180] Z. Papp, I. Edes, S. Fruhwald, et al. *Int. J. Cardiol*. **2012**, *159*, 82–87.

[181] a) A. Mebazaa, M. S. Nieminen, M. Packer, et al. *JAMA*. **2007**, *297*, 1883–1891; b) M. Packer, W. Colucci, L. Fisher, et al. *JACC Heart Fail*. **2013**, *1*, 103–111.

[182] a) T. Sorsa, P. Pollesello, P. Permi, T. Drakenberg, I. Kilpeläinen, *J. Mol. Cell. Cardiol.* **2003**, *3*, 1055–1061; b) I.M. Robertson, O. K. Baryshnikova, M. X. Li, B.D. Sykes, *Biochemistry*, **2008**, *47*, 7485–7495.

[183] a) H. Haikala, I. B. Linden, *J. Cardiovasc. Pharmacol*. **1995**, *26*, 10–19; b) P. Pollesello, M. Ovaska, J. Kaivola, et al. *J. Biol. Chem*. **1994**, *269*, 28584–28590; c) Q. Kleerekoper, J. A. Putkey, *J. Biol. Chem*. **1999**, *274*, 23932–23939.

[184] S. Szilágyi, P. Pollesello, J. Levijoki, P. Kaheinen, H. Haikala, I. Édes, et al, *Eur. J. Pharmacol*. **2004**, *486*, 67–74.

[185] a) D. Farmakis, J. Alvarez, T. B. Gal, D. Brito, F. Fedele, C. Fonseca, et al. *Int. J. Cardiol.* **2016**, *222*, 303–312; b) E. Grossini, C. Molinari, P.P. Caimmi, F. Uberti, G. Vacca, *Br. J. Pharmacol*. **2009**, *156*, 250–261.

[186] a) R. J. Solaro, P. Bousquet, J. D. Johnson, *J. Pharmacol. Exp. Ther*. **1986**, *238*, 502–507; b) file was downloaded from Protein Data Bank, entry 1DTL, and generated with PyMOL; https://www.rcsb.org/structure/1DTL.

[187] Y. Li, M. L. Love, J. A. Putkey, C. Cohen, *Proc. Natl. Acad. Sci. U. S. A.* **2000**, *97*, 5140–5145.

[188] a) X. Wang, M. X. Li, B. D. Sykes, *J. Biol. Chem.***2002**, *277*, 31124–31133;

[189] For more details about chimera and its preparation, see the paper indicated in reference 1 of chapter 4.

[190] E. J. Hennessy, S. L. Buchwald, *J. Am. Chem. Soc.* **2003**, *125*, 12084–12085.

[191] K. E. Andersen, J. L. Sørensen, J. Lau, B. F. Lundt, H. Petersen, P. O. Huusfeldt, P. D. Suzdak, M. D. Swedberg, *J. Med. Chem.* **2001,** *44,* 2152–2163.

[192] S. Andrews, S. J. Burgess, D. Skaalrud, J. X. Kelly, D. H. Peyton, *J. Med. Chem.* **2010**, *53*, 916–919.

[193] T. Jeffery, *Tet. Lett*. **1985**, *26*, 2667–2670.

[194] J. P. Wolfe, R. A. Rennels, S. L. Buchwald, *Tetrahedron,* **1996***, 52*, 7525–7546.

[195] D. Bebbington, N. J. T. Monck, S. Gaur, A. M. Palmer, K. Benwell, V. Harvey, C. S. Malcolm, R. H. P. Porter, *J. Med. Chem*. **2000**, *43*, 2779–2782.

[196] R. Suzuki, A. Mikami, H. Tanaka, H. Fukushima, Patent: EP 2172453 A1, **2010.**

[197] J. P. Wolfe, S. L. Buchwald, *J. Org. Chem.* **2000**, *65*, 1144–1157.

[198] D. Zhu, R. Wang, J. Mao, L. Xu, F. Wu, B. Wan, B. *Journal of Molecular Catalysis A: Chemical,* **2006,** *256***,** 256–260.

[199] H. Tuerdi, H. J. Chao, J. X. Qiao, T. C. Wang, T. Gungor, Patent: US 2005/261244 A1,**2005.**

[200] W. Shan, A. V. Gavai, J. A. Balog, Patent: WO 2014/047390 A1, **2014.**

Appendix I: Selected NMR Spectra
(Chapter 2)

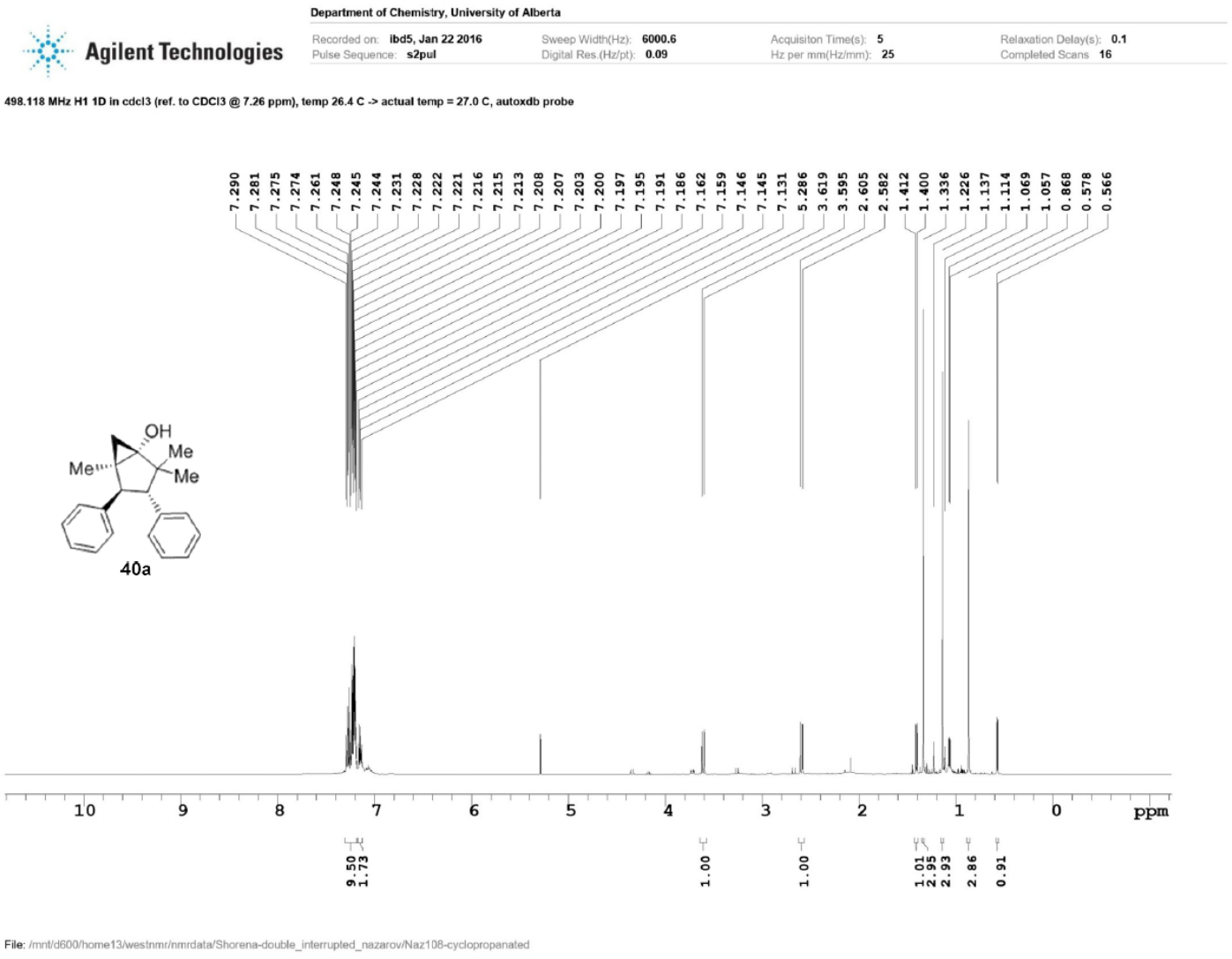
Department of Chemistry, University of Alberta
Agilent Technologies
Recorded on: ibd5, Jan 22 2016
Pulse Sequence: s2pul
Sweep Width(Hz): 6000.6
Digital Res.(Hz/pt): 0.09
Acquisiton Time(s): 5
Hz per mm(Hz/mm): 25
Relaxation Delay(s): 0.1
Completed Scans 16
498.118 MHz H1 1D in cdcl3 (ref. to CDCl3 @ 7.26 ppm), temp 26.4 C -> actual temp = 27.0 C, autoxdb probe
7.290 7.281 7.275 7.274 7.261 7.248 7.245 7.244 7.231 7.228 7.222 7.221 7.216 7.215 7.213 7.208 7.207 7.203 7.200 7.197 7.195 7.191 7.186 7.162 7.159 7.146 7.145 7.131 5.286 3.619 3.595 2.605 2.582 1.412 1.400 1.336 1.226 1.137 1.114 1.069 1.057 0.868 0.578 0.566
OH
Me
Me
Me
40a
10 9 8 7 6 5 4 3 2 1 0 ppm
9.50 1.73 1.00 1.00 1.01 2.95 2.93 2.86 0.91
File: /mnt/d600/home13/westnmr/nmrdata/Shorena-double_interrupted_nazarov/Naz108-cyclopropanated

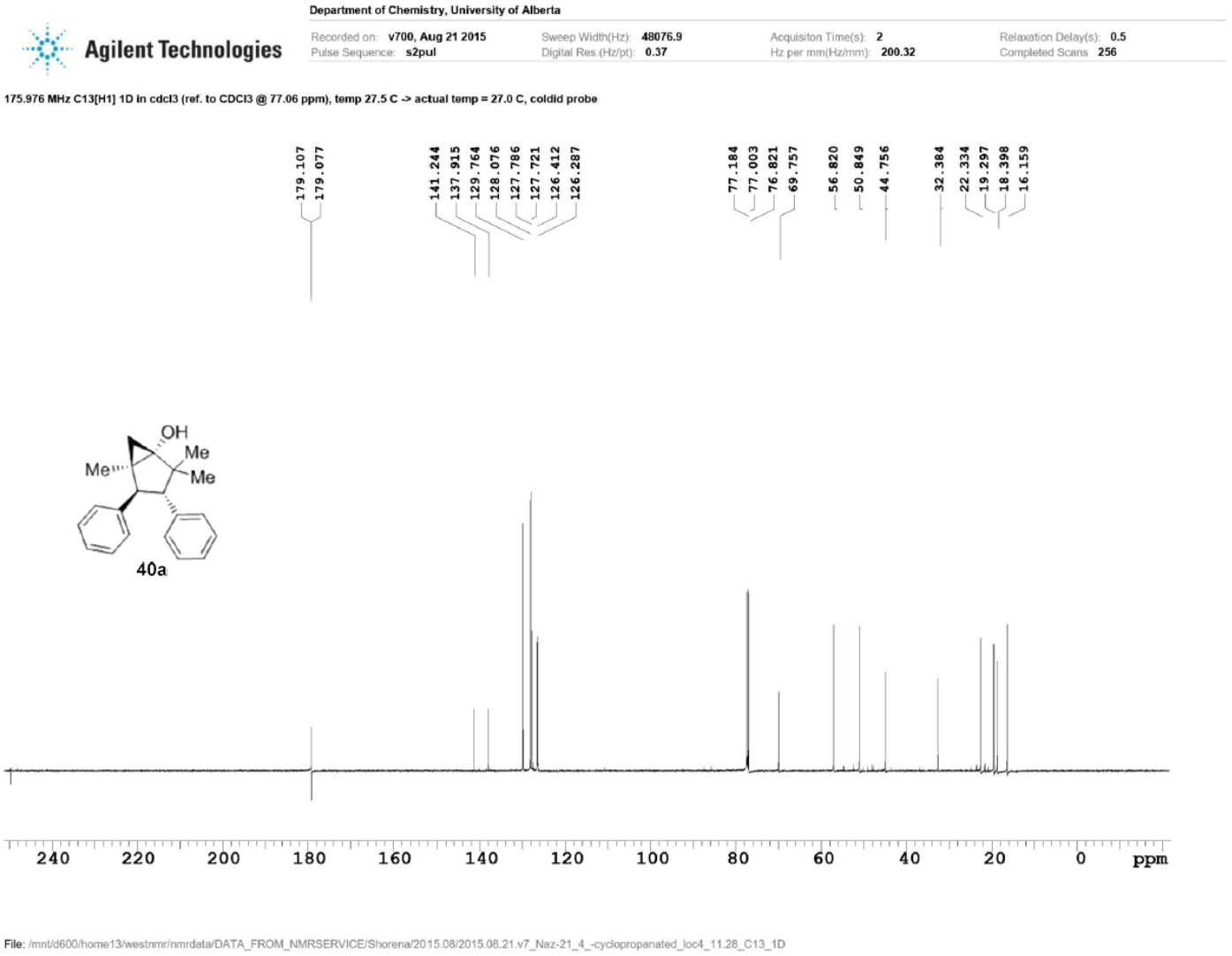
Department of Chemistry, University of Alberta
Agilent Technologies
Recorded on: v700, Aug 21 2015
Pulse Sequence: s2pul
Sweep Width(Hz): 48076.9
Digital Res.(Hz/pt): 0.37
Acquisiton Time(s): 2
Hz per mm(Hz/mm): 200.32
Relaxation Delay(s): 0.5
Completed Scans 256
175.976 MHz C13[H1] 1D in cdcl3 (ref. to CDCl3 @ 77.06 ppm), temp 27.5 C -> actual temp = 27.0 C, coldid probe
179.107
179.077
141.244
137.915
129.764
128.076
127.786
127.721
126.412
126.287
77.184
77.003
76.821
69.757
56.820
50.849
44.756
32.384
22.334
19.297
18.398
16.159
OH
Me
Me
Me
40a
240
220
200
180
160
140
120
100
80
60
40
20
0
ppm
File: /mnt/d600/home13/westnmr/nmrdata/DATA_FROM_NMRSERVICE/Shorena/2015.08/2015.08.21.v7_Naz-21_4_-cyclopropanated_loc4_11.28_C13_1D

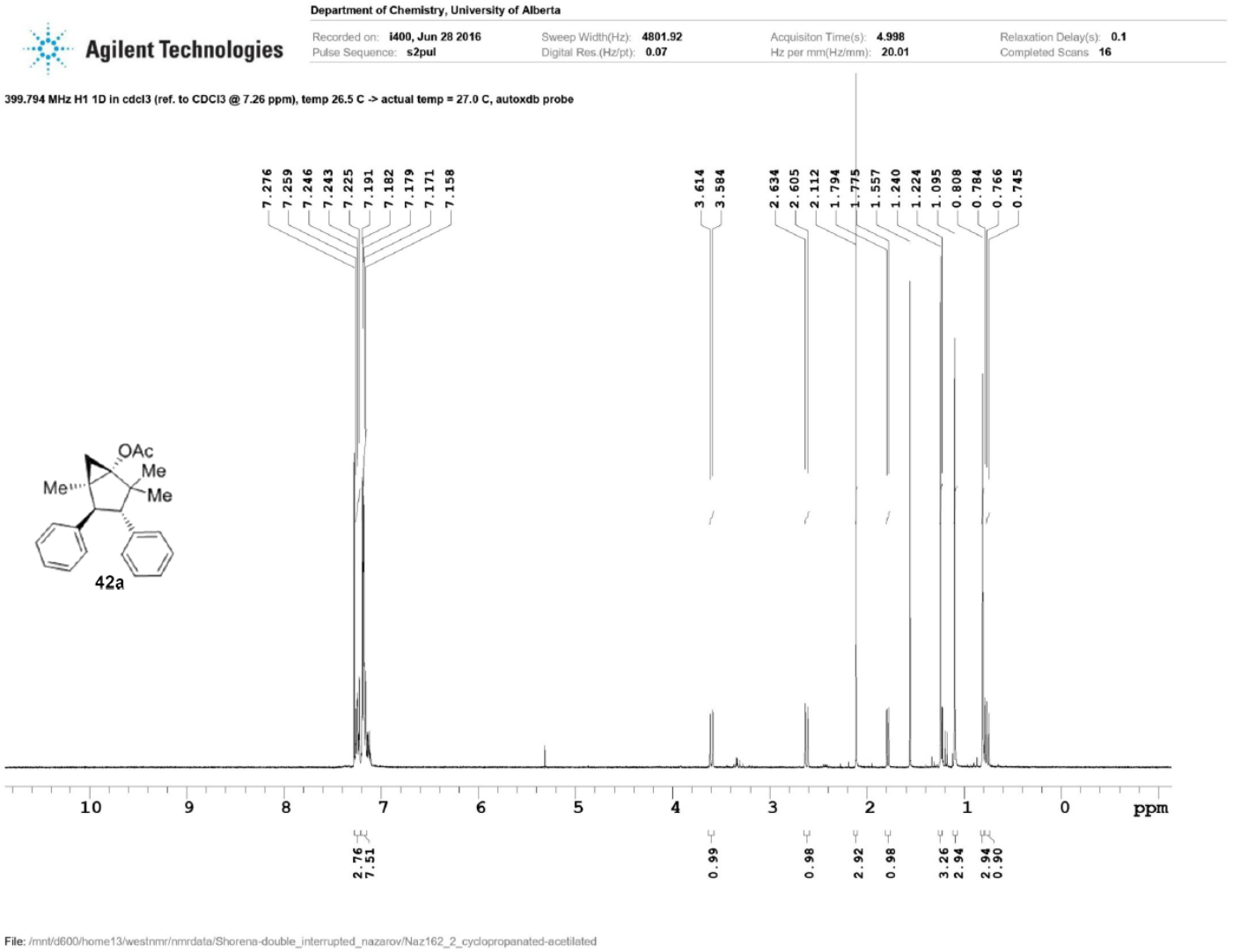
Department of Chemistry, University of Alberta
Agilent Technologies
Recorded on: i400, Jun 28 2016
Pulse Sequence: s2pul
Sweep Width(Hz): 4801.92
Digital Res.(Hz/pt): 0.07
Acquisiton Time(s): 4.998
Hz per mm(Hz/mm): 20.01
Relaxation Delay(s): 0.1
Completed Scans 16
399.794 MHz H1 1D in cdcl3 (ref. to CDCl3 @ 7.26 ppm), temp 26.5 C -> actual temp = 27.0 C, autoxdb probe
7.276
7.259
7.246
7.243
7.225
7.191
7.182
7.179
7.171
7.158
3.614
3.584
2.634
2.605
2.112
1.794
1.775
1.557
1.240
1.224
1.095
0.808
0.784
0.766
0.745
OAc
Me
Me
Me
42a
10
9
8
7
6
5
4
3
2
1
0
ppm
2.76
7.51
0.99
0.98
2.92
0.98
3.26
2.94
2.94
0.90
File: /mnt/d600/home13/westnmr/nmrdata/Shorena-double_interrupted_nazarov/Naz162_2_cyclopropanated-acetilated

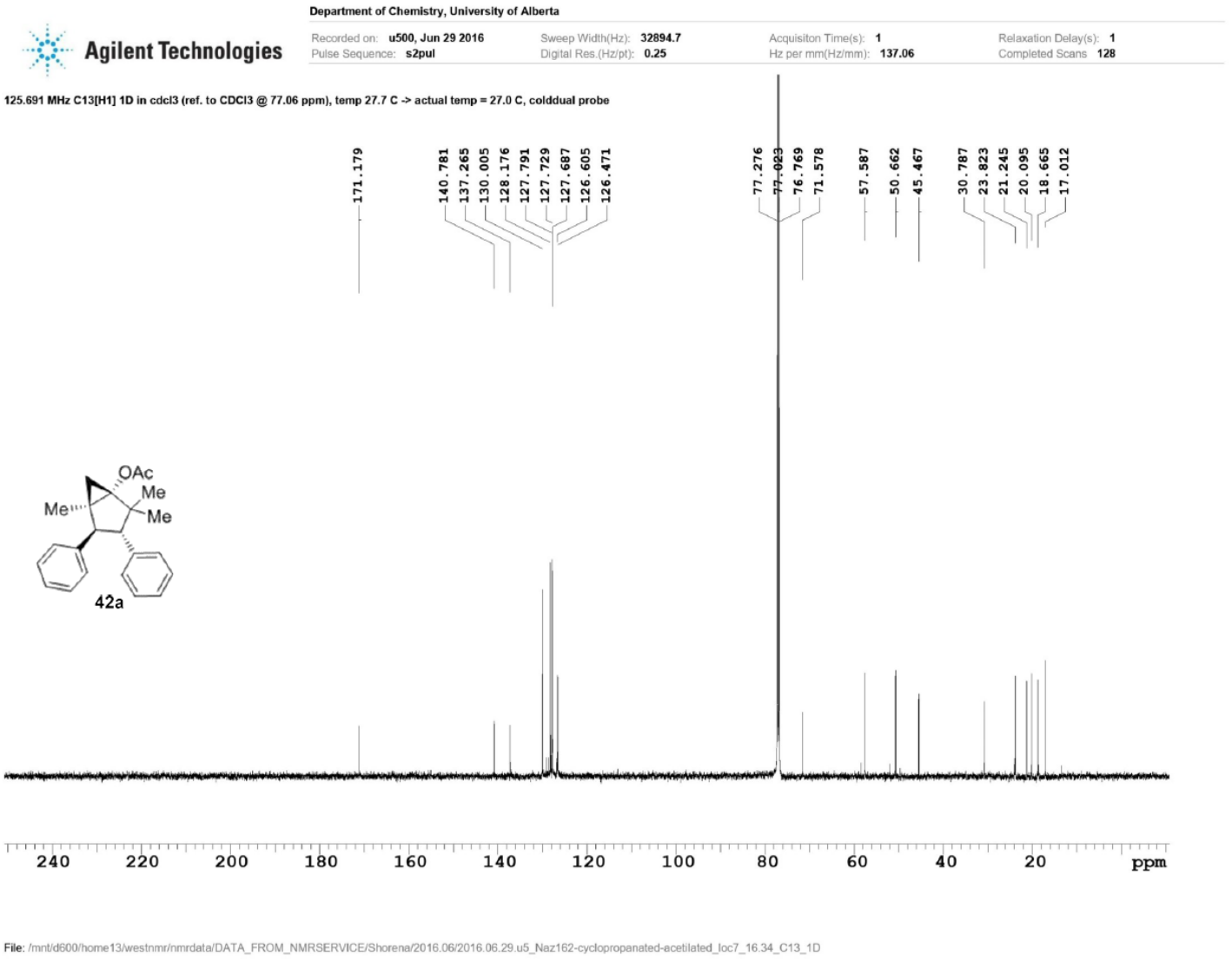
Department of Chemistry, University of Alberta
Agilent Technologies
Recorded on: u500, Jun 29 2016
Pulse Sequence: s2pul
Sweep Width(Hz): 32894.7
Digital Res.(Hz/pt): 0.25
Acquisiton Time(s): 1
Hz per mm(Hz/mm): 137.06
Relaxation Delay(s): 1
Completed Scans 128
125.691 MHz C13[H1] 1D in cdcl3 (ref. to CDCl3 @ 77.06 ppm), temp 27.7 C -> actual temp = 27.0 C, colddual probe
171.179
140.781
137.265
130.005
128.176
127.791
127.729
127.687
126.605
126.471
77.276
77.023
76.769
71.578
57.587
50.662
45.467
30.787
23.823
21.245
20.095
18.665
17.012
OAc
Me
Me
Me
42a
240
220
200
180
160
140
120
100
80
60
40
20
ppm
File: /mnt/d600/home13/westnmr/nmrdata/DATA_FROM_NMRSERVICE/Shorena/2016.06/2016.06.29.u5_Naz162-cyclopropanated-acetilated_loc7_16.34_C13_1D

Department of Chemistry, University of Alberta

Agilent Technologies

Recorded on: u500, Apr 12 2017	Sweep Width(Hz): 6009.62	Acquisiton Time(s): 5	Relaxation Delay(s): 0.1
Pulse Sequence: PRESAT	Digital Res.(Hz/pt): 0.09	Hz per mm(Hz/mm): 25.04	Completed Scans 32

499.797 MHz H1 1D in cdcl3 (ref. to CDCl3 @ 7.26 ppm)
temp 27.7 C -> actual temp = 27.0 C, colddual probe

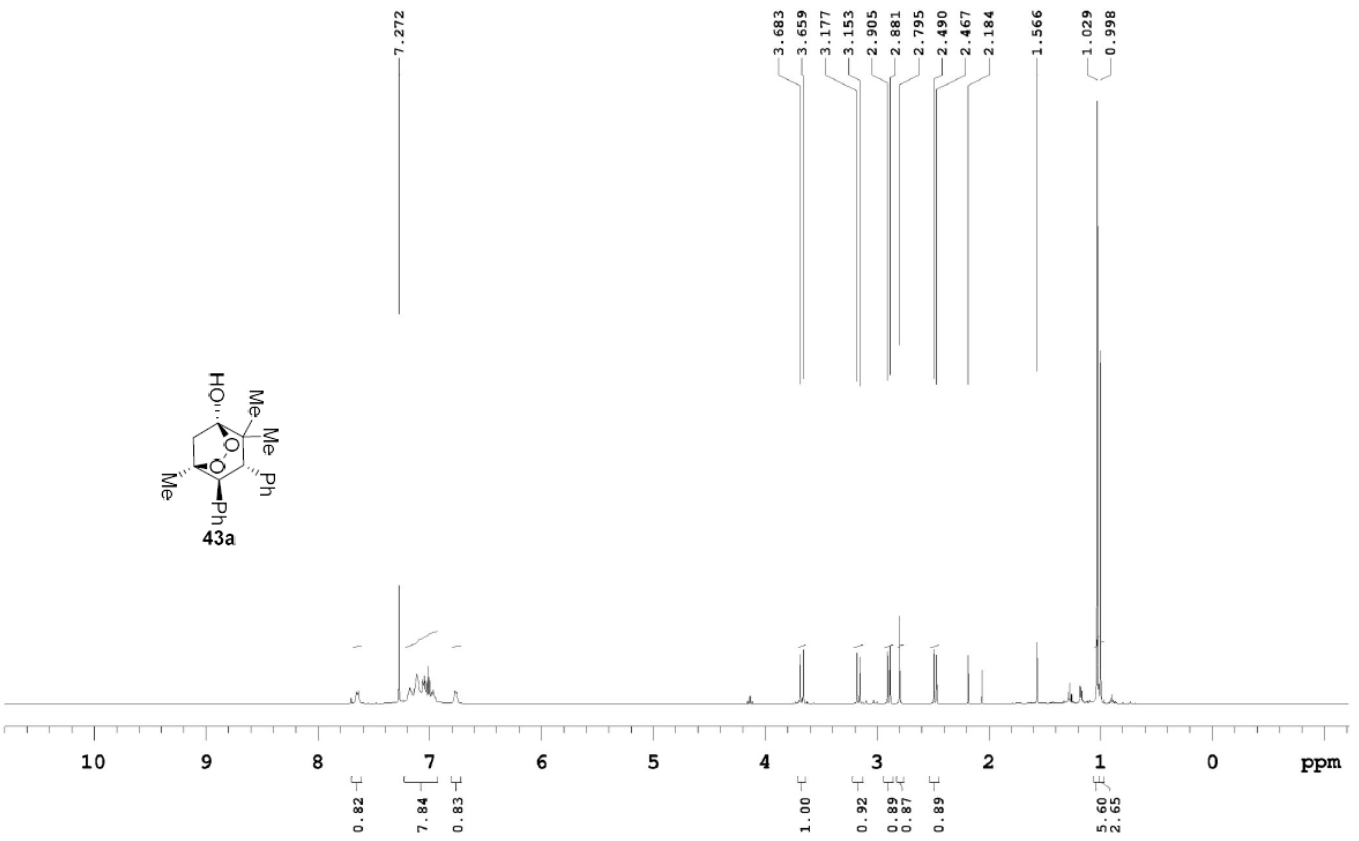

File: /mnt/d600/home13/westnmr/nmrdata/DATA_FROM_NMRSERVICE/Shorena/2017.04/2017.04.12.u5_Naz_46-1-bridged_peroxide-acceptable_spectrum_loc1_12.44_H1_1D

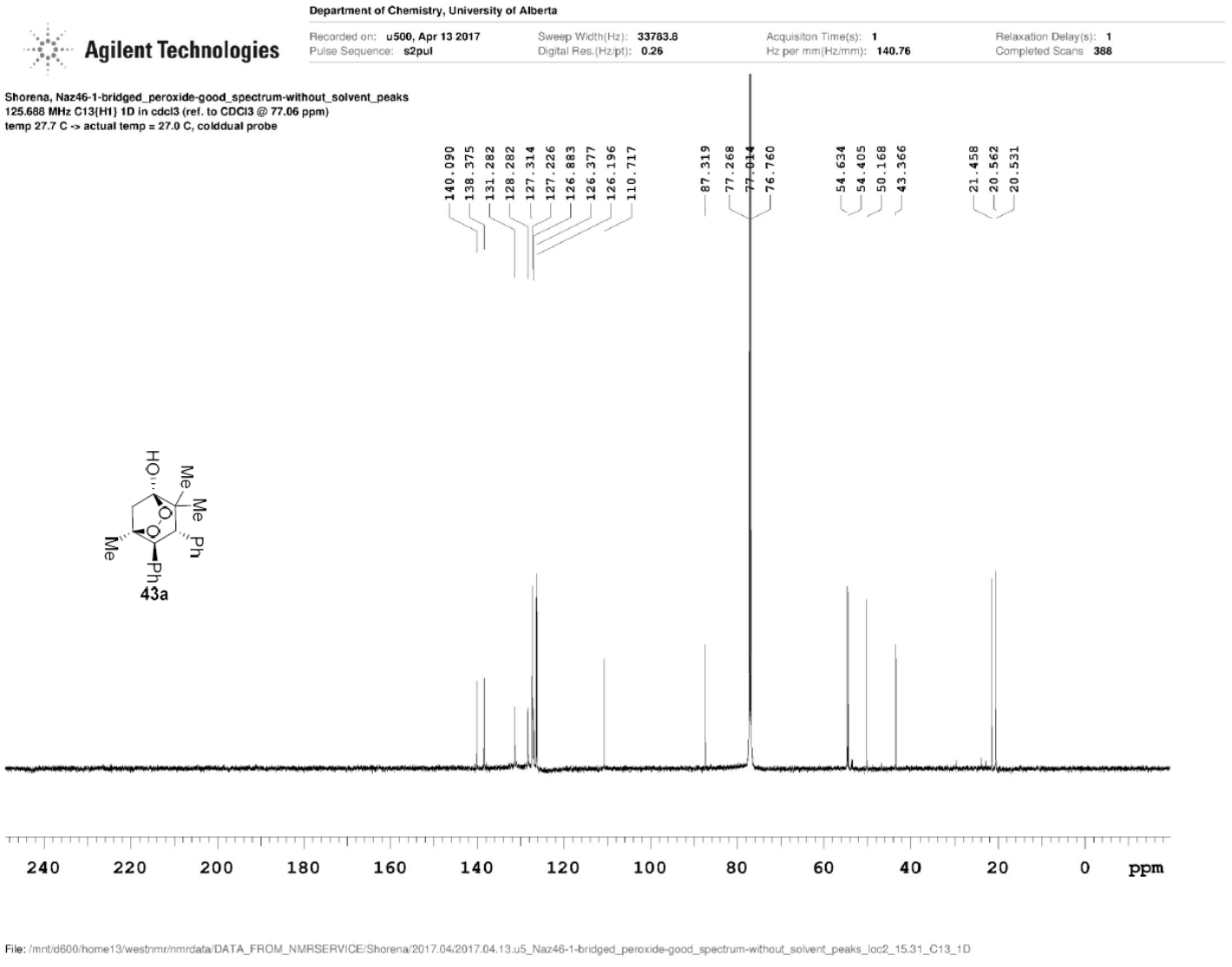
Department of Chemistry, University of Alberta
Agilent Technologies
Recorded on: u500, Apr 13 2017
Pulse Sequence: s2pul
Sweep Width(Hz): 33783.8
Digital Res.(Hz/pt): 0.26
Acquisiton Time(s): 1
Hz per mm(Hz/mm): 140.76
Relaxation Delay(s): 1
Completed Scans 388
Shorena, Naz46-1-bridged_peroxide-good_spectrum-without_solvent_peaks
125.688 MHz C13{H1} 1D in cdcl3 (ref. to CDCl3 @ 77.06 ppm)
temp 27.7 C -> actual temp = 27.0 C, colddual probe
140.090
138.375
131.282
128.282
127.314
127.226
126.883
126.377
126.196
110.717
87.319
77.268
77.014
76.760
54.634
54.405
50.168
43.366
21.458
20.562
20.531
HO
Me
Me
Ph
Me
Ph
43a
240
220
200
180
160
140
120
100
80
60
40
20
0
ppm
File: /mnt/d600/home13/westnmr/nmrdata/DATA_FROM_NMRSERVICE/Shorena/2017.04/2017.04.13.u5_Naz46-1-bridged_peroxide-good_spectrum-without_solvent_peaks_loc2_15.31_C13_1D

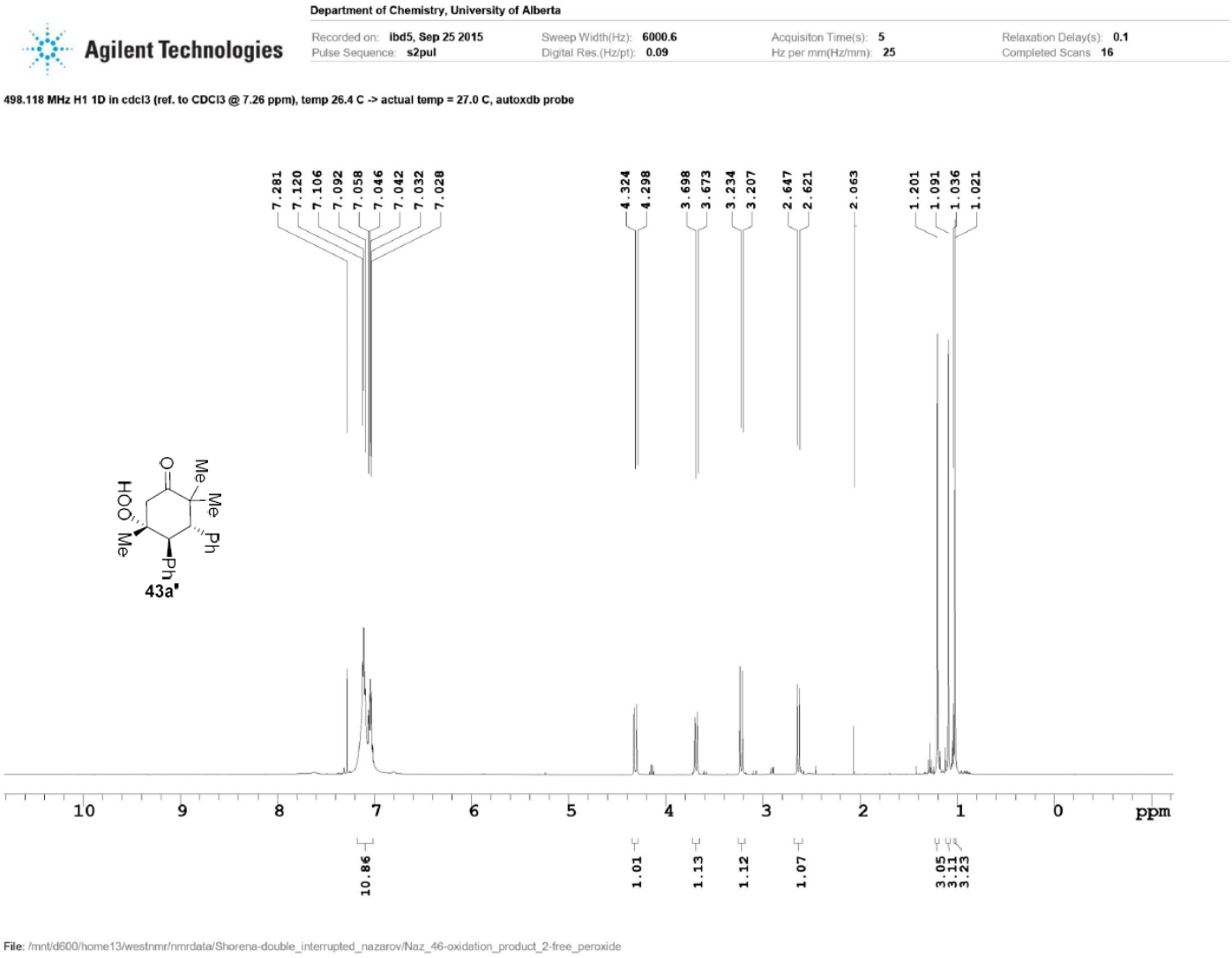
Department of Chemistry, University of Alberta
Agilent Technologies
Recorded on: ibd5, Sep 25 2015
Pulse Sequence: s2pul
Sweep Width(Hz): 6000.6
Digital Res.(Hz/pt): 0.09
Acquisiton Time(s): 5
Hz per mm(Hz/mm): 25
Relaxation Delay(s): 0.1
Completed Scans 16
498.118 MHz H1 1D in cdcl3 (ref. to CDCl3 @ 7.26 ppm), temp 26.4 C -> actual temp = 27.0 C, autoxdb probe
7.281
7.120
7.106
7.092
7.058
7.046
7.042
7.032
7.028
4.324
4.298
3.698
3.673
3.234
3.207
2.647
2.621
2.063
1.201
1.091
1.036
1.021
HOO
Me
O
Me
Me
Ph
Ph
43a'
10
9
8
7
6
5
4
3
2
1
0
ppm
10.86
1.01
1.13
1.12
1.07
3.05
3.11
3.23
File: /mnt/d600/home13/westnmr/nmrdata/Shorena-double_interrupted_nazarov/Naz_46-oxidation_product_2-free_peroxide

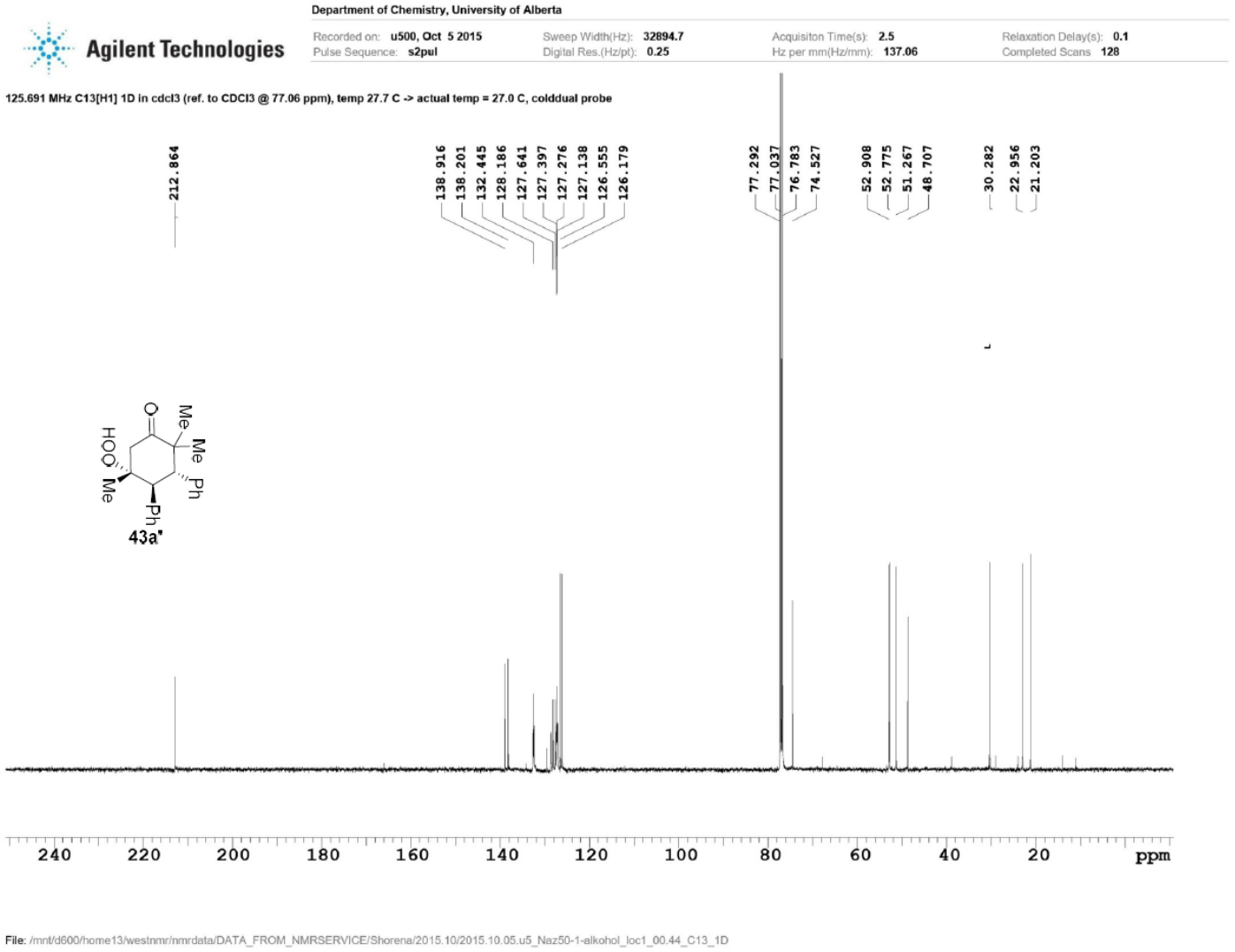
Department of Chemistry, University of Alberta
Agilent Technologies
Recorded on: u500, Oct 5 2015
Pulse Sequence: s2pul
Sweep Width(Hz): 32894.7
Digital Res.(Hz/pt): 0.25
Acquisiton Time(s): 2.5
Hz per mm(Hz/mm): 137.06
Relaxation Delay(s): 0.1
Completed Scans 128
125.691 MHz C13[H1] 1D in cdcl3 (ref. to CDCl3 @ 77.06 ppm), temp 27.7 C -> actual temp = 27.0 C, colddual probe
212.864
138.916
138.201
132.445
128.186
127.641
127.397
127.276
127.138
126.555
126.179
77.292
77.037
76.783
74.527
52.908
52.775
51.267
48.707
30.282
22.956
21.203
HOOC
Me
Me
Ph
Ph
43a'
240
220
200
180
160
140
120
100
80
60
40
20
ppm
File: /mnt/d600/home13/westnmr/nmrdata/DATA_FROM_NMRSERVICE/Shorena/2015.10/2015.10.05.u5_Naz50-1-alkohol_loc1_00.44_C13_1D

Department of Chemistry, University of Alberta

Agilent Technologies

Recorded on:	i400, Oct 1 2015	Sweep Width(Hz):	4801.92	Acquisiton Time(s):	4.998	Relaxation Delay(s):	0.1
Pulse Sequence:	s2pul	Digital Res.(Hz/pt):	0.07	Hz per mm(Hz/mm):	20.01	Completed Scans	16

399.794 MHz H1 1D in cdcl3 (ref. to CDCl3 @ 7.26 ppm), temp 26.5 C -> actual temp = 27.0 C, autoxdb probe

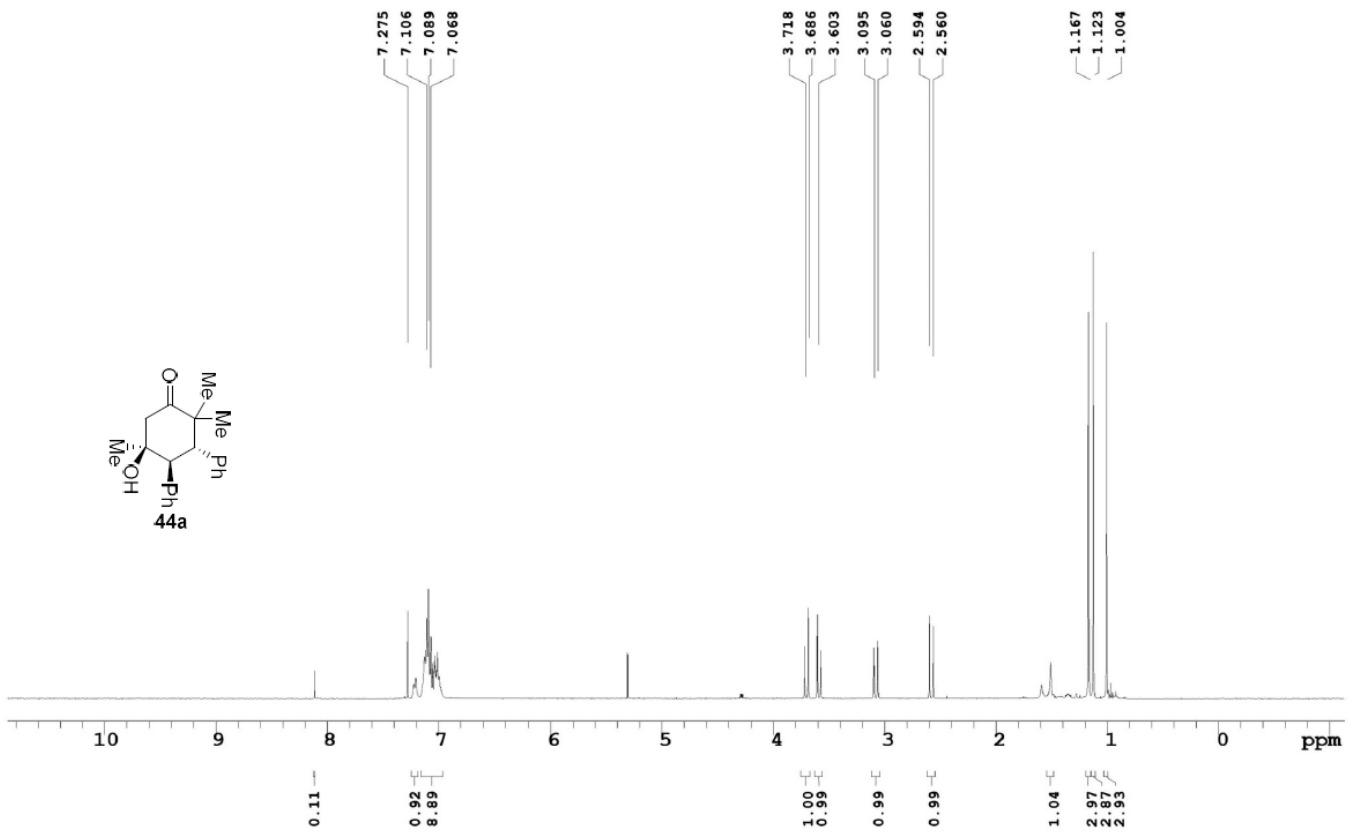

File: /mnt/d600/home13/westnmr/nmrdata/Shorena-double_interrupted_nazarov/Naz_50-1-alkohol

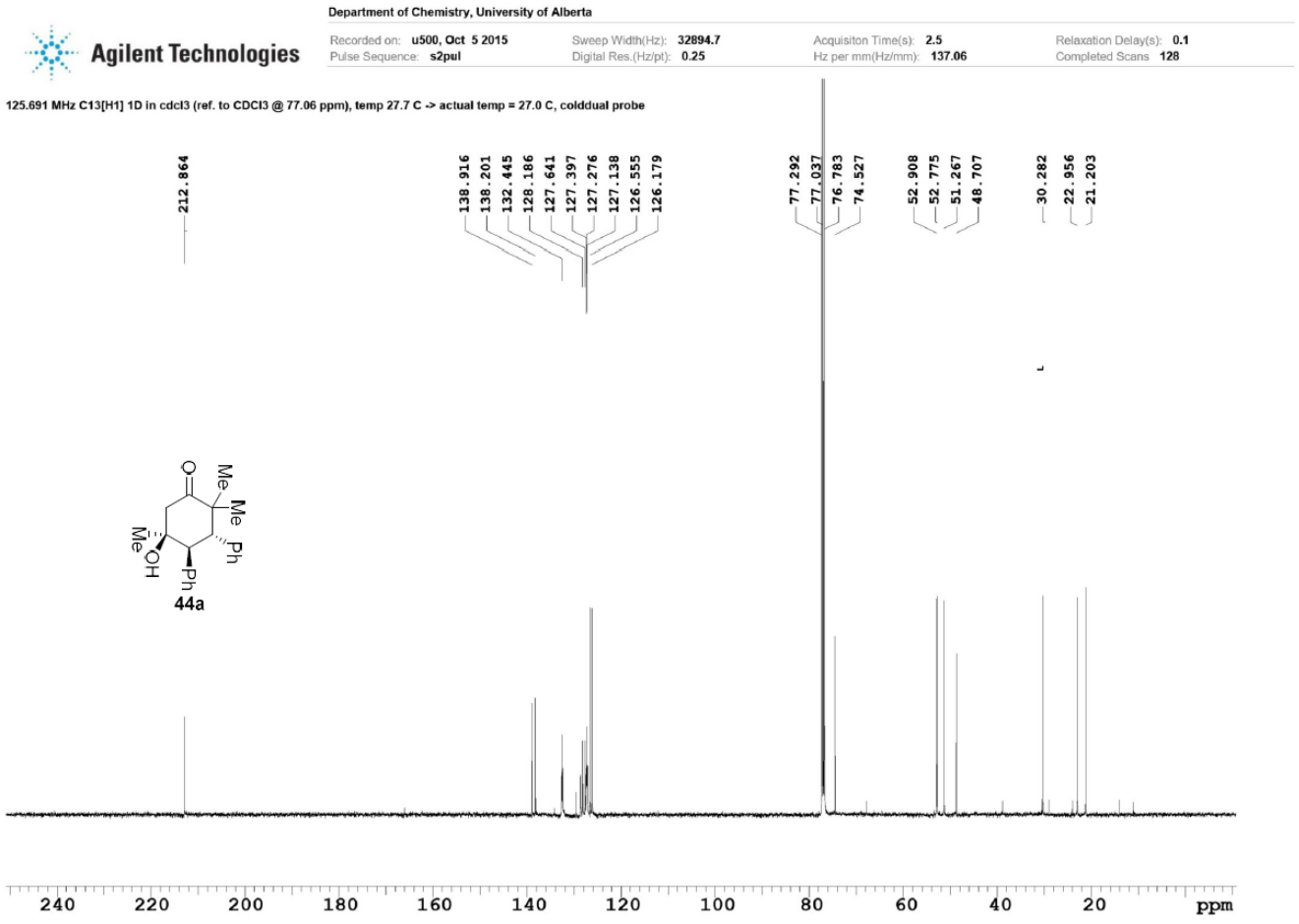
Agilent Technologies
Department of Chemistry, University of Alberta
Recorded on: u500, Oct 5 2015
Pulse Sequence: s2pul
Sweep Width(Hz): 32894.7
Digital Res.(Hz/pt): 0.25
Acquisiton Time(s): 2.5
Hz per mm(Hz/mm): 137.06
Relaxation Delay(s): 0.1
Completed Scans 128
125.691 MHz C13[H1] 1D in cdcl3 (ref. to CDCl3 @ 77.06 ppm), temp 27.7 C -> actual temp = 27.0 C, colddual probe
212.864
138.916
138.201
132.445
128.186
127.641
127.397
127.276
127.138
126.555
126.179
77.292
77.037
76.783
74.527
52.908
52.775
51.267
48.707
30.282
22.956
21.203
Me
Me
Ph
OH
Me
Ph
44a
240
220
200
180
160
140
120
100
80
60
40
20
ppm
File: /mnt/d600/home13/westnmr/nmrdata/DATA_FROM_NMRSERVICE/Shorena/2015.10/2015.10.05.u5_Naz50-1-alkohol_loc1_00.44_C13_1D

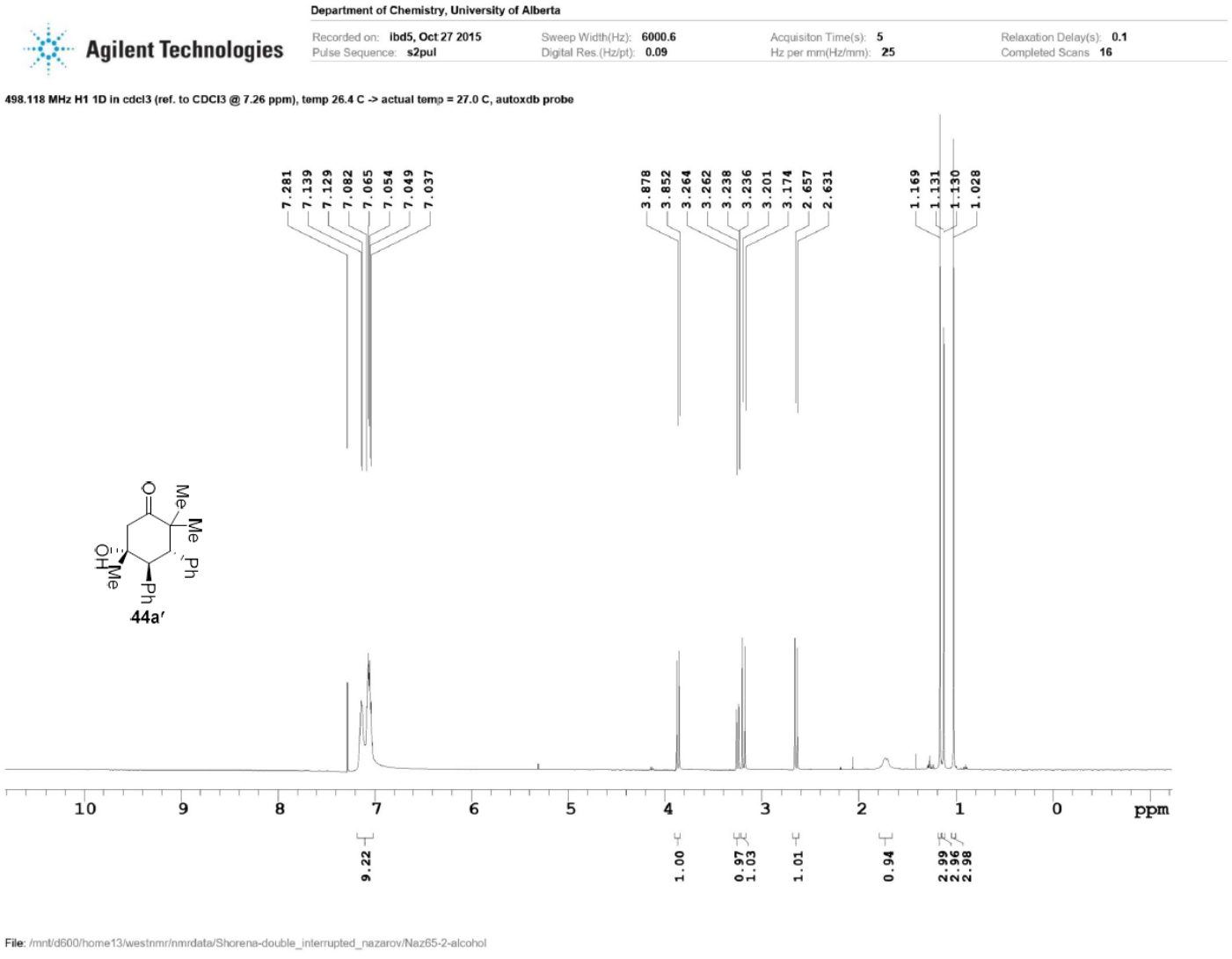
Department of Chemistry, University of Alberta
Agilent Technologies
Recorded on: ibd5, Oct 27 2015
Pulse Sequence: s2pul
Sweep Width(Hz): 6000.6
Digital Res.(Hz/pt): 0.09
Acquisiton Time(s): 5
Hz per mm(Hz/mm): 25
Relaxation Delay(s): 0.1
Completed Scans 16
498.118 MHz H1 1D in cdcl3 (ref. to CDCl3 @ 7.26 ppm), temp 26.4 C -> actual temp = 27.0 C, autoxdb probe
7.281
7.139
7.129
7.082
7.065
7.054
7.049
7.037
3.878
3.852
3.264
3.262
3.238
3.236
3.201
3.174
2.657
2.631
1.169
1.131
1.130
1.028
Me
Me
Ph
OH
Me
Ph
44a′
10
9
8
7
6
5
4
3
2
1
0
ppm
9.22
1.00
0.97
1.03
1.01
0.94
2.99
2.98
2.98
File: /mnt/d600/home13/westnmr/nmrdata/Shorena-double_interrupted_nazarov/Naz65-2-alcohol

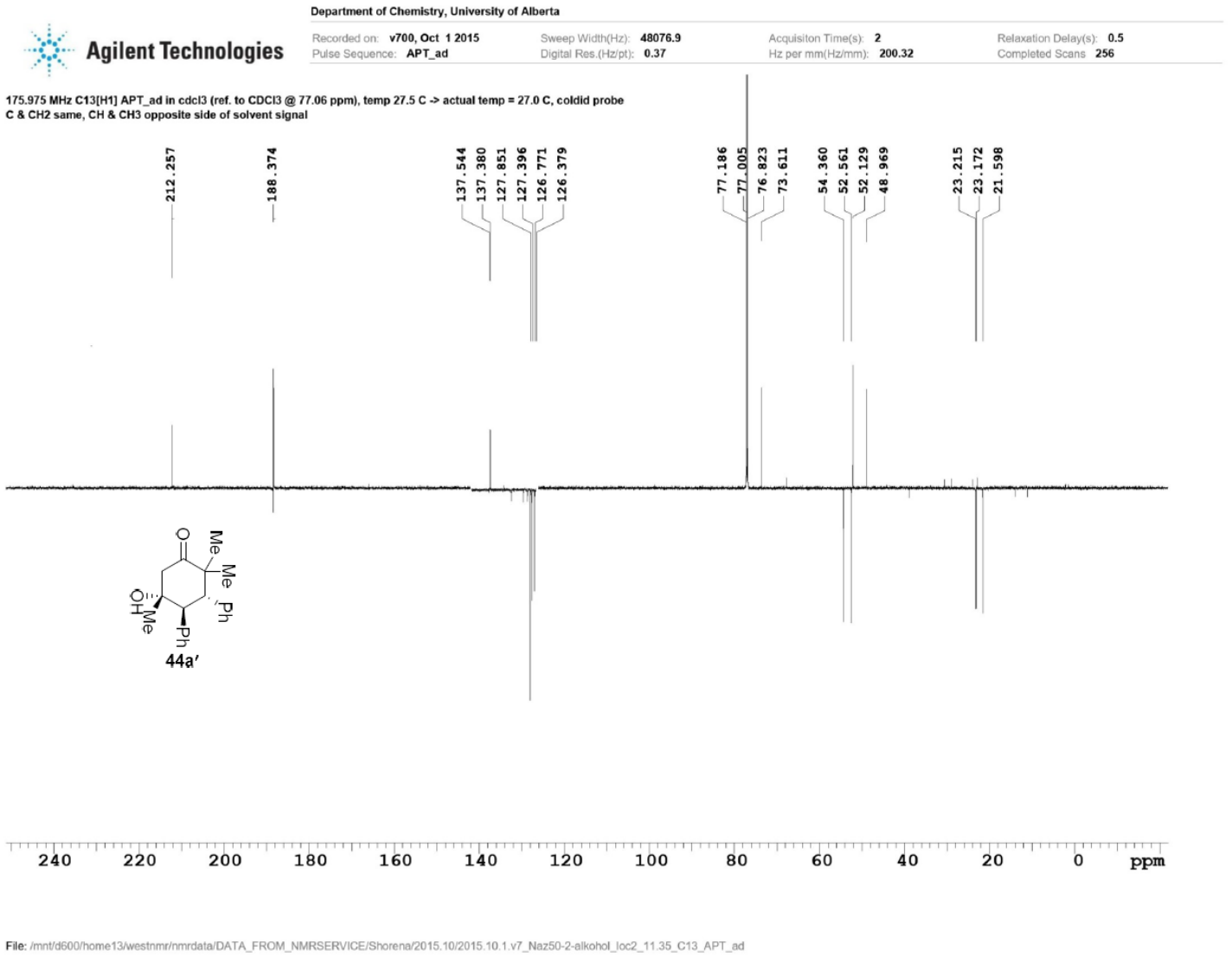
Department of Chemistry, University of Alberta
Agilent Technologies
Recorded on: v700, Oct 1 2015
Pulse Sequence: APT_ad
Sweep Width(Hz): 48076.9
Digital Res.(Hz/pt): 0.37
Acquisiton Time(s): 2
Hz per mm(Hz/mm): 200.32
Relaxation Delay(s): 0.5
Completed Scans 256
175.975 MHz C13[H1] APT_ad in cdcl3 (ref. to CDCl3 @ 77.06 ppm), temp 27.5 C -> actual temp = 27.0 C, coldid probe
C & CH2 same, CH & CH3 opposite side of solvent signal
212.257
188.374
137.544
137.380
127.851
127.396
126.771
126.379
77.186
77.005
76.823
73.611
54.360
52.561
52.129
48.969
23.215
23.172
21.598
O
Me
Me
Ph
OH
Me
Ph
44a′
240
220
200
180
160
140
120
100
80
60
40
20
0
ppm
File: /mnt/d600/home13/westnmr/nmrdata/DATA_FROM_NMRSERVICE/Shorena/2015.10/2015.10.1.v7_Naz50-2-alkohol_loc2_11.35_C13_APT_ad

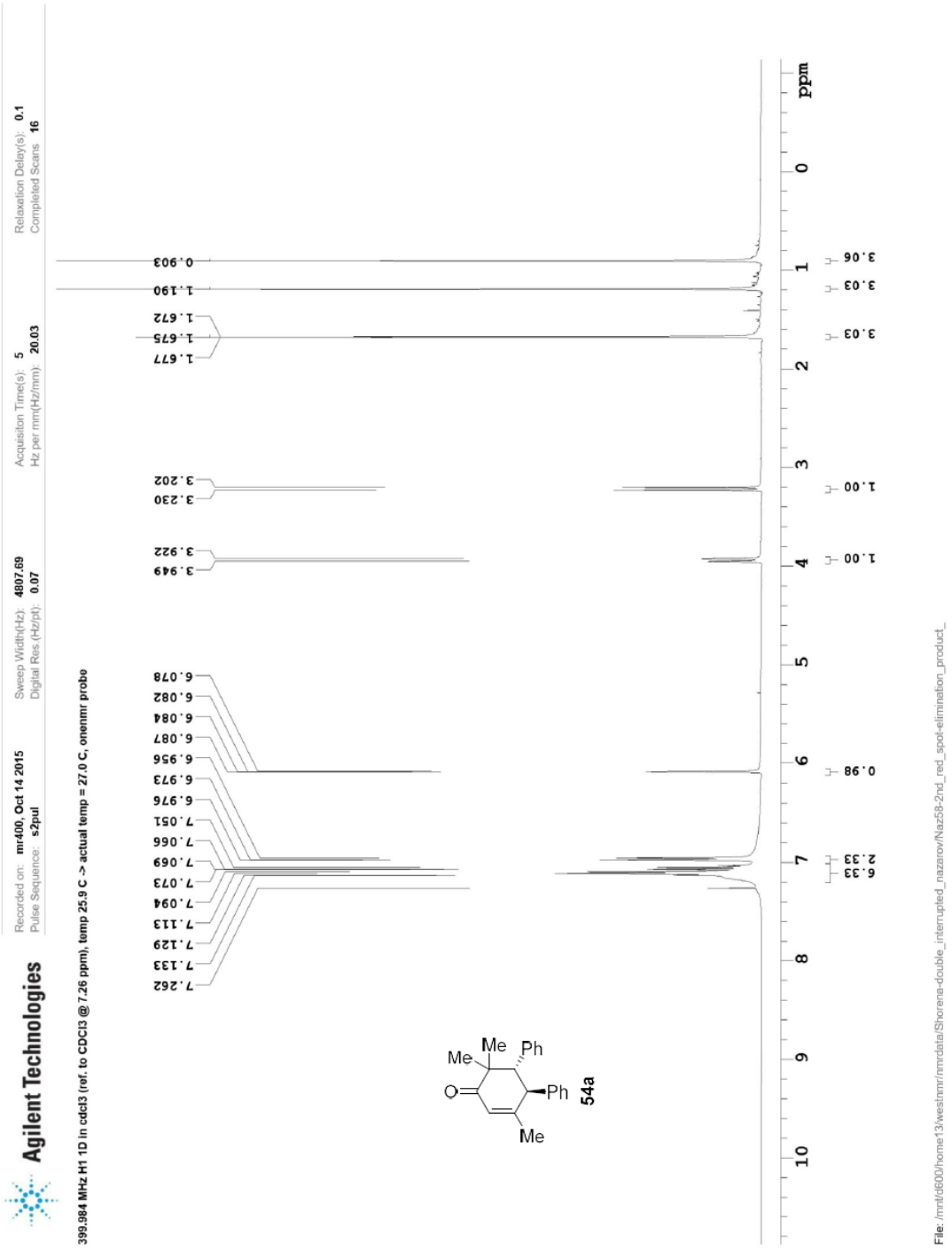
Department of Chemistry, University of Alberta
Agilent Technologies
Recorded on: mr400, Oct 14 2015
Pulse Sequence: s2pul
Sweep Width(Hz): 4807.69
Digital Res.(Hz/pt): 0.07
Acquisition Time(s): 5
Hz per mm(Hz/mm): 20.03
Relaxation Delay(s): 0.1
Completed Scans 16
399.984 MHz H1 1D in cdcl3 (ref. to CDCl3 @ 7.26 ppm), temp 25.9 C -> actual temp = 27.0 C, onenmr probe
7.262
7.133
7.129
7.113
7.094
7.073
7.069
7.066
7.051
6.976
6.973
6.956
6.087
6.084
6.082
6.078
3.949
3.922
3.230
3.202
1.677
1.675
1.672
1.190
0.903
6.33
2.33
0.98
1.00
1.00
3.03
3.03
3.06
ppm
Me
Me
Ph
Ph
O
Me
54a
File: /mnt/d600/home13/westnmr/nmrdata/Shorena-double_interrupted_nazarov/Naz58-2nd_red_spot-elimination_product_

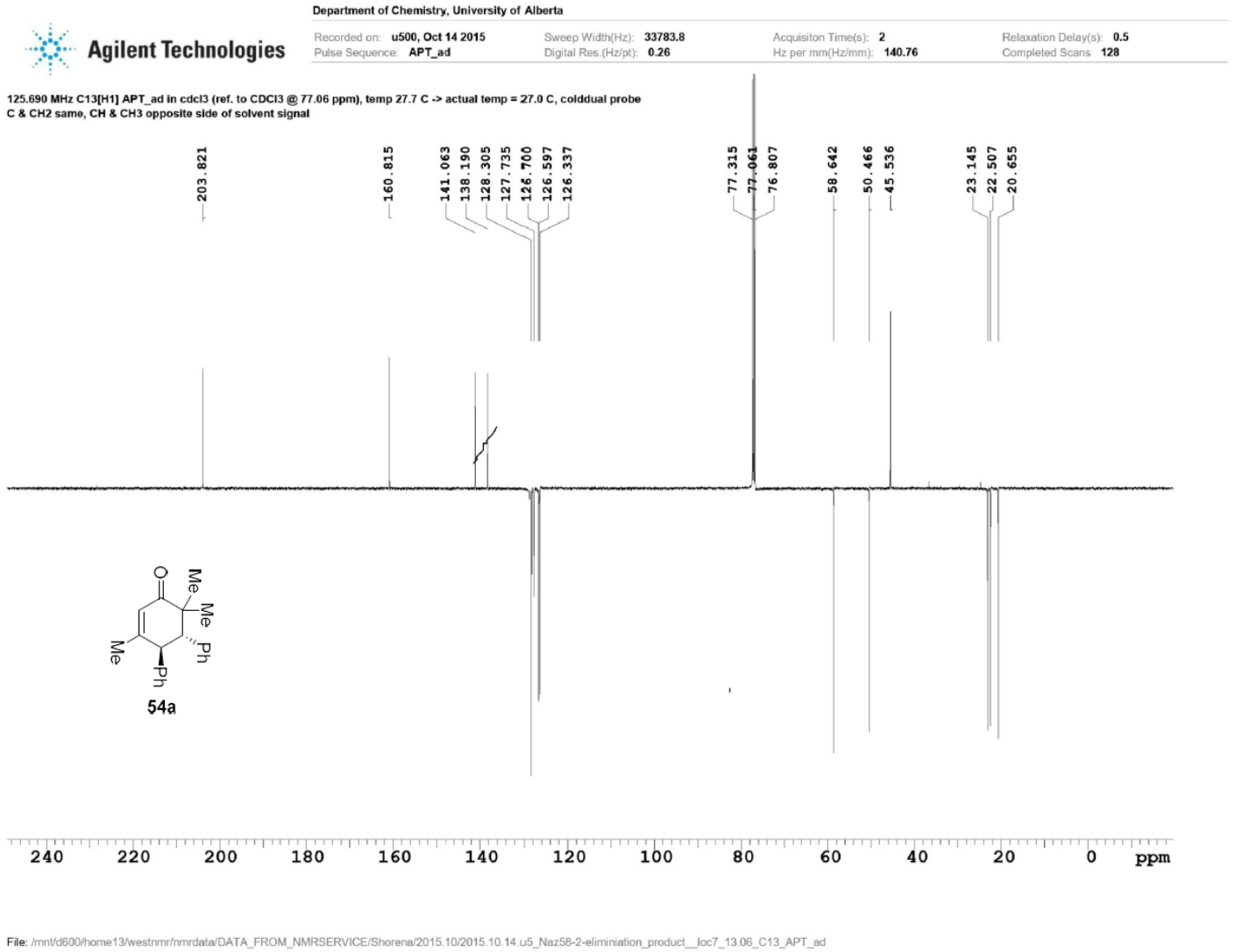
Department of Chemistry, University of Alberta
Agilent Technologies
Recorded on: u500, Oct 14 2015
Pulse Sequence: APT_ad
Sweep Width(Hz): 33783.8
Digital Res.(Hz/pt): 0.26
Acquisiton Time(s): 2
Hz per mm(Hz/mm): 140.76
Relaxation Delay(s): 0.5
Completed Scans 128
125.690 MHz C13[H1] APT_ad in cdcl3 (ref. to CDCl3 @ 77.06 ppm), temp 27.7 C -> actual temp = 27.0 C, colddual probe
C & CH2 same, CH & CH3 opposite side of solvent signal
203.821
160.815
141.063
138.190
128.305
127.735
126.700
126.597
126.337
77.315
77.061
76.807
58.642
50.466
45.536
23.145
22.507
20.655
O
Me
Me
Ph
Me
Ph
54a
240
220
200
180
160
140
120
100
80
60
40
20
0
ppm
File: /mnt/d600/home13/westnmr/nmrdata/DATA_FROM_NMRSERVICE/Shorena/2015.10/2015.10.14.u5_Naz58-2-eliminiation_product__loc7_13.06_C13_APT_ad

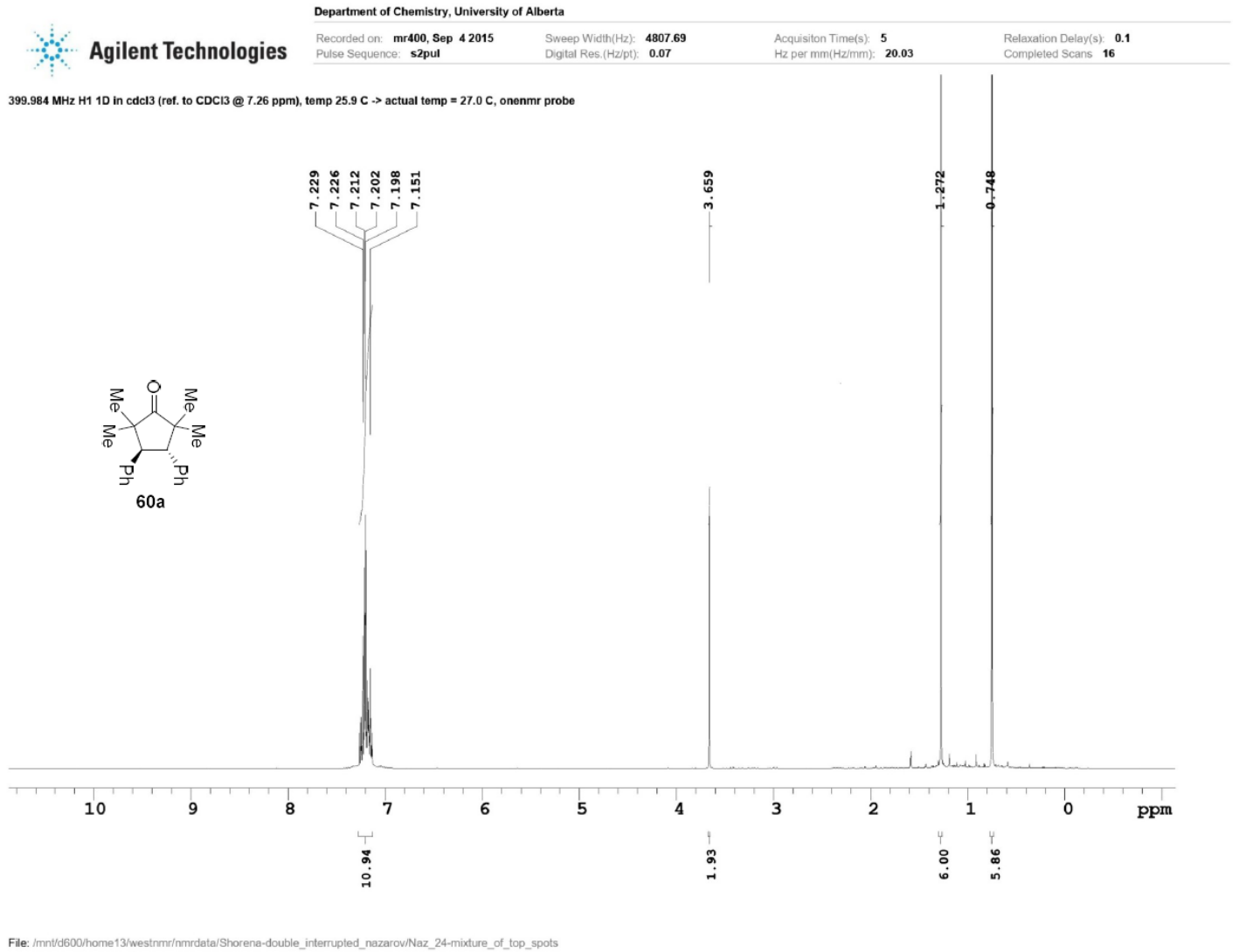
Department of Chemistry, University of Alberta
Agilent Technologies
Recorded on: mr400, Sep 4 2015
Pulse Sequence: s2pul
Sweep Width(Hz): 4807.69
Digital Res.(Hz/pt): 0.07
Acquisiton Time(s): 5
Hz per mm(Hz/mm): 20.03
Relaxation Delay(s): 0.1
Completed Scans 16
399.984 MHz H1 1D in cdcl3 (ref. to CDCl3 @ 7.26 ppm), temp 25.9 C -> actual temp = 27.0 C, onenmr probe
7.229
7.226
7.212
7.202
7.198
7.151
3.659
1.272
0.748
Me
Me
Me
Me
Ph
Ph
60a
10
9
8
7
6
5
4
3
2
1
0
ppm
10.94
1.93
6.00
5.86
File: /mnt/d600/home13/westnmr/nmrdata/Shorena-double_interrupted_nazarov/Naz_24-mixture_of_top_spots

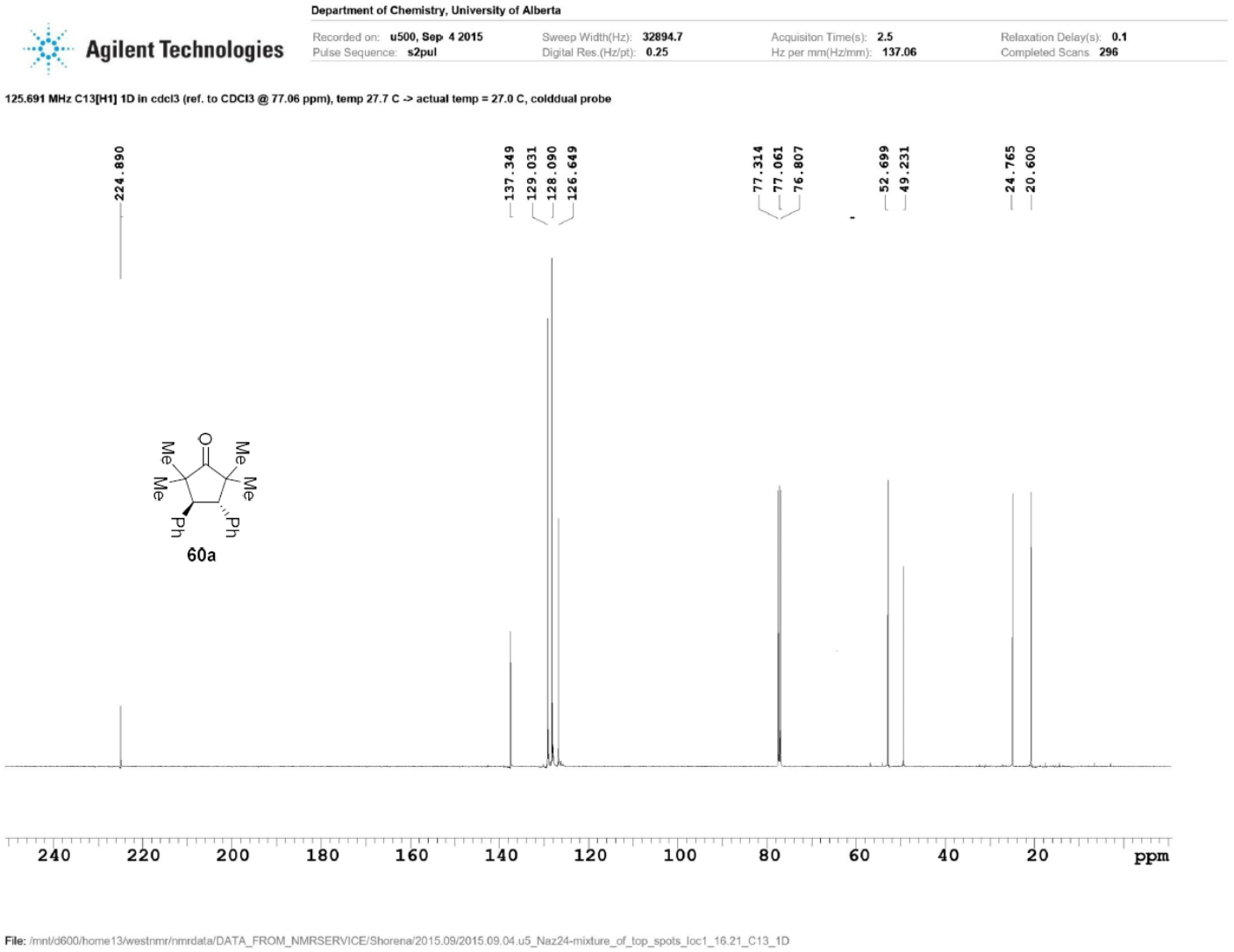
Department of Chemistry, University of Alberta
Agilent Technologies
Recorded on: u500, Sep 4 2015
Pulse Sequence: s2pul
Sweep Width(Hz): 32894.7
Digital Res.(Hz/pt): 0.25
Acquisiton Time(s): 2.5
Hz per mm(Hz/mm): 137.06
Relaxation Delay(s): 0.1
Completed Scans 296
125.691 MHz C13[H1] 1D in cdcl3 (ref. to CDCl3 @ 77.06 ppm), temp 27.7 C -> actual temp = 27.0 C, colddual probe
224.890
137.349
129.031
128.090
126.649
77.314
77.061
76.807
52.699
49.231
24.765
20.600
Me
Me
Me
Me
Ph
Ph
60a
240
220
200
180
160
140
120
100
80
60
40
20
ppm
File: /mnl/d600/home13/westnmr/nmrdata/DATA_FROM_NMRSERVICE/Shorena/2015.09/2015.09.04.u5_Naz24-mixture_of_top_spots_loc1_16.21_C13_1D

Appendix II: Selected NMR Spectra

(Chapter 3)

Department of Chemistry, University of Alberta

Agilent Technologies

Recorded on: **ibd5, May 9 2018**	Sweep Width(Hz): **6000.6**	Acquisiton Time(s): **5**	Relaxation Delay(s): **0.1**
Pulse Sequence: **s2pul**	Digital Res.(Hz/pt): **0.09**	Hz per mm(Hz/mm): **25**	Completed Scans **16**

498.118 MHz H1 1D in cdcl3 (ref. to CDCl3 @ 7.26 ppm)
temp 26.9 C -> actual temp = 27.0 C, autoxdb probe

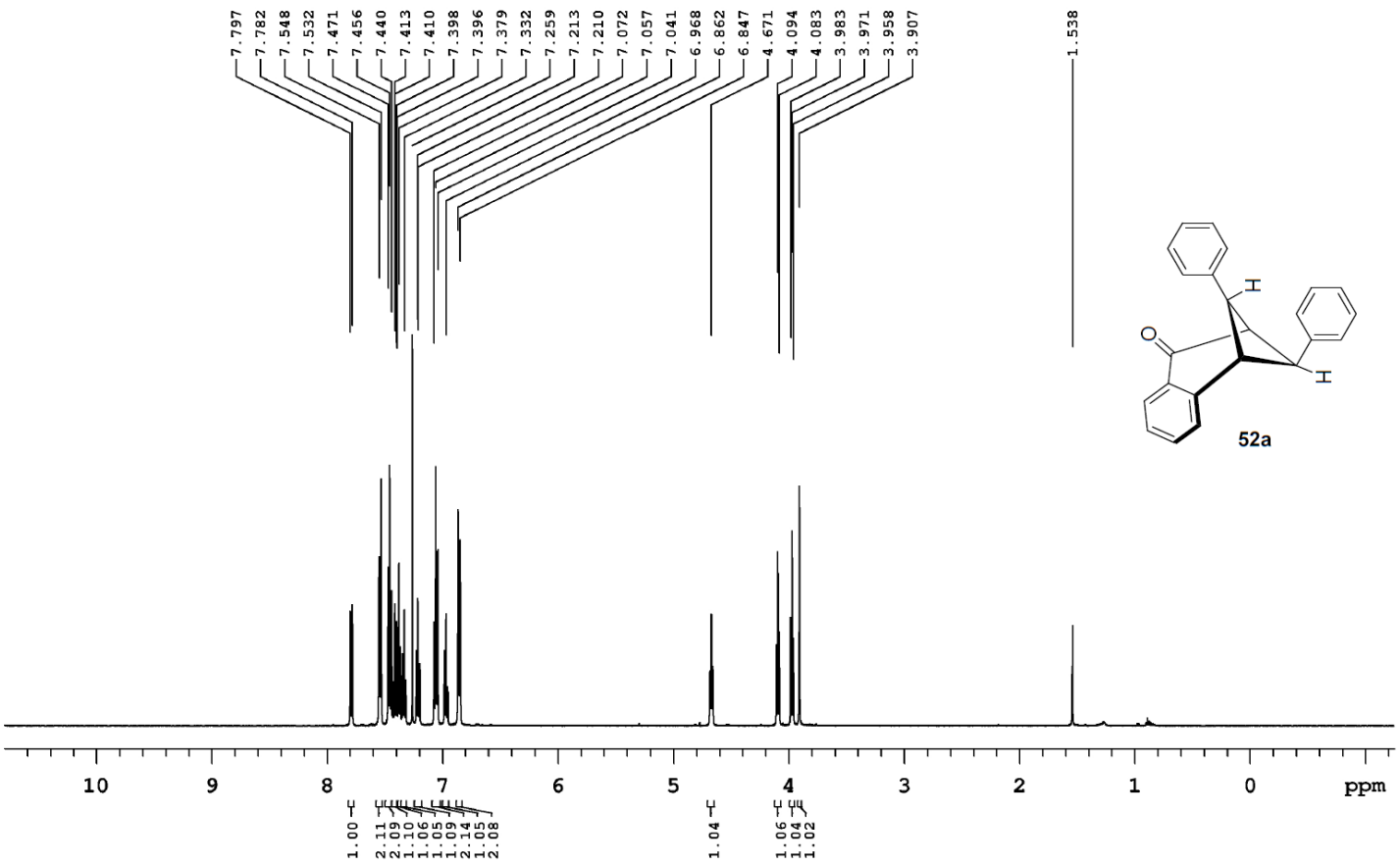

File: /mnt/d600/home13/westnmr/nmrdata/ShorenaFolders/2-2-products-et-al/2018.06.20.d6_Naz_3-156-1-BF3_on_model_substrate_nonsymmetrical_H1_1D

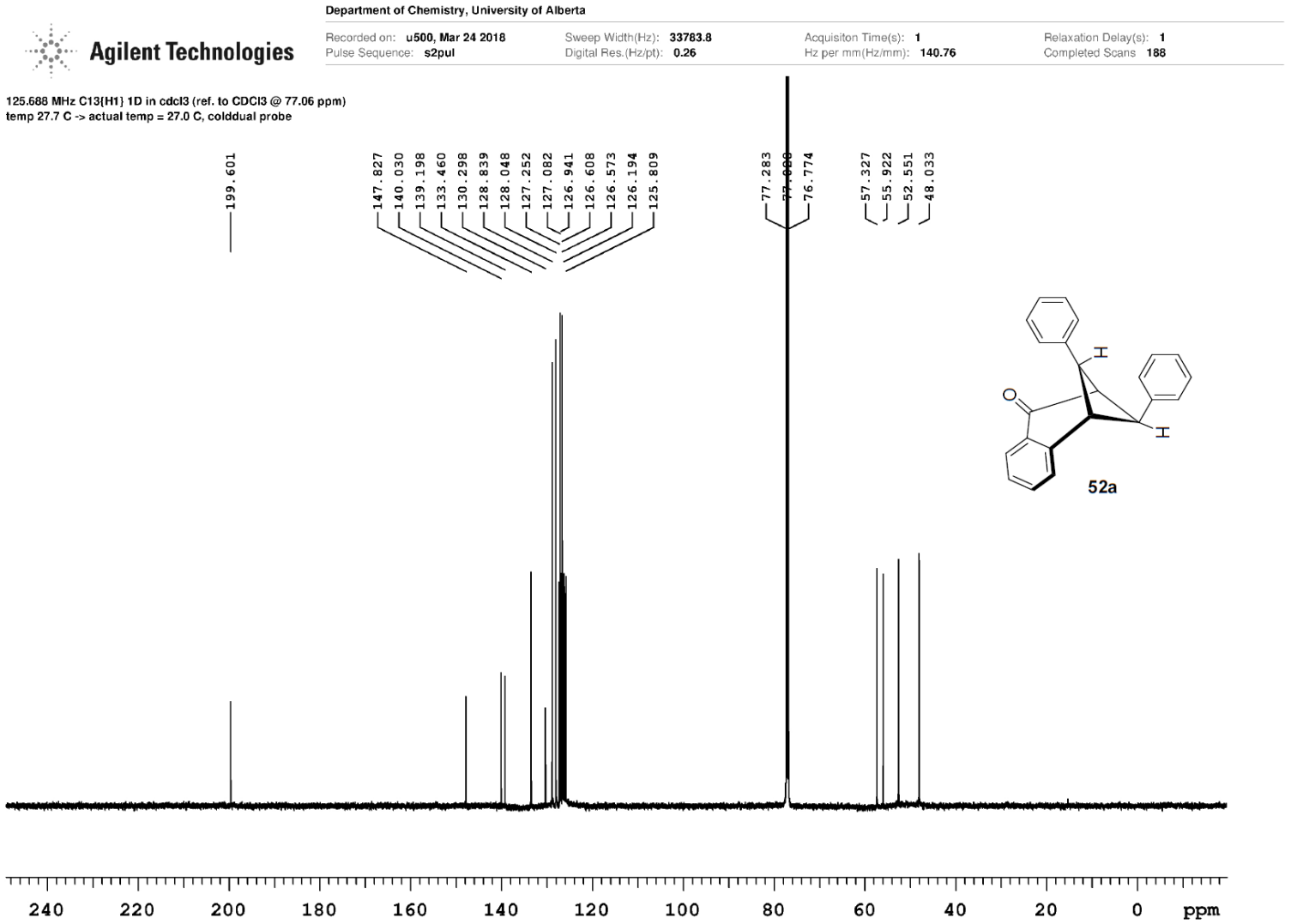

File: /mnt/d600/home13/westnmr/nmrdata/ShorenaFolders/2-2-products-et-al/2018.06.20.d6_Naz_3-156-1-BF3_on_model_substrate_nonsymmetrical_C13_1D

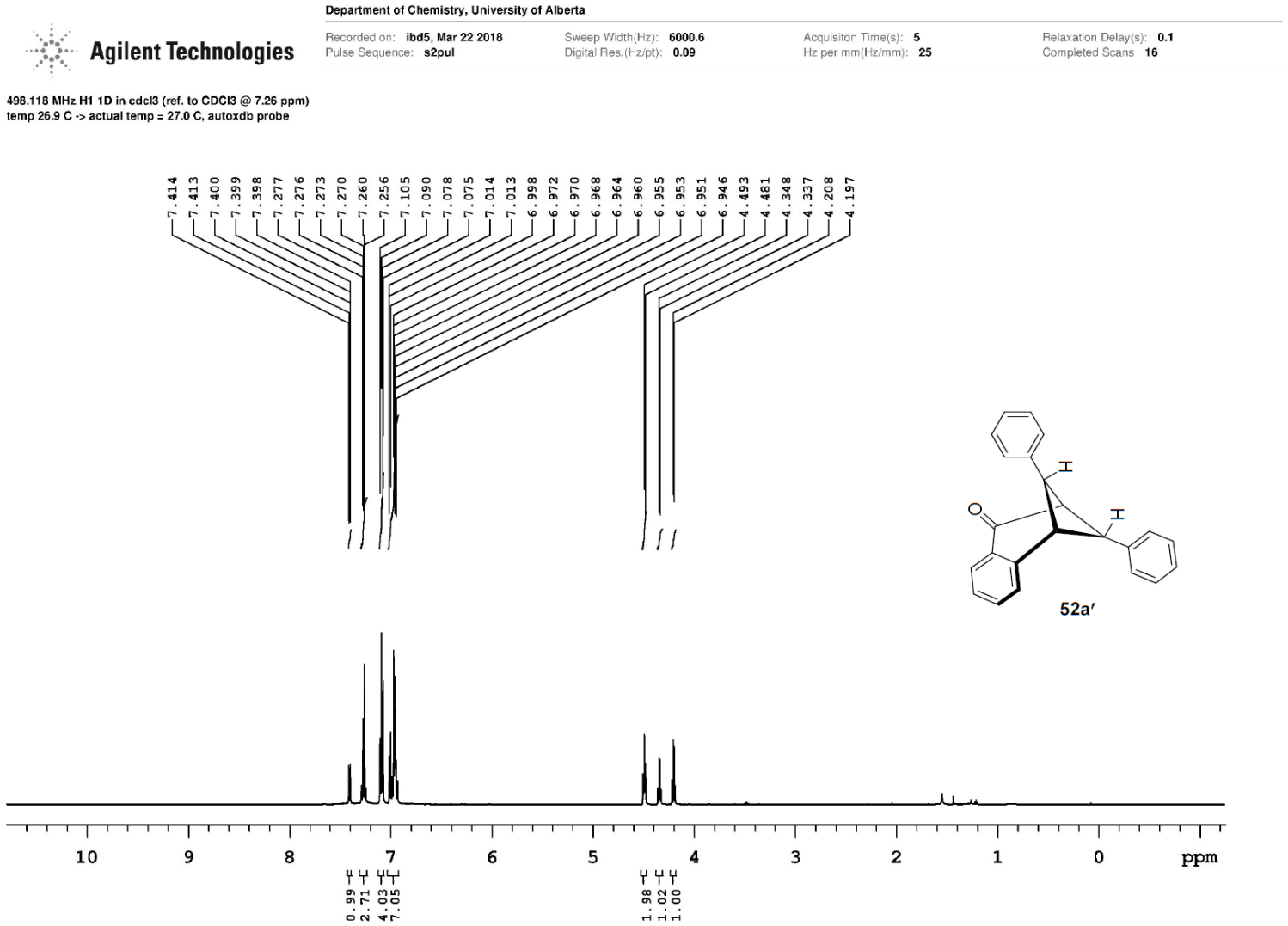

File: /mnt/d600/home13/westnmr/nmrdata/ShorenaFolders/2-2-products-et-al/2018.06.20.d6_Naz_3-156-prod_2-symmetrical-with_BF3_on_model_substr_H1_1D

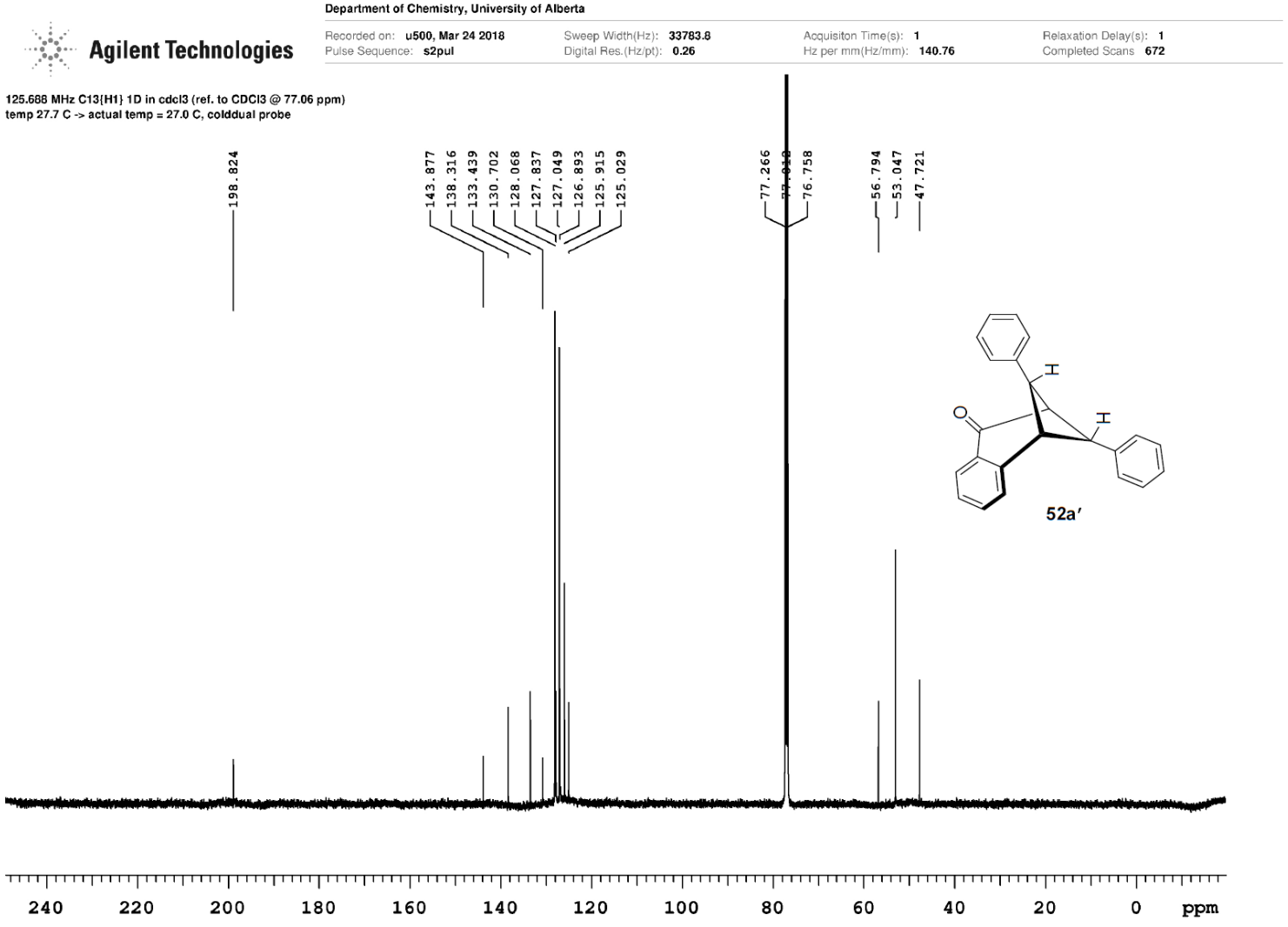

File: /mnt/d600/home13/westnmr/nmrdata/ShorenaFolders/2-2-products-et-al/2018.06.20.d6_Naz_3-156-prod_2-symmetrical-with_BF3_on_model_substr_C13_1D

Department of Chemistry, University of Alberta

Agilent Technologies

Recorded on: ibd5, Apr 25 2018	Sweep Width(Hz): 6000.6	Acquisiton Time(s): 5	Relaxation Delay(s): 0.1
Pulse Sequence: s2pul	Digital Res.(Hz/pt): 0.09	Hz per mm(Hz/mm): 25	Completed Scans 16

498.118 MHz H1 1D in cdcl3 (ref. to CDCl3 @ 7.26 ppm)
temp 26.9 C -> actual temp = 27.0 C, autoxdb probe

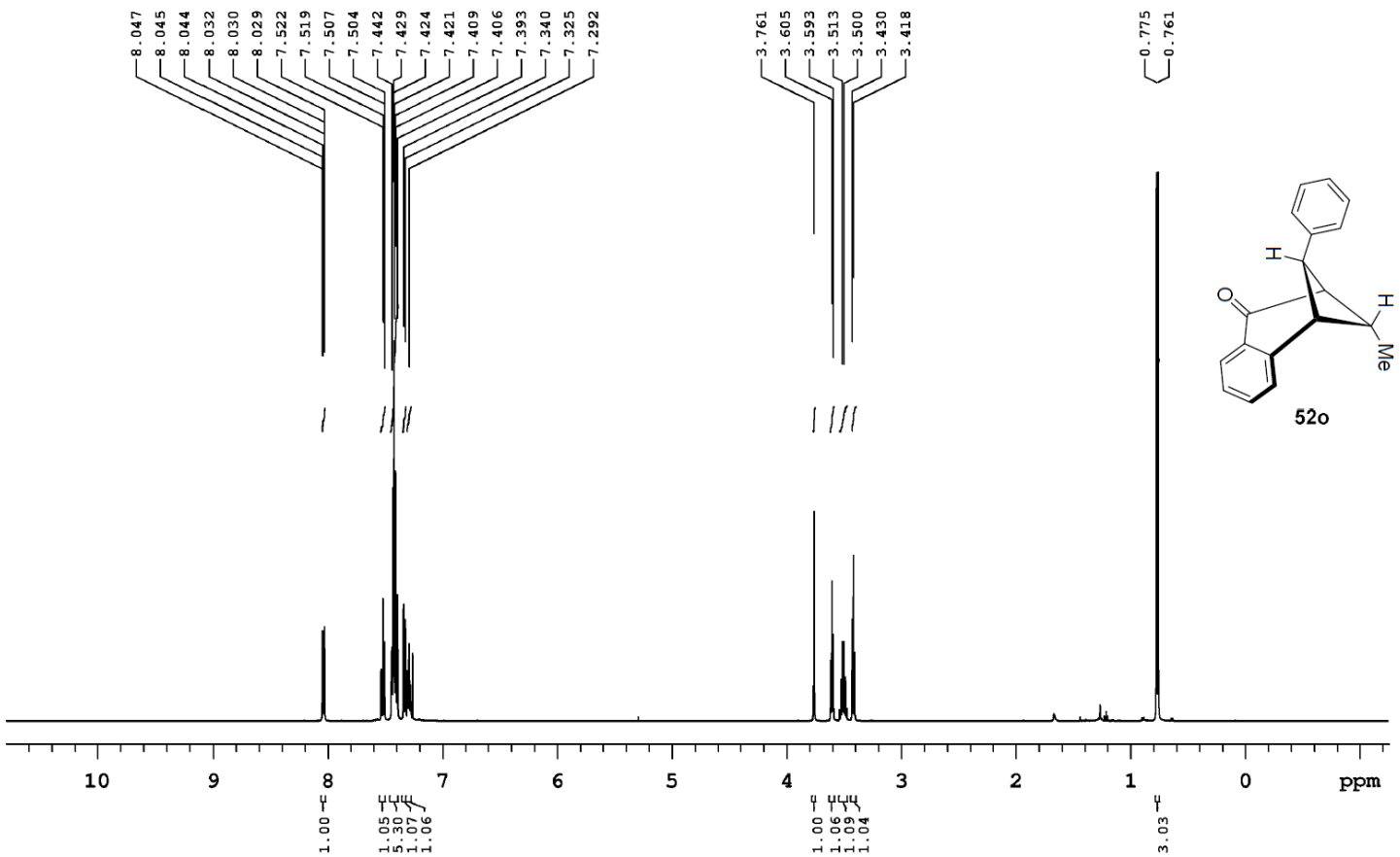

File: /mnt/d600/home13/westnmr/nmrdata/ShorenaFolders/2-2-products-et-al/2018.06.21.d3_Naz_4-18-1-BF3_on_Pn_Me-ed_H1_1D

Department of Chemistry, University of Alberta

Agilent Technologies

Recorded on: u500, Apr 25 2018	Sweep Width(Hz): 33783.8	Acquisiton Time(s): 1	Relaxation Delay(s): 1
Pulse Sequence: s2pul	Digital Res.(Hz/pt): 0.26	Hz per mm(Hz/mm): 140.76	Completed Scans 12

125.688 MHz C13{H1} 1D in cdcl3 (ref. to CDCl3 @ 77.06 ppm)
temp 27.7 C -> actual temp = 27.0 C, colddual probe

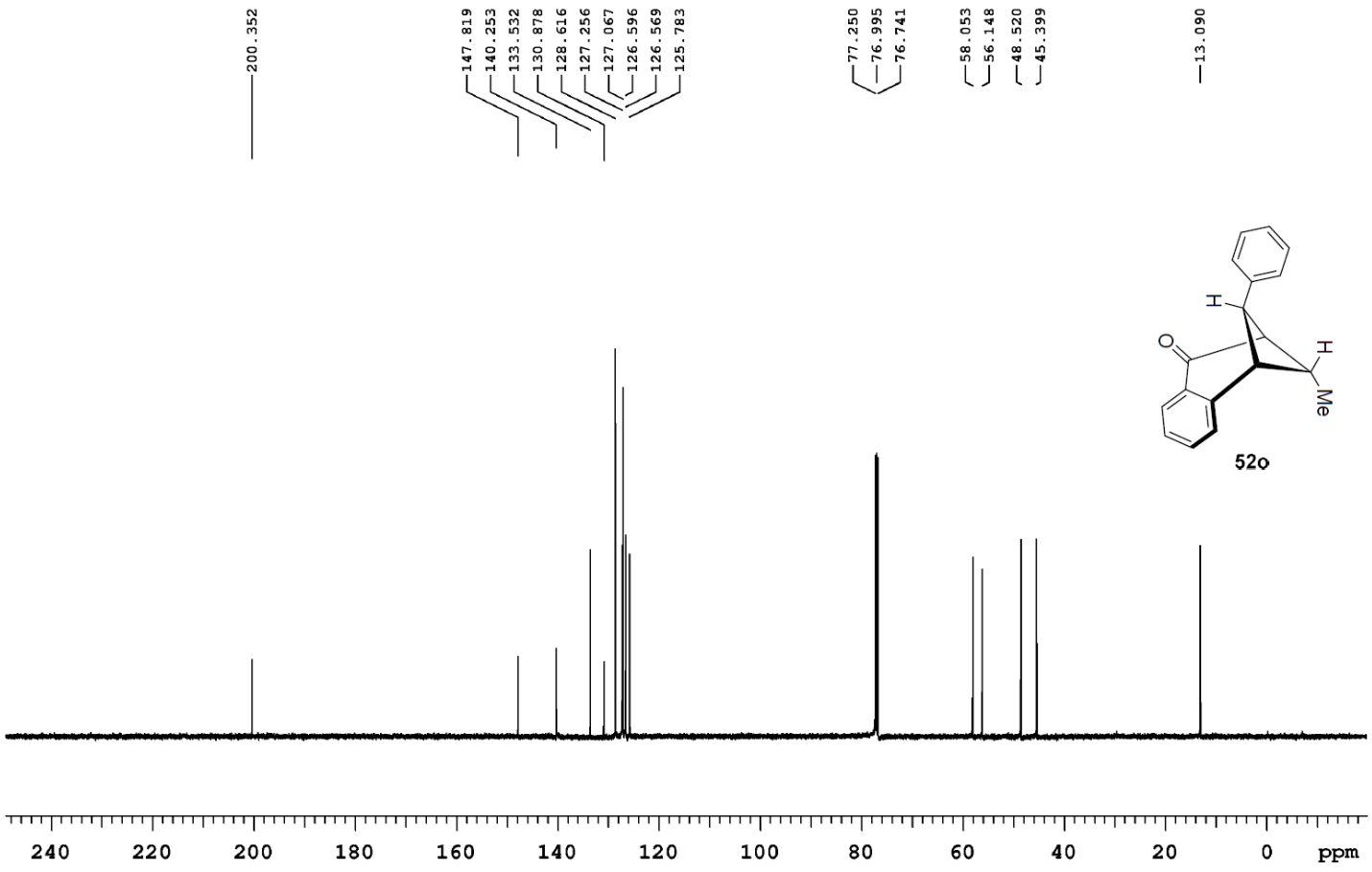

File: /mnt/d600/home13/westnmr/nmrdata/ShorenaFolders/2-2-products-et-al/2018.06.21.d3_Naz_4-18-1-BF3_on_Pn_Me-ed_C13_1D

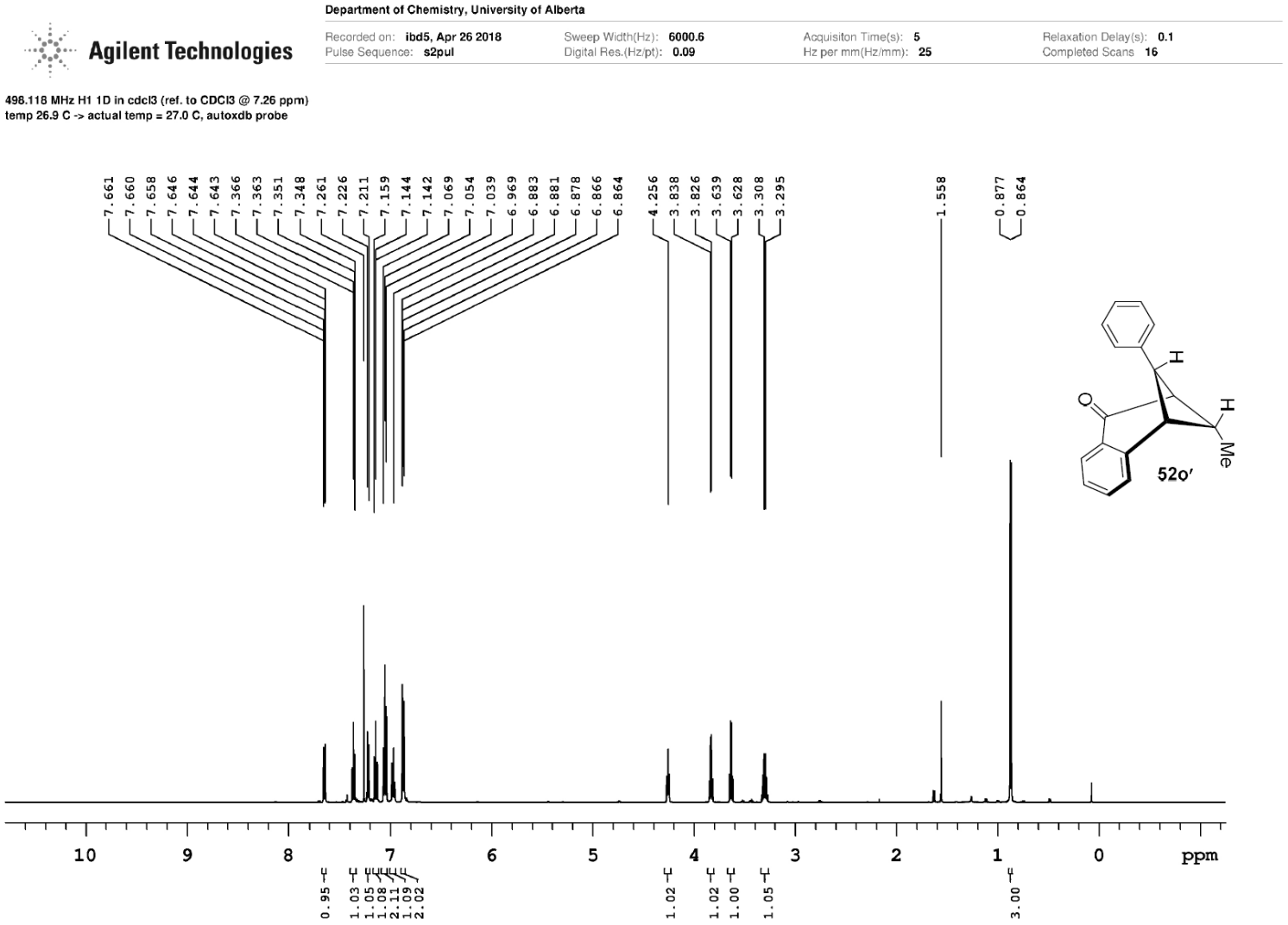
Department of Chemistry, University of Alberta
Agilent Technologies
Recorded on: ibd5, Apr 26 2018
Pulse Sequence: s2pul
Sweep Width(Hz): 6000.6
Digital Res.(Hz/pt): 0.09
Acquisiton Time(s): 5
Hz per mm(Hz/mm): 25
Relaxation Delay(s): 0.1
Completed Scans 16
498.118 MHz H1 1D in cdcl3 (ref. to CDCl3 @ 7.26 ppm)
temp 26.9 C -> actual temp = 27.0 C, autoxdb probe
7.661
7.660
7.658
7.646
7.644
7.643
7.366
7.363
7.351
7.348
7.261
7.226
7.211
7.159
7.144
7.142
7.069
7.054
7.039
6.969
6.883
6.881
6.878
6.866
6.864
4.256
3.838
3.826
3.639
3.628
3.308
3.295
1.558
0.877
0.864
H
O
H
Me
52o′
10
9
8
7
6
5
4
3
2
1
0
ppm
0.95
1.03
1.05
1.08
2.11
1.09
2.02
1.02
1.02
1.00
1.05
3.00
File: /mnt/d600/home13/westnmr/nmrdata/ShorenaFolders/2-2-products-et-al/2018.06.21.d3_Naz_4-18-2-BF3_on_Pn_Me-ed_H1_1D

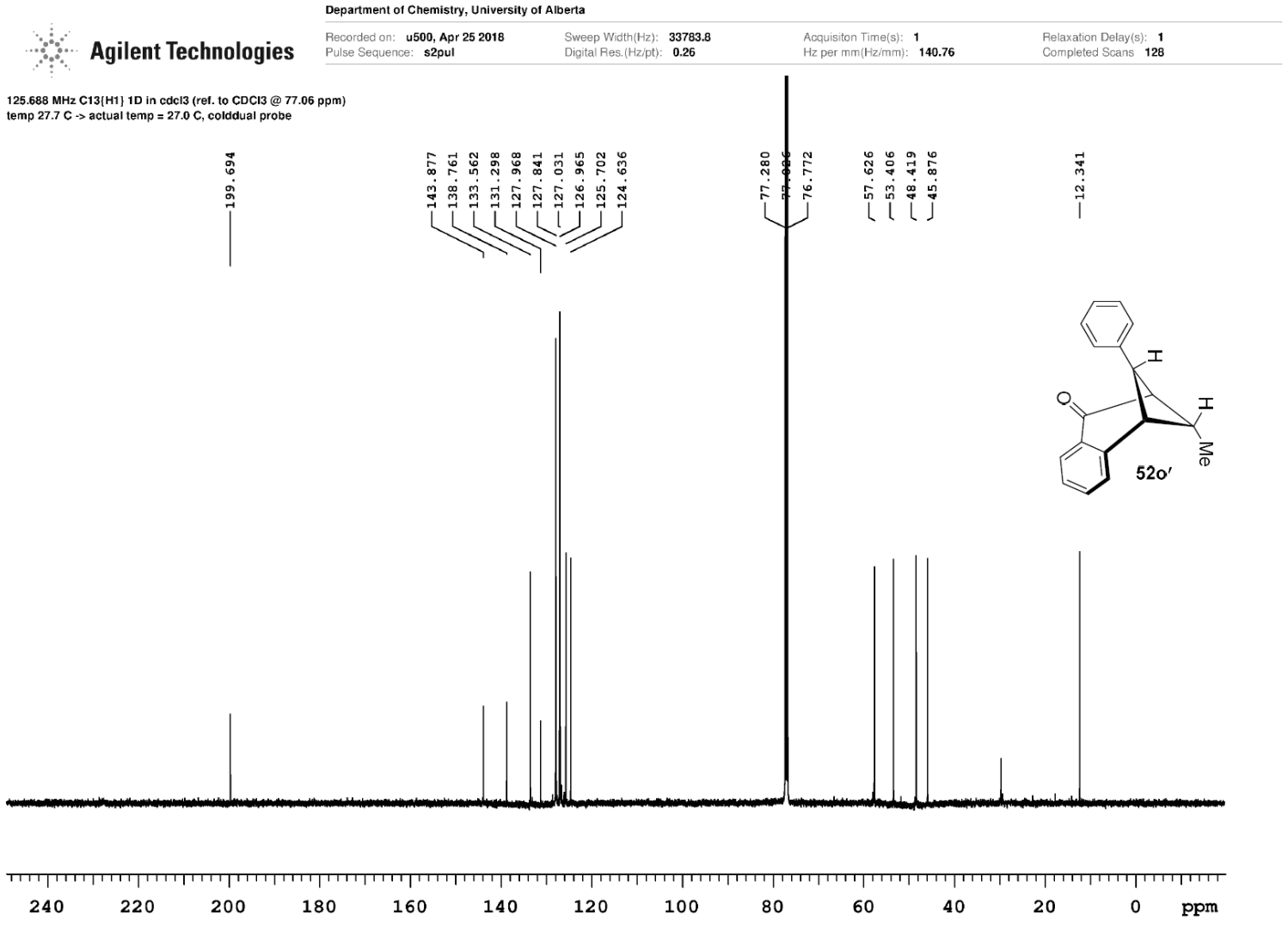

File: /mnt/d600/home13/westnmr/nmrdata/ShorenaFolders/2-2-products-et-al/2018.06.21.d3_Naz_4-18-2-BF3_on_Pn_Me-ed_C13_1D

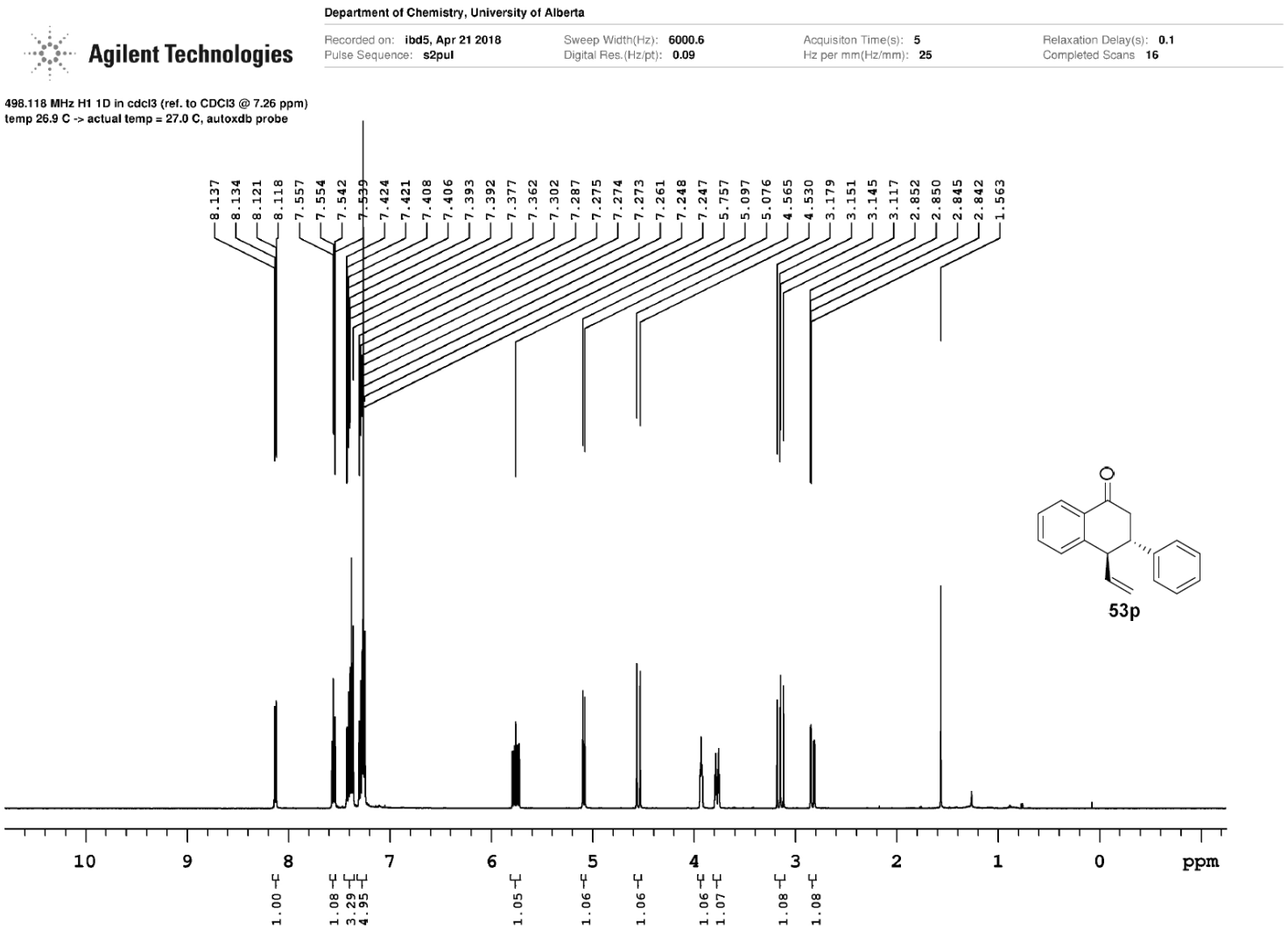

File: /mnt/d600/home13/westnmr/nmrdata/ShorenaFolders/2-2-products-et-al/2018.06.21.d3_Naz_4-6-BF3_on_Me_Ph-ed-pure-heat_at_85_H1_1D

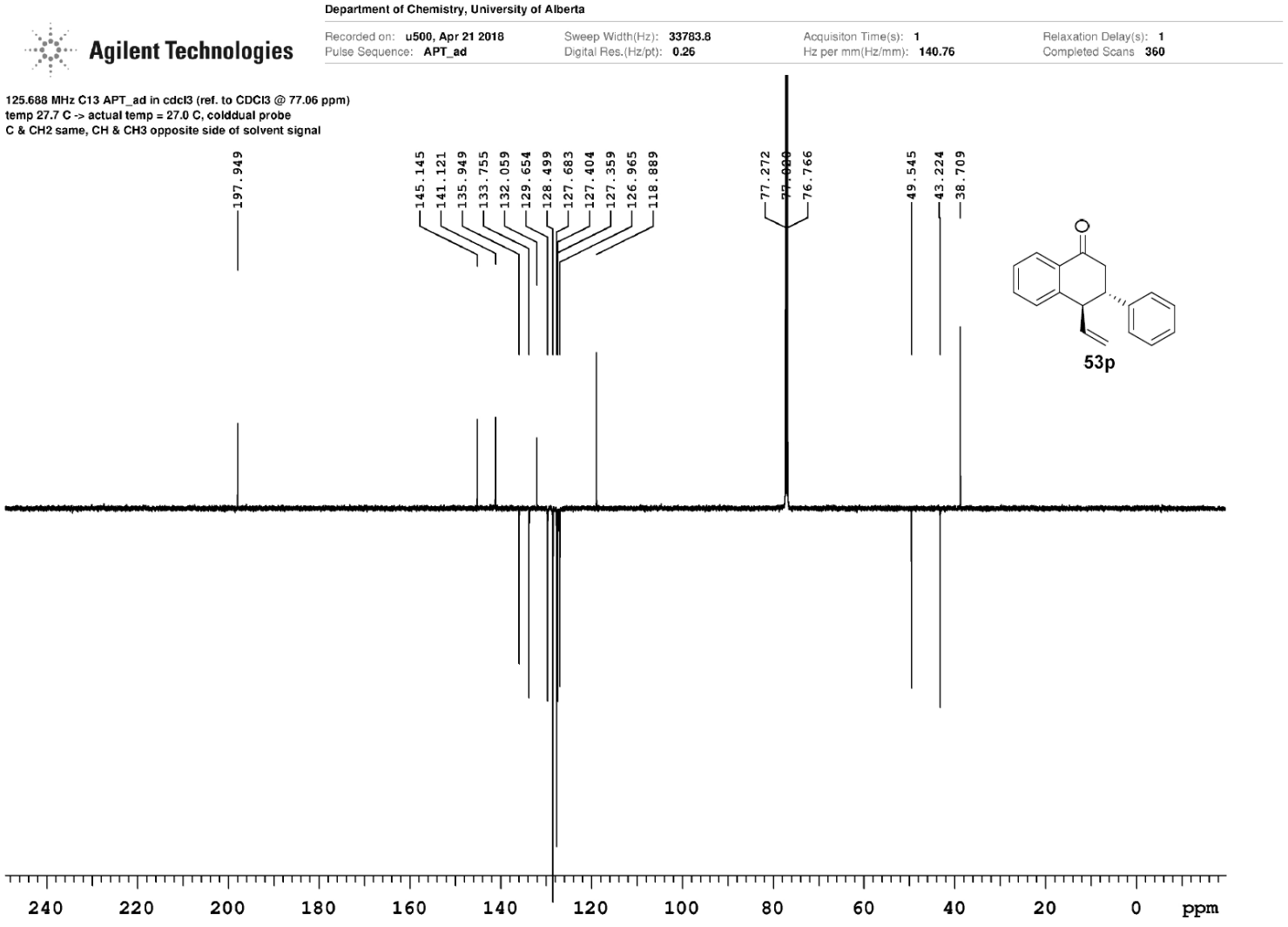

File: /mnt/d600/home13/westnmr/nmrdata/ShorenaFolders/2-2-products-et-al/2018.06.21.d3_Naz_4-6-BF3_on_Me_Ph-ed-pure-heat_at_85_C13_APT_ad

Department of Chemistry, University of Alberta

Agilent Technologies

Recorded on: **i600, Apr 9 2018**	Sweep Width(Hz): **7183.91**	Acquisiton Time(s): **5**	Relaxation Delay(s): **0.1**
Pulse Sequence: **s2pul**	Digital Res.(Hz/pt): **0.11**	Hz per mm(Hz/mm): **29.93**	Completed Scans **16**

599.926 MHz H1 1D in cdcl3 (ref. to CDCl3 @ 7.26 ppm)
temp 25.8 C -> actual temp = 27.0 C, autoxid probe

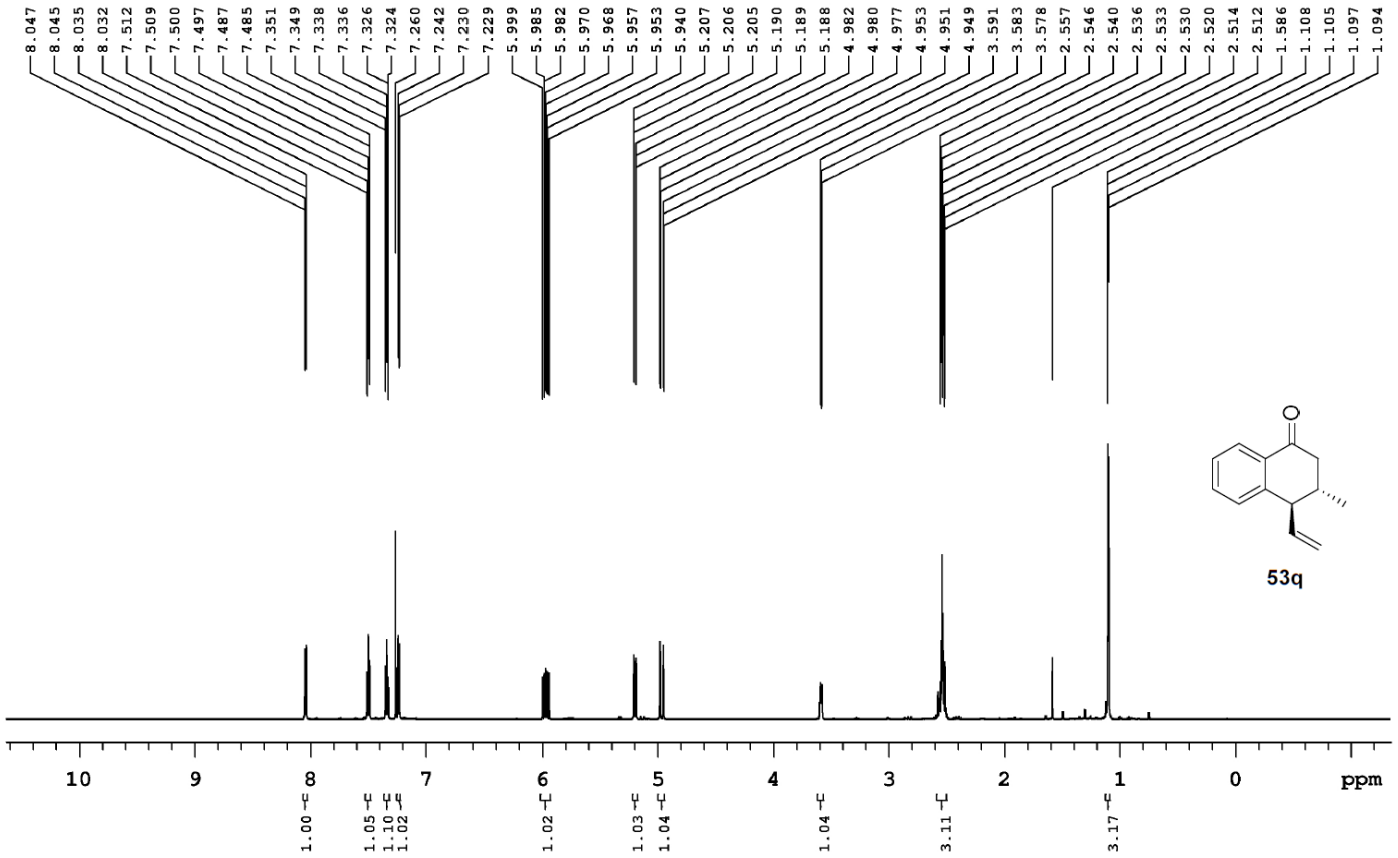

53q

File: /mnt/d600/home13/westnmr/nmrdata/ShorenaFolders/2-2-products-et-al/2018.06.21.d3_Naz_3-168-BF3_on_2XMe-ed_trienone_H1_1D

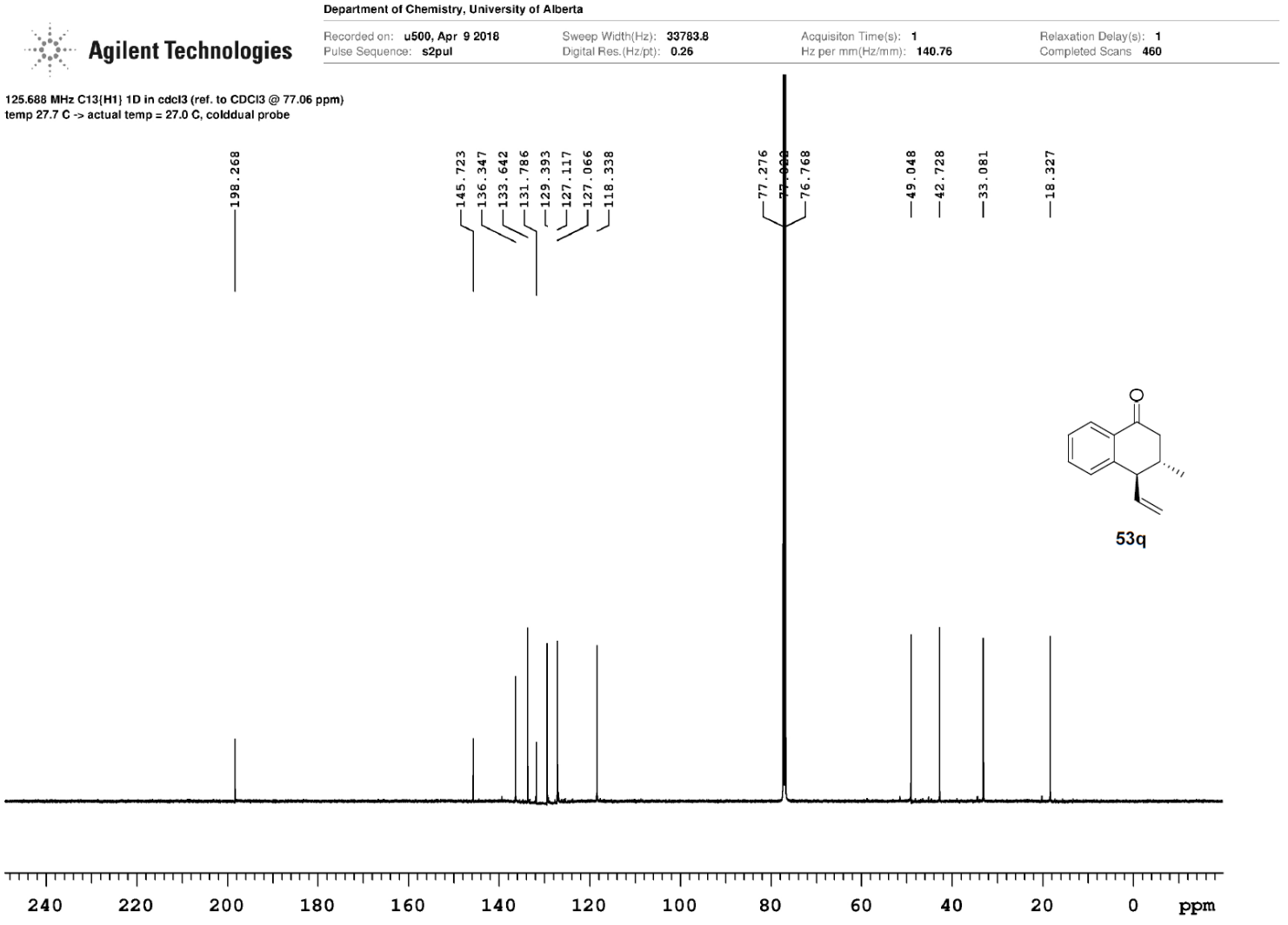
Department of Chemistry, University of Alberta
Agilent Technologies
Recorded on: u500, Apr 9 2018
Pulse Sequence: s2pul
Sweep Width(Hz): 33783.8
Digital Res.(Hz/pt): 0.26
Acquisiton Time(s): 1
Hz per mm(Hz/mm): 140.76
Relaxation Delay(s): 1
Completed Scans 460
125.688 MHz C13{H1} 1D in cdcl3 (ref. to CDCl3 @ 77.06 ppm)
temp 27.7 C -> actual temp = 27.0 C, colddual probe
198.268
145.723
136.347
133.642
131.786
129.393
127.117
127.066
118.338
77.276
77.000
76.768
49.048
42.728
33.081
18.327
53q
240
220
200
180
160
140
120
100
80
60
40
20
0
ppm
File: /mnt/d600/home13/westnmr/nmrdata/ShorenaFolders/2-2-products-et-al/2018.06.21.d3_Naz_3-168-BF3_on_2XMe-ed_trienone_C13_1D

Department of Chemistry, University of Alberta

Agilent Technologies

Recorded on: **ibd5, May 27 2018**	Sweep Width(Hz): **6000.6**	Acquisiton Time(s): **5**	Relaxation Delay(s): **0.1**
Pulse Sequence: **s2pul**	Digital Res.(Hz/pt): **0.09**	Hz per mm(Hz/mm): **25**	Completed Scans **16**

498.118 MHz H1 1D in cdcl3 (ref. to CDCl3 @ 7.26 ppm)
temp 26.9 C -> actual temp = 27.0 C, autoxdb probe

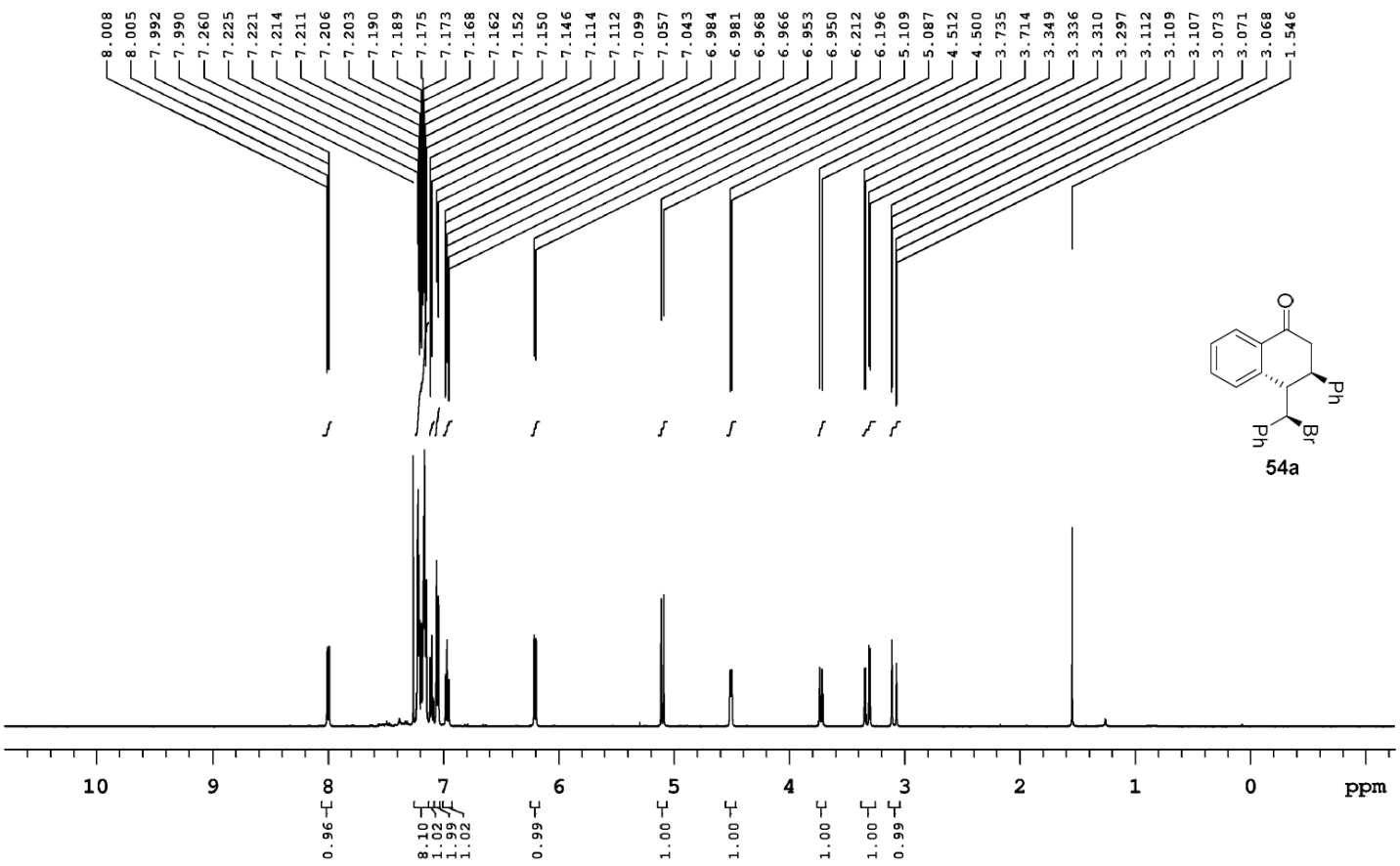

File: /mnt/d600/home13/westnmr/nmrdata/ShorenaFolders/2-2-products-et-al/2018.06.21.d3_Naz_II-198-1-BBr3_on_model_substrate_H1_1D

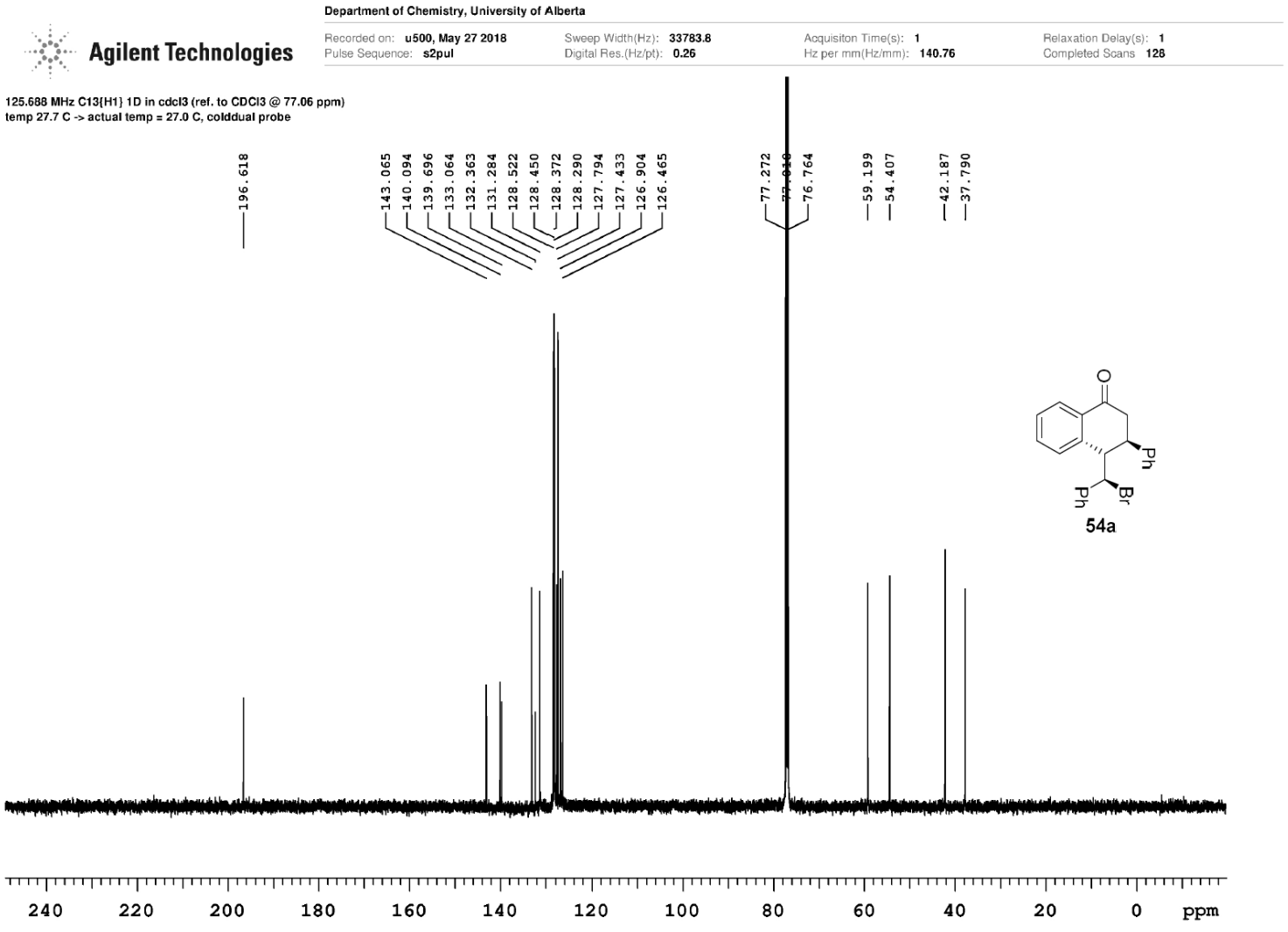

File: /mnt/d600/home13/westnmr/nmrdata/ShorenaFolders/2-2-products-et-al/2018.06.21.d3_Naz_II-198-1-BBr3_on_model_substrate_C13_1D

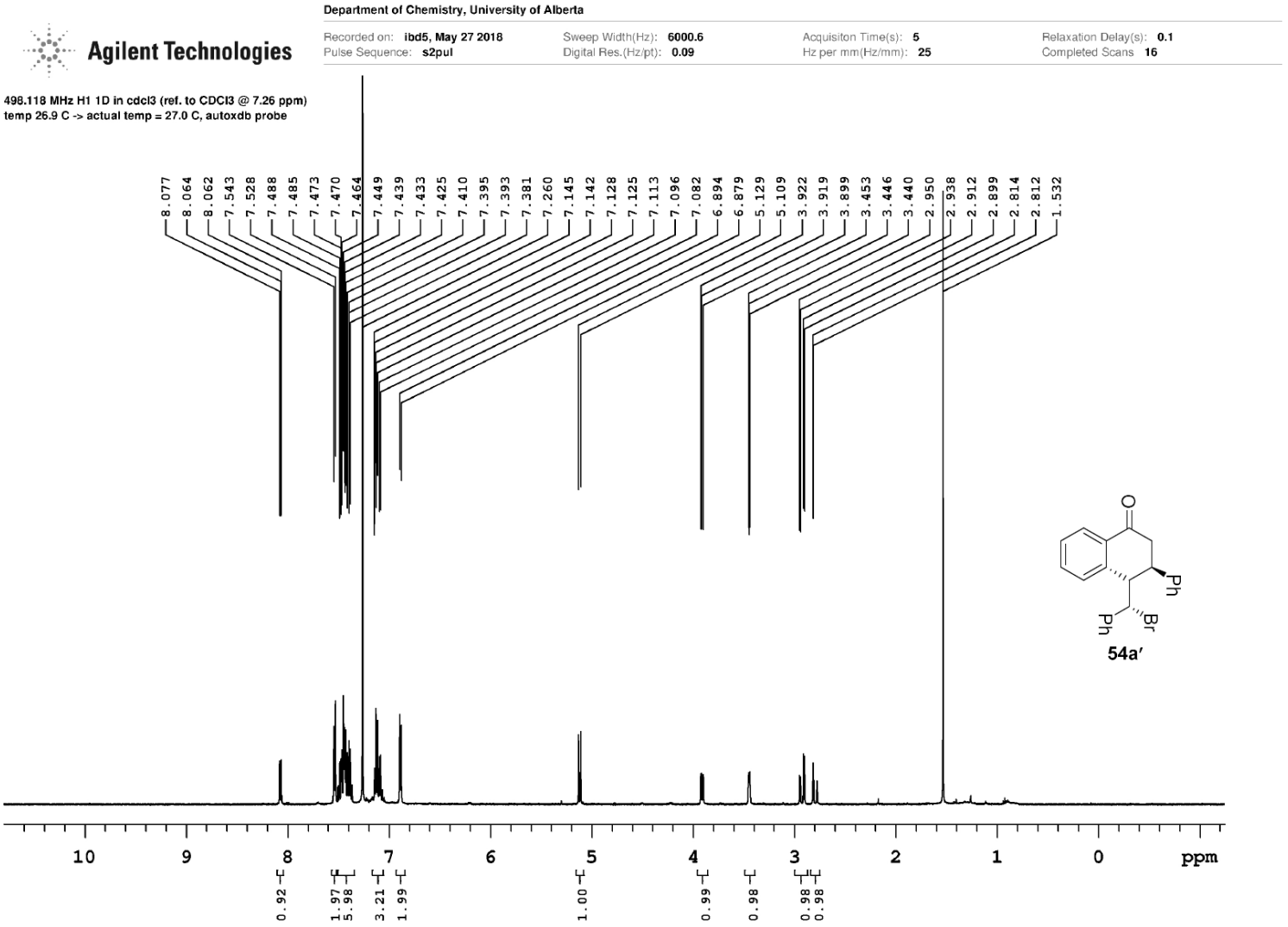

File: /mnt/d600/home13/westnmr/nmrdata/ShorenaFolders/2-2-products-et-al/2018.06.21.d3_Naz_II-198-2-BBr3_on_model_substrate_H1_1D

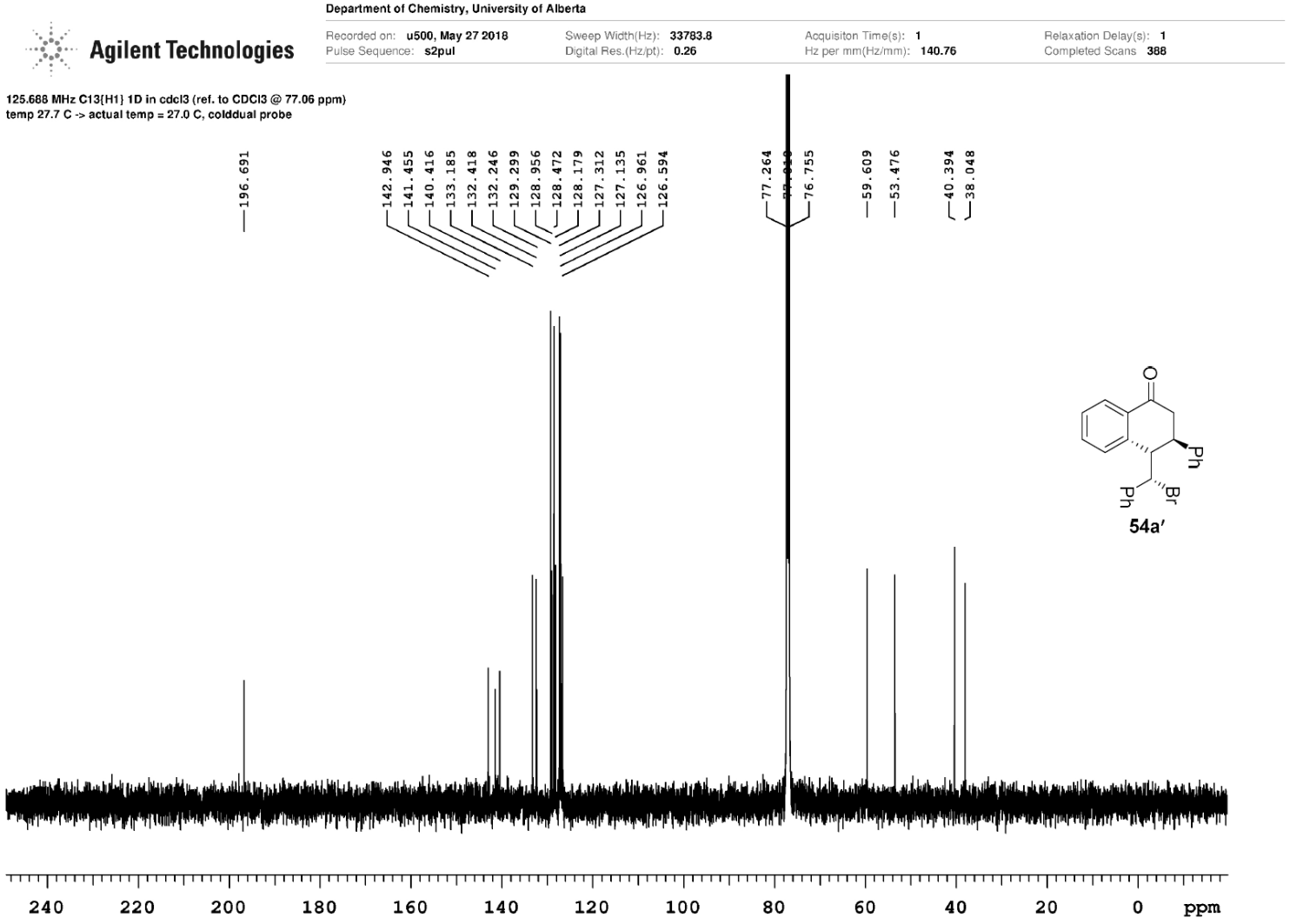

File: /mnt/d600/home13/westnmr/nmrdata/ShorenaFolders/2-2-products-et-al/2018.06.21.d3_Naz_II-198-2-BBr3_on_model_substrate_C13_1D

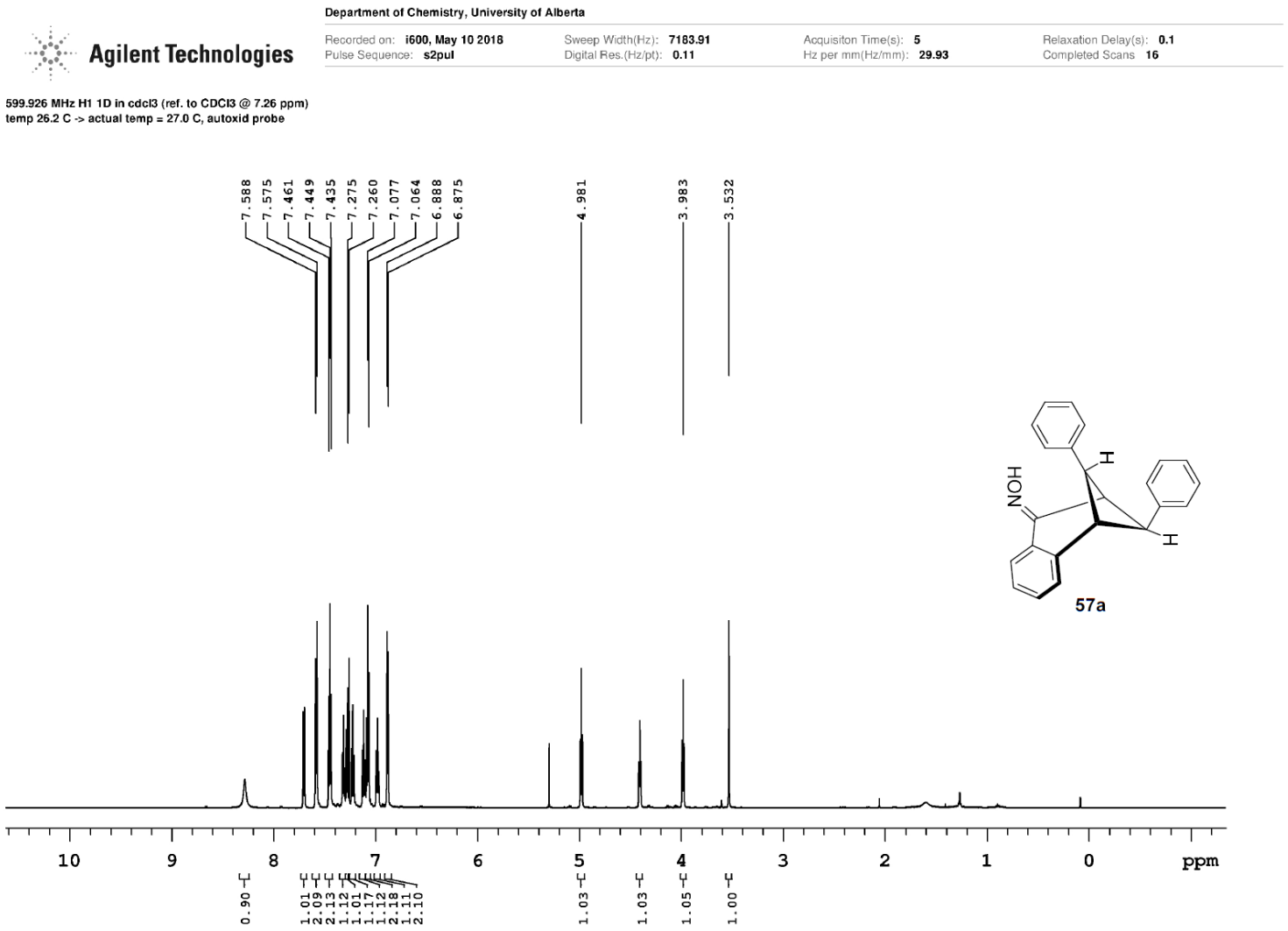
Department of Chemistry, University of Alberta
Agilent Technologies
Recorded on: i600, May 10 2018
Pulse Sequence: s2pul
Sweep Width(Hz): 7183.91
Digital Res.(Hz/pt): 0.11
Acquisiton Time(s): 5
Hz per mm(Hz/mm): 29.93
Relaxation Delay(s): 0.1
Completed Scans 16
599.926 MHz H1 1D in cdcl3 (ref. to CDCl3 @ 7.26 ppm)
temp 26.2 C -> actual temp = 27.0 C, autoxid probe
7.588
7.575
7.461
7.449
7.435
7.275
7.260
7.077
7.064
6.888
6.875
4.981
3.983
3.532
HON
H
H
57a
10
9
8
7
6
5
4
3
2
1
0
ppm
0.90
1.01
2.09
2.13
1.12
1.01
1.17
1.12
2.18
1.11
2.10
1.03
1.03
1.05
1.00
File: /mnt/d600/home13/westnmr/nmrdata/ShorenaFolders/2-2-products-et-al/2018.06.21.d3_Naz_4-46-oxime_H1_1D

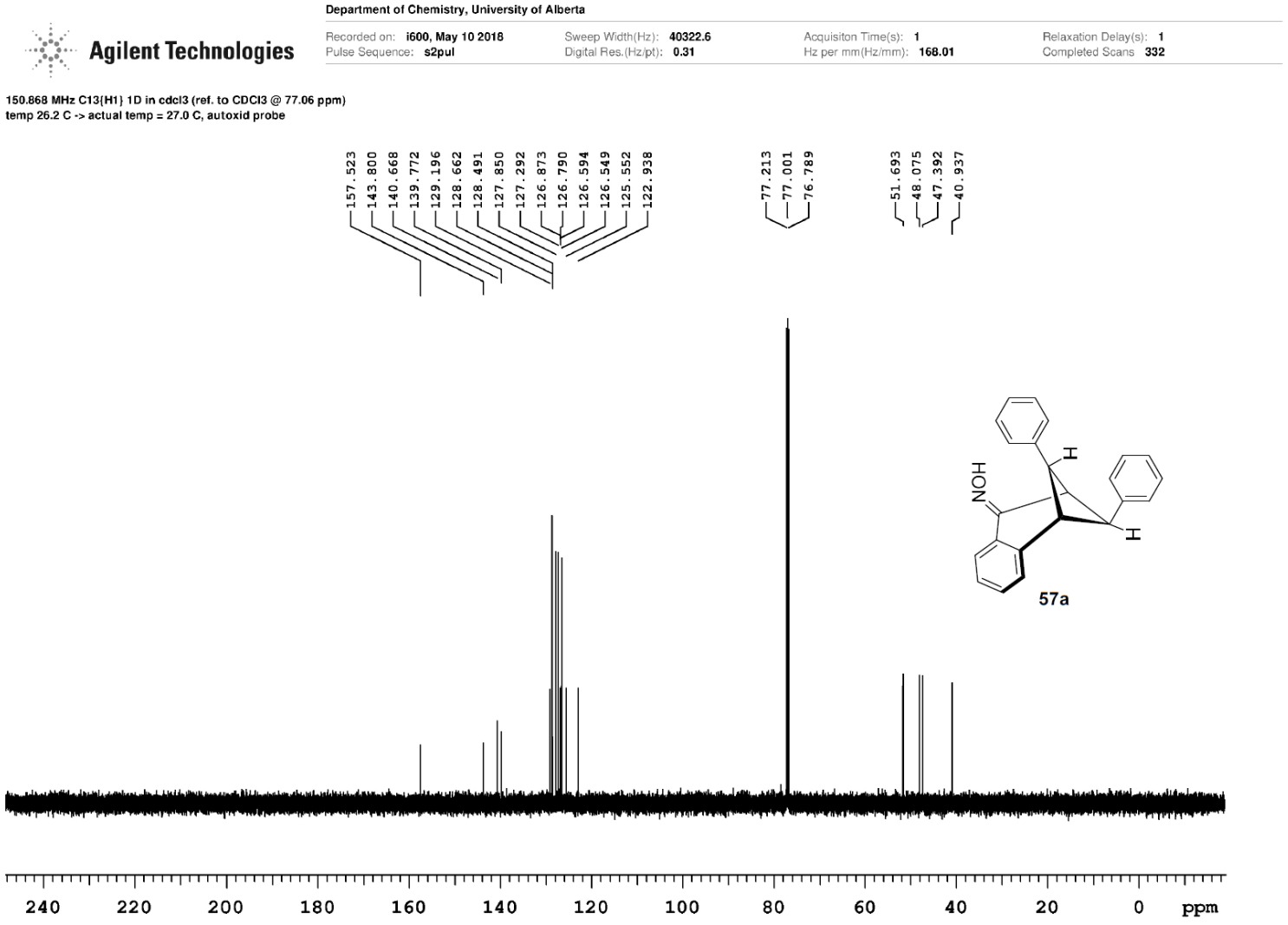

File: /mnt/d600/home13/westnmr/nmrdata/ShorenaFolders/2-2-products-et-al/2018.06.21.d3_Naz_4-46-oxime_C13_1D

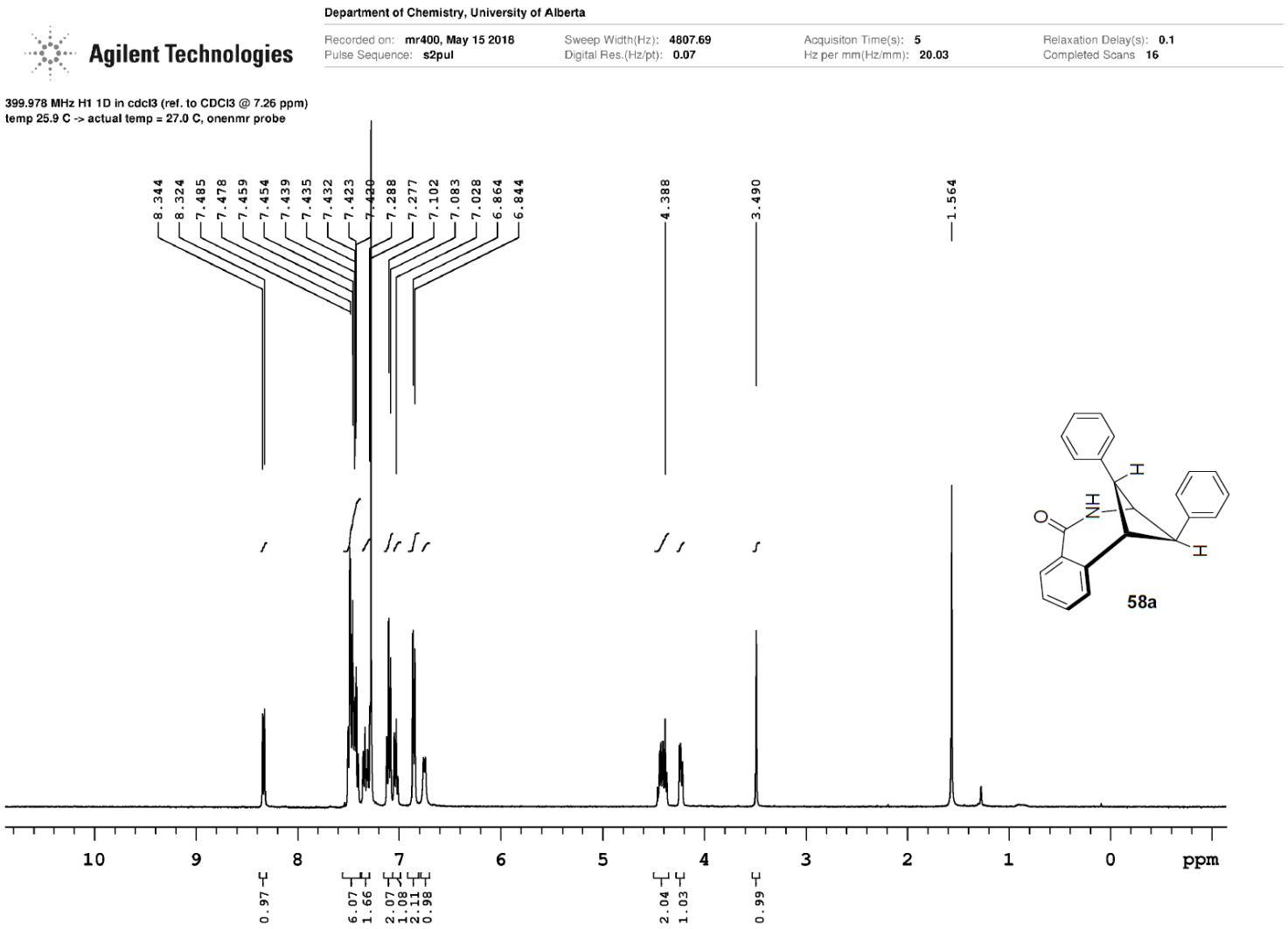

File: /mnt/d600/home13/westnmr/nmrdata/ShorenaFolders/2-2-products-et-al/2018.06.21.d3_Naz_4-50-amide_H1_1D

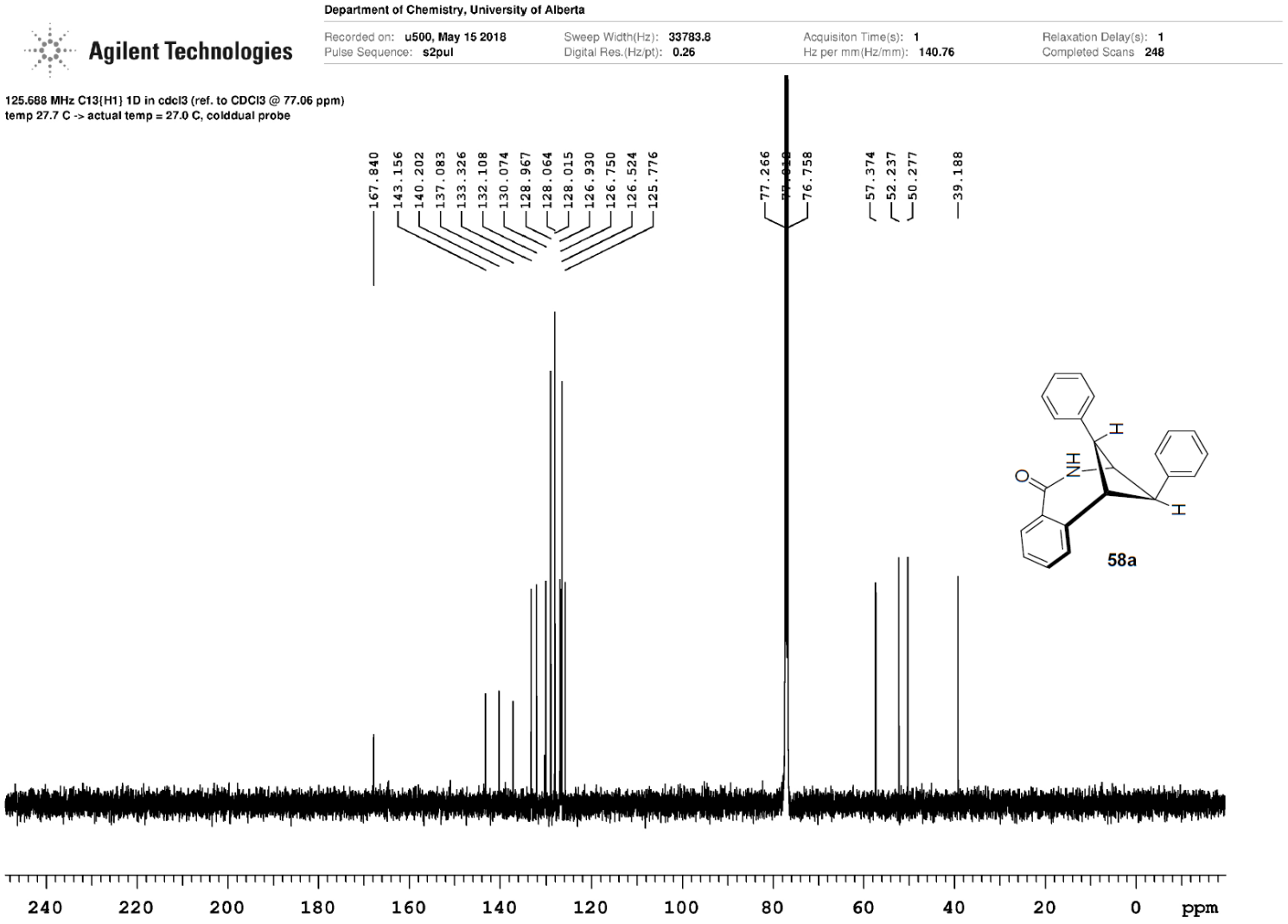

File: /mnt/d600/home13/westnmr/nmrdata/ShorenaFolders/2-2-products-et-al/2018.06.21.d3_Naz_4-50-amide_C13_1D

Department of Chemistry, University of Alberta

Agilent Technologies

Recorded on: **ibd5, May 22 2018**	Sweep Width(Hz): **6000.6**	Acquisiton Time(s): **5**	Relaxation Delay(s): **0.1**
Pulse Sequence: **s2pul**	Digital Res.(Hz/pt): **0.09**	Hz per mm(Hz/mm): **25**	Completed Scans **16**

498.118 MHz H1 1D in cdcl3 (ref. to CDCl3 @ 7.26 ppm)
temp 26.9 C -> actual temp = 27.0 C, autoxdb probe

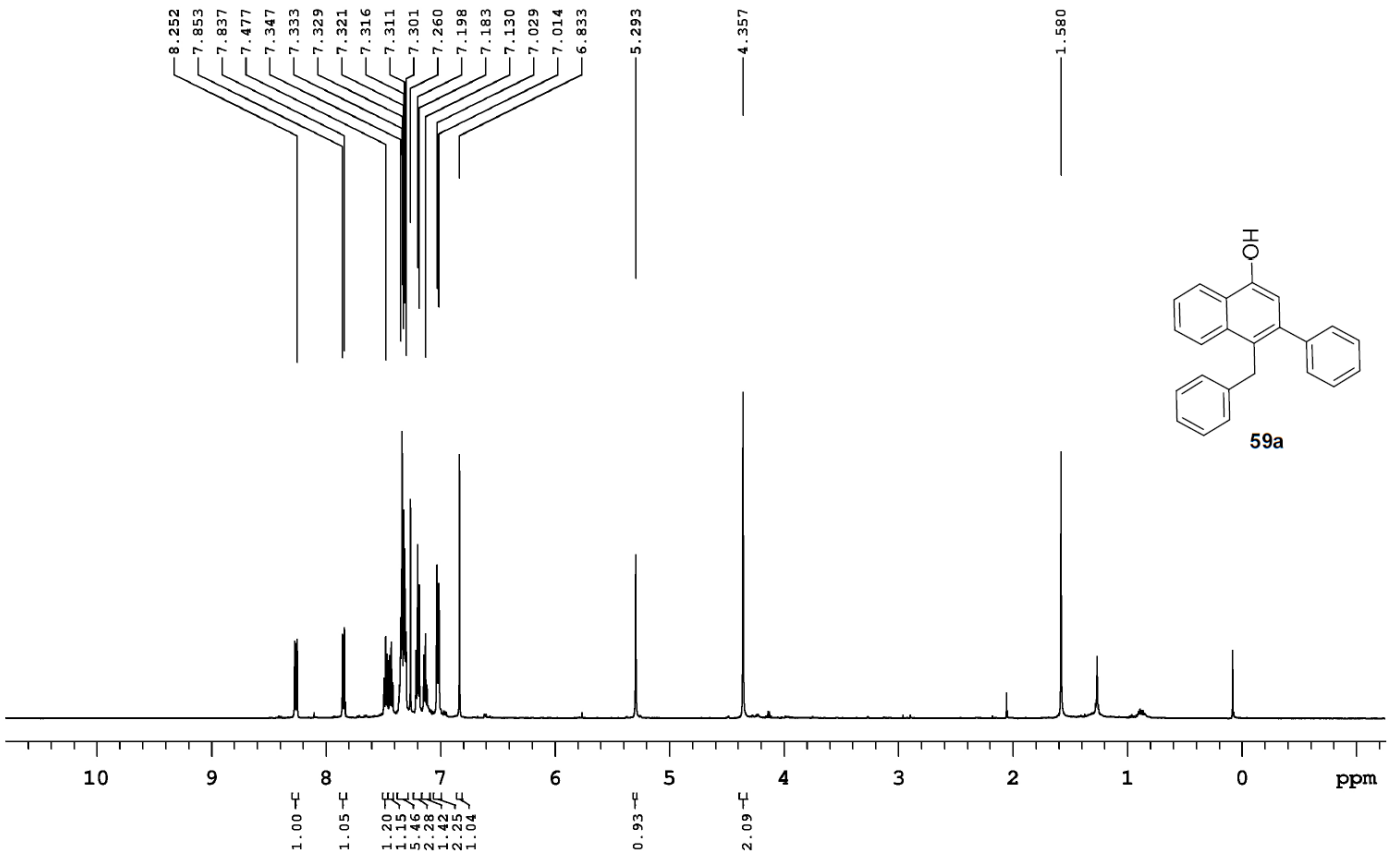

File: /mnt/d600/home13/westnmr/nmrdata/ShorenaFolders/2-2-products-et-al/2018.06.21.d3_Naz_4-52-naphthol_H1_1D

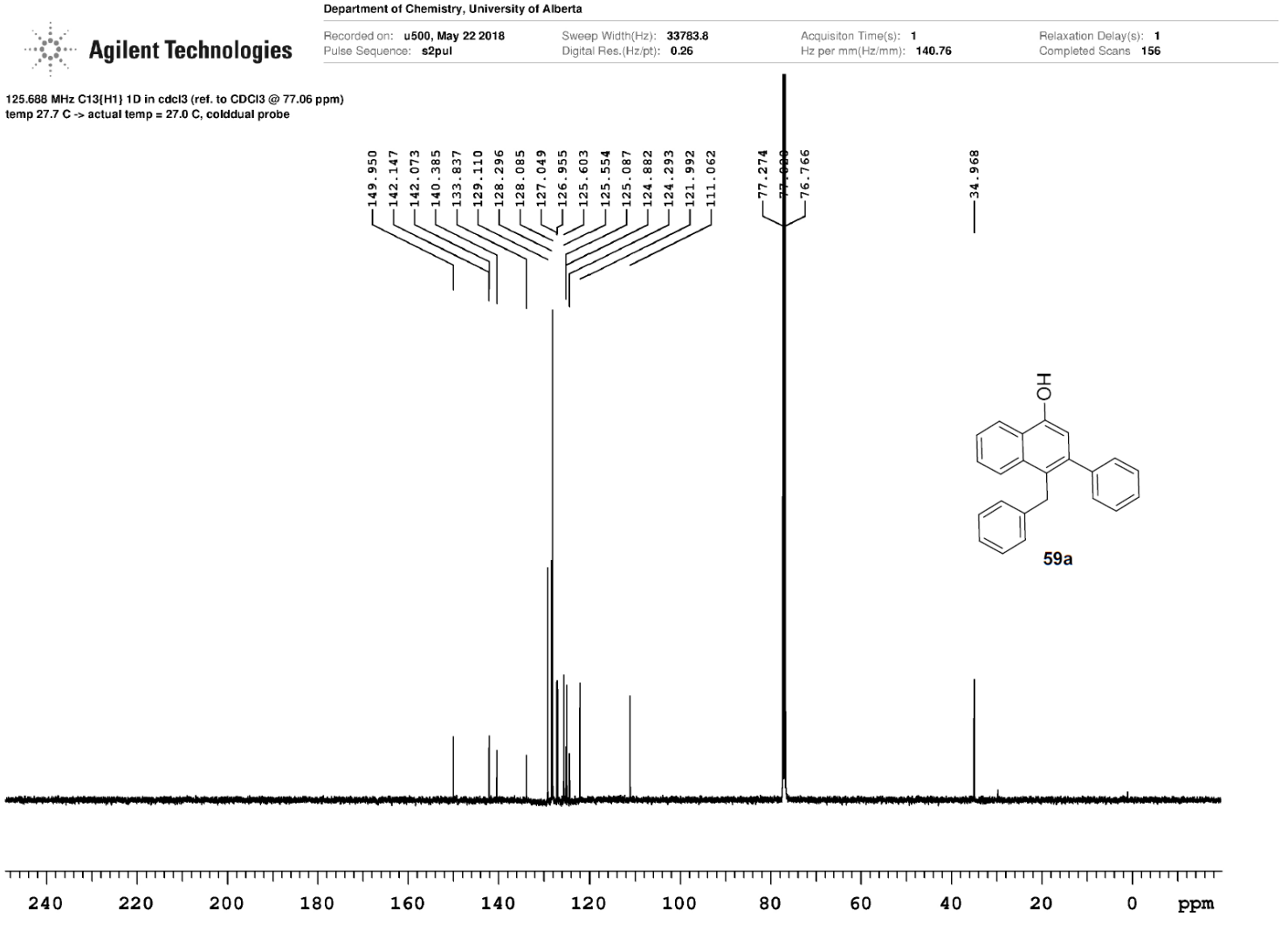

File: /mnt/d600/home13/westnmr/nmrdata/ShorenaFolders/2-2-products-et-al/2018.06.21.d3_Naz_4-52-naphthol_C13_1D

Appendix III: X-ray Crystallographic Data for Compound 42a

(Chapter 2)

STRUCTURE REPORT

XCL Code: FGW1601 **Date:** 22July2016

Compound: 2,2,5-Trimethyl-3,4-diphenylbicyclo[3.1.0]hex-1-yl acetate

Formula: $C_{23}H_{26}O_2$

Supervisor: F. G. Wes

Crystallographer: R. McDonald

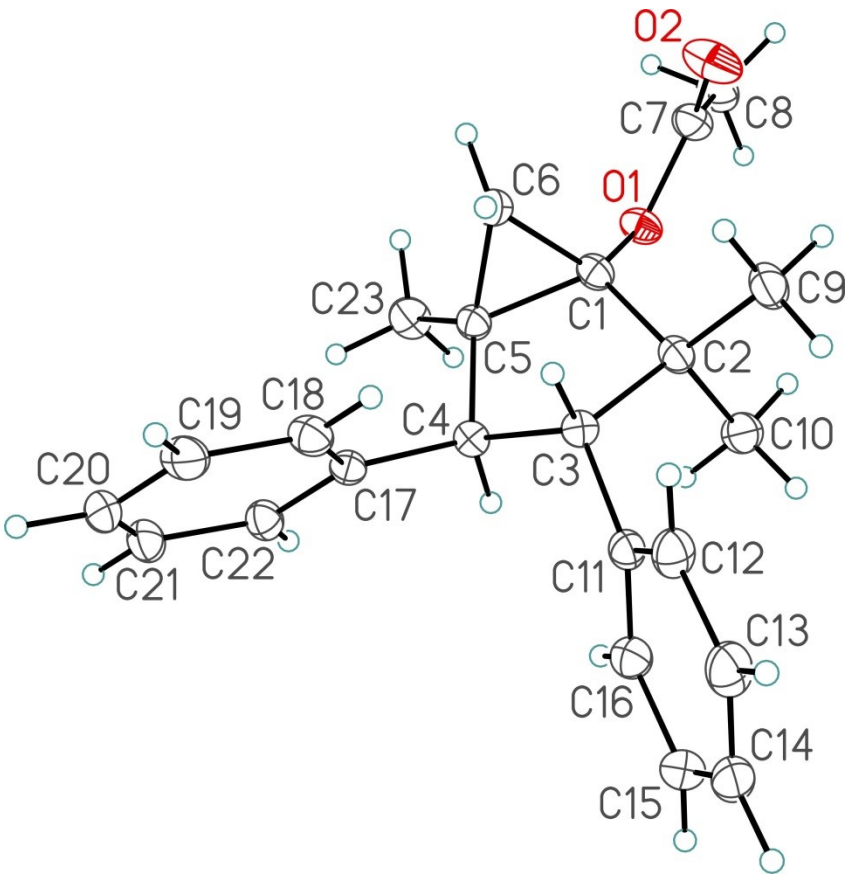

Figure 1. Perspective view of the 2,2,5-trimethyl-3,4-diphenylbicyclo[3.1.0]hex-1-yl acetate molecule showing the atom labelling scheme. Non-hydrogen atoms are represented by Gaussian ellipsoids at the 30% probability level. Hydrogen atoms are shown with arbitrarily small thermal parameters.

Table 1. Crystallographic Experimental Details

A. Crystal Data	
formula	$C_{23}H_{26}O_2$
formula weight	334.44
crystal dimensions (mm)	0.33 × 0.30 × 0.17
crystal system	orthorhombic
space group	$P2_12_12_1$ (No. 19)
unit cell parameters[a]	
	a (Å) 7.5221 (9)
	b (Å) 14.6773 (18)
	c (Å) 16.859 (2)
	V (Å^3) 1861.3 (4)
	Z 4
ρ_{calcd} (g cm^{-3})	1.193
μ (mm^{-1})	0.074
B. Data Collection and Refinement Conditions	
diffractometer	Bruker PLATFORM/APEX II CCD[b]
radiation (λ [Å])	graphite-monochromated Mo Kα (0.71073)
temperature (°C)	–80
scan type	ω scans (0.4°) (10 s exposures)
data collection 2θ limit (deg)	55.30
total data collected	11401 (-8≤h≤9, -19≤k≤19, -21≤l≤22)
independent reflections	4253 (R_{int} = 0.0411)
number of observed reflections (*NO*)	3528 [$F_o^2 \geq 2\sigma(F_o^2)$]
structure solution method	direct methods/dual space (*SHELXD*[c])
refinement method	full-matrix least-squares on F^2 (*SHELXL–2014*[d])
absorption correction method	Gaussian integration (face-indexed)
range of transmission factors	1.0000–0.8748
data/restraints/parameters	4253 / 0 / 228
Flack absolute structure parameter[e]	1(2)
goodness-of-fit (*S*)[f] [all data]	1.074
final R indices[g]	
	R_1 [$F_o^2 \geq 2\sigma(F_o^2)$] 0.0486
	wR_2 [all data] 0.1292
largest difference peak and hole	0.268 and –0.205 e Å^{-3}

[a]Obtained from least-squares refinement of 2467 reflections with 4.84° < 2θ<43.60°.

[b]Programsfor diffractometer operation, data collection, data reduction and absorption correction were those supplied by Bruker.

(continued)

Table 1. Crystallographic Experimental Details (continued)

[c]Schneider, T. R.; Sheldrick, G. M. *Acta Crystallogr.***2002**, *D58*, 1772-1779.

[d]Sheldrick, G. M. *Acta Crystallogr.***2015**, *C71*, 3–8.

[e]Flack, H. D. *Acta Crystallogr.***1983**, *A39*, 876–881; Flack, H. D.; Bernardinelli, G. *Acta Crystallogr.***1999**, *A55*, 908–915; Flack, H. D.; Bernardinelli, G. *J. Appl. Cryst.***2000**, *33*, 1143–1148. The Flack parameter will refine to a value near zero if the structure is in the correct configuration and will refine to a value near one for the inverted configuration.The low anomalous scattering power of the atoms in this structure (none heavier than oxygen) implies that the data cannot be used for absolute structure assignment, thus the Flack parameter is provided for informational purposes only. The structure is assigned based on the stereochemistry of the precursor compounds.

[f]$S = [\Sigma w(F_o^2 - F_c^2)^2/(n - p)]^{1/2}$ (n = number of data; p = number of parameters varied; $w = [\sigma^2(F_o^2) + (0.0540P)^2 + 0.2230P]^{-1}$ where $P = [\mathrm{Max}(F_o^2, 0) + 2F_c^2]/3$).

[g]$R_1 = \Sigma||F_o| - |F_c||/\Sigma|F_o|$; $wR_2 = [\Sigma w(F_o^2 - F_c^2)^2/\Sigma w(F_o^4)]^{1/2}$.

Appendix IV: X-ray Crystallographic Data for Compound 52a

(Chapter 3)

STRUCTURE REPORT

XCL Code: FGW1704 **Date:** 18May 2017

Compound: 2,9-Diphenyl-2,3-dihydro-1,3-methanonaphthalen-4(1*H*)-one

Formula: $C_{23}H_{18}O$

Supervisor: F. G. West **Crystallographer:** R. McDonald

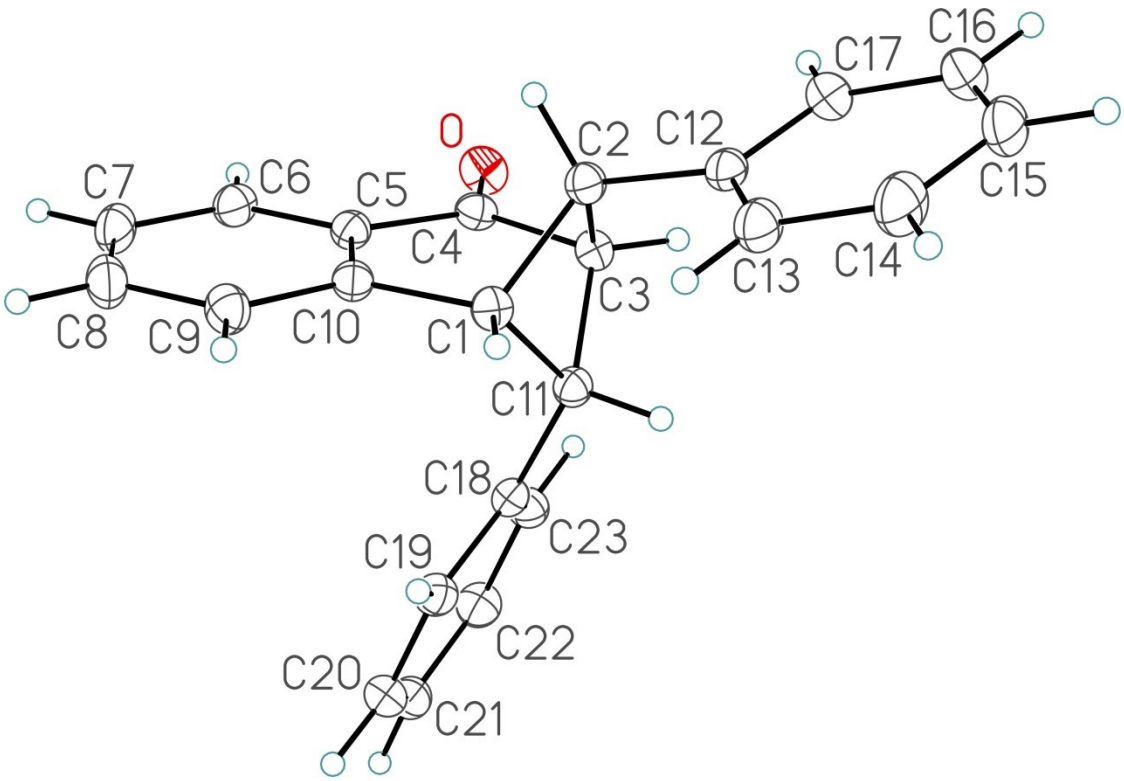

Figure 1. Perspective view of the 2,9-diphenyl-2,3-dihydro-1,3-methanonaphthalen-4(1*H*)-one molecule showing the atom labelling scheme. Non-hydrogen atoms are represented by Gaussian ellipsoids at the 30% probability level. Hydrogen atoms are shown with arbitrarily small thermal parameters.

Table 1. Crystallographic Experimental Details

A. Crystal Data	
formula	$C_{23}H_{18}O$
formula weight	310.37
crystal dimensions (mm)	0.44×0.30 × 0.23
crystal system	orthorhombic
space group	*Pbca* (No. 61)
unit cell parameters[a]	
	a (Å) 11.5317 (4)
	b (Å) 14.3687 (5)
	c (Å) 19.7918 (7)
	V (Å^3) 3279.4 (2)
	Z 8
ρ_{calcd} (g cm^{-3})	1.257
μ (mm^{-1})	0.075
B. Data Collection and Refinement Conditions	
diffractometer	Bruker PLATFORM/APEX II CCD[b]
radiation (λ [Å])	graphite-monochromated Mo Kα (0.71073)
temperature (°C)	–80
scan type	ω scans (0.3°) (15 s exposures)
data collection 2θ limit (deg)	56.69
total data collected	29767 (-15≤*h*≤15, -18≤*k*≤19, -26≤*l*≤26)
independent reflections	4097 (R_{int} = 0.0245)
number of observed reflections (*NO*)	3395 [$F_o^2 \geq 2\sigma(F_o^2)$]
structure solution method	direct methods/dual space (*SHELXD*[c])
refinement method	full-matrix least-squares on F^2 (*SHELXL–2014*[d])
absorption correction method	Gaussian integration (face-indexed)
range of transmission factors	1.0000–0.9434
data/restraints/parameters	4097 / 0 / 217
goodness-of-fit (*S*)[e] [all data]	1.049
final *R* indices[f]	
	R_1 [$F_o^2 \geq 2\sigma(F_o^2)$] 0.0424
	wR_2 [all data] 0.1217
largest difference peak and hole	0.281 and –0.208 e Å^{-3}

[a]Obtained from least-squares refinement of 9958 reflections with 4.98° < 2θ<53.28°.

[b]Programs for diffractometer operation, data collection, data reduction and absorption

correction were those supplied by Bruker.

(continued)

Table 1. Crystallographic Experimental Details (continued)

[c]Schneider, T. R.; Sheldrick, G. M. *Acta Crystallogr.***2002**, *D58*, 1772-1779.

[d]Sheldrick, G. M. *Acta Crystallogr.***2015**, *C71*, 3–8.

[e]$S = [\Sigma w(F_o^2 - F_c^2)^2/(n - p)]^{1/2}$ (n = number of data; p = number of parameters varied; $w = [\sigma^2(F_o^2) + (0.0632P)^2 + 0.7023P]^{-1}$ where $P = [\mathrm{Max}(F_o^2, 0) + 2F_c^2]/3$).

[f]$R_1 = \Sigma||F_o| - |F_c||/\Sigma|F_o|$; $wR_2 = [\Sigma w(F_o^2 - F_c^2)^2/\Sigma w(F_o^4)]^{1/2}$.

Appendix V: X-ray Crystallographic Data for Compound 52f

(Chapter 3)

STRUCTURE REPORT

XCL Code: FGW1709 **Date:** 11October 2017

Compound: 2,9-Di(naphthalen-1-yl)-2,3-dihydro-1,3-methanonaphthalen-4(1*H*)-one
Formula: $C_{31}H_{22}O$

Supervisor: F. G. West

Crystallographer:R. McDonald

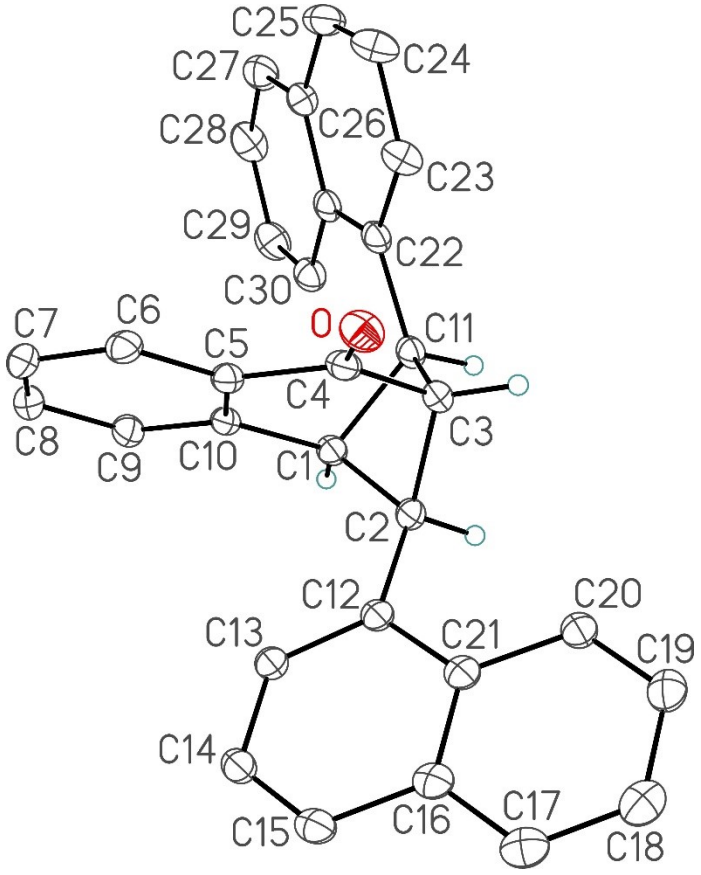

Figure 1. Perspective view of the 2,9-di(naphthalen-1-yl)-2,3-dihydro-1,3-methanonaphthalen-4(1*H*)-one molecule showing the atom labelling scheme. Non-hydrogen atoms are represented by Gaussian ellipsoids at the 30% probability level. The hydrogen atoms attached to C1, C2, C3, and C11 are shown with arbitrarily small thermal parameters; aromatic-ring hydrogens are not shown.

Table 1. Crystallographic Experimental Details

A. Crystal Data	
formula	$C_{31}H_{22}O$
formula weight	410.48
crystal dimensions (mm)	0.46×0.22 × 0.20
crystal system	triclinic
space group	$P\bar{1}$(No. 2)
unit cell parameters[a]	
	a (Å) 8.3472 (2)
	b (Å) 10.2108 (2)
	c (Å) 12.6979 (3)
	α (deg) 101.0417 (9)
	β (deg) 95.8912 (12)
	γ (deg) 100.7152 (8)
	V (Å^3) 1032.93 (4)
	Z 2
ρ_{calcd} (g cm^{-3})	1.320
μ (mm^{-1})	0.601
B. Data Collection and Refinement Conditions	
diffractometer	Bruker D8/APEX II CCD[b]
radiation (λ [Å])	Cu Kα (1.54178) (microfocus source)
temperature (°C)	–100
scan type	ω and ϕ scans (1.0°) (5 s exposures)
data collection 2θ limit (deg)	147.84
total data collected	7274 (-10≤h≤10, -12≤k≤12, -15≤l≤15)
independent reflections	4001 (R_{int} = 0.0228)
number of observed reflections (*NO*)	3740 [$F_o^2 \geq 2\sigma(F_o^2)$]
structure solution method	direct methods/dual space (*SHELXD*[c])
refinement method	full-matrix least-squares on F^2 (*SHELXL–2014*[d])
absorption correction method	Gaussian integration (face-indexed)
range of transmission factors	1.0000–0.6984
data/restraints/parameters	4001 / 0 / 289
goodness-of-fit (*S*)[e] [all data]	1.062
final R indices[f]	
	R_1 [$F_o^2 \geq 2\sigma(F_o^2)$] 0.0432
	wR_2 [all data] 0.1241
largest difference peak and hole	0.276 and –0.264 e Å^{-3}

[a]Obtained from least-squares refinement of 9968 reflections with 7.16° < 2θ<147.86°.

(continued)

Table 1. Crystallographic Experimental Details (continued)

[b]Programs for diffractometer operation, data collection, data reduction and absorption correction were those supplied by Bruker.

[c]Schneider, T. R.; Sheldrick, G. M. *Acta Crystallogr.***2002**, *D58*, 1772-1779.

[d]Sheldrick, G. M. *Acta Crystallogr.***2015**, *C71*, 3–8.

[e]$S = [\Sigma w(F_o^2 - F_c^2)^2/(n - p)]^{1/2}$ (n = number of data; p = number of parameters varied; $w = [\sigma^2(F_o^2) + (0.0724P)^2 + 0.2222P]^{-1}$ where$P = [\mathrm{Max}(F_o^2, 0) + 2F_c^2]/3)$.

[f]$R_1 = \Sigma||F_o| - |F_c||/\Sigma|F_o|$; $wR_2 = [\Sigma w(F_o^2 - F_c^2)^2/\Sigma w(F_o^4)]^{1/2}$.

Appendix VI: X-ray Crystallographic Data for Compound 52l

(Chapter 3)

STRUCTURE REPORT

XCL Code: FGW1802 **Date:** 21February 2018

Compound: 2-(4-methylphenyl)-9-[4-(trifluoromethyl)phenyl]-2,3-dihydro-1,3-methanonaphthalen-4(1*H*)-one

Formula: $C_{25}H_{19}F_3O$

Supervisor: F. G. West

Crystallographer: M. J. Ferguson

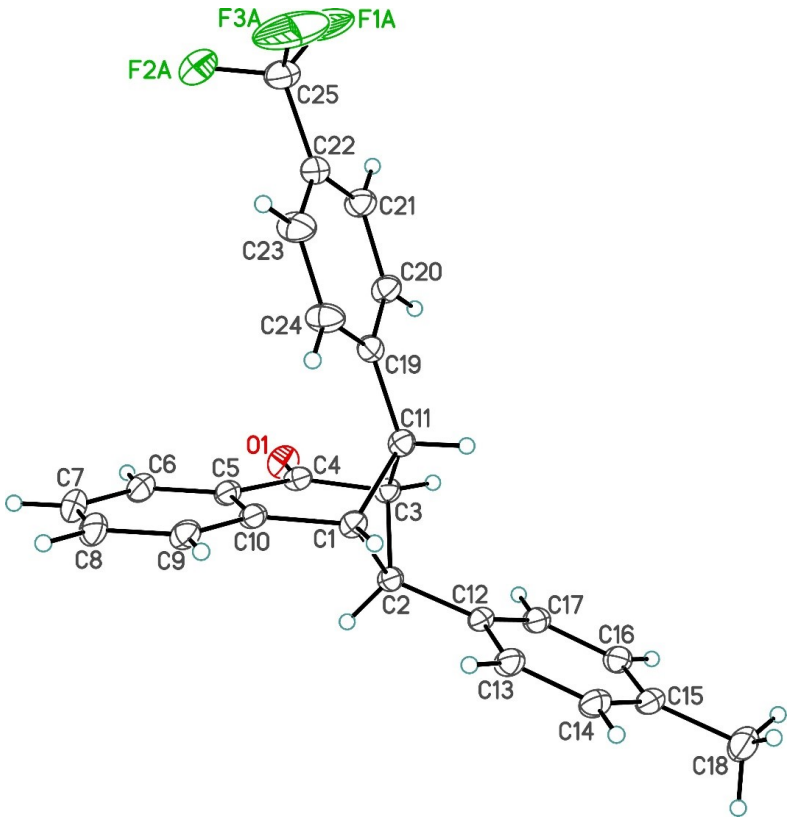

Figure 1. Perspective view of the 2-(4-methylphenyl)-9-[4-(trifluoromethyl)phenyl]-2,3-dihydro-1,3-methanonaphthalen-4(1*H*)-one molecule showing the atom labelling scheme. Only the major orientation of the disordered CF_3 group is shown. Non-hydrogen atoms are represented by Gaussian ellipsoids at the 30% probability level. Hydrogen atoms are shown with arbitrarily small thermal parameters.

Table 1. Crystallographic Experimental Details

A. Crystal Data	
formula	$C_{25}H_{19}F_3O$
formula weight	392.40
crystal dimensions (mm)	0.40×0.14×0.04
crystal system	orthorhombic
space group	$Pca2_1$ (No. 29)
unit cell parameters[a]	
	a (Å) 8.5514(2)
	b (Å) 12.5087(3)
	c (Å) 18.3036(4)
	V (Å^3) 1957.88(8)
	Z 4
ρ_{calcd} (g cm^{-3})	1.331
μ (mm^{-1})	0.829
B. Data Collection and Refinement Conditions	
diffractometer	Bruker D8/APEX II CCD[b]
radiation (λ [Å])	Cu Kα (1.54178) (microfocus source)
temperature (°C)	–100
scan type	ω and ϕ scans (1.0°) (5 s exposures)
data collection 2θ limit (deg)	135.38
total data collected	11838 (-9≤h≤8, -15≤k≤15, -21≤l≤21)
independent reflections	3455 (R_{int} = 0.0239)
number of observed reflections (*NO*)	3376 [$F_o^2 \geq 2\sigma(F_o^2)$]
structure solution method	intrinsic phasing (*SHELXT-2014*[c])
refinement method	full-matrix least-squares on F^2 (*SHELXL–2016*[d])
absorption correction method	Gaussian integration (face-indexed)
range of transmission factors	0.9906–0.8498
data/restraints/parameters	3455 / 0 / 291
Flack absolute structure parameter[e]	–0.01(5)
goodness-of-fit (*S*)[f] [all data]	1.039
final *R* indices[g]	
	R_1 [$F_o^2 \geq 2\sigma(F_o^2)$] 0.0307
	wR_2 [all data] 0.0804
largest difference peak and hole	0.123 and –0.151 e Å^{-3}

[a]Obtained from least-squares refinement of 9873 reflections with 7.06° < 2θ<144.00°.

[b]Programs for diffractometer operation, data collection, data reduction and absorption correction were those supplied by Bruker.

(continued)

Table 1. Crystallographic Experimental Details (continued)

[c]Sheldrick, G. M. *ActaCrystallogr.***2015**, *A71*, 3–8. (*SHELXT-2014*)

[d]Sheldrick, G. M. *ActaCrystallogr.***2015**, *C71*, 3–8. (*SHELXL-2016*)

[e]Flack, H. D. *ActaCrystallogr.***1983**, *A39*, 876–881; Flack, H. D.; Bernardinelli, G. *ActaCrystallogr.***1999**, *A55*, 908–915; Flack, H. D.; Bernardinelli, G. *J. Appl. Cryst.***2000**, *33*, 1143–1148. The Flack parameter will refine to a value near zero if the structure is in the correct configuration and will refine to a value near one for the inverted configuration.

[f]$S = [\Sigma w(F_o^2 - F_c^2)^2/(n - p)]^{1/2}$ (n = number of data; p = number of parameters varied; $w = [\sigma^2(F_o^2) + (0.0533P)^2 + 0.1759P]^{-1}$ where $P = [\mathrm{Max}(F_o^2, 0) + 2F_c^2]/3$).

[g]$R_1 = \Sigma||F_o| - |F_c||/\Sigma|F_o|$; $wR_2 = [\Sigma w(F_o^2 - F_c^2)^2/\Sigma w(F_o^4)]^{1/2}$.

Appendix VII: X-ray Crystallographic Data for Compound 54a

(Chapter 3)

STRUCTURE REPORT

XCL Code: FGW1708 **Date:** 1August 2017

Compound: 4-{Bromo(phenyl)methyl}-3-phenyl-3,4-dihydronaphthalen-1(2*H*)-one (***racemate***)

Formula: $C_{23}H_{19}BrO$

Supervisor: F. G. West

Crystallographer: R. McDonald

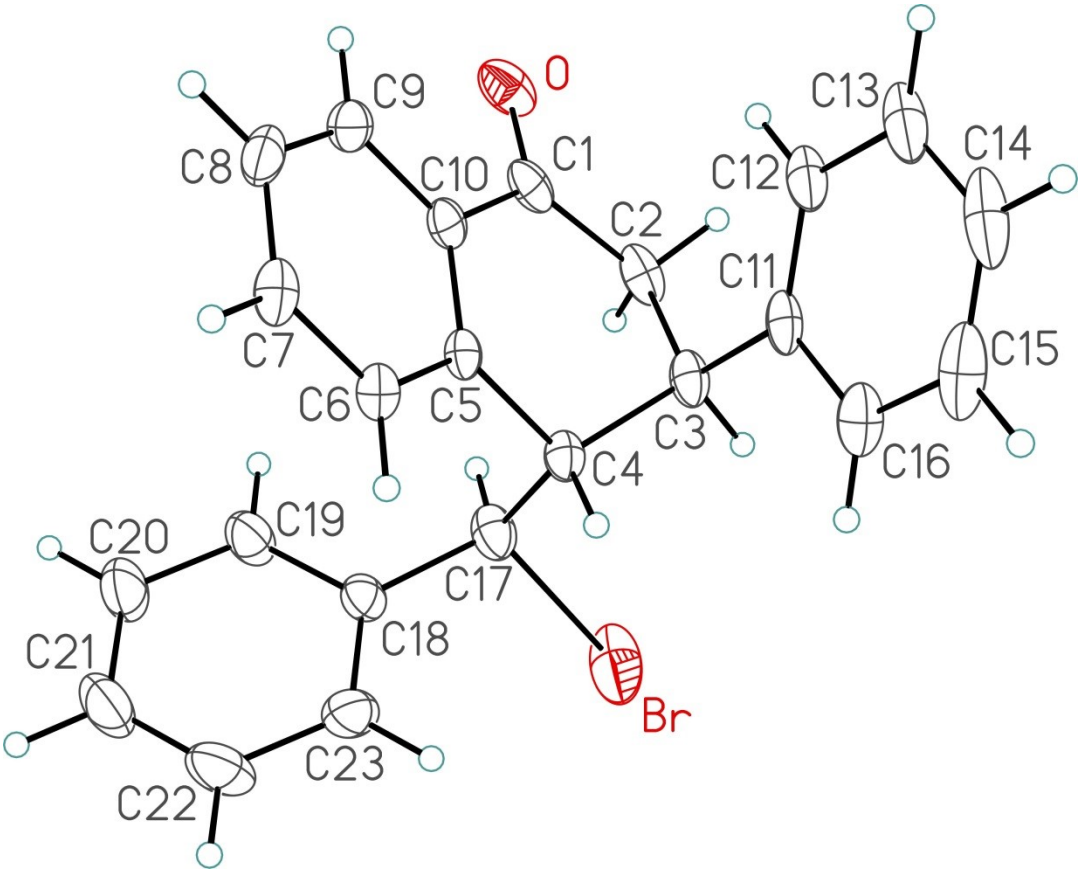

Figure 1. Perspective view of the 4-{bromo(phenyl)methyl}-3-phenyl-3,4-dihydronaphthalen-1(2*H*)-one molecule showing the atom labelling scheme. Non-hydrogen atoms are represented by Gaussian ellipsoids at the 30% probability level. Hydrogen atoms are shown with arbitrarily small thermal parameters.

Table 1. Crystallographic Experimental Details

A. Crystal Data	
formula	$C_{23}H_{19}BrO$
formula weight	391.29
crystal dimensions (mm)	0.40×0.27 × 0.12
crystal system	monoclinic
space group	*C*2/*c* (No. 15)
unit cell parameters[a]	
	a (Å) 19.1521 (3)
	b (Å) 18.7707 (3)
	c (Å) 10.8273 (2)
	β (deg) 102.6636 (7)
	V (Å^3) 3797.71 (11)
	Z 8
ρ_{calcd} (g cm^{-3})	1.369
μ (mm^{-1})	2.988
B. Data Collection and Refinement Conditions	
diffractometer	Bruker D8/APEX II CCD[b]
radiation (λ [Å])	Cu Kα (1.54178) (microfocus source)
temperature (°C)	–100
scan type	ω and ϕ scans (1.0°) (5 s exposures)
data collection 2θ limit (deg)	147.47
total data collected	13008 (-23≤*h*≤23, -23≤*k*≤23, -12≤*l*≤13)
independent reflections	3838 (R_{int} = 0.0301)
number of observed reflections (*NO*)	3576 [$F_o^2 \geq 2\sigma(F_o^2)$]
structure solution method	direct methods/dual space (*SHELXD*[c])
refinement method	full-matrix least-squares on F^2 (*SHELXL–2014*[d])
absorption correction method	Gaussian integration (face-indexed)
range of transmission factors	0.8788–0.5768
data/restraints/parameters	3838 / 0 / 227
extinction coefficient (*x*)[e]	0.00067(6)
goodness-of-fit (*S*)[f] [all data]	1.085
final *R* indices[g]	
	R_1 [$F_o^2 \geq 2\sigma(F_o^2)$] 0.0466
	wR_2 [all data] 0.1118
largest difference peak and hole	0.816 and –1.542 e Å^{-3}

[a]Obtained from least-squares refinement of 9768 reflections with 6.68° < 2θ< 146.58°.
[b]Programs for diffractometer operation, data collection, data reduction and absorption correction were those supplied by Bruker.

(continued)

Table 1. Crystallographic Experimental Details (continued)

[c]Schneider, T. R.; Sheldrick, G. M. *Acta Crystallogr.***2002**, *D58*, 1772-1779.

[d]Sheldrick, G. M. *Acta Crystallogr.***2015**, *C71*, 3–8.

[e]$F_c^* = kF_c[1 + x\{0.001F_c^2\lambda^3/\sin(2\theta)\}]^{-1/4}$ where k is the overall scale factor.

[f]$S = [\Sigma w(F_o^2 - F_c^2)^2/(n - p)]^{1/2}$ (n = number of data; p = number of parameters varied; $w = [\sigma^2(F_o^2) + (0.0369P)^2 + 7.3578P]^{-1}$ where $P = [\mathrm{Max}(F_o^2, 0) + 2F_c^2]/3$).

[g]$R_1 = \Sigma||F_o| - |F_c||/\Sigma|F_o|$; $wR_2 = [\Sigma w(F_o^2 - F_c^2)^2/\Sigma w(F_o^4)]^{1/2}$.